Cortical plasticity, dynamic neural fields and self-organization

Georgios Detorakis

UNIVERSITÉ DE LORRAINE

École doctorale IAEM Lorraine

Plasticité corticale, champs neuronaux dynamiques et auto-organisation

(Cortical plasticity, dynamic neural fields and self-organization)

THÈSE

présentée et soutenue publiquement le 23/10/2013

pour l'obtention du

Doctorat de l'Université de Lorraine

(mention informatique)

par

Georgios Is. DETORAKIS

Composition du jury

Directeurs :	ROUGIER Nicolas, Chargé de recherche à l'INRIA Nancy Grand-Est. ALEXANDRE Frédéric, Directeur de recherche à l'INRIA Sud-Ouest.
Rapporteurs :	BERRY Hugues, Chargé de recherche à l'INRIA Rhone-Alpes. GAUSSIER Philippe, Professeur à l'Université de Cergy-Pontoise
Examinateurs :	SHULZ Daniel, Directeur de recherche à CNRS Gif-sur-Yvette. CONTASSOT-VIVIER Sylvain, Professeur à l'Université de Lorraine.

Laboratoire Lorrain de Recherche en Informatique et ses Applications — UMR 7503

Loria
Laboratoire lorrain de recherche en informatique et ses applications

Mis en page avec la classe thloria.

Résumé

L'objectif de ce travail est de modéliser la formation, la maintenance et la réorganisation des cartes corticales somesthésiques en utilisant la théorie des champs neuronaux dynamiques. Un champ de neurones dynamique est une équation intégro-différentiel qui peut être utilisée pour décrire l'activité d'une surface corticale. Un tel champ a été utilisé pour modéliser une partie des aires 3b de la région du cortex somatosensoriel primaire et un modèle de peau a été conçu afin de fournir les entrées au modèle cortical. D'un point de vue computationel, ce modèle s'inscrit dans une démarche de calculs distribués, numériques et adaptatifs. Ce modèle s'avère en particulier capable d'expliquer la formation initiale des cartes mais aussi de rendre compte de leurs réorganisations en présence de lésions corticales ou de privation sensorielle, l'équilibre entre excitation et inhibition jouant un rôle crucial. De plus, le modèle est en adéquation avec les données neurophysiologiques de la région 3b et se trouve être capable de rendre compte de nombreux résultats expérimentaux. Enfin, il semble que l'attention joue un rôle clé dans l'organisation des champs récepteurs du cortex somato-sensoriel. Nous proposons donc, au travers de ce travail, une définition de l'attention somato-sensorielle ainsi qu'une explication de son influence sur l'organisation des cartes au travers d'un certain nombre de résultats expérimentaux. En modifiant les gains des connexions latérales, il est possible de contrôler la forme de la solution du champ, conduisant à des modifications importantes de l'étendue des champs récepteurs. Celà conduit au final au développement de zones finement cartographiées conduisant à de meilleures performances haptiques.

Mots-clés: plasticité corticale, les champs neuronaux, auto-organisation, somatosensoriel cortex, attention.

Abstract

The aim of the present work is the modeling of the formation, maintenance and reorganization of somatosensory cortical maps using the theory of dynamic neural fields. A dynamic neural field is a partial integro-differential equation that is used to model the cortical activity of a part of the cortex. Such a neural field is used in this work in order to model a part of the area 3b of the primary somatosensory cortex. In addition a skin model is used in order to provide input to the cortical model. From a computational point of view the model is able to perform distributed, numerical and adaptive computations. The model is able to explain the formation of topographic maps and their reorganization in the presence of a cortical lesion or a sensory deprivation, where balance between excitation and inhibition plays a crucial role. In addition, the model is consistent with neurophysiological data of area 3b. Finally, it has been shown that attention plays a key role in the organization of receptive fields of neurons of the somatosensory cortex. Therefore, in this work has been proposed a definition of somatosensory attention and a potential explanation of its influence on somatotopic organization through a number of experimental results. By changing the gains of lateral connections, it is possible to control the shape of the solution of the neural field. This leads to significant alterations of receptive fields sizes, resulting to a better performance during the execution of demanding haptic tasks.

Keywords: cortical plasticity, neural fields, self-organization, somatosensory cortex, attention.

Ελευτεριά θα πει να μάχεσαι στη γης χωρίς ελπιδα.
Νίκος Καζαντζάκης, 1883-1957.

Acknowledgments

« ἀρχή σοφίας ὀνομάτων ἐπίσκεψις »
(Αντισθένης, 445-360 π.Χ.)

I would like to express my heartfelt gratitude to my advisor Dr. Nicolas Rougier for his continue support during my dissertation and research, for his patience, immense knowledge and his continue presence all these three years. His guidance was invaluable and useful to me during my dissertation preparation. Moreover, I own him a big thank you because of his help in my settling in Nancy.

Besides my advisor, I would like to thank Dr. Frédéric Alexandre, my co-advisor, for his helpful hints and advices in all these years, and especially during the writing of the present thesis. Moreover, I would like to thank Dr. Thierry Viéville and Dr. Axel Hutt for their interesting and useful conversations and mathematical tips.

I would like to express my deepest appreciation to the members of my dissertation committee, Dr. Berry Hugues, Prof. Philippe Gaussier, Dr. Daniel Shulz and Prof. Contassot-Vivier Sylvain.

I thank my officemates Maxime Rio, Carolina Saavedra, Benoit Chappet de Vangel, Meysam Hashemi and Meropi Topalidou and the "postdoctoral fellows" Pedro Garcia Rodriguez, Nicoles Voges and Laure Buhry who were a source of joy, laughter and patience during these years. Moreover, I would like to thank my former officemate, Carlos Carvajal.

And finally I would like to thank my father Isidoros, who set me on the road and my mother Theonymfi. Furthermore, I would like to thank my brothers, Manolis and Antonis. Special thanks go to my grandfather Manolis for his continue support from the beginning of my studies all these years. Additionally, a big thank you goes to my lost grandparents Georgios, Marianthi and Maria, who passed on me the virtue of education and learning.

In memory of my beloved cousin, Marianthi.

Contents

List of figures

List of tables

Introduction (in French)

Le cortex somatosensoriel primaire est une partie du cortex cérébral qui est, avec le cortex moteur, l'un des premiers cortex développés et parmi les plus importants. Il est divisé en quatre aires (1,2,3 a et 3b) et chacune de ces aires est consacrée au traitement spécifique d'un type d'information. Ainsi, l'aire 3b traite les informations relatives au toucher et à la pression. En effet, il existe au niveau de la peau des mécano-récepteurs (cellules de Merkel) qui collectent ces informations et les transmettent à la moelle épinière, puis au thalamus et enfin au cortex somatosensoriel primaire. L'objectif de cette thèse est d'étudier la formation de cartes topographiques au sein du cortex somatosensoriel primaire en utilisant comme cadre de calcul la théorie de champs neuronaux dynamiques.

Lorsque l'on regarde en détail les zones du cortex somatosensoriel primaire, on peut remarquer que chaque zone contient une carte somatotopique du corps. Cela signifie que dans la région 3b, il existe une carte qui représente la surface de la peau de chaque partie du corps. Ces cartes sont développées au cours des périodes pré et post natale. Au début du développement, les neurones migrent vers leurs positions finales et établissent des connexions (synapses) avec les autres neurones et avec leurs entrées. Par la suite, des processus simultanés de compétition et de coopération, vont provoquer la formation des cartes somatotopiques. Il y a encore quelques années, la communauté scientifique pensait que ces cartes sensorielles (somatotopique - cortex, somatosensoriel, rétinotopiques - cortex visuel, tonotopique - cortex auditif) avaient un caractère immuable à la fin de la période de développement ; la période critique. Les travaux de David Hubel et Torsten Wiesel ont défini cette période critique comme étant une fenêtre de temps durant laquelle le cerveau peut se développer et demeure relativement plastique. Au delà de cette période, le cerveau ne pourrait plus se modifier aussi facilement. Or quelques années plus tard, John Kaas et Michael M. Merzenich ont montré que la théorie de Hubel et Wiesel n'était pas correcte. Ils ont constaté que le cerveau, même adulte, demeure plastique et peut, dans une moindre mesure, se modifier suite à un accident vasculaire cérébral par exemple. Au cours des deux décennies passées, de grands progrès ont été réalisés quant à la compréhension de la plasticité corticale et il est aujourd'hui largement admis que le cortex cérébral demeure plastique au delà de la période critique, de même que pour les autres structures cérébrales mais aussi, et de façon plus étonnante, pour la moelle épinière.

En outre, le cortex somatosensoriel primaire est sous l'influence de nombreuses autres zones du cerveau, à la fois corticales et sous-corticales, et se trouve en particulier influencé par des processus de haut niveau telle que l'attention. Ce processus cognitif peut se définir simplement comme la capacité à traiter en priorité (et en profondeur) une partie de l'information au détriment des autres informations disponibles, qui peuvent être moins importantes ou moins significatives. Par exemple, lorsque l'on recherche une cible particulière dans une scène visuelle, il est important de pas prêter attention aux nombreux distracteurs qui peuvent être présents. On parle alors d'attention visuelle. Or, il existe aussi une attention somatosensorielle qui, si elle est moins connue, joue néanmoins un rôle très important dans notre perception du monde. Elle reste cependant peu étudiée et il n'existe à l'heure actuelle que deux théories dominantes (et

contradictoires) quant à son effet sur la formation des cartes somatotopiques. Nous cherchons donc à comprendre comment les neurones du cortex somatosensoriel peuvent coopérer pour former des cartes topographiques qui soient bien organisées. Pour répondre à cette question, il nous faut aussi déterminer quel type d'information est nécessaire et quel est le mécanisme mathématique ou numérique qui puisse décrire efficacement le phénomène d'auto-organisation et de ré-organisation en cas de lésions corticales ou de privations sensorielles. De plus, nous souhaitons définir ce qu'est l'attention somatosensorielle et comprendre son influence sur la formation des cartes à long terme et sur les performances haptiques à court terme.

D'un point de vue strictement informatique, on peut considérer les cartes corticales comme des cartes auto-organisées, c'est à dire qu'elles réalisent une quantification vectorielle des entrées perceptives en grande dimension (i.e. le nombre de capteurs) vers une topologie d'ordre 2. L'un des algorithmes les plus connus pour réaliser une telle quantification sont les cartes auto-organisatrices de Kohonen (SOM). Le coeur de l'algorithme est basé sur la notion de neurone gagnant (winner-takes-all) qui désigne le neurone le plus proche de la donnée présentée. La notion de voisinage entre les neurones (la carte est dotée d'une topologie) permet ensuite de faire apprendre les neurones au prorata de leur distance au neurone gagnant. Cet algorithme connaît d'innombrables variantes mais (presque) toutes reposent sur un apprentissage hors-ligne, c'est à dire un apprentissage où l'ensemble des données est connu a priori. Une amélioration notable de cet algorithme est l'algorithme DSOM (pour Dynamic Self-Organising Map) qui permet quant à lui d'effectuer un apprentissage en ligne et en continu en utilisant un paramètre d'élasticité. Il nécessite cependant lui aussi la notion de neurone gagnant qui demeure peu compatible avec les neurosciences. Le modèle LISSOM est plus intéressant en ce sens qu'il permet de rendre compte de l'organisation du cortex visuel primaire en tenant compte des entrées thalamiques et des interaction corticales. Cependant, son usage reste limité au cas visuel en raison d'une paramétrisation peu robuste aux changements

Au vu de ces objections, il nous a donc semblé nécessaire de définir un certain nombre de critères et de propriétés qu'il est souhaitable pour un modèle de respecter afin de pouvoir rendre compte de la plasticité corticale. Le modèle que nous proposons s'inscrit dans cette démarche et se base sur la théorie des champs de neurones dynamiques auquel il a été adjoint une règle d'apprentissage permettant l'émergence de représentations topologiquement organisées. Un modèle de peau a aussi été conçu afin de fournir au modèle de cortex des entrées réalistes vis-à-vis des connaissances actuelles sur les mécano-récepteurs. Comme nous le verrons dans le document, ce modèle est capable de s'auto-organiser et de pallier partiellement les effets de lésions corticales ou cutanées. Le modèle peut être décrit très simplement par un système de deux équations différentielles continues en temps et en espace et rendant compte respectivement de l'évolution de l'activité d'une population de neurones et de l'évolution des poids montants de la population :

$$\left.\begin{aligned} \tau\frac{\partial u(\mathbf{x},t)}{\partial t} &= -u(\mathbf{x},t) + \int_\Omega w_l(\mathbf{x},\mathbf{y})(\alpha f(u(\mathbf{y},t)))d\mathbf{y} + \alpha\frac{1}{k}|s(\mathbf{z},t) - w_f(\mathbf{x},t)| \\ \frac{\partial w_f(\mathbf{x},t)}{\partial t} &= \gamma\left(s(\mathbf{z},t) - w_f(\mathbf{x},t)\right)\int_\Omega w_e(\mathbf{x},\mathbf{y})(\alpha f(u(\mathbf{y},t)))d\mathbf{y} \end{aligned}\right\} \quad (1)$$

où $u(\mathbf{x},t)$ décrit l'activité de la population à la position $\mathbf{x}$ et au temps t, w_f représente les poids montants, w_l représente les poids latéraux, α est une constante de temps. Les simulations se font alors via une discrétisation (en temps et en espace) et une intégration standard des équations différentielles. La fonction w_l est généralement une différence de gaussiennes (voire même une différence d'exponentielles) de sorte que l'on a des excitations à courte portée et des inhibitions à longue portée, reflétant ainsi les données de la biologie. Pour que l'auto-organisation puisse avoir lieu au sein du modèle, il a été nécessaire dans un premier temps de doter le champ d'une

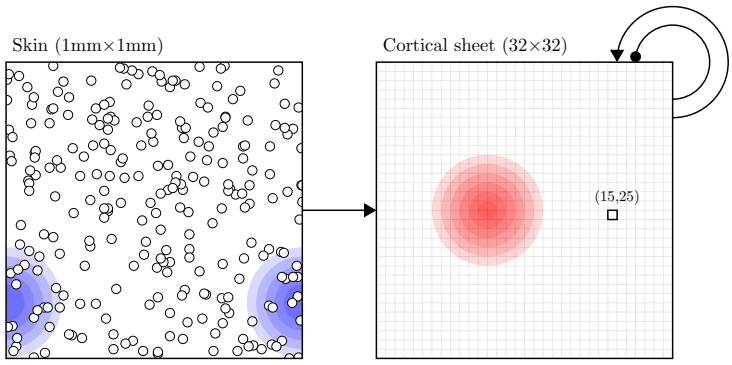

propriété numérique qui permet à celui-ci, à partir d'une entrée donnée, de se relaxer de telle sorte que l'activité maximale du champ correspond à l'activité en entrée. Cette propriété correspond de fait à une mesure et lors du processus d'apprentissage, l'activité du champ reflète alors une mesure implicite de l'adéquation des entrées avec les prototypes mémorisés par le modèle, ce que nous avons pu montrer expérimentalement. Une autre propriété numérique qui a été introduite correspond à la forme même de la solution du champ qui peut être déformée en fonction d'un paramètre contrôlant l'étendue de la solution. Celle-ci peut être forte et étroite ou bien large et faible, reflétant dans une certaine mesure les effets de l'attention. De plus, et pour des valeurs particulières des paramètres, il est possible d'avoir des solutions localisées (on parle de bulle unique) ou bien des solutions multiples (2 bulles dans notre cas) reflétant ainsi la possibilité de discriminer une stimulation simple ou double, selon la distance entre les stimuli.

L'objectif principal du modèle proposé est de comprendre la formation et l'organisation des cartes somatotopiques du cortex somatosensoriel primaire. Dans ce contexte, le modèle doit rendre compte de la formation initiale des cartes topographiquement organisées, mais aussi de la réorganisation de ces mêmes cartes en cas de lésion corticale (e.g. accident vasculaire cérébral par exemple) ou de privation sensorielle (e.g. brûlure profonde, amputation, etc.). Nous avons dans un premier temps modélisé une petite surface de peau, de l'ordre de $1mm^2$, se situant à l'extrémité d'un doigt qui est l'une des zones les plus denses en termes de récepteurs. Nous avons muni la zone considérée d'un ensemble de 256 récepteurs répartis de façon quasi-uniforme sur l'ensemble de la surface. Un stimulus appliqué en un point P est alors échantillonné en tenant compte de l'élasticité de la peau qui induit une excitation de l'ensemble des récepteurs proches du point P de façon proportionnelle à leur distance au site de stimulation. Plus précisément, nous avons utilisé une fonction gaussienne. Ces informations de pressions (256 valeurs scalaires) sont alors transmises au modèle de cortex qui est, comme nous l'avons souligné, un champ de neurone. Celui-ci a été paramétré de sorte qu'il y ait à tout instant une solution unique sous forme d'une bulle localisée. Cette activité du champ, qui reflète l'adéquation entre la stimulation et ce qui a déjà été mémorisé par le champ (au niveau des entrées montantes), module l'apprentissage des entrées montantes qui se fait de façon simultanée et continue. Au final, nous montrons numériquement comment une carte topographiquement bien organisée peut émerger suite au processus d'apprentissage. Nous avons évalué le comportement du modèle selon différents critères afin notamment de pouvoir faire le lien avec la biologie et les différent résultats expérimentaux disponibles. Aussi, à la fin de chaque simulation, nous avons extrait les champs récepteurs de chaque neurone du modèle nous permettant alors de situer ceux-ci sur la surface de la peau, en considérant le centre de masse des champs récepteurs. Nous avons pu alors constater visuellement que le modèle était bien organisé, ce qui a été confirmé par une mesure objective de cette bonne organisation (mesure $dx - dy$). En extrapolant la position de ces champs récepteurs via un processus de diffusion, nous avons

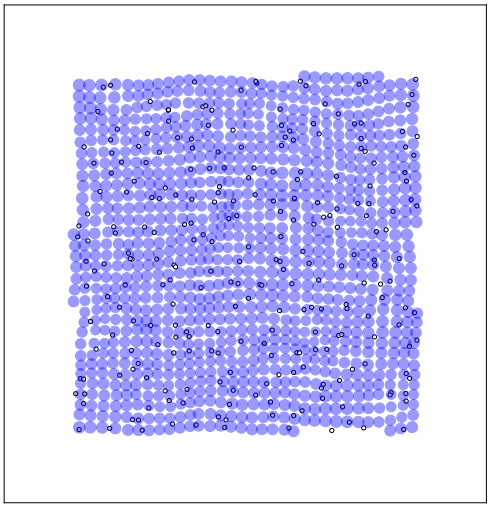

montré une densité quasi-uniforme de ceux poids sur la surface de la peau, indiquant ainsi que l'ensemble de la surface est "bien représentée". Nous avons ensuite étudié 3 types de lésions corticales (type I, II et III) et 3 types de lésions cutanées (type I, II et III). Pour les lésion corticales, nous avons considéré qu'un certain nombre de neurones étaient dysfonctionnels, c'est à dire qu'ils ne participaient plus, ni à l'activité globale du champ, ni à l'apprentissage. Pour les lésions cutanées, nous avons considéré qu'un certain nombre de récepteurs devenaient silencieux quelle que soit la stimulation. Les trois types de lésions correspondent de plus à 3 situations topologiques distinctes, le type I étant topologiquement équivalent à la situation normale et le type III induisant une variété topologique nouvelle. Pour l'ensemble de ces lésions, le modèle est capable de se réorganiser plus ou moins complètement selon le type de lésion et son étendue (25% de la surface considérée ici).

Dans le cas de la privation sensorielle, les champs récepteurs concernés migrent vers de nouvelles positions sur la surface de la peau selon un processus en trois étapes. Il y a d'abord une expansion du champ récepteur, suivie d'une migration et enfin d'une contraction sur le nouveau site. Dans le cas d'une lésion corticale, les neurones voisins aux neurones dysfonctionnels ont tendance à coopter les territoires perdus via une expansion et une migration de leurs champs récepteurs sans phase de contraction. Cependant, cette réorganisation n'est pas totale notamment parce que le connexions latérales sont fixes et n'autorisent pas de changements de la topologie intrinsèque du champ : un neurone voisin d'une neurone dysfonctionnel conserve cette relation de voisinage. Une perspective logique de ce travail consisterait à pouvoir aussi modifier les connections latérales afin de pouvoir moduler la topologie.

Nous avons dans un deuxième temps étudié la notion d'attention somatosensorielle en identifiant celle-ci avec la possibilité de moduler la forme de la solution du champ. Le mécanisme proposé repose sur la modulation de gain des liaisons horizontales. En définissant une région d'intérêt sur la surface de la peau, il est alors possible de moduler la réponse du modèle selon que le stimulus se trouve ou non dans cette zone. Si un stimulus se trouve dans la zone, le champ est modulé de façon à offrir une solution de faible étendue mais de forte amplitude. Cette modulation de la réponse induit des conséquences directes sur l'apprentissage et les champs récepteurs des neurones subissent alors des modifications importantes. Nous avons constaté numériquement une plus grande densité de champs récepteurs dans la zone d'intérêt avec des champs récepteurs significativement plus petits. Ces effets sont d'autant plus forts s'ils accompagnent la formation initiale des cartes. Ainsi, si il est possible de moduler la réponse à court terme, seul l'apprentis-

sage permet de conserver ces propriétés sur le long terme. L'interprétation de ces résultats nous a conduit à proposer les lobes frontaux et temporaux comme origines possibles de ce signal attentionnel qui pourrait être de nature cholinergique, en accord avec plusieurs études expérimentales. Suite à quoi, nous proposons aux expérimentalistes un certain nombre d'expériences permettant de valider ou d'invalider nos hypothèses. Au final, le modèle proposé est robuste, complètement distribué et repose sur un nombre restreint d'hypothèses. Il permet d'expliquer, avec les mêmes mécanismes, la formation initiale des cartes somatotopiques, la capacité à se réorganiser en cas de lésion corticale ou cutanée, et le rôle et l'influence de l'attention somatosensorielle. En cela, le modèle propose une explication simple des mécanismes sous-jacent à la plasticité corticale.

Ce travail est organisé en deux grandes parties. La première partie introduit des éléments de neurobiologie, de neuroanatomie et de neurophysiologie concernant le système nerveux central et plus particulièrement le cortex primaire somatosensoriel. Ces éléments permettent d'introduire notamment les données expérimentales concernant la région 3b et de comprendre les questions attenantes concernant les mécanismes de la plasticité corticale et du rôle supposé de l'attention. La deuxième partie de ce travail est consacrée à la formalisation mathématique et à la résolution numérique du problème. Par conséquent, le premier chapitre introduit les champs de neurones dynamiques ainsi que les principaux résultats connus. Le second chapitre présente la quantification vectorielle et les principes de l'auto-organisation et trois modèles neuronaux représentatifs d'auto-organisation sont illustrés. Enfin, le troisième chapitre présente un modèle détaillé de la zone 3b du cortex somatosensoriel ainsi que les principaux résultats concernant la formation initiale des cartes, la réorganisation face à des lésions corticales et cutanées et le rôle de l'attention dans l'apprentissage. Enfin, nous présentons les perspectives ce travail dans le conclusion générale.

Introduction

The problem of Brain and Mind is not something new. Ancient Greeks tried to answer to some very essential and basic questions about what is the brain, and how does it work? What is the consciousness and how does it emerge? They tried to find out where is the *home* of the soul and how a soul can be connected and interact with the body. Is the body a prison for the soul or it is something absolutely necessary for the existence of the brain and the mind itself?

Plato and Aristotle tried to treat the mind-body problem. Aristotle believed that the mind emerges from the soul, instead of Plato, who believed that the body and the mind (soul) are two different entities and the soul can exist without the body, but the body is incapable of living without the soul, since it is not able to understand the abstraction of the universe. More recently proposed philosophical treatments are those provided by Descartes, Kant and Popper. Descartes believed that the mind is over the body and it is able to control the body through the pineal gland. Kant claimed that the mind and body problem can be studied as an embedded a priori knowledge of some of the aspects of the real world. For Popper, the problem is more complicated since he distinguished three major objects. The mind, the matter and the creation of the mind (abstract meanings created by the mind itself).

The main point that has to be designated is the connection between mind and body. The brain is an organ, that serves specific operations and tasks, from simple tasks such as regulation of the body temperature to highly complex tasks such as attention and even more complex; consciousness.

From the very early theories of Aristotle and Plato to the more recent theories of Popper and Kant, a lot of scientific data have come to the light. In this era, it is known that the brain is a constituent part of the body, and vice versa. The body needs the brain and the brain needs the body in order for both to work properly. The body acts as the mediator between the environment and the brain, providing it later with all the necessary information. The brain, in turn, processes the information in order to interact with the environment.

Aristotle, when he tried to describe the anatomy and the biology of animals and humans made some assumptions about the brain. In one of his masterpiece of work, "On the parts of Animals", readers can found the quote:

> *And of course, the brain is not responsible for any of the sensations at all. The correct view is that the seat and source of sensation is the region of the heart.*

Since the era of Aristotle, many things have changed. In the 21^{st} century, the information about the brain is enormous. It has been now revealed that the brain itself is a highly complex dynamic system. Dynamic in the sense that it can learn (be plastic), evolve and adapt itself in the presence of different conditions. Furthermore and on the contrary of older studies, the brain is known to be plastic for a lifetime. It was the pioneer work of Hubel and Wiesel that establishes the doctrine of hardwired brain. They managed to provide evidence that the brain after a period following childhood (the so-called critical period) was not able to learn anymore. After some years, neuroscientists such as John Kaas and Michael M. Merzenich showed that the theory of

Hubel and Wiesel was not correct. They found that even the adult brain has the ability to learn and recover in the presence of brain damages, such as strokes.

In addition a lot of work has been done in the domain of medical imaging and new recording techniques have been established aiming at a better understanding of the brain and finally of the consciousness itself. New phenomena have also been unrevealed and described. Neuroscientists have shed light on many different aspects of the behavior of animals and human beings. Let alone the biology, the biochemistry and the neurophysiology. In this quest for knowledge, mathematics and computer science play an important and vital role, providing new tools and insights and explaining, through a more theoritical point of view, neurophysiological data. This can lead to the development of new theories and to the improvement of previous ones.

From a mathematical perspective, the problem of modeling the brain and understanding its complex phenomena through equations is a challenging one. A big progress has been made in the few last decades, starting from the models of spiking neurons, such as the Hodgkin-Huxley model, which is the the most well-known representative model of that category. Other models, belonging to the class of rate models, trying to describe the same phenomena but using different kind of equations, have come into the game. Models such the one of Cowan and Wilson and later that of Amari have contributed to the understanding of the brain.

The natural expansion of the mathematical models, is the computational and the numerical one. Many of the aforementioned equations have been used in order to develop computational models able to simulate parts of the brain and/or study several phenomena that take place in the brain. Other applications that can be considered are related to robotics. Many of those models are also used in order to render robots capable of acquiring behavior like animals or humans. This could be used for medical purposes or for the further study of the brain itself.

What a brain is, is more or less roughly known. The brain consists of two hemispheres and several different centers and nuclei. They are groups of neurons forming complex neural networks, that serve different, multiple, distributed and complex computations. Computations must not be understood here in the strict sense of computer science but at a more abstract level. The most evolved and modern (according to evolution theory) part of the brain is the cerebral cortex. This is the part of the brain that renders human beings able to think rationally, to do plans, to take decisions, to pay attention on something or on somebody.

An important part of the cerebral cortex corresponds to sensory systems. These systems provide an interface between receptors spreading on all over the body and the brain. Body receptors gather information about the external and the internal environment. They transmit that information to the brain for further processing. The most well-known sensory region is the visual cortex. This is the most well-studied one and a lot of different theories have been postulated about it. Another important cortex, as much important as the visual one, is the somatosensory cortex. The somatosensory cortex is mainly responsible for haptic information, temperature, pain, posture and body position information. In combination with the motor cortex, it is able to move the body and to protect it from the threats of the external environment, because of the haptic information it provides.

Primary somatosensory cortex is an ordered topographic map that contains neurons encoding a part of the skin of the body, for instance. Any body part is represented in the primary somatosensory cortex, following more or less an homonculus organization. This means that specific parts of the primary somatosensory cortex are devoted to specific body parts. Therefore, an interesting question is, how the neurons of primary somatosensory cortex are able to compete and cooperate with each other in order to establish such topographic map? What is the kind of information that they need and what is the possible computational and/or mathematical

mechanism that could describe the phenomenon of self-organization of neurons. Therefore, in the present work a model about self-organization of primary somatosensory cortex is proposed. The model is based on the theory of dynamic neural fields and takes advantage of an Oja-like learning rule in order to achieve topographic maps. In addition, a model of the skin has been considered as an inevitable and necessary part of the model, because a simultaneous simulation of the body and the brain is more plausible and reliable than a strict mathematical model that does not take into consideration any kind of sensory external information. Furthermore, the model is able to recover from cortical lesions and sensory deprivation conditions. This means that it can react as the brain cortex does when it faces a stroke, for instance, or a sensory deprivation, respectively.

In addition to the primary sensory cortices and the very basic brain areas, the subcortical ones (such as thalamus, brainstem, spinal cord), there are several higher order areas, which are responsible for more complex and advanced tasks. For instance, areas in the prefrontal cortex are responsible for attention and other areas in frontal cortex are responsible for working memory. Temporal lobe, for instance, plays a crucial role in language comprehension. Other areas in parietal lobe are capable of combining different sensory modalities in order to express a specific behavior. A very important higher order cognitive function of the brain cortex is attention. Attention means the capability of the brain to ignore irrelevant information during the execution of a task and to concentrate only to the relevant (attended) information. As the visual system is the most well-studied system, attention has been also extensively studied in this system. In this work attention has also been studied from a computational point of view in order to examine the effects on primary somatosensory cortex. How attention can affect the sensation of haptic information and how the performance of a subject during an attentional task can be increased? To address these questions, it has been proposed that a gain control mechanism of lateral (horizontal) connections is able to induce dramatic changes on the receptive fields of the neurons of primary somatosensory cortex.

The proposed model is able to capture cortical phenomena such as ordered topographic maps formation, maintenance and recovery in the presence of cortical lesions or sensory deprivation. The model takes advantage of the dynamic neural fields theory and the Oja learning rule in order to accomplish its objectives. In addition, attentional effects on receptive fields of neurons of primary somatosensory cortex have been studied. The proposed mechanism, driven by attention, is the gain modulation of horizontal connections. In addition, a strong remark is the need for training in combination with attention. That's because attention, by its own, in the long-term is not sufficient to promote long-lasting changes in the performance of a subject. Therefore training is a constituent part of achieving optimal performance. The proposed model uses a small amount of parameters in order to achieve self-organization. This renders the model easy to implement, reliable and robust enough. The model is able to learn for a lifetime, after its critical period of learning. Furthermore, it can be considered as distributed and is completely unsupervised. Furthermore, two interesting properties of dynamic neural fields have been described in this work. The first has to do with the ability of a neural field to relax its activity at the maximum value of its input regarding the parameters. The second one has to do with a dynamic change of solution of a neural field, providing two different kinds of persistent solutions (bumps). Both can be extracted by the same equation by changing only one parameter. Both properties have been used during this dissertation in order to explain neurophysiological phenomena.

Therefore, this work is organised into two major parts. The first part introduces the neurobiology, neuroanatomy and neurophysiology of the central nervous system and especially the primary somatosensory cortex. Hence, in the first part the central nervous system of mam-

mals is presented and some very basic terms are explained. In the second chapter the primary somatosensory cortex and especially area 3b are illustrated. Neurophysioligical data about topographic organization and reorganization in the presence of cortical lesions or sensory deprivations are also put forward. In addition, higher order cognitive functions are also discussed. The second part of this work is devoted to the mathematical and computational modeling of the problem. Therefore, the first chapter is an introduction to neural networks modeling and neural fields equations. In the second chapter the computational principles and aspects of self-organization are discussed. Three main types of self-organizing neural networks are illustrated (Kohonen-SOM, Dynamic SOM and LISSOM). Finally, in the third chapter the outcoming model of this work is introduced. A few preliminar results are illustrated and then a detailed model of area 3b of the primary somatosensory cortex is discussed. In addition, some interesting results about cortical reorganization and attentional affects on area 3b are also taken into consideration. In the end, the general conclusions of this work are set forth.

Part I

Neuroscience background

Mind is infinite and self-ruled, and is mixed with nothing, but is alone itself by itself.

(Anaxagoras, 500-428 B.C.)

1 Central Nervous System (CNS)

Contents

Almost all animals on the planet earth, especially the vertebrates, have a nervous system, which is responsible from the very basic functions of the reptiles up to the most higher cognitive functions of the human brain cortex.

A typical nervous system is composed of two major parts. The central (CNS) and the peripheral nervous system (PNS), [1, Ch. 1, p. 18]. The latter contains the autonomic nervous system (sympathetic and parasympathetic), that is responsible for gastrointestinal system, regulation of functions of internal organs and glands and the "fight-or-flight" condition, [2, Part. 6, p. 795]. The central nervous system is the main coordinator of the body as it processes the received information from both the outer environment and the interior of the body, [2, Ch. 2, p. 31]. Moreover, higher order cognitive functions, which participate in the vast repertoire of behavior

are a result of complex cooperative functions of complex neural networks lying in the central nervous system.

The rest of the chapter pertains to the central nervous system, presenting briefly the most basic and important structures neglecting the details and the peripheral nervous system.

1.1 Basic elements of CNS

The CNS is a complex of neural networks composed of different living materials. From a macroscopic point of view, the CNS of mammals is divided in two major parts, the brain and the spinal cord, [1, Ch. 1, p. 18]. The brain is located in the cavity of the head and is composed of cells (gray matter) and cables or axons (white matter). Moreover the brain floats in cerebrospinal fluid, where it is protected from harmful substances by the blood-brain barrier and is divided into two hemispheres. Each hemisphere consists of the cortex, which is the outer and most phylogenetically developed part of the brain and of nuclei, which are groups of neurons located at several subcortical structures of the brain, [2, Ch. 2, p. 35]. Each brain hemisphere carries through different tasks, [3]. For instance, left hemisphere is more specialized in speech process and subconsciousness processing of grammar instead of the right hemisphere, which can process imaginary states in a more flexible way, [4]. This means that each hemisphere has a dominant function over the other one, something which is known as hemisphere lateralization. The two hemispheres are connected with each other by the corpus callosum, which is a bridge between the two hemispheres. Humans corpus callosum, for instance, is composed by $300 - 400$ million contralateral cables, [5]. In addition, the brain is organized in a decussated fashion, which means that the left hemisphere is responsible for the right part of the body and vice versa.

1.1.1 Cells of CNS

The very basic elements of CNS are the neurons and the glial cells. The neurons are the single processing units of the CNS, that process and transmit information. Next paragraphs are dedicated to neurons and how they work. Before diving into details about neurons, it's worth to mention some interesting and valuable information about glial cells. Glial cells are something like supporting players and play an important role in neural axons myelination. Glial cells produce the myelin that insulate the neurons, [6, Ch. 2,p. 20]. Another important function of glial cells is the uptake of neurotransmitters and recently it has been proposed that they are also involved in the neural computations by forming complex networks and building the so-called tripartite synapses, [7]. Among other operations are the regulation of presynaptic terminals of neuromascular junction, promoting the growth of neurons and taking care of nutrient of neurons. During development, glial cells guide neurons to migrate properly and collect the debris after neurons death, [2, Ch. 3, p. 47].

1.1.2 What is a neuron?

Neurons are the very basic elements of the CNS and a schematic representation of a neuron is illustrated in figure 1.1. They are the cells that execute the computations in order to process the information and to transmit it to other neurons and/or to other structures such as muscles. Moreover, other types of neurons receive information or transduce information from external or internal environment of the body and convey the information towards the CNS for further process. Therefore, a first classification can be made according to the way that a neuron conveys information. Hence, there are three types of neurons,

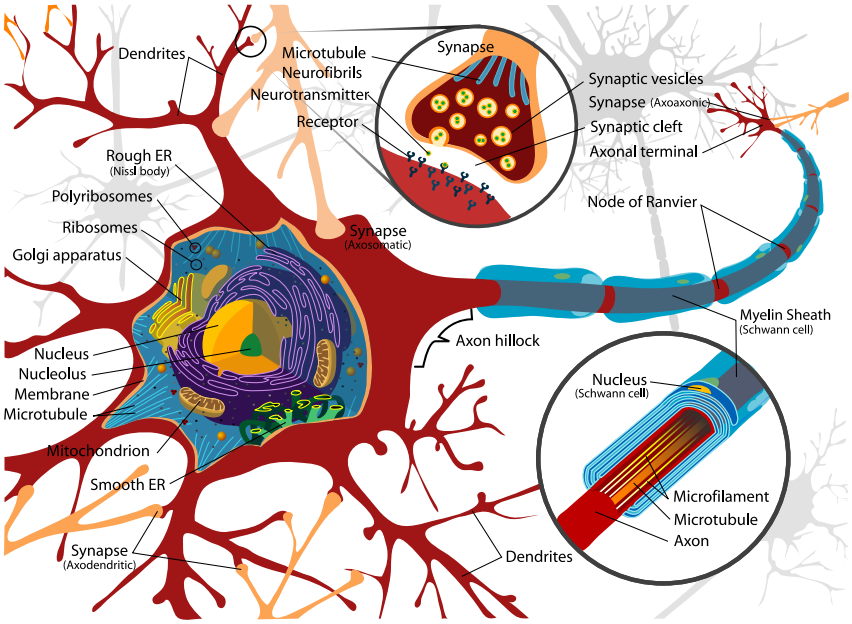

Figure 1.1: **A schematic representation of a neuron.** In this schematic the very basic cellular organelles and structures are apparent. The soma, axon, dendrites and synapses are illustrated. (Figure from Wikipedia, under a Creative Commons Attribution-Share Alike 3.0 Unported)

- Afferent neurons, that convey information from periphery to the brain.
- Efferent neurons that transmit information.
- And interneurons, that act locally within the brain and have inhibitory properties, [6, Ch. 2, p. 21].

Neurons are cells that consist of four main components. The soma of the neuron, where the most of the cell structures and organs live. The soma is the place where the protein synthesis takes place. The second important part of a neuron is the axon, which is a very long thin fiber that conveys and transmit the information to other neurons or structures. Some of the cell structures like microfilaments and microtubules also live there. The connection point between axon and soma is called axon hillock and is the most excitable part of the neuron. Axon transmits the action potentials, that will be described later in this chapter. The third part of a neuron is the axon terminals, where the synapses live and the transmission of chemical neurotransmitters takes place. The fourth component of a neuron are the dendrites. Dendrites are cellular structures, that emerge mainly from the soma and act as the main input of the neuron via dendritic spines, [2, Ch. 4, p. 59].

Another classification depending on the morphology of the neurons also exists. Therefore, there are three main classes. First is the unipolar or pseudounipolar neurons, where axon and dendrites can be found on a single process. Second is the bipolar neurons, that have two processes one for the axon and one for the dendrites. The third class is the multipolar neuron, that have one process, which is the axon and other multiple processes that serve as dendrites. Some examples of multipolar neurons are the pyramidal neurons of cortex, motor neurons of spinal cord and Purkinje cells of cerebellum, [6, Ch. 2, p. 24]. In figure 1.2 are illustrated some different types of neurons. In addition neurons can be classified according to the chemical neurotransmitter

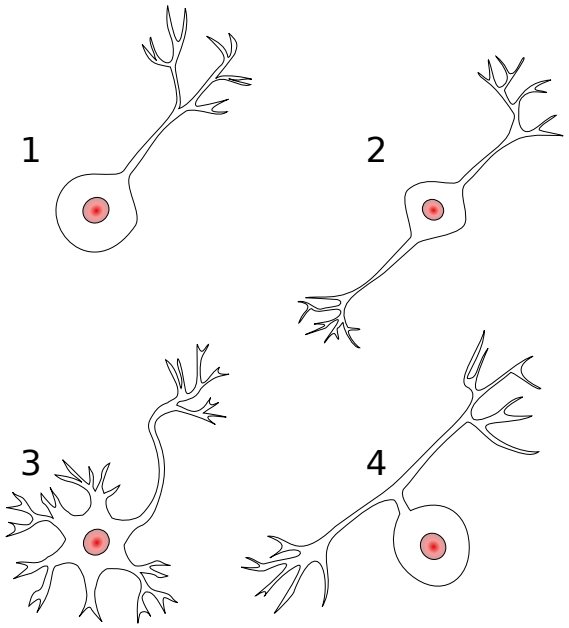

Figure 1.2: **Four types of neurons. 1** A unipolar neuron, **2** bipolar neuron, **3** multipolar neuron, **4** pseudounipolar neuron. (Figure from Wikipedia, under a Creative Commons Attribution-Share Alike 3.0 Unported)

they express. There are two major classes, the excitatory neurons that excite other neurons and express excitatory neurotransmitter like glutamate. In contrary the neurons that inhibit (suppress activity of) other neurons and express inhibitory chemical neurotransmitter like GABA are called inhibitory neurons. More details about this classification can be found in the dedicated neurotransmitters paragraph of the present chapter, [2, Ch. 3, p. 45].

1.1.3 How does a neuron work?

A neuron is an electrical excitable mean that takes advantage of ion pumps and ion channels in order to keep in balance the membrane potential, the difference between interior and exterior electrical potential of a neuron. Ion pumps promote ions (calcium, potassium, sodium and chloride) exchange between the inner and the exterior part of a neuron. Moreover, ion channels, that are transmembranic proteins, gate the ions permitting the inflow and the outflow of ions. There are two major ion channels, the ligand-based that open and close in the presence of specific chemical molecules and the voltage-based that open and close according to differences in membrane potential. The voltage-gated ion channels are mainly responsible for generation and transmission of action potentials, [6, Ch. 2, p. 21], [2, Ch. 3, p. 41].

Action potential

The term action potential refers to a short-time event that takes place on a neuron, and is nothing more than a spontaneous increase of membrane potential followed by a decrease. This up and down process of membrane potential is a local phenomenon and because of the continuous placement of ion channels on the axon of a neuron it is able to transmit along the axon. Hence, action potential is the major communication component between neurons and/or neurons and

other peripheral structures.

In a few words, an action potential is an electrical pulse that consists of four main temporal events. To begin with, the membrane potential of a neuron has a resting potential at about -70mV, which means that through ion pumps and without any stimulation a neuron can keep steady the electrical currents on its membrane. If a stimulus is applied on a neuron then there are two main outcomes depending on the threshold of the neuron. Usually the threshold of a neuron is about -55mV. The first outcome is the triggering of an action potential if the stimulus is strong enough to overpass the threshold. The presynaptic neuron or neurons, transmit via the neurotransmitters the signal to open the ion gates on the postsynaptic neuron. This causes the excitatory postsynaptic potential (EPSP). If the summation of the EPSPs leads to the overpass of the firing threshold then an action potential rises (rising phase) till it reaches a maximum value-a peak. This peak is usually near +40mV. After the rising phase, follows a falling phase where the potential tends to return back to its initial resting level. Near the end of the falling phase the membrane potential goes below the initial resting potential for a while-a period called refraction period-and after this refraction period it returns back to the resting potential (-70mV). The second outcome is that of a weak stimulus, that is not able to overpass the threshold and hence there is no action potential. The rising phase till reaching the peak is called depolarization and the falling phase is called hyperpolarization, [6, Ch. 6, p. 105], [6, Ch. 7, pg. 125], [6, Ch. 9, p. 140], [2, Ch. 5, p. 87,p. 111]. Furthermore, the duration of an action potential depends on the type of the neuron and the properties of the cell membrane. Typically an action potential lasts for few milliseconds. A schematic of an action potential (or spike or neuron impulse) is depicted in figure 1.3. Depending on the temporal properties of action potentials of a neuron there is one more classification of neurons. There are three different types of neurons, first, the tonic neurons that show sustained responses and continuously generate action potentials, even in the absence of a stimulus. Second, is the bursting (or phasic) neurons, that fire a bunch of action potentials and then they remain mostly silent. Finally, there is the class of fast spiking neurons, that fire at extremely high frequencies and in a tonic fashion.

Neurotransmitter

Neurotransmitters are chemical substances, that participate in the signal transduction between neurons. In order to communicate, two neurons, need to establish and exchange some kind of information, like two persons trying to communicate with each other. In order to establish a communication channel between two neurons, a signal that triggers the initiation of the communication is necessary. This signal is the presynaptic action potential that regulates the gating of calcium and/or potassium presynaptic channels. These channels, in turn, change the ionic currents inside the presynaptic neuron terminal and the vesicles that contain the neurotransmitters are released to the synaptic cleft. Neurotransmitters bind on the postsynaptic membrane receptors of the same kind, promoting an opening of ion channels or triggering second messengers pathways. This results in a generation of an action potential on the post-synaptic cell.

In the CNS, and especially, in the brain there are several different neurotransmitters. The five most important are, first, the glutamate, that is an excitatory neurotransmitter found in the brain and in the spinal cord. Second, acetylcholine is also an excitatory neurotransmitter that binds on muscarinic and nicotinic receptors. Third, dopamine is a very important molecule that plays an important role in a lot of brain functions, such as emotional arousal, motor behavior, motivation and pleasure. A similar chemical substance is the serotonin, which regulates appetite, sleep, mood, memory, learning and other functions. Finally, γ-Aminobutyric acid (GABA) is the most important inhibitory neurotransmitter, [6, Ch. 15, p. 280], [6, Ch. 253, p. 253].

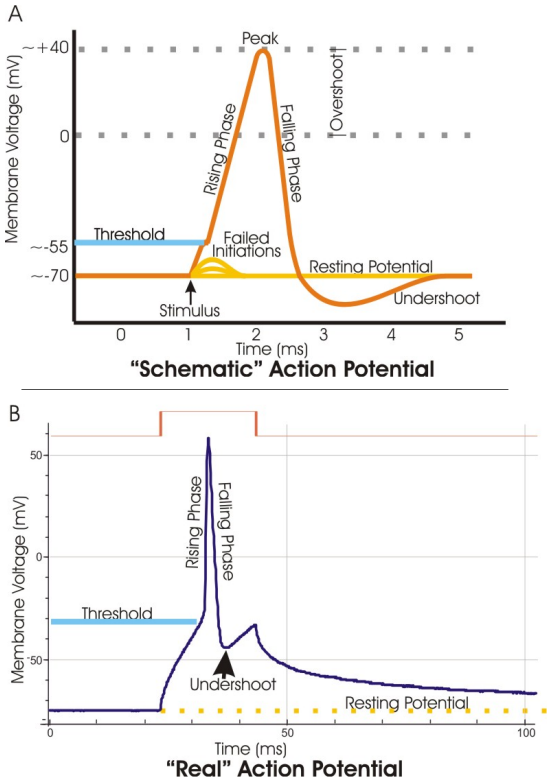

Figure 1.3: **Action potential (spike) schematic representation. A** An artificial spike accompanied by a short explanation of each phase. **B** A real action potential (spike). (Figure from Wikipedia, under a Creative Commons Attribution-Share Alike 3.0 Unported)

Synapse

The synapse is the most important part in the communication of two cells. As it has been mentioned in previous paragraphs, two cells can communicate and exchange information by sending and receiving neurotransmitters. This is a kind of chemical signaling and it takes place in specific parts of neurons. This place is called synaptic cleft. Besides this chemical communication of neurons there is the electrical communication, which is more direct and takes place at the gap junctions. The chemical synapses and the neurotransmitters have been described in the previous

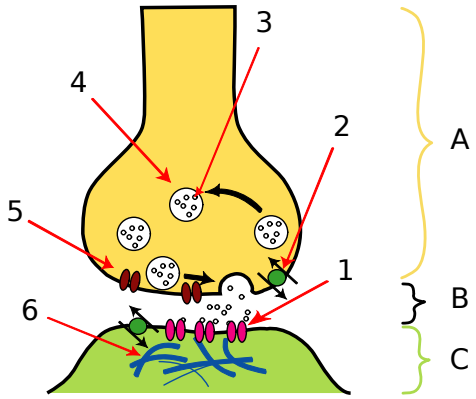

Figure 1.4: **Chemical synapse schematic.** **A** Axon terminal lies on a presynaptic neuron, **B** synaptic cleft, **C** postsynaptic dendrite, **1** postsynaptic receptor where presynaptic neurotransmitters bind and open the gates, **2** reuptake bump of presynaptic cell, that clean up the diffused neurotransmitters, **3 neurotransmitters**, that bind on postsynaptic receptors, **4** presynaptic synaptic vesicle in which neurotransmitters are packed, **5** calcium voltage-gated channels that gated by action potentials and thus they regulate the neurotransmitters release. In some cases there may exist potassium channels. **6** Postsynaptic density, is a protein that is involved in receptors organization. (Figure from by Wikipedia and readapted, under a Creative Commons Attribution-Share Alike 3.0 Unported)

paragraph, and a schematic of a chemical synapse is illustrated in figure 1.4. In contrary, in an electrical synapse pre- and postsynaptic neurons membranes are in touch and can communicate directly by using electrical signals. This electrical charges are in reality ions that pass from the presynaptic cell to the postsynaptic one via the so-called gap junctions. Gap junctions are therefore a special kind of communication channels and because of the direct exchanging of ions they are faster than chemical synapses. The cons of a gap junction is that the transmitted signal cannot be changed, since there is no gain, [6, Ch. 10, p. 177]. In figure 1.5 is illustrated a gap junction.

1.2 Structure of CNS

As it has been mentioned in the introduction of the present chapter the vertebrates nervous system is divided into the central and the peripheral. The present work examines the somatosensory system, which is part of the central nervous system and more precisely the primary somatosensory cortex. The somatosensory cortex is the highest processing center of the somatosensory system and is located at the brain cortex. Brain cortex is just one of the many different structures of the central nervous system. In this section, the structures of the central nervous system are revised

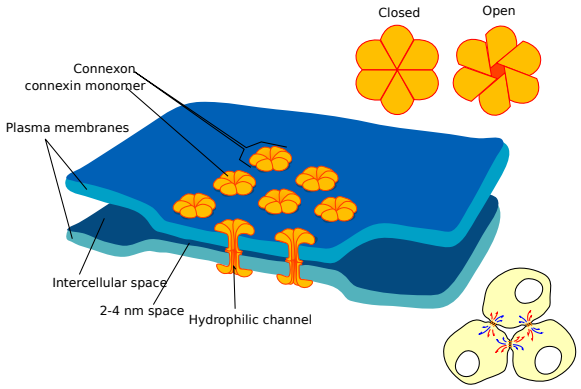

Figure 1.5: **A gap junction schematic.** A gap junction is formed between two neurons membranes and one gap junction can consists of several funnels. Each funnel, in turn, consists of two connexons. Connexos are the hemi-channels, that can be open or closed as it is depicted on the upper right corner. The ionic current flows through the connexons and thus the signal is transmitted from the presynaptic to the postsynaptic cell. Connexons permit also to smaller molecules to pass through. (Figure from Wikipedia and readapted, under a Creative Commons Attribution-Share Alike 3.0 Unported)

and their major functions are described. Moreover, a short description of the neural systems that are hosted in the neocortex follows. The following short description of the structures is based on a review of the two classical textbooks in neuroscience, *Fundamental Neuroscience*, [2] and *Principles of Neural Science*, [6]. Therefore, unless it is stated otherwise, the arguments and the findings are described in the two aforementioned textbooks.

1.2.1 Structures of CNS

Spinal cord

The first structure of the CNS from bottom to up is the spinal cord. Spinal cord is the main place where the motorneurons lie and therefore it plays a very important role in locomotion of vertebrates and in the movement of other parts of the body such as hands. Spinal cord is also the main channel of communication between periphery and brain structures. This means that almost all the signals that must be transmitted to and from periphery pass through the spinal cord. Exceptions are the signals from and to the eyes, the olfactory system and the somatosensory information concerning the head. The spinal cord contains the tracts from motor areas of the brain, which are responsible for motor commands, afferent tracts that convey somatosensory information to thalamus, and also tracts to/from cerebellum and other brain motor areas.

Brainstem

Brainstem is the next structure after the spinal cord and acts as a bridge connecting spinal cord and brain. Brainstem constitutes the main gate of cranial nerves, providing motor and sensory afferent/efferent fibers to the face and neck. Brainstem is very important because all motor and somatosensory tracts pass through it in order to reach cerebellum, cortex and other subcortical structures of the CNS. Moreover, brainstem has a vital role, because of its involvement in the

control of very basic functions of the body, such as respiratory, cardiovascular operation and other significant operations.

Hypothalamus

Hypothalamus is a part of the brain that locates above the brainstem and contains a small number of nuclei (group of neurons and neural networks) that are responsible for metabolic functions of the body and regulation of autonomic nervous system. Moreover, hypothalamus coordinates functions as circadian rhythms and is the orchestra leader of hormones. Therefore is connected to many different parts of the brain.

Pituitary gland

Pituitary gland or hypophysis is an endocrine gland, which sprouts out from the brain as a branch at the bottom of the hypothalamus. However, pituitary gland is not part of the brain and it secretes nine different hormones, that play an important role in homeostasis. Some of the most important functions that are regulated by those hormones are pain relief, temperature regulation, metabolism, growth and blood pressure. Another interesting function is the involvement in the so-called "fight or flight" condition. In this condition, when an animal is in danger it has to decide if it will fight or it will abandon the fight and leave. In such conditions the arc of thalamus-hypothalamus-pituitary-adrenal gland is activated and cortisol is produced. This results in an elevated blood pressure, higher heart rates and generally prepares the body to be engaged in a dangerous situation.

Thalamus

The thalamus is above hypothalamus and is the most important relay station of sensory and motor information from/to brain cortex to/from periphery and other brain structures. Thalamus plays an important role in the visual system since the lateral geniculus nucleus lies on thalamus. Another important function is its participation in somatosensory pathway and in the process of somatosensory information. Because of its vital role in somatosensory processing system, a more comprehensive examination takes place in the next chapter.

Hippocampus

Hippocampus is a part of cerebral cortex and is important for memory consolidation. It promotes the storage of memories passing from the short-term memory to long-term memory. In addition, hippocampus participates in spatial navigation. About memory formation, hippocampus is believed to participate actively in formation of new memories, that are relevant to experienced events, [8].

Basal Ganglia

Basal ganglia is a group of nuclei, that are working synergistically as a unit. The basal ganglia is a group of four major nuclei.

- Striatum, which acts as the input gate of basal ganglia.
- Pallidum, contains two major parts, where inhibitory GABAergic neurons live. The Globus Pallidus internal (GPi) and the Glopus Pallidus external (GPe). GPi projects mainly to the thalamus.

- Substantia Nigra, is also consists of two main parts. The Substantia Nigra reticulata (SNr) and Substantia Nigra compacta (SNc). The former is the main output of basal ganglia, that projects to the thalamus.

- Subthalamic nucleus is an excitatory nucleus (glutamate) and the main function of this nucleus is to excite GPi and SNr.

The anatomical details of the basal ganglia is out of scope therefore they are not mentioned in the present work. Although, the major functions of the basal ganglia is the voluntary motor control, learning habits, procedural learning some cognitive functions, action selection and some emotional functions, [9, 10].

Cerebellum

Cerebellum is an archaic structure present in a lot of organisms. In latin language cerebellum means little brain, which describes perfectly the cerebellum. Cerebellum consists of two hemispheres and it has in addition a cortical structure like the brain. In cerebellum cortex live the most powerful neurons of the CNS, the Purkinje cells. The circuitry of the cerebellum is complex and is out of scope of the present work. Nevertheless, cerebellum is involved in motor control, and it receives strong input from motor structures of the spinal cord and of the brain, [11]. A more modern view of the functionality of the cerebellum has been proposed by Doya in [12]. Doya proposes that since cerebellum consists of different independent modules each module probably acts as a computation unit dedicated to different tasks. Moreover, Doya claims that cerebellum executes supervised learning in contrary to basal ganglia (reinforcement learning) and cortex (unsupervised learning).

1.2.2 The Neocortex (brain cortex)

From a more phylogenetic point of view the most developed structure of the brain of some vertebrates is the brain cortex. As it has been already mentioned the brain cortex follows a major organization according to the two hemispheres. The brain cortex is mainly responsible for high order cognitive functions such as memory, attention, planning, decisions taking/making, language, and consciousness. This paragraph describes the structural and functional organization as well as the main systems of the brain cortex.

Brain cortex structure

The brain cortex or cerebral cortex has a different structure from any other structure of the CNS. It consists of six different layers, each contains different kind of cells and operates different kind of functions. More analytically, the numbering of layers begins from outer part of the brain cortex towards the inner part close to white matter.

- **Layer I (One) or molecular layer**: This is the outer layer and it is consists of a few cells, such as stellate cells. In this layer there are a lot of dendrites of neurons of deeper layers. This layer plays an important role to feedback flux of information.

- **Layer II (Two) or external granule cell layer**: The second layer (sometimes this layer and layer III are considered as one) contains small pyramidal neurons (the main excitatory neurons of cerebral cortex), and stellate cells.

- **Layer III (Three) or external pyramidal cell layer**: is comprised of a vast number of different kind of pyramidal neurons. In this layer as well as in I and II there are the apical dendrites of neurons of layers V and VI. Layers from I to III are the main targets of interhemispheric corticocortical afferents. Layer III is the major source of corticocortical efferents.
- **Layer IV (Four) or internal pyramidal cell layer**: There are granule cells and this layer is the main entry of information from periphery to the cortex via thalamus. Hence, layer IV is the main connection port of the thalamus to the cerebral cortex. Moreover, a vast number of intrahemispheric afferent connections terminates to this layer.
- **Layer V (Five) or internal pyramidal cell layer**: In this layer large pyramidal neurons can be found. In contrary to layer IV, layer V is the main output connection of the cerebral cortex to the outer world. This means that efferent connections to subcortical structures starts from this layer.
- **Layer VI (Six) or multiform layer**: It contains a lot of different types of cells and is the frontier of the cortex with white matter. This layer and layer IV are reached by the basal dendrites of neurons lying in layer III and IV. Layer VI is the main connection of the cerebral cortex to the thalamus by using both excitatory and inhibitory synapses, [13].

There are some exceptions of cortical areas that do not underlie to the aforementioned cortical organization rule. A such area is the agranular cortex (precentral gyrus), which is characterized by an utter absence of layer IV.

In the cerebral cortex there are two major types of neurons, the excitatory one and the inhibitory one. Excitatory neurons are mostly the pyramidal neurons that are large pyramidal-shaped neurons, that use mainly glutamate as neurotransmitter. In contrary to pyramidal neurons, interneurons make inhibitory connections and there are six major types in the cerebral cortex, [14]. Inhibitory neurons use GABA as the principal neurotransmitter.

Another important organization structure of the cerebral cortex is the minicolumn and the hypercolumn. The former is a vertical column running from the outer surface of the cerebral cortex to the white matter. It has a diameter of about $30-80\mu$m and contains about of $80-120$ neurons, [15, 16]. Neurons within a minicolumn respond to more or less the same kind of information. The meaning of hypercolumn was firstly described by Hubel and Wiesel, [17], and it is referred to a collection of cortical columns of different kind of information. In a hypercolumn multiple and adjacent columns communicate with each other via horizontal connections.

Cortical areas

The cerebral cortex is anatomically divided into four distinct lobes, frontal temporal, occipital and parietal. Each lobe contains many different areas each of them is responsible to accomplish different operations and to process different kind of information. For instance, occipital lobe contains the visual cortices, which are responsible for vision. In addition two more areas are the insular and the cingulate cortices. In figure 1.6 are illustrated the four lobes and the anatomical position of each on the brain.

More analytically, the frontal lobe, which is illustrated in blue color in figure 1.6 is the most anterior part of the brain and the most developed part of the brain cortex in humans compared to other mammals. This lobe contains neural networks that are connected with most of the rest of the brain cortex and the subcortical areas of the brain. It has been considered as the key player in high order cognitive functions, such as attention, social behavior, emotions, short-term

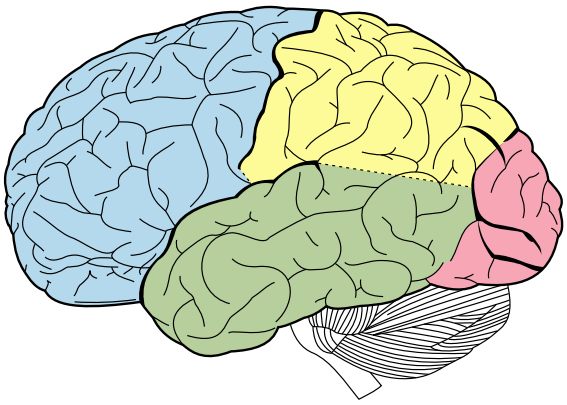

Figure 1.6: **Schematic view of the four brain cortex lobes.** In blue is illustrated the frontal lobe, in green the temporal lobe, in yellow the parietal lobe and in pink the occipital lobe. In addition the cerebellum is depicted in white and black stripes indicating its characteristic anatomical structure. The vertical thick black curve indicates the central sulcus or Rolando fissure and the horizontal one indicates the lateral or Sylvian sulcus. (Figure from Wikipedia and readapted, under a Creative Commons Attribution-Share Alike 3.0 Unported)

memory (e.g. working memory), planning, future actions prediction and forecasting. Frontal lobe also, contains the motor cortex, which is responsible for motor preparation, planning and action.

The temporal lobe plays an important role in the processing of auditory, visual and memory functions. For instance, hippocampus is located in temporal lobe, rendering the temporal lobe responsible for the formation of new memories in cooperation with limbic system. Temporal lobe is also a vital part of language comprehension, since the primary auditory area (responsible for auditory stimuli processing and perception) is located in temporal lobe and Wernicke's area (speech comprehension) is located in temporal lobe, too. Furthermore, temporal lobe, anterior and posterior, plays a very important role in high order visual processing, such as object recognition and perception.

Occipital lobe contains the first stages of the visual system. There is the primary visual cortex (V1) as well as the second, third, fourth and fifth visual cortices. These areas are responsible for seeing and visual information processing and visual perception. For instance, V1 is the most important part of the visual system since it is a highly precision well-defined topographic map of spatial visual information. Another important example is area MT or V5, which is involved in perception of motion.

Finally, parietal lobe contains the associative areas, which integrate sensory information from different sensory areas, such as visual and somatosensory information. An example of a such associative area is the LIP area which combines visual and motor information, playing an important role in oculomotor tasks. Another part of the parietal lobe is the somatosensory cortex, which is responsible for somatic information such as touch, proprioception, nociception and temperature.

1.3 Cortical plasticity

During the investigation of brain over the years, a lot of things and beliefs about its functionality and anatomy have changed. One of the most important hypothesis in neuroscience is the one about the doctrine of brain plasticity. Brain plasticity is, in simple words, the alterations, that can take place over time within the brain. Hubel and Wiesel influenced deeply the belief of neuroscientists, when they publish their article about synaptic plasticity of the visual system, [18]. They claimed that brain visual cortex of cats is plastic only within a time window over their lifetime. This time window is the so-called critical period, and after that period brain is not plastic anymore. This leaded neuroscientists to believe that brain was extremely plastic only at the very early stages of development and over the years it turns into something static and hardwired.

In contrary, today, it is well known that the very strong arguments and ideas of Hubel and Wiesel is not exactly true. It has been shown by many researchers, such as Kaas, [19] and Merzenich, [20] that brain is not static at all. It is now known that brain is prone to continuous learning till the end of its life. Of course the rate of learning is not constant, decaying over years, as it has been shown by several studies on humans, [21].

1.3.1 What is plasticity?

Plasticity is an intrinsic property of the brain. It is one of the most important properties and principles of functionality of the brain in the game of evolution and adaptation. Plasticity is the process by which the brain learns and changes its representations according to experience, environmental and body alterations, physiologic changes. All these operations take place under the scope of genomes entangling also many biological and chemical mechanisms, [22].

During the lifetime of a brain, zillion of trillion of events take place, that affect directly and indirectly the circuitry of the brain and its functionality. At the very early stages of development brain forms synapses and connections. A vast number of these connections will vanish in the future progress of development and other will be enforced. This process leads to a well-shaped formation of brain circuits. In this process, experience plays also a key role, since it promotes the strengthening and the elimination of many connections, leading to the formation of cortical maps, [23, 24, 25]. In addition experience-dependent plasticity promotes development of cortical maps and specific connectivity patterns within brain cortex according to Sur et al., [26].

Brain cortex is composed of many different systems as it has been mentioned in the previous section. Each system contains other subsystems, but the general principle of functionality is the topographic organization. Peripheral organs send information to the cerebral cortex in a topographic way, which means that neighboring places of periphery are represented by neighboring neurons in the cortex. The question, that immediately emerges, is when and how such a topographically organized map emerges? Such a map is built over time and after its formation, it remains dynamic. Cortical neurons after the very first moments of the fetus life in utero have started a competition-cooperation process, which leads to the formation of the topographic maps. Some examples of well-known topographic maps is the primary visual cortex and the primary somatosensory cortex, [20, 27]. Primary cortices are those, who receive input directly from the thalamus (except the olfactory cortex) and the topographic organization is more vivid there than in other higher order cortical areas. Cortical plasticity induces also alterations at the topography of cortical maps in the presence of cortical lesions or loss of sensory information, [19, 28, 29, 30]. More details about cortical plasticity of primary somatosensory cortex will be discussed in the next chapter.

1.3.2 Plasticity over time

Plasticity develops over time and passes through three different phases, roughly speaking. The first phase is the formation and differentiation of neurons, including the migration of neurons to their final positions. The second phase is the so-called critical period. During this period the brain is unmitigatedly plastic and it can learn very rapidly. A lot of complex processes take place during this process. A lot of neural connections die out and other become stronger. During this period sensory input establishes. The third and last period is the adulthood. In this period the brain is still plastic and dynamic but the rate of learning has decreased. Moreover, the brain is able to recover from lesions and it can cope with really harmful situations, [31].

1.3.3 Mechanisms of plasticity

Until now nothing has been mentioned about the underlying mechanisms of plasticity. Plasticity by itself is a very complex process and still today the complete figure of how plasticity works is obscured. In this paragraph some of the very basic plasticity mechanisms are reviewed, starting from the short-term plasticity (synaptic enhancement and synaptic depression) and proceeding to the long-term plasticity (long-term potentiation and long-term depression).

Synaptic enhancement

Synaptic enhancement is a short-term plasticity mechanism, that can be found at the synaptic level. When an action potential arrives at the synaptic terminal of a presynaptic neuron, it triggers a neurotransmitters release according to a given probability. The increase of the releasing probability leads to a temporally enhancement of synaptic strength, [32].

Synaptic depression

Synaptic depression, or synaptic fatigue, has to do with the depletion of the resources of neurotransmitters. Synaptic depression is input-specific, which means that it affects part of the synaptic input of a neuron without altering responsiveness to all inputs of the neuron. This implies according to Abbott et. all [33] a gain regulating mechanism of slow-firing rate afferents.

Long-term potentiation

Long-term potentiation or LTP is one of the two major long-lasting plasticity mechanisms. LTP develops between two neurons, when they are stimulated simultaneously. This coincident activation of neurons leads to an enhancement of synaptic strength, and because of the long-lasting stimulation, LTP involves a lot of cellular mechanisms producing new proteins maintaining the synaptic strength memorized and elevated, [34]. This kind of memory has to do with the remaining calcium quantities at the presynaptic cell, [6, Ch. 14, p. 275]. This residuals of calcium acts as a history record of cell's activity. The LTP mechanism is a candidate mechanism for learning and memories formation in hippocampus, for instance, [35].

Long-term depression

Long-term depression or LTD is the inverse process of LTP. In this case, homosynaptic (refers to a specific synapse and its history of activation) and heterosynaptic (refers to the alterations in synaptic strength because of the activity of other neurons) synaptic strength weakening takes place, [36]. This synaptic strength reduction can last for days, weeks or months. LTD implicates

also complex cellular processes and protein synthesis, such as LTP. LTD is mostly expressed in cerebellum and hippocampus, but it has been found in other brain areas, too. LTD as well as LTP is based on pre- and postsynaptic neurons and is mainly related to the calcium concentrations, [34, 37] and both are experience-dependent.

1.3.4 Hebbian-like plasticity

Hebb theory

In the previous paragraphs the very basic types of plasticity mechanisms were introduced. An important question that emerges directly is how one can obtain plasticity changes in order to learn or to remember. An answer to that question has been proposed by Donald O. Hebb in his book "The organization of behavior" in 1949, [38]. Hebb wrote,

> *When an axon of cell A is near enough to excite cell B and repeatedly or persistently takes part in firing it, some growth process or metabolic change takes place in one or both cells such that A's efficiency, as one of the cells firing B, is increased, (D.O. Hebb, 1949).*

In simple words Hebb described a process of learning, by using the term of associations. This means that if a neuron is active and drive another neuron then strong connections between them can be developed. These connections are nothing more than statistical associations of firing patterns of neurons. This simple learning rule has been used, and is still used, by many researchers in order to describe learning (plastic) processes in the brain. There are several different variations of Hebb rule. One of the most important is the Oja's rule, which is the realization of a need for a stable learning rule. The Hebb rule is not stable and in the presence of a continuously present stimulus can easily run away leading to non-desirable conditions. Oja's rule takes the advantage of normalization and of an anti-Hebb term in order to prevent such run-away condition.

Spike-timing-dependent plasticity

Spike-timing-dependent plasticity or STDP is a learning rule, which is believed to implement experience-dependent Hebb plasticity *in vivo*. STDP is related to the temporal properties of the pre- and postsynaptic neurons and it is engaged to LTP and LTD. It has been assumed that STDP may drive changes in primary visual cortex V1 and in primary somatosensory cortex during sensory deprivations, [36]. STDP acts as the way a Hebbian-like learning rule acts in a specific and short time asymmetric window of milliseconds. The main result of STDP is the temporal correlation of presynaptic arriving spikes with the emitting spikes of postsynaptic neuron, [39]. This means that if a presynaptic spike arrives just before the firing of a postsynaptic spike then that synapses is enforced leading to an LTP. On the other hand if an arrival spike occurs after the postsynaptic one then the synapse becomes weaken, driving an LTD. STDP is applicable on both excitatory and inhibitory synapses.

Is everything about Hebb?

In contrary to Hebbian plasticity and all the so-far known synaptic plasticity mechanisms, such as STDP, there has been mentioned a non-Hebbian synaptic plasticity mechanism, that induces LTD. Recent findings by Rodriguez-Moreno et al. in [40] indicate that there is a special kind of synaptic plasticity that has nothing to do with the Hebbian learning rule. That p-LTD, as it is

mentioned, is a spike pattern dependent LTD (p-LTD) mechanism that is completely independent from the postsynaptic neuron activity. In addition, it engages some different mechanisms rather than the ones that t-LTD (STDP for instance) implicates. In the work of Rodriguez-Moreno et al. they found p-LTD in the barrel cortex of rats, and more precisely in synapses of layer V to layer II/III. Such a remark could lead in the future in new learning rules, that would be able to explain developmental phenomena of the cortex, since p-LTD is present only during the early stages of development.

1.3.5 Homeostatic plasticity

Homeostatic plasticity is a term introduced and firstly described by Gina Turrigiano and Sascha Nelson in [41]. On the one hand homeostasis is a property of a biological system that maintains the internal state of the organism stable and keeps the internal conditions at an equilibrium. On the other hand Hebbian synaptic plasticity is a process that adjusts the synaptic strength according to some learning rules, which may be somehow unstable. Therefore, a mechanism that promotes stability and keeps the average neural activity stable is probably a homeostatic mechanism. Such a mechanism should be able to adjust synaptic strength of a neuron according to the network activity in order to prevent synaptic strength from run away. In [42, 43] a profusion of different synaptic mechanisms has been proposed including among others synaptic scaling, AMPA and BDNF mechanisms.

1.3.6 Metaplasticity

Metaplasticity is another form of synaptic plasticity. It has been introduced firstly by Wickliffe Abraham and Mark Bear in [44]. Metaplasticity relates to the proposition of a biological implementation of balancing mechanisms of Hebbian learning rules. Metaplasticity as homeostatic plasticity is engaged in experience-dependent plasticity. Metaplasticity is the plasticity of synaptic plasticity implying that the synaptic plasticity is indirectly affected by other factors than neurotransmitters, hormones and other substances. It is present when a "priming" activity puts in the game some molecular mechanisms, that in turn regulate the synaptic strength minutes, hours or days after the primary event occured. In simple words experience-dependent modifications of inhibition, dendritic excitability, NMDA receptors function and neuromodulation can affect the future LTP and LTD, [36]. In this sense, one can claim that metaplasticity takes advantage of the history of neuron activity, [45]. Metaplasticity can also be related to Bienenstock, Cooper and Munro model (BCM theory) about visual cortex and orientation selectivity, [46].

1.4 Summary

CNS is the major regulator and controller of the body, since the brain and the spinal cord are the two major components of it. Structures of CNS receive and process information from the outer environment and the body in order to keep the body fully operational within the environment. Spinal cord transmits the signals from and to the brain and takes care of the reflexes. The brain contains a vast number of structures, that process different kinds of information and/or produce different kinds of outputs. The cerebral cortex processes visual, auditory, somatic and other sensations. In the cerebral cortex there are regions responsible for planning, decisions making, speaking (comprehension and production), perception, object recognition, memories, attention and many others. The thalamus provides input to the cerebral cortex, hypothalamus is the main regulator of the very basic functions of the body such as homeostasis. The basal ganglia

participate in the reinforcement learning of motor actions. Cerebellum controls the movements and other cognitive functions. Hippocampus is a huge store of memories (declarative) and it is also involved in spatial navigation.

In the core of each CNS structure the main component is the neuron. A neuron can be considered as a powerful computational device. It can receive, process and transmit information. Each neuron is connected with other neurons via synapses, forming neural networks. Communication between neurons takes place via the transmission of action potentials and the release of chemical neurotransmitters or via gap junctions. Neurons need some kind of support, which is provided by the glial cells. Glial cells take care of neurons nutrients, clean up the dead neurons and aid neurons communications, by forming glial neural networks.

From the beginning of life of a mammal, neurons form neural networks and they start to adapt their synapses in order to establish optimal and proper connections rendering themselves operational. These neural networks can learn over time and this learning is the adjustment of the synaptic strength. This property of the brain to adapt to the stimuli and learn according to experience is called plasticity. Plasticity is expressed by different kinds of mechanisms and has different impacts on different parts of the CNS. For instance, in hippocampus plasticity is expressed by long-term potentiation (LTP) and long-term depression (LTD). Furthermore, most of the plasticity learning rules can be explained by a very simple principle, proposed by Donald O. Hebb. Hebb proposed that neurons that fire together wire together.

Can the brain understand the brain? Can it understand the mind? Is it a giant computer, or some other kind of giant machine, or something more?

(David Hubel,1926-)

2 Somatosensory System and Area 3b

Contents

The somatosensory cortex is the part of the brain cortex that is responsible for the somatosensory information processing. The term somatosensory information embraces four basic types of modalities: touch sensation, temperature, proprioception and nociception. More precisely, touch sensation refers to the information about touch, pressure or vibrations on the skin. Temperature refers to the information about warm and cold stimuli on the skin, proprioception refers to the information about the posture of the body (e.g. angles of joints, muscles tension) and nociception alludes to the information about pain, [2, Ch. 1, p. 581]. The information is conveyed from peripheral receptors to the somatosensory cortex through afferent fibers, in a hierarchical fashion, [47]. In addition, information conveyed to the cortex is not diffused randomly, but it is distributed and organized topographically and according to a modality pattern of cortical organization, [48, 49].

One of the most well-studied functions of somatosensory system is this of touch. Touch sensation is very important in everyday life. Everybody uses this sensation in order to do a lot of

different tasks every day, as for example the perception of different kinds of objects. Therefore, area 3b of primary somatosensory cortex has been chosen in this work to be the neurophysiological model. This means that the computational model captures the basic organization and operations of area 3b of primary somatosensory cortex. The rest of the modalities have been neglected. Hence, in the rest of the chapter, only the touch sensation modality is taken into consideration.

2.1 Organization

2.1.1 Receptors

At the basis of the somatosensory system there are the ganglion cells, which are pseudo-unipolar neurons. Pseudo-unipolar means that they split their axon in two parts in a shape of a T. The target surface can be an external surface (e.g. skin) or an internal surface such as muscles or bones. The second part of the ganglion cell is named the central axon and this part makes synapses with the spinal cord neurons in order to transmit the information to higher order subcortical and cortical areas, [2, Ch. 25, p. 582]. In figure 2.1 is depicted such a pseudo-unipolar cell. Depending on the type of target modality, there exist different types of receptors. In the

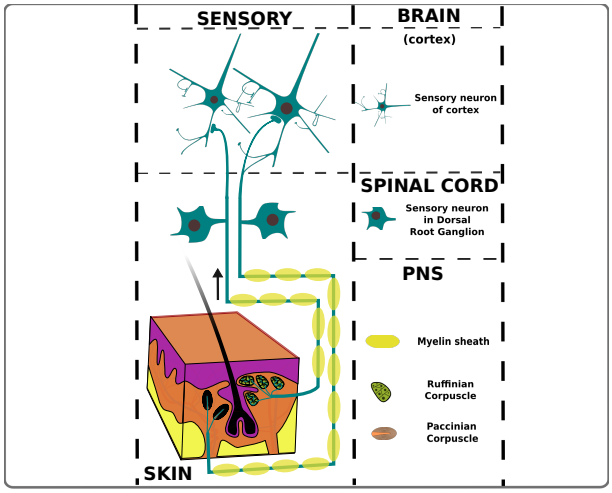

Figure 2.1: **Schematic of somatosensory information flow.** A skin volume is depicted with two out of the four major mechanoreceptors. A pseudo-unipolar ganglion is depicted in navy blue color making synapses with the receptors from one side and with a pyramidal neuron on the other side. (Figure from Wikipedia and reproduced under a Creative Commons Attribution-Share Alike 3.0 Unported)

somatosensory system there are four different types of receptors depending on the modality, touch, temperature, nociception and finally proprioception, [50, 51, 52].

The most important receptors of the somatosensory system are classified in different categories according to the modality they are responsible for. Therefore according to [6, Ch. 22, p. 433] there are seven different types of mechanoreceptors regarding touch and haptic sensation. Four types of thermoreceptors, four types of nociceptors and five types of proprioceptors. Throughout this work only the modality of touch is discussed in full details and therefore from

now and on the discussion about somatosensory system will be restricted to the parts, which are related to touch sensation.

Four out of seven mechanoreceptors lying in the skin are the most important and extensively studied. Each of these four mechanoreceptors is responsible for conveying specific type of information to the upper level of the somatosensory pathway. The distinction of these receptors can be done in two different ways. The first discrimination deals with the type of information they transmit and the second one with the neurophysiology of the receptors themselves, [53].

The information that is transmitted to the upper levels of somatosensory pathway can be related to pressure, texture, flutter, motion skin stretch and vibration, [54]. More precisely, Merkel cells are responsible for pressure, texture and form information, [55, 56]. Meissner corpuscles transmit information about fluttering of skin and motion on the skin. Ruffini corpuscles convey information related to skin stretch and finally Pacinian corpuscles can detect vibrations on the skin, [57, 58]. The aforementioned categorization has been done according to the transmitted

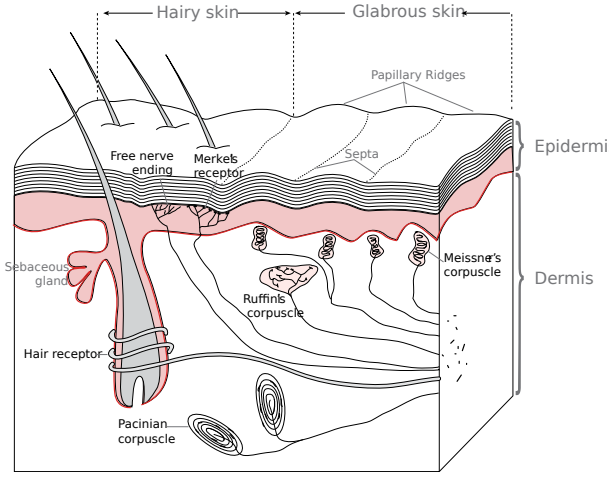

Figure 2.2: **Section of a skin volume.** The four major types of skin mechanoreceptors are illustrated (Merkel cells, Ruffini, Pacinian and Meissner corpuscles). Moreover, their position within the skin volume and their shape are depicted in this figure. (Figure from Wikipedia and reproduced under a Creative Commons Attribution-Share Alike 3.0 Unported)

information from each receptor that also expresses some physiological properties. The most important property is the adaptation rate of each receptor. There are two basic adaptation rates, the slow and the fast, [59, 60]. On the one hand slowly adapting mechanoreceptors respond to a continuous stimulus. They fire continuously and rhythmically as the stimulus is present and the rate of discharge is proportional to the applied pressure caused by the stimulus. On the other hand, rapidly adapting mechanoreceptors respond only on the onset and the offset of the stimulus. Their firing rate is inversely proportional to the pressure intensity. Merkel cells and Ruffini corpuscles are two types of slowly adapting mechanoreceptors, instead of Meissner and Pacinian corpuscles, which are rapidly adapting mechanoreceptors, [61]. In figure 2.2 are illustrated the four different types of skin mechanoreceptors and their position in the skin layers.

2.1.2 Subcortical areas

At the next level of organization of somatosensory pathway there are the subcortical structures. These structures are composed by neural populations (nuclei), which are specialized in the processing of different kinds of information. The somatosensory pathway of touch is divided in two

streams. The first stream reaches cortex through the trigeminal nerve, which conveys information from the face skin and the second one converges to the somatosensory cortex via the dorsal column lemniscal system and transmits information about the skin of the rest of the body, [62, 63]. In figure 2.3 both dorsal column-medial lemniscus and trigeminal systems are illustrated. The

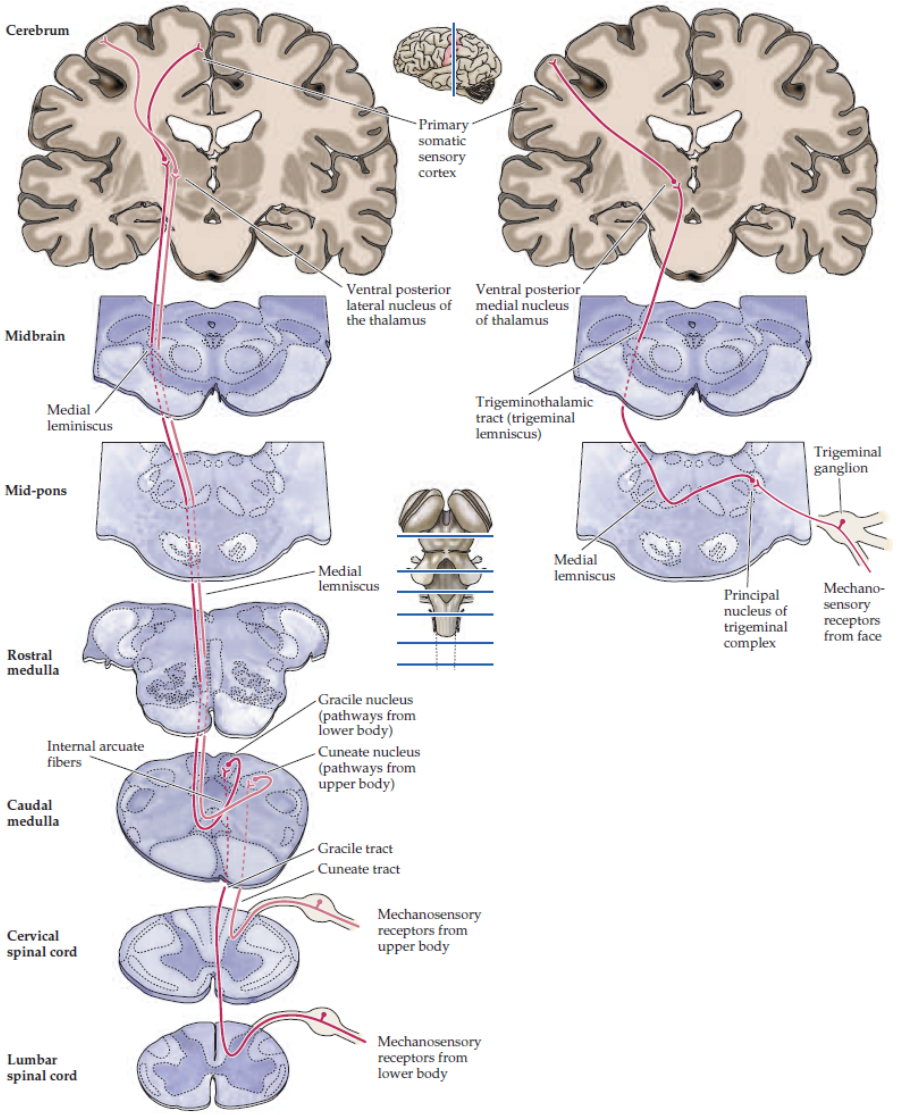

Figure 2.3: **Ascending pathways.** An artistic representation of ascending somatosensory pathways. All the relay stations are indicated from the dorsal root ganglion to primary somatosensory cortex. (Reproduced with written permission by *Neuroscience, 3rd Edition*, [1, p. 201]

flow of information from skin receptors to brain cortex follows a long distance pathway passing through different relay stations. Hence, skin mechanoreceptors transduce the stimulus to firing rate patterns, conveying the information to neuron pools within spinal cord. From spinal cord, information is transmitted to the brain stem and from there to the thalamus till it reaches finally the primary and secondary somatosensory cortices, [64] and [65, Ch. 10, p. 146].

The subcortical areas, which are involved in the transmission of information to somatosensory cortex, starting from the lower level and ascending to the upper level, are the medulla, the pons, the midbrain and the thalamus. In addition the first relay is the spinal cord. Each of these areas has a specific and discrete role in the information processing and conveying. The spinal cord, and more precisely the dorsal column system (DCS) is the first relay station and is the place where the dorsal root ganglion cells live. The root ganglion cells are divided into two major classes. The gracile and the cuneate fascicles. The former is a tract regards information about proprioception from lower limbs and trunk and the latter about upper limbs, and associated truck and neck. Both systems form topographic maps as well as the trigeminal system which is devoted to information originating from face and upper neck, [66, Ch. 8, pg. 103]. At the next level there is the medulla where information crosses the midline, the so-called sensory decussation. After that checkpoint, information travels via the dorsal column medial lemniscal system and the next relay station is the medial lemniscus of pons and midbrain, where neurons receive input from trigeminal nerve, dorsal column, spinal cord and the lateral cervical nucleus. Finally information converges to the thalamus. It is remarkable that throughout this ascending pathway information remains topographically organized. This is more obvious in the thalamic level and even more in the cortical level (see next subsection). This pathway transmits information from mechanoreceptors and proprioceptors. Modality of temperature conveyed by thermoreceptors follows the dorsal horn pathway, [66, Ch. 8, p. 103], [67], [68, Ch. 28, p. 1059]. Thalamus is the last relay station

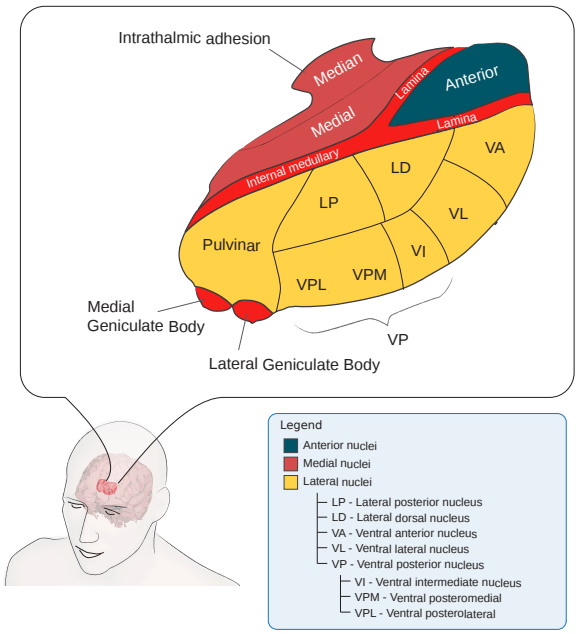

Figure 2.4: **Schematic representation of thalamus and its nuclei.** (Figure from Wikipedia under a Creative Commons Attribution-Share Alike 3.0 Unported)

before information reaches somatosensory cortex. Thalamus is also the most important relay in this pathway in the sense that the information is finely topographically organized, [69]. In figure 2.4 an artistic view of the thalamus is depicted. Two nuclei of thalamus are important in somatic sensory information processing. Both nuclei are part of the ventral posterior (VP) part of thalamus. The first is the ventral posterolateral nucleus (VPL) and the second one is the ventral mediolateral nucleus (VPM). VPL is the part of the thalamus, which is responsible

for haptic sensory information coming from the body and for proprioception information. VPL projects directly to layers III and IV of Broadman areas 3a, 3b, 1 and 2. These areas comprise the primary somatosensory cortex. Moreover, VPL sends some less strong connections directly to the second somatosensory cortex SII. In contrary VPM processes neural information related to face and intraoral structures conveyed by the trigeminal nerve. Between the two thalamic structures VPM and VPL there exists the so-called arcuate lamella, which is a natural frontier made by white matter, [67].

As it has been already mentioned thalamus is topographically organized. Therefore, there are some kind of somatotopic maps, which are neural representations of body parts, who send information to the cortex. Moreover, thalamus has been shown to be plastic and can reorganize its representations in the presence of lesions, for instance sensory deprivations, [70, 71] (see subsections below for more details about lesions and reorganization).

Another interesting aspect, that promotes the topographic organization of the thalamus and of the cortex as well is the notion of dermatomes, [72]. Dermatomes are skin areas enervated by a single spinal nerve. This means that all the receptors within a specific skin area transmit their information to a specific nerve and this in turn conveys that information directly towards the spinal cord and from there to upper hierarchical levels, [73]. In later chapters there will be a more detailed explanation of the dermatomes of the hand since the skin of the palm is the main biological model of this work. Dermatomes are crucial for the further description of the cortical organization itself, because the skin surface of the body is represented in the somatosensory cortex according to the dermatomes and the representation order of dermatomes is reversed at the cortical level, [74]. A schematic illustration of dermatomes can be found in figure 2.5.

2.1.3 Cortical areas

The primary somatosensory cortex is the main convergence side of the somatic information and it can be found in the anterior parietal cortex, posterior of the central sulcus and the primary motor cortex, [75, 76, 77]. In figure 2.7 is illustrated a schematic of the primary somatosensory cortex and its anatomical position. Thalamic afferent fibers converge to the primary somatosensory cortex making synapses at cortical levels III and IV. Both excitatory and inhibitory connections can be found in this feed-forward circuit. The excitatory pyramidal neurons of layer IV receive direct input from the thalamus at a percentage of 15% of the synapses. Although, these synapses are strong enough and express a synchronization pattern, which is able to drive cortical activity and to transmit the proper somatic information to the upper hierarchical levels of somatosensory pathway, [78]. The primary somatosensory cortex or SI is divided into four distinct areas, area 1, 2, 3a and 3b. All four areas receive input from the thalamus and project to other cortical areas and to some subcortical areas such as basal ganglia, anterior pulvinar, spinal cord, the pons and with feed-back connections to the thalamus, [68, Ch. 28, p. 1076]. Each area is committed to process different kind of information and in a topographically organized fashion. For instance, in figure 2.6 a rough schematic of topographic organization of somatosensory cortex is illustrated. Moreover, the so-called perceptive homunculus, [79], is illustrated in the same figure, indicating the cortical representations and the extent of each representation.

Area 3b

This is the most well-known area of primary somatosensory cortex. In figure 2.7 is illustrated the area 3b within SI. Usually area 3b is considered as the primary somatosensory cortex. In this area there is a topographic map of the cutaneous receptors of the body. Anatomically, the

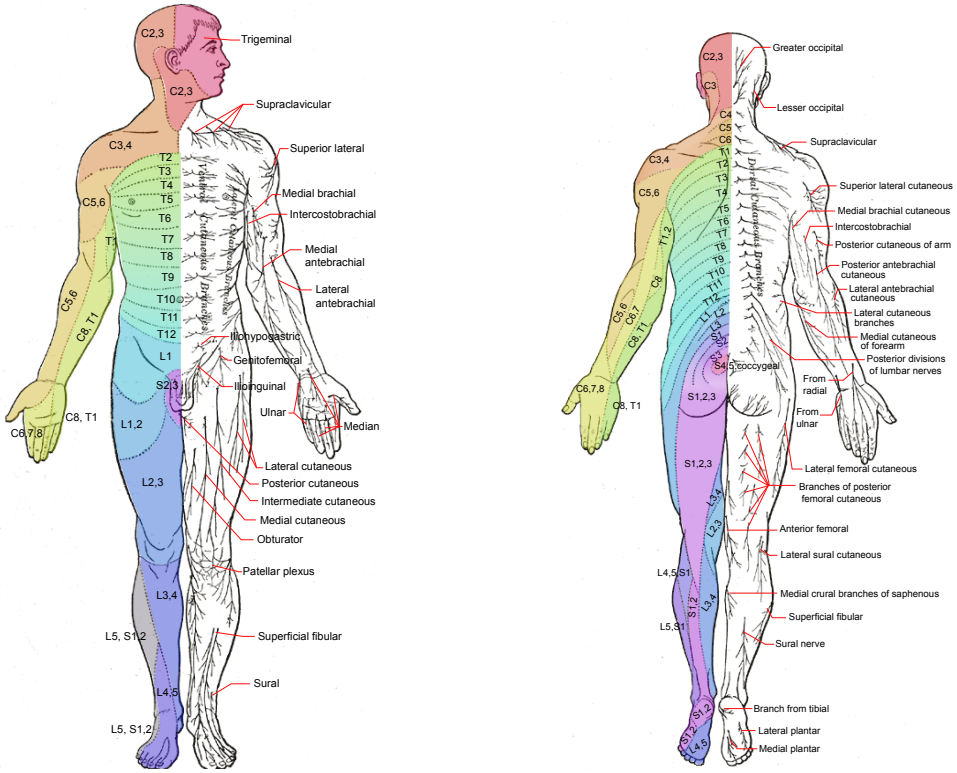

Figure 2.5: **Dermatomes** On the left side is illustrated the anterior dermatomes and on the right side the posterior dermatomes. (Figure from Wikipedia under a Creative Commons Attribution-Share Alike 3.0 Unported)

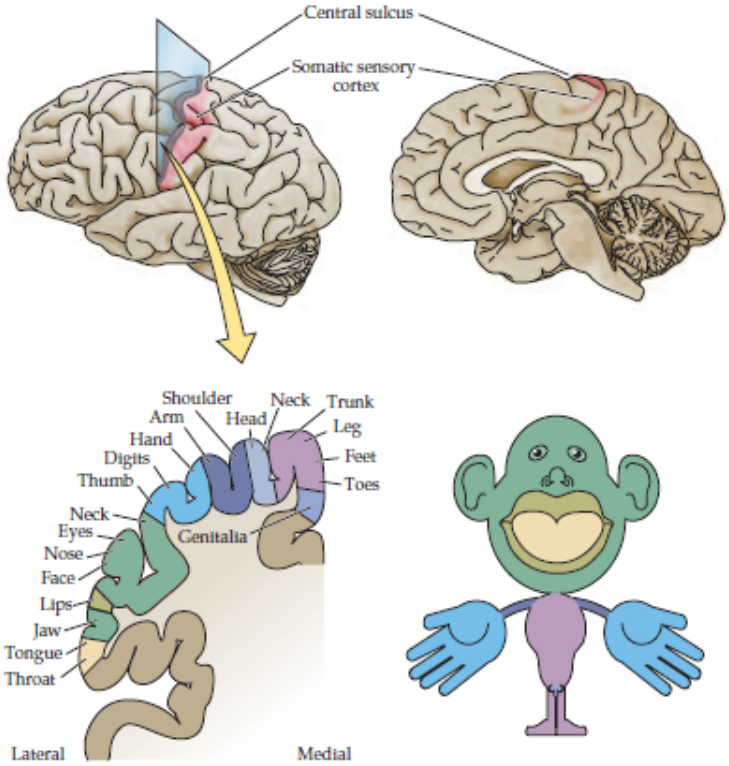

Figure 2.6: **Homunculus.** A schematic illustration of the primary somatosensory cortex (SI), which is located posteriorly of central sulcus. In the lower panel, a homunculus as it has been described by Penfield in [79] is illustrated. (Reproduced with written permission by *Neuroscience, 3rd Edition*, [1, p. 205]

representations of the face and tongue lie on lateral part of the cortex. Representations of foot lie medial, digits of the foot and hand more rostrally and pads of palm and sole of the foot more caudal. Area 3b receives input from thalamus (VPM and VPL) and projects with feed-forward connections to areas 1, 2 and S2. All these three areas project back to area 3b with feedback connections, [77, 80, 81, 82] and [68, Ch. 28, p. 1075]. Moreover, there are feedback connections arising from layer VI of the somatosensory cortex to VP [83]. The receptive fields of neurons of area 3b are typically simple. Simple in a sense that it is composed by an excitatory center and an inhibitory disc around the excitatory center.

Area 3a

Area 3a can be found in the deepest part of the primary somatosensory cortex, as it is depicted in figure 2.7. Neurons of area 3a respond mostly to stimulation of muscle spindles and other deep receptors, [84, 77]. Therefore, neurons encode information about movements and sometimes they are affected by behavioral intentions. The main input of this area is coming from VPS and area 3b, in turn, project to area 2 and to S2, [68, Ch. 28,p. 1076] and [85].

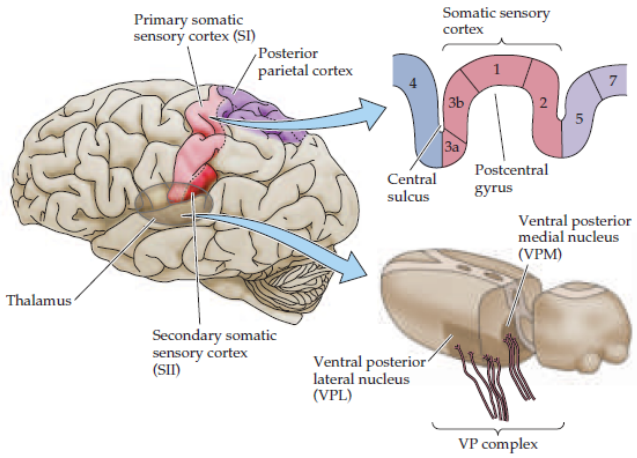

Figure 2.7: **Primary somatosensory cortex.** The four distinct cortical areas 3a, 3b, 1, 2 of SI are also displayed. (Reproduced with written permission by *Neuroscience, 3rd Edition*, [1, p. 204]

Area 1

Area 1 contains a representation of the body surface. This area is next to area 3b and it can be considered as a mirror area of 3b, [86]. This means that the anatomical organization of area 1 follows the one of area 3b. Neurons of area 1 receives mostly information from rapidly adapting receptors and their receptive fields exhibit a typical complex pattern. Receptive fields of neurons of area 1 are also larger than the ones of area 3b, [82]. Some of the neurons have been shown to be affected by the ongoing feature motor behavior following a somatic stimulus. Furthermore, the main input of area 1 is provided by area 3b, VPM and VPL. Neurons of area 1 project directly to area 2 and S2 and receive feedback connections from those areas, [68, Ch. 28, p. 1075].

Area 2

In area 2 there exist a complex representation of the body cutaneous and noncutaneous receptors. Neurons of area 2 have large and complex receptive fields and they respond to certain shapes of objects and movements directions on the skin surface, [87, 88]. Moreover, neurons of area 2 combine information about limb and digit position with tactile information, [68, Ch. 28, p. 1076]. The main input to area 2 is originated from VPS, areas 1, 3a, 3b, primary motor cortex and S2.

2.1.4 A few words about secondary somatosensory cortex

Secondary somatosensory cortex (SII) is a higher order cortical area of the somatosensory system. It was firstly found by Adrian in 1940, [89]. At the beginning Adrian believed that SII exists only in the brain of cats. Later, Penfield et al., [90] showed that SII does exist in the brain cortex of many different primate species including humans. Today is well-known that SII is located at the upper part of parietal operculum and is composed by three main areas. The parietal ventral area (PV), area S2, ventral somatosensory area (SV) and in humans including also areas 40 and 43, [91, 92]. Moreover, SII contains mainly two somatosensory maps of the body surface, in PV and SV. Neurons of these representations have extensively large receptive fields, [93, 94]. Another interesting finding is the involvement of SII in attentional effects. It has been shown, [95], that attention strongly influences the neurons of SII during the execution of demanding haptic tasks.

2.2 Development of somatosensory cortex

Brain development is the most important process of the nervous system. Since the topic of this work is related to the somatosensory cortex, the discussion is limited to the cortical development. Cortical development process can be divided into four discrete phases or periods depending on the age of the organism. Therefore, there is the fetal period where the brain starts forming from the neural plate. Childhood period, which is very important because of the very fast learning rate and the highly plastic abilities of the brain. Then there is the puberty and finally, adulthood. In contrast with what it was originally believed about cortical plasticity and development, according to Hubel and Wiesel [18], it is now known that the brain remains plastic during almost its entire lifetime, [96].

The formation of brain cortex starts from the most anterior part of the neural plate. Neural plate (part of the embryonic ectoderm) initially forms the neural tube and from the telencephalon (anterior part) the brain cortex and the two cerebral hemispheres emerge, [6, Ch. 52. p. 1019] (the description of the whole process is out of the scope of the present work, see the part VIII of [6] for more details). An important part of the brain cortex development is the emergence of topographic maps. Neurons during development migrate to their final positions on the brain according to different chemical signals and they form synapses with each other and with other neurons from spinal cord and via those they connect with the periphery (body parts). Once neurons have locked on their positions and have established their connections, they start to develop specific patterns of activation. These patterns of activity drive, in turn, the self-organization of the topographic maps. Neurons receive input from the periphery and they cooperate and compete with each other in order to take over peripheral representations, [2, Ch. 18. p. 401]. In figure 2.8 are illustrated the different periods of the brain cortex. It is apparent that there are two main distinct periods based on the activity of the neural circuits. The first one is characterized by the absence of activity and is the aforementioned period of neural formation and migration. In this period, synapses start forming and spontaneous activity is present as well, [97]. Then

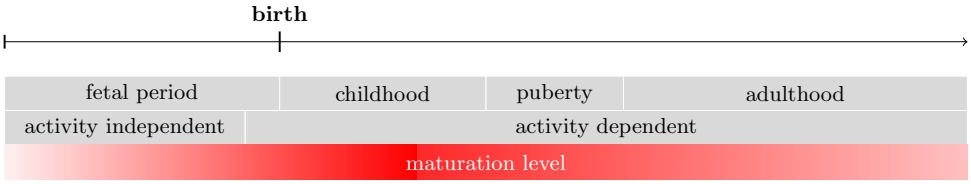

Figure 2.8: **Developmental brain periods.** A time line of the four main periods of brain development.

the second period of development begins. This second period is activity dependent. This means that neurons have already formed the proper synapses and communicate by producing spikes and other forms of signals. Because the most part of neural activity is driven by external stimuli (environmental) it is also called experience-dependent and the plasticity which refers to this period is named experience-dependent plasticity, [98].

It has already been mentioned that spontaneous activity is the first type of activity which is present in the prenatal developing cortex. This kind of activity patterns are present also in the postnatal developing period as it has been shown by different studies, [98, 99, 31]. The significance of the spontaneous activity is its contribution to the initial formation of the somatosensory cortex and it is claimed that it is crucial for the later postnatal development of cortex, [100]. In the case of somatosensory cortex, spontaneous activity has been shown to emerge as spindle bursts, forming a primitive network. This network, later in the development life, of rat promotes the final formation of the topographic maps, [31]. This process has been proposed to be driven by some basic chemical signals and transmitters such as serotonin. More precisely, in the barrel cortex of rats, thalamocortical afferent connections seem to play an important role in the formation of the topographic map. Thalamocortical connections aid the uptake of serotonin (HT-5), that contributes to the synaptic growth, [101].

The aforementioned observed spindle bursts caused by an early motor activity, indicates that motor and somatosensory cortices develop simultaneously. This is in line with neuroimaging data about cortical maturation. Gogtay et al in [21] have conducted an extended and long-term investigation of maturation level, (a schematic is indicated in figure 2.8). The results reveal that primary motor and somatosensory cortices are the first developing cortices. The maturation level increases till roughly the end of puberty and then starts descending. This can also introduce modifications at the level of lateral connections.

During the development of the cerebral cortex, probably the most important period is the so-called critical period. Critical period is a time window in the lifetime of a primate, where the brain is highly plastic, and the columnar and laminar connections of cortical neurons cover a large area of the cortical sheet, [102]. As time passes, the lateral connections and the column size change according to experience and to the thalamocortical connections, which have been formed and fixed earlier (before the critical period) probably because of the spontaneous activity. The key player in the formation of the topographic map and in the shaping of lateral connections during critical period is the experience-driven activity and the balance between excitation and inhibition, [103]. Within topographic maps of somatosensory cortex excitation and inhibition of neurons promote the competition and the cooperation during development. If there is no balance between the two there are some malformation problems in the somatotopic maps. For instance, it has been shown that administering GABA alters the shape of the receptive fields of neurons triggering changes at the topographic level of somatotopic map, [104]. Another characteristic of this balance is the stimulus selectivity of neurons. In [105] authors have shown that the dynamic

properties of excitatory and inhibitory connections are the basic mechanism of the stimulus selectivity.

Concluding, the development of topographic maps in the somatosensory cortex is an extremely complex but highly precise process. The history begins from the genesis of neurons and the migration of them towards their final positions. Then a primitive activity triggers the initial cooperation and competition process among neurons until the critical period. In the critical period, neurons form their receptive fields according to their input and finally the lateral connections reorganized in order to acquire a quasi final shape. The term "quasi" highlights the dynamic nature of the cortical synapses, that are able to adapt themselves under different circumstances depending on the internal and external states of the body.

2.3 Reorganization

Brain cortex as it has been analyzed in the previous sections is a dynamic complex neural network which expresses highly precision operations and is able to adapt to any kind of internal and external changes. For instance, it has been found that in dorsolateral striatum a reorganization takes place during the acquisition and consolidation of a new skill, [106].

In a few words, brain cortex is a plastic material, like the play dough of the children. This means that it can still learn and reorganize itself, during its lifetime. Of course, this does not happen all the time at the same rate. In the adulthood for instance the rate of reorganization is slower than the corresponding rate of learning during puberty. Recently, some works have shown that some subcortical areas, such as thalamus and brainstem, are also subjected to reorganization, [71, 107, 108, 109] and [110].

An interesting and at the same time useful case of reorganization of brain cortex is the one taking place after a cortical lesion or a sensory deprivation. The underlying mechanisms of such a reorganization remain unclear and in some extent unknown. However, cortical neurons can still recover the functionality of the lost cortical territory and replace the dead neurons, keeping the body operational.

2.3.1 Cortical lesion

A cortical lesion is a damage of the cortex, which renders some of the cortical neurons dead or non-functional. Cortical lesions are strokes because of vascular disorders, hematomas caused by traumatic brain injuries, tumors and some other syndromes. Some cortical lesions can also be caused *in vivo* in rats, monkeys, cats or other animal subjects.

In the presence of a cortical lesion a population of neurons usually becomes silent. These neurons represent a skin surface of the body. After a lesion and the death of the cortical neurons the cortical representation of the corresponding skin surface does not exist and is not represented any more. In contrary, the input to the cortex is still present and provides information to the rest of the neurons. This remaining input triggers the competition and cooperation process and some cascade phenomena leading to a reorganization of the SI. Reorganization enables the neurons in the vicinity of the damaged representation to take over the lost functions resulting in new receptive fields of the unaffected neurons. Hence, after a cortical reorganization neurons have learnt new representations.

There is a vast number of studies of cortical lesions in humans and other primates as well. The most common cortical lesion in humans is the vascular disorder such as strokes. Rapp et al. in [111] studied the case of damage of left hemisphere at the level of somatosensory cortex and more precisely the damages were located at the level of hand representation of SI. The

main finding of this study is the reorganization of the non-damaged neurons. These neurons, after reorganization, were able to respond to stimuli from skin surfaces that were previously represented by the damaged cortical area. Furthermore, the localization of the stimulus was not preserved but the detection of the stimuli was normal as before the cortical lesion. Hamdy et al. in [112] investigated the case of cortical lesions at the cortical representation of swallowing motor cortex. In this study the unaffected representation in the undamaged hemisphere was larger after reorganization and recovery. Other studies of cortical reorganization are those provided by Sober et al., [113] and Nishibe et al., [114]. In the former authors studied the changes in receptive fields of cortex using neurophysiological recordings and computational models. In the later, a piece of motor cortex was removed and then the reorganization of the rest of the areas was recorded and studied. In both cases, recordings revealed that the cortex was able to reorganize itself in the presence of a lesion or ablation and the neurons in vicinity took over the input of the damaged representations.

Another important study is the one of Carlson and Burton [115] where both primary and second somatosensory cortices were removed in order to determine the underlying processes of reorganization. After partial removal of SI some of the previous functions were still operable. The ablation of SII leaded to non-significant alterations in the perception of objects size, but a temporary delay in the perception of texture of surfaces.

Cortical reorganization process can also be induced by a pharmacological treatment. This means that a chemical substance is administered to the subjects in a targeted cortical area. Usually, one of those sustances is the muscimol. Muscimol is a $GABA_A$ agonist and therefore can mimic a cortical lesion at the cortical site where it has been injected. Such conditions can also be paired with cortical stimulation in order to study cortical lesions and how reorganization is taking place. Other substances promote the reorganization by increasing the performance of learning as it has been shown by [116]. In some other cases pharmacological administration can lead to faster and better results of recovery after a cortical lesion or an injury, by promoting cortical reorganization, [117].

2.3.2 Sensory deprivation

Sensory deprivation is the loss of sensory information and therefore cortical neurons are not able to receive any kind of somatic information from the deprived skin areas. A possible cause of sensory deprivation is the peripheral nerve damage. Another cause of sensory deprivation is the loss of a body part following an amputation.

More precisely, if a body part is amputated then the skin information of that part of the body is no longer available. Therefore the neurons, that respond to this information are now "orphans". They remain silent for a while but after some time they acquire new inputs because of some cortical mechanisms which activate the reorganization process. The mechanisms are the same as in the case of a cortical lesion.

More precisely, Merzenich and Kaas have shown in their work [118] that after a sectioning of median nerve of owl and squirrel monkeys, reorganization of the primary somatosensory cortex takes place. Digits representations, which are devoted to median nerve, undergo an organization. This means that the unresponsive representations (unresponsive because of the lack of input) become responsive in the presence of other inputs. The possible unmasking mechanism is discussed in the next subsection. In the same flavor, Manger et al. [119] studied the case of a digit amputation on a macaca nemestrina. In this case the representation of digit 2 is under reorganization and at the end of the process of reorganization the stump of the digit is represented in the place of the amputated digit 2. This indicates that the silent neurons because of the amputation,

can reorganize themselves by acquiring new inputs from the unaffected skin areas close to the amputated body part. Jain et al. [120] cut the dorsal column of monkeys and they noticed that after eight months the face representation had covered the whole area 3b, pointing out that the thalamocortical connections are very important for the organization and reorganization of somatosensory cortex. More examples about sensory deprivations can be found in three review works, [121, 122, 123].

The phenomenon of reorganization of subcortical structures is also extremely interesting. As it has been investigated by Florence and Jones in [70] and [71], respectively, thalamus and brain stem are subjected to reorganization to some extent. The reorganization is not so massive as in the cortex but still, these structures are able to reorganize themselves in the presence of an injury or a sensory deprivation. Rosenzweig et al. [124] proposed in their work that the spinal cord is also subjected to reorganization due to spontaneous activity after spinal cord injuries. A more general study about reorganization of somatosensory pathway has been conducted by Faggin et al. in [125]. They studied a large portion of the somatosensory pathway including somatosensory cortex, thalamus and brainstem. They found that all three structures are capable of reorganization following a sensory deprivation.

2.3.3 Underlying mechanisms of reorganization

The reorganization after a cortical lesion or a sensory deprivation is a temporal multi-phase process. The temporal evolution of reorganization can be divided in three or two phases depending on the point of view. Therefore, according to Foeller and Feldman [126] three distinct phases compose the temporal evolution, starting from the unmasking of some previously masking thalamocortical connections. Sensory deprivation, for instance, interrupts the input to some cortical representations resulting in a silence of that cortical representation. Since the affected cortical representation is silent, the excitatory neurons do not fire any more, leading to a reduction of inhibition. This reduction of inhibition reveals the latent and divergent thalamocortical connections. It has been shown that GABA mechanisms can control and affect the shape of the receptive fields of somatosensory cortex, [127]. This disturbance of balance between excitation and inhibition leads to an expansion of the receptive fields of neurons, [27, 128]. In the second phase neurons continue to expand their receptive fields and their activity rebounds, [129]. In the third and last phase the receptive fields undergo shrinkage and the balance of excitation and inhibition reestablishes, [104]. This last phase, especially, when it is considered at the very late stages acts somehow as a somatotopic consolidation, according to [130]. This somatic consolidation leads to a better refinement of the receptive fields of neurons. Some authors prefer to distinct two phases instead of three, such as Florence, Jain and Kaas do in [29]. A boost to the reorganization process could be the naturalistic environments, as it has been claimed in [131]. According to this study caged rats were unable to achieve a good refinement of somatosensory cortex receptive fields instead of naturalistic housed rats, who managed to develop fine receptive fields. This could be useful during humans rehabilitation after strokes, for instance.

2.4 Higher order cognitive functions

As it has been mentioned, so far, brain consists of several different anatomical and functional systems. There are the subcortical systems, the primary cortical systems and there are some associative and higher order centers that integrate information from primary cortical, subcortical and other higher cortical areas. For instance, lateral intraparietal cortex (LIP area) neurons integrate motor and spatial visual information, [132].

Furthermore, there are other areas, mostly lying in prefrontal and frontal cortices, which are involved in the processing of complex behaviors. Some areas of frontal cortex have been proposed to contribute to consciousness, [133]. Moreover, frontal cortex seems to play an important role in the so-called executive functions, [134]. Executive system has to take care of the execution, maintenance and control of high order cognitive functions such as attention, working memory and task switching among others, [135, 136, 137].

So far, the primary somatosensory cortex has been studied, from the perspective of the development of the somatotopic maps to the recovery from cortical lesions and sensory deprivations. In this section another aspect, related to high order functions of the brain, is under investigation. This aspect is the attention and how it can affect the receptive fields of neurons of primary somatosensory cortex. Therefore in the next subsection the implications of attention on primary somatosensory cortex are discussed.

2.4.1 Attention

Attention is a cognitive process that promotes some aspects of one stimulus against others. This means, for instance, that if someone would like to select an object among others, their brains ignore information emitting from the irrelevant objects and promote information relative to the desired object. In somatosensory cortex Hsiao [138] has studied extensively the effects of attention and he with his colleagues have shown that attention is engaged in the modification of RFs of both primary and secondary somatosensory cortices. Similarly, Braun and colleagues [139] have reported such engagement of attention in the primary somatosensory cortex using neuroimaging techniques.

The exact underlying mechanisms of attention are not yet known. There are some hypotheses about the circuitry and the molecular mechanisms that are engaged in attentional modulation of receptive fields of somatosensory cortex, but still there is no definite answer of how attention affects the receptive fields. However, several studies on attention have concluded that the origin of the attentional mechanism most probably involves many different networks from both cortical and sub-cortical brain areas and involves complex chemical mechanisms as well as different higher order cognitive functions such as working memory, planning and prediction.

Sarter et al. in [140] proposed two distinct neural networks, one bottom-up and one top-down, that can be implied in attention. They proposed that an attentional signal may reach the SI through the basal forebrain system after the implication of a more complex network. This latter network has been proposed to be a switching system involving insular cortex, dorsolateral prefrontal cortex, posterior parietal cortex, ventromedial prefrontal cortex, posterior cingulate cortex and anterior cingulate cortex, according to Menon and Uddin, [141]. The main point is that the insular cortex acts as a switch between two different prefrontal networks leading to an attentional effect through saliency occurring in anterior insular cortex. In addition Sarter et al. [140] proposed that a neural network, which engages the basal forebrain corticopetal cholinergic system is probably the origin of the attention affecting SI. Furthermore this cholinergic system is affected directly by the prefrontal cortex and hence it can be considered as an output of the prefrontal cortex to the somatosensory cortices.

It is generally known, that neurons communicate via chemical and electrical synapses. This means that probably attention also affects the chemical communication of the neurons of target area. Juliano et al. [142] found that the cholinergic depletion prevents expansion of somatosensory topographic maps, providing evidence for the involvement of some cholinergic substances such as acetylcholine (ACh) in the alterations of receptive fields of neurons. In addition Tremblay et al. [143, 144] and Rasmusson and Dykes in [145] have shown that the co-activation of

somatosensory cortex (by cutaneous stimulation) and the basal forebrain leads to an enhancement of activity responses of the neurons of somatosensory cortex (in cats). These two different works can provide evidence that acetylcholine, probably is the most suitable candidate for the chemical molecule promoting attentional phenomena.

Besides the studies about neural circuitry and molecular basis of attentional phenomena in somatosensory cortex there are also some other interesting neurophysiological and computational studies such as [146, 147, 148] and [149], respectively, that have revealed strong evidence about attention. According to these works attention affects primary somatosensory cortex in a very specific way. It seems that there is a smart mechanism, which promotes the suspending of the irrelevant aspects of a stimulus by promoting the most interesting ones. This mechanism works directly on the receptive fields of neurons of sensory areas. Therefore, if a stimulus lies on the center of a RF of a neuron, the neuron tends to shrink its RF around the stimulus. Nevertheless, when a stimulus is located close to the center of the RF (but outside of the center) the neuron shifts the RF towards the stimulus position by expanding the RF.

In conclusion, attention is a highly complex cognitive process, that involves several different neural mechanisms, circuits and molecules, due to affect the receptive fields of the target neurons. The receptive fields are modified by attention by virtue of promoting some aspects of the input stimulus/stimuli against some other aspects, which are out of interest.

2.5 Summary

The somatosensory system is responsible for the processing of information related to touch, pain, temperature and body posture. Receptors of different kinds are spread over every squared-inch of the body. Mechanoreceptors convey information from skin towards the somatosensory cortices through spinal cord and thalamus. Thermal receptors transmit information relevant to temperature and nociceptive receptors transduce signals into pain information. In addition, proprioceptive receptors convey information from muscles and joints towards somatosensory cortices in order to provide information to the brain about body posture. This information is vital in the process of movement planning and execution. The somatosensory system is topographically organized. This means that structures such as thalamus, primary and secondary somatosensory cortices contain body topographical organization.

These topographic maps emerge during development. They are formed by a self-organization process driven by experience, postnatal, and to some extent by genetics prenatally. Because the cerebral cortex is highly plastic, it has the ability to reorganize such topographic maps in the presence of a cortical lesion (e.g. strokes) or a sensory deprivation (e.g. limb amputation). These conditions affect directly the organization of the topographic maps and cause dramatic changes in the receptive fields of neurons. Furthermore, other higher cognitive functions such as attention can cause dramatic alterations of receptive fields without causing massive reorganization of the topographic maps.

Conclusions of the first part

In the last decades, in the field of neuroscience, it has been done a big progress. A large part of the nervous system (central and peripheral) of mammals has been investigated. These investigations have helped scientist to understand several biological phenomena that take place in the nervous system. However, a lot of questions remain unanswered, and provoke further research. This has led to the development of new techniques and new branches of neuroscience. Such a branch is the computational neuroscience. Computational neuroscience is the branch of neuroscience that combines mathematics and computer science in order to explain the brain mechanisms and the corresponding neurophysiological data.

This work is focused on the mathematical and computational aspects of the somatosensory cortex. As it has been mentioned in the second chapter, somatosensory cortex is responsible for processing of information related to proprioception, touch, nociception and temperature. This particular cortex is very important and it plays a vital role in other higher order functions of the brain and the body. For instance, the somatosensory cortex plays a crucial role in the generation of movements, since the information for the body posture (proprioception) is processed by somatosensory cortex. Another interesting aspect of the somatosensory cortex is the process of haptic information. Everybody, every day in their lives have to treat with haptic tasks, rendering the somatosensory cortex one of the most valuable parts of the brain.

The somatosensory cortex has been studied extensively. The neurophysiology and the anatomy of somatosensory cortex are well-known and there is a vast number of bibliographic references about them. However, there are plenty of questions that have to be answered. For instance, the underlying mechanisms of the somatosensory cortex reorganization in the presence of a lesion remain largely unknown. Therefore, all those data render the somatosensory cortex one of the most suitable candidates for further studying, mostly by using mathematical and computational models. Moreover, because of the direct connection to the motor cortex and the associative cortices, somatosensory cortex constitutes the beginning for making more realistic models of motion and perception.

In this context, this work is devoted mostly to three different aspects of the primary somatosensory cortex, and more precisely about the area 3b of primary somatosensory cortex. Area 3b is responsible for processing haptic information and lies posterior to central sulcus close to the primary motor cortex. In this area a fine somatotopic map of the body parts can be found, as it has been described by many researchers. The first aspect that the present work is trying to cope with is the formation of this somatotopic map. How a bunch of neurons, receiving information from many different areas of the body can self-organize themselves in order to provide a topographic map of the skin of the body parts.

The second aspect, relates to the maintenance of the cortical representations of body parts over time and how neurons of area 3b can face cortical lesions and sensory deprivations. This means that in the case of a cortical lesion some of the neurons are dead and the rest of the unaffected neurons are able to take over and recover a part of the lost functions of area 3b. In the case of sensory deprivation some of the neurons do not receive input and hence they have to

find new inputs and new skin regions to represent in order to stay alive and useful. In both cases there are a lot of neurophysiological data, but still the underlying mechanisms remain to some extent unknown. Therefore, the model must be able to explain such phenomena and moreover to be capable of reproducing and recovering from such lesions or sensory deprivations.

The third aspect, is the effects of higher order cognitive functions on the area 3b. Such a cognitive process is the attention. Attention, in simple words, is the ability of the brain to suppress non-interesting aspects of an input signal and to promote the interesting aspects. Attention has been extensively studied in the visual system, and there are plenty of computational and mathematical models that can explain some aspects of visual attention. The most interesting part of visual attention, is how attention affects the receptive fields of the neurons. Similar findings have been reported also for the primary and secondary somatosensory cortices. Thus a potential model of somatosensory attention is probably affected by an attentional signal, which modifies the receptive fields according to the neurophysiological data.

In the next part of this work there is an introduction to the very basic mathematical and computational principles on which the model is based. Then the introduction and the description of the model follow and finally the results of the model are set forth.

Part II

Modeling

Introduction

We introduced in the first part of the document the problem of topographic organization. The anatomy, the connections and the functions of area 3b of the primary somatosensory cortex were de- scribed as well as some of the working hypothesis of how self-organization is achieved in the cerebral cortex using known plasticity mechanisms. We would like now to introduce a computational model of area 3b of the primary somatosensory cortex, which aim at explaining how self-organization is achieved through learning as well as the role and the influence of somatosensory attention, which is a lesser known phenomenon. But before diving into the details of this specific model, we would like to explain first why we think a new model is necessary to explain self-organization and why models from the literature may have failed at capturing some important properties. As we explained earlier in this document, the work of Hubel and Wiesel [17] has been very influential in the scientific community and promoted the idea of fixed cortical representations following the post-natal developmental period. It has been thus believed for quite a long time (roughly from the 50's to the late 80's) that the cortex was somehow frozen (or static) after childhood. This drew some dramatic consequences in the computational community since virtually all models of self-organization from this period take great care of reporting static representation at the end of the self-organization. One of the most well-known model is the Kohonen Self-Organised Map (SOM) which was one of the first model to explain computationally the self-organization process. This model has in turn greatly influenced both the neurosciences and the machine learning communities. Today, there exist literally a myriad of variants of this algorithm and virtually all of them ends up with static representation. In this context, the work of Kass and Merzenich [118] came as a shock since their studies provided clear experimental evidences for a massive cortical reorganization after a peripheral nerve injury or amputation in the adult monkey (in the somato-sensory cortex). Their findings have been since confirmed by several other and independent experiments in both rats, monkeys and humans [30]. However, if this is today a known fact in neurosciences, this did not ignite an equivalent revolution in computational modeling. The computational mechanism behind self-organization, self-reorganization and lifelong learning remain to be found. This motivated our research for finding a computational model that would give account on these properties.

Our working hypotheses is that self-organization takes place at the level of the thalamocortical feed-forward connections while lateral connections are believed to drive the competition and regulate the homeostasis of the system in order to keep in balance between excitation and inhibition. In this context, the role of somatosensory attention become prominent since it allows to finely allocate representations where they are most needed. Therefore, we propose a model of area 3b of the primary somatosensory cortex based on the theory of dynamic neural fields. We modeled a region of $1mm^2$ of the index finger glabrous skin, by using 256 receptors quasi-uniformly distributed. This distribution is very close to the distribution of the Merkel's discs mechanoreceptors in the skin layers, which are responsible for touch and pressure modalities. The main core of the model is a dynamic neural field, which describes the cortical dynamics, coupled with an Oja-like learning rule. We adapted the original Amari's neural field equation

and we use a difference of Gaussians for the lateral connections kernel and a linear rectification for the firing rate function. We also use a specific set of parameters such that the dynamic answer of the field reflects to some extent the intensity of the stimulus. Said differently, the maximum of the persistent activity solution (a.k.a. bump) of the neural field is also the maximum value of the input signal. Using such property, we can avoid the use of any explicit distance functions in order to measure the distances between inputs vectors and the codebooks of the model. The model is really unsupervised in the sense that there is no need for a central supervisor to compute the winning unit. Furthermore, the dynamic nature of the neural field offers another benefit. Due to its dynamic nature, the gains of the lateral connections can be modified such as modifying the profile of the solution and make it either wider or thinner compared to the nominal answer. And last but not least, the neural field equation is able to express a dual behavior in terms of solutions. Using the same aforementioned set of parameters, we can obtain a one or two bump solutions by modifying a single parameter. The model has been also coupled with a modified Oja learning rule. It is now known that the Oja learning rule develops associations between pre- and post-synaptic neurons (like a Hebbian learning rule) and regulates the synaptic scaling. The latter is performed through a power term of the Oja learning rule. We propose a new version of the Oja learning rule, which preserves the properties of the original one, but we replaced the power term of synaptic scaling with a more biologically plausible one. The new proposed rule is able to act continuously on the feed-forward thalamocortical connections rendering the model able to learn continuously over time.

The model, when repeatedly presented with random samples, explains the emergence of self-organization of area 3b of the primary somatosensory cortex. Once the so-called "critical period" is achieved, a map of the skin patch is present and topographically organized. Interestingly enough, the learning process leads to the stabilization of the representation while the learning rate (like every other parameters) remain constant. This mean the model is and remains plastic. It can cope with lesions by reorganizing its representations As it was mentioned previously, Kaas and Merzenich foiled the theories about cortical reorganization. They showed that area 3b of the primary somatosensory cortex can handle hazardous conditions such as cortical lesions and/or sensory deprivations. In both cases, the neurons of area 3b have to adapt their receptive fields and to tune their properties to a new condition. This reorganization takes place in three distinct phases (even if some authors mention two). In the first phase there is a silencing of neurons response due to the cortical lesion or to the loss of input. In the second and the third phases, the reorganization actually happens. Previously silent connections become unmasked and active, the axons of the neurons are sprouted in order to capture new inputs and make new connections and finally the new synapses are strengthened and a shrinkage of the receptive fields takes place. We thus decided to cause three different types of lesions (cortical and sensory deprivations) in order to study further how the size of a lesion affects the reorganization and if the locus of the lesion also affects the reorganization. The model copes with all the six lesion cases (three cortical and three sensory deprivations), reorganizing the topographic maps. The main outcome of those experiments is that the balance between excitation and inhibition is critical, and even if the lateral connections do not change, the thalamocortical connections are the prominent side of reorganization.

Self-organization can also be further refined by somatosensory attention. It has been proposed that attention is critical in learning tactile discrimination tasks. However, the two dominant theories of somatosensory attention are somehow contradictory. One the one hand, a part of researchers believe that only intensive stimulation and continuous learning can improve the performance of a subject. On the other hand, some others believe that attention is a critical component such that without attention, nobody would be able to perform demanding tasks.

We think that our model can be used in order to study how attention reorganizes the area 3b and if there is any improvement of the performance when attention is considered. Therefore, we propose an experimental set up, where a region of the skin patch is selected as the attended region, and when a stimulus appears in this region the gains of lateral connections are modified by the attention signal. This can lead to a shrinkage of receptive fields corresponding to the representations of the attended region and to a migration of the rest of the receptive fields towards the attended region. Moreover, the cortical representations can increase their sizes. The experiment consists of three different stages. The first refers to the intensive stimulation, where no attention is required. The second has to do only with attention and the third one is a hybrid of the first and the second ones. We think that a combination of attention and intensive stimulation can lead to a better performance during the execution of a demanding haptic task.

However, even if the model is able to explain data related to the somato-sensory cortex, it is only half part of the whole picture. We got the touch, but we need the body as explained by [150]. This problem refers to the understanding of how the human brain manages to form representations of the body over development and how perception of haptic modalities is developed. In this context, we propose that the present model can be used in a closed loop of sensorimotor integration in order to explain the perception of voluntary movements of fingers and how the brain can perceive and localize a touch on the skin surface. The proposed circuit includes the somatosensory cortex (areas 3a, 3b, 1), motor cortex (M1) and associative areas (area 5).

The second part is organized as follows. The first chapter introduces the theory of dynamic neural fields and the main equation that is used in this work. The second chapter describes the problem of self-organization from a computational point of view and three basic self-organizing maps models are presented (Kohonen, DSOM and LISSOM). In the last chapter the DNF-SOM model is introduced and some simple examples of the model are given. Then the actual model of area 3b is presented as well as all the relevant results concerning formation, maintenance, reorganization and attention.

Number is the ruler of forms and ideas, and the cause of gods and deamons.

(Pythagoras, 570-495 B.C.)

1 Neural Fields

Contents

In the decade of 1950 Beurle introduced in his article [151] a mathematical theory about a mass of cells describing neural populations using nonlinear dynamical systems as a mathematical framework. This theory is the ancestor of the later Wilson-Cowan model. Wilson and Cowan, [152, 153] developed a mathematical model of neural populations. Their model describes two neural populations, one excitatory and one inhibitory with sigmoid firing rate functions. From a mathematical point of view this model is very important since it can be used for studying different kind of mathematical problems such as waves, oscillations, fronts and others. Four years later, 1977, Amari published a very influential article about neural fields. In [154] he introduced a simplified (one equation) model of a neural population. Instead of the Wilson-Cowan dynamical system, Amari's neural field is an integro-differential equation which is able to describe the cortical dynamics.

More precisely, a neural field equation describes the spatio-temporal evolution of the average activity or the mean firing rate of a population of neurons at the cortical level. The Amari's equation is defined on a continuum and is, therefore, continuous in both time and space. Moreover,

such neural field provides a way to understand neural population codes [155] and how activity patterns emerge within the cortex from populations of neurons.

Neural fields are also excellent tools to study activity patterns. Coombes in [156] reviews some of the neural field equation properties, and what kind of behaviors and patterns one can achieve. For instance, bumps, travelling waves, fronts, travelling pulses and Turing patterns can emerge from a neural field. Moreover, breathers can also appeared in a two-dimensional neural field according to Folias et al. [157].

Another approach of neural fields is the one introduced by Markounikau et al. [158], where two interconnected population of neurons are used to analyse the non-linear characteristics of visual cortex activity dynamics. The use of different cortical layers in a model is also an interesting behavior of neural fields as Folias et al. investigate in [159]. In this model a pair of interacting neural fields layers can maintain a persistent bump (i.e. the bump solution is sustained after input removal), while the two layers exhibit different bumps properties.

Stationary bumps are solutions of neural fields of great interest. Such solutions can emerge from a neural field equation using a difference of Gaussians as lateral connections function. The bump solutions have been studied extensively by [160, 161] in the context of working memory and by Faye et al. in [162]. In the present thesis work the stationary bump-solutions can be exploited in order to drive self-organization processes.

1.1 Neurons and neural networks modeling

The goal of computational neuroscience is to investigate the theoretical and computational aspects of neurons and neural networks. As it has been described in the first part, the basic component of the CNS is the neuron. A neuron is a powerful computational unit since it has the ability to receive, process and transmit a huge number of information. Several model have been proposed that describe the function of a neuron and how information is gathered, transmitted and integrated. The simplest model is the one proposed by McCulloch and Pitts in 1943, [163]. According to this model a neuron is a binary device that sums up all the input (one or multiple) and depending on a threshold value, the neuron responds or not. The McCulloch-Pitts model is a completely artificial model and generalizes in a very abstract way the function of a neuron. More modern models of McCulloch-Pitts neurons use non-linearity in order to achieve better and more reliable results. On the contrary, the model provided by Hodgkin and Huxley, [164] is more realistic, since it is based on the neurophysiology of the squid giant axons. The so-called Hodgkin-Huxley model is a system of differential equations, describing the dynamics of currents, conductances and membrane potential producing spikes. A simplification of the Hodgkin-Huxley model is the FitzHugh-Nagumo model, [165]. This is a two-dimensional coupled dynamical system, which is able to mimic the spike generation of squid giant axons.

The next level of modeling is the neural networks. In this level of modeling the model contains from two to many thousands of neurons, interconnected either with a predefined way or a random one. Spiking neurons, are point processes driven by ordinary differential equations (temporal dynamics only). Neural networks can also be formed by interconnected spiking neurons (spiking neural networks). One can find a fully description of spiking neural networks in the book of Wolfram Gerstner, [166].

Another type of neural networks is the firing rate model. These kind of models use different types of neural populations (usually two, one excitatory and one inhibitory), and they can capture the dynamics of the populations describing several phenomena of the brain such as working memory and attention. The firing rate models can be used in order to study both

temporal and spatial phenomena. Such a model is a neural field.

In addition to the aforementioned neural networks, there are a lot of other different types of them. A very old artificial neural network (historically the first one) is the so-called perceptron introduced by Rosenblatt in 1960, [167]. An evolution of the perceptron is the multilayer perceptron (a multi-layer feed-forward neural network supported by a back-propagation learning rule), which is a nice tool used in functions fittings and classification problems as well in prediction problems and error estimations. These models sometimes are also called supervised neural networks since their learning rules need a supervisor (a teacher) in order to update their synaptic strengths. These can be done by comparing the desired output of the network with the actual output of the network.

Another type of neural network is the Hopfield, introduced by John Hopfield in 1982, [168]. A Hopfield neural network is able to form memories and it can be used in storing/recalling spatial patterns. Furthermore, a Hopfield network can be studied analytically in terms of statistical mechanics and an Energy functional can be found explicitly introducing the capacity of the model, [169]. This model belongs to the class of unsupervised neural networks. This means that, on contrary to feed-forward networks, there is no need for a supervisor in order the network to update its synaptic strengths.

In the class of unsupervised neural networks there is also the self-organizing maps. This kind of neural networks can capture the features of the input space and can reduce and compress the input space into a lower dimension. Usually such a network can reduce high dimensional problems to one- or two-dimensional ones. The result of such networks is a topographic map of the input encoded into the synaptic strengths of the network. A well-known self-organizing map is the Kohonen SOM (Self-Organizing Map), introduced firstly by Grossberg, [170] and then by Kohonen, [171].

Stephen Grossberg and Gail Carpenter, developed in 80s and 90s a theory about how the brain processes information by introducing several neural network models that use supervised and unsupervised learning rules. The theory is named ART after the Adaptive resonance theory and a gentle introduction, written by Grossberg and Carpenter themselves, to ART can be found in the book of Michael Arbib, *The handbook of brain theory and neural networks*, [172].

The rest of the chapter is devoted to neural fields and the derivation of the equation that has been used throughout the present work. Neural fields are unsupervised recurrent neural networks and have many different applications as it has been mentioned in the introduction of the present chapter.

1.2 Derivation of neural fields equations

The main idea of neural field is the mathematical description of the dynamics of a neural population. In a neural population there are a lot of different types of cells as it has been described in previous chapters. In this section the analysis provided by Ermentrout in [173] and in Faugeras [174] is followed.

Let k to be the number of populations of neurons, $\mathcal{V}_k(t)$ be the membrane potential of population (average) k at time t. Moreover, the firing rate of each population is given by $\mathcal{R}_k(t) = f_k(\mathcal{V}_k(t))$, where f is a non-linear function usually a sigmoid function.

Assuming that there are two different neural populations which are interconnected, the action potentials from one population to the other can be seen as pre- and postsynaptic potentials, respectively. Let k and l be the two interconnected neural populations. The postsynaptic potential, $\mathcal{P}_{kl}$ is a time function depending on the time that one spike arrives at the synapse and

the time period after that arrival. This can be formulated as $\mathcal{P}_{kl}(t-t_0)$, where t_0 is the arrival time and t is the time after that arrival.

Using the notation of postsynaptic potential, one can extract the average membrane potential of one neural population simply by taking the linear sum of $\mathcal{P}_{kl}$. Therefore, the average membrane potential of population k driven by the presynaptic potentials rising at arrival times t_m from neural population l is given by,

$$\mathcal{V}_k(t) = \sum_{l,m} \mathcal{P}_{kl}(t - t_m). \tag{1.1}$$

Moreover, the firing rate of population k can be predicted by using $\mathcal{R}_k$. This can be done by integrating the arriving spikes over the time. Let assume that the firing rate between within an arrival interval, t and $t + dt$, is given by $\mathcal{R}_k(t)dt$. This leads to the following equation,

$$\begin{aligned} \mathcal{V}_k(t) &= \sum_l \int_t^{t_0} \mathcal{P}_{kl}(t-a)\mathcal{R}_l(a)da \\ &= \sum_l \int_t^{t_0} \mathcal{P}_{kl}(t-a) f_l(\mathcal{V}_l(a))da. \end{aligned} \tag{1.2}$$

Equation (1.2) can be rewritten as

$$\mathcal{R}_k(t) = f_k\Big(\sum_l \int_t^{t_0} \mathcal{P}_{kl}(t-a)\mathcal{R}_l(a)da\Big). \tag{1.3}$$

In order to end up with the derivation of the neural field equations, two assumptions must be made one for each class of equations. The first assumption has been made by Hopfield in [175] and it states that *the shape of the postsynaptic potential is independent of the presynaptic population* and lead to the derivation of the voltage-based model. On the other hand, the voltage-based model is based on a second assumption that states, *the shape of a postsynaptic potential depends on the presynaptic neuron.* The first assumption is formulated as

$$\mathcal{P}_{kl}(t) = \mathcal{W}_{kl}\mathcal{P}_k(t), \tag{1.4}$$

where $\mathcal{W}_{kl}$ is the strength of the postsynaptic potentials and $\mathcal{P}_k(t)$ is the shape of the postsynaptic potential. When the strength, $\mathcal{W}_{kl}$ is positive, population l excites population k and vice-versa. In addition, assuming that the postsynaptic potential is given by the following equation,

$$\mathcal{P}_{kl}(t) = \exp(-\frac{t}{\tau_k})H(t), \tag{1.5}$$

where H is a Heaviside function and τ is a time constant, the following expression emerges,

$$\tau_k \frac{d\mathcal{P}_k(t)}{dt} + \mathcal{P}_k(t) = \tau_k \delta(t). \tag{1.6}$$

This final equation can lead to a system of ordinary differential equations, which describes the dynamic evolution and behavior of a neural population (cortical sheet). Because of the neurophysiology of a cortical sheet one has to take into account the thalamic input. This cause a modification to the differential equations adding an extra term, I. Hence,

$$\tau_k \frac{d\mathcal{V}_k(t)}{dt} = -\mathcal{V}_k(t) + \sum_l \mathcal{W}_{kl} f_l(\mathcal{V}_l(t)) + I_k(t) \tag{1.7}$$

Furthermore, following the second assumption, equation (1.4) turns into

$$\mathcal{P}_{kl}(t) = \mathcal{W}_{kl}\mathcal{P}_l(t). \tag{1.8}$$

And similarly to the voltage-based model and assuming that the activity is given by the equation,

$$V_l(t) = \int_{t_0}^{t} \mathcal{P}_l(t-a)\mathcal{R}_l(a)da. \tag{1.9}$$

one can end up to the following system of differential equations,

$$\tau_k \frac{dV_k(t)}{dt} = -V_k(t) + f_k\Big(\sum_l \mathcal{W}_{kl}V_l(t) + I_k(t)\Big). \tag{1.10}$$

The last step in order to achieve the neural field equation is to take the continuum limit of equations (1.7) and (1.10). By doing this the neural field equations for voltage-based and activity-based models emerge as it is given by the following two equations, respectively,

$$\tau \frac{\partial \mathbf{V}(x,t)}{\partial t} = -\mathbf{V}(x,t) + \int_\Omega \mathbf{W}(x,y)f(\mathbf{V}(y,t))dy + \mathbf{I}(x,t) \tag{1.11}$$

$$\tau \frac{\partial \mathbf{V}(x,t)}{dt} = -\mathbf{V}(x,t) + f\Big(\int_\Omega \mathbf{W}(x,y)\mathbf{V}(y,t)dy + \mathbf{I}(x,t)\Big). \tag{1.12}$$

where Ω is a compact close subset of $\mathbb{R}^n$.

1.3 Amari's Neural Field Equation

The simplest form of a neural field equation is the Amari's equation. Amari in [154] described a one-dimensional neural field equation and its theoretical analysis providing a stationary solution stability proof and a classification of stationary solutions. A two-dimensional case of that equation was firstly analyzed by Taylor in [176]. Since then a lot of studies around neural fields have taken place. More details can be found in two reviews by Coombes, [156] and Bressloff, [177].

The Amari's neural field equation is described by the following equation in one-dimension,

$$\tau \frac{\partial u(x,t)}{\partial t} = -u(x,t) + \int w(x-y)f(u(y,t))dy + h + s(x,t), \tag{1.13}$$

where $u(x,t)$ is the local activity of a population of neurons at position x and time t. τ is the temporal decay synaptic constant, $w(x-y)$ is the synaptic strength of lateral connections between position x and y. Throughout this work the lateral connections, w, are isotropic and homogeneous, which means that $w(|x-y|) = w(x,y)$. $f(u(y,t))$ is the firing rate function, h is the resting potential and $s(x,t)$ is the thalamic input to the cortical sheet (neural population).

In Amari's work the connectivity function, w (or synaptic footprint) is considered to be a mexican hat function. This is because of lateral inhibition, implying a short-range excitation and long-range inhibition. Therefore, neurons close to the center of w form excitatory connections with their neighbors, instead of the remote neurons which form inhibitory connections. Moreover, Amari has done his analysis using as firing rate function $f(u(x,t))$ a Heaviside. In panel A of figure 1.1 is illustrated a Heaviside firing rate function. Panel B displays lateral connections, w, of "Mexican hat" type, and in panel C is depicted a solution of equation (1.13) corresponding to the

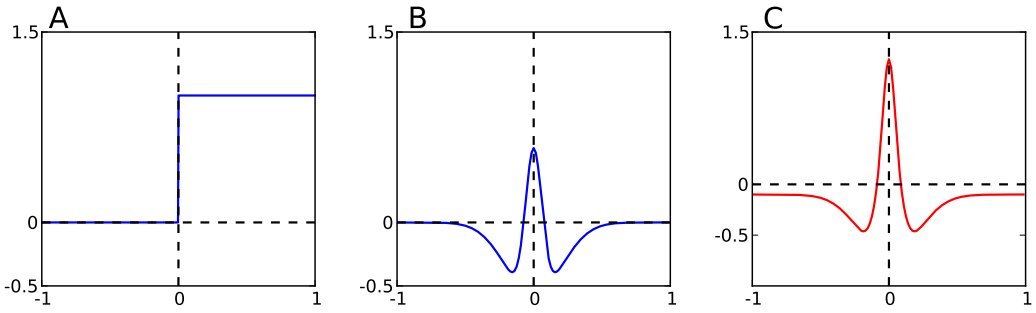

Figure 1.1: **Amari's bump solution**. **A** A Heaviside function, **B** synapses connection strength kernel, **C** solution of equation (1.13)

.

lateral connections illustrated in panel B. Equation (1.13) can be generalized in two-dimensions as,

$$\tau \frac{\partial u(\mathbf{x},t)}{\partial t} = -u(\mathbf{x},t) + \int w(\mathbf{x}-\mathbf{y}) f(u(\mathbf{y},t)) d\mathbf{y} + h + s(\mathbf{x},t), \tag{1.14}$$

Amari in [154] defined some useful mathematical structures by virtue of analysis of equation (1.13). First, the excited region (or excitation region) of a neural field is defined to be

$$R_\theta[u] = \{x \in \mathbb{R}^n | u(x,t) > \theta\}, \tag{1.15}$$

where θ is a threshold. Thus one can define a localized solution by using the definition of excited region. More precisely, a stationary bump solution defined as the excited region of a neural field. This means that a localized solution is a pattern $u(x)$ whose excited region is a finite interval. Moreover, this pattern decays to zero as $|x|$ approaches infinity. Another useful structure is $W(x)$ that is defined by

$$W(x) = \int_0^x w(y) dy \tag{1.16}$$

The localized solution is non-zero only within the excited region, which can be rewritten as $R_\theta[u] = (a_1, a_2)$, where a_1 and a_2 are the two endpoints of the excited region and the length of $R_\theta[u]$ is $a_2 - a_1 \because a_2 > a_1$. Because the neural field is homogeneous, the stationary solution is also translation invariant and hence $R_\theta[u] = (0, a)$. From equation (1.16) it is clear that $W(0) = 0$ and $W(x) = -W(-x)$. Moreover, maximum and minimum values of W are defined respectively by the following two equations,

$$W_m = \max_{x>0} \{W(x)\} \tag{1.17}$$

$$W_\infty = \lim_{x \to \infty} W(x) \tag{1.18}$$

W_m indicates the maximum value of the integral of w ($W(x)$) and W_∞ is the minimum value of $W(x)$. Both values are useful in the characterization of the solutions of neural fields. Moreover, $W(x)$ can be used in order to construct a stationary solution of equation (1.13). This solution is described by the following equation,

$$u(x) = W(a) + h \tag{1.19}$$

All the aforementioned mathematical structures can be used in the following theorem about the characterization of a solution of a neural field. There are three different types of solutions of a neural field according to [154]. The solutions are summarized by the following definition.

Definition 1. *The three different types of a neural field solution depending on the excited region $R[u]$ are defined to be:*

1. $\phi-$**solution** *When $R[u] = \phi$, i.e. there is no excited region, due to $u(x) \leq 0$.*
2. $\infty-$**solution** *When the whole region $R[u]$ is excited.*
3. $\alpha-$**solution** *When a finite interval (α_1, α_2) of the region $R[u]$ is excited.*

The theorem was introduced by Amari in [154] and states that:

Theorem 1. *In the absence of input $s(x,t)$:*

1. *There exists a ϕ-solution iff $h < 0$.*
2. *There exists an ∞-solution iff $2W_\infty > -h$.*
3. *There exists an α-solution (a local excitation of length α) iff $h < 0$ and $\alpha > 0$ satisfies $W(a) + h = 0$*

In order to classify the possible solutions of a Amari's neural field one can use the theorem 1. This theorem has some limitations as for instance the absence of input. It is not applicable in the case where the neural field has also a thalamic input $s(x,t)$. Nevertheless, this problem can be circumvented by following the work of Kubota et al., [178], where the authors examine the case of a one-dimensional neural field with external input, $s(x,t)$. Another interesting work about neural fields solutions is the one by Werner, [179] where the author studies the circular stationary solutions of two-dimensional neural fields.

1.4 Dynamic Neural Field (DNF)

Similarly to Amari's equation (1.13) one can define a new equation of neural field. These equations are named as dynamic neural fields since they exhibit a dynamic behavior. Throughout this work the following dynamic neural field equation is used.

$$\tau \frac{\partial u(\mathbf{x},t)}{\partial t} = -u(\mathbf{x},t) + \alpha \int_\Omega w_l(|\mathbf{x}-\mathbf{y}|) f(u(\mathbf{y},t)) d\mathbf{y} + \alpha i(\mathbf{x},t) + h \tag{1.20}$$

where the cortical domain Ω is a spatial continuum (a subset of $\mathbb{R}^2$), α is a scaling factor, $i(\mathbf{x},t)$ is the thalamic input to the cortical sheet. $w_l(|\mathbf{x}-\mathbf{y}|)$ is the connectivity function of lateral connections. The lateral connections obey the short-range excitation long-range inhibition rule. Therefore,

$$w_l(x) = w_e(x) - w_i(x), \tag{1.21}$$

where $w_e(x)$ is the excitatory part and $w_i(x)$ is the inhibitory one, defined as follows:

$$w_e(x) = K_e \exp\Big(-\frac{x^2}{2\sigma_e^2}\Big) \text{ and } w_i(x) = K_i \exp\Big(-\frac{x^2}{2\sigma_i^2}\Big) \tag{1.22}$$

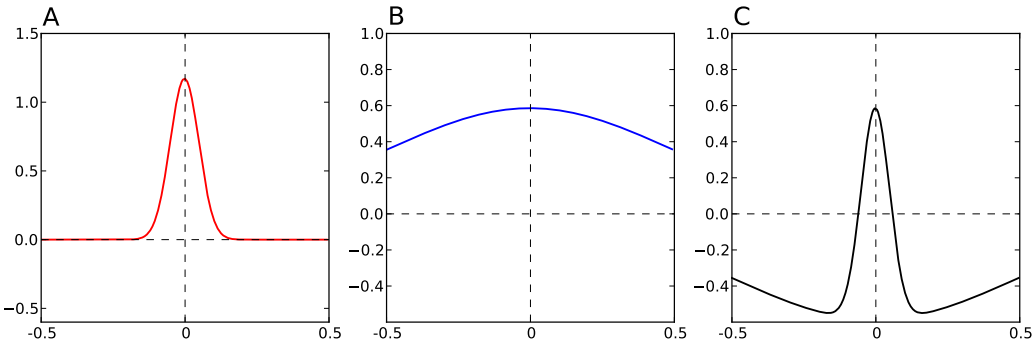

Figure 1.2: **A realization of kernel function A** Excitatory part of kernel, **B** inhibitory part of kernel (see equation (1.22)), **C** the kernel function according to equation (1.21).

with K_e, K_i being the gains (amplitudes), σ_e, σ_i being the variances of the excitatory and inhibitory Gaussian functions respectively, such that generally we consider $\sigma_e \ll \sigma_i$. In figure 1.2 is displayed a realization of the kernel function, w_l. Equation (1.20) is in two-dimensions, similarly one can define the one-dimensional equation. In addition, w_l has the following important properties. w_l is

- an even function, i.e. $w_l(-x) = w_l(x)$,
- positive on an interval $(-x_1, x_1)$, and $w(-x_1) = w(x_1) = 0$,
- decreasing on $(0, x_1)$,
- negative or zero outside of the interval $(-x_1, x_1)$,
- continuous on $\mathbb{R}$ and its integral over $\mathbb{R}$ is finite,
- $\sup_{x \in \mathbb{R}^m} ||w_l(x, \cdot)||_{L^1(\mathbb{R}^m)} \leq C_{w_l}$,
- and finally it has a global maximum at $K_e - K_i$.

Furthermore, the firing rate function $f(x)$ is considered to be a rectification function (piecewise linear function) given by

$$f(x) = \begin{cases} x, & \text{if } x > 0 \\ 0, & \text{if } x \leq 0 \end{cases} \tag{1.23}$$

Salinas et al. [180] have used the same firing rate function in order to obtain some specific behaviors in a model similar to equation (1.20). Furthermore, bump solutions can also be found by using different kind of firing rate functions such as sigmoid function, $\frac{1}{1+\exp(-x)}$ or sigmoid-like functions such as $\frac{x}{\sqrt{1+x^2}}$, $\frac{x}{1+|x|}$, $\tanh(x)$, $\frac{2}{\pi}\arctan(\frac{\pi}{2}x)$.

The integral of w_l over the excited area $R[u]$ can be computed according to equation (1.16) as

$$\begin{aligned} W(x) &= \int_0^x w_l(y)dy \\ &= \int_0^x w_e(y) - w_i(y)dy \\ &= \int_0^x K_e e^{-\frac{y^2}{2\sigma_e^2}} - K_i e^{-\frac{y^2}{2\sigma_i^2}} dy \\ &= \frac{\sqrt{2\pi}}{2}\Big(K_e\sigma_e \text{erf}\Big(\frac{1}{2}\frac{\sqrt{2}x}{\sigma_e}\Big) - K_i\sigma_i \text{erf}\Big(\frac{1}{2}\frac{\sqrt{2}x}{\sigma_i}\Big)\Big) \end{aligned} \tag{1.24}$$

In figure 1.3 is illustrated the $W(x)$ and the values of W_m and W_∞ computed for $w_l(x) = 1.5\text{exp}\Big(\frac{-x^2}{50}\Big) - 0.75\text{exp}\Big(\frac{-x^2}{2}\Big)$. Another important quantity is the integral $\int_\Omega w_l(x)dx$. This

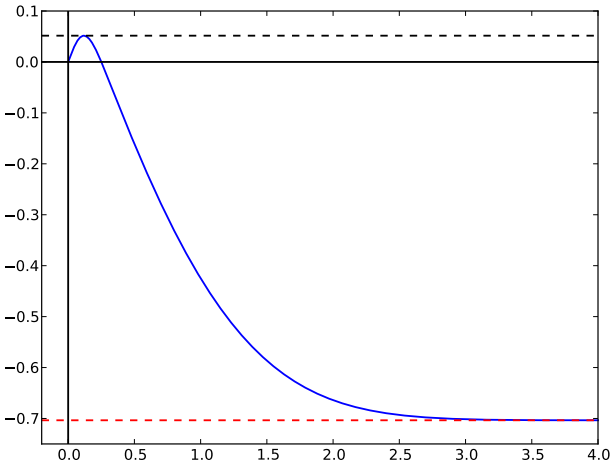

Figure 1.3: **Numerical computation of** $W(x)$**.** The blue curve is the numerical integration of $w_l(x) = 1.5\text{exp}\Big(\frac{-x^2}{50}\Big) - 0.75\text{exp}\Big(\frac{-x^2}{2}\Big)$. The blue dashed line indicates W_m and the red dashed line indicates W_∞.

calculation is useful for the analysis of equation (1.20). Therefore the integrals of w_l for one and two dimensions are given by the following two equations,

$$\int_{-\infty}^{\infty} w_l(x)dx = \sqrt{2\pi}\Big(K_e\sigma_e - K_i\sigma_i\Big) \tag{1.25}$$

$$\int_{-\infty}^{\infty}\int_{-\infty}^{\infty} w_l(\mathbf{x},\mathbf{y}) = 2\pi\Big(K_e\sigma_e - K_i\sigma_i\Big) \tag{1.26}$$

In addition a simple bump solution of equation (1.20) is depicted in figure 1.4. In order to obtain that solution a simple two-dimensional Gaussian function has been applied as input to the dynamic neural field equation, (1.20). Moreover, a theoretical analysis of equation (1.20), such as the one in Amari's equation (1.13), is extremely difficult because of the firing rate function. Therefore, another theoretical analysis must be considered. Hence, in the next section a theoretical analysis of the existence of a solution of equation (1.20) is conducted. In addition a linear stability of the stationary solution has been done in order to define the stability of the solution. The stability of stationary solutions is important in the sense of self-organization. An unstable stationary solution of equation (1.20) would result in an ill-organized map.

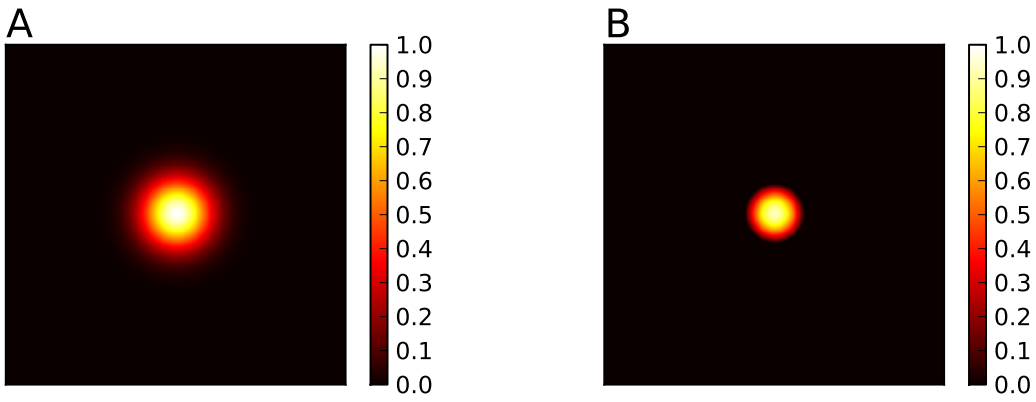

Figure 1.4: **A realization of a two-dimensional neural field. A** Input, $i(\mathbf{x},t)$ of the equation (1.20). The input is a simple Gaussian. **B** The solution of the neural field described by equation (1.20)

1.5 Linear stability of bump solutions

In the previous paragraph the dynamic neural field equation was introduced. In this paragraph, a linear stability analysis according to [181], is being done. In order to proceed to linear stability analysis, the stationary solution of equation (1.20) must be defined. In the following analysis the parameters τ and h are considered equal to 1 and 0, respectively (in order to be in accordance with later simulations). Hence, when $\frac{\partial u(\mathbf{x},t)}{\partial t} = 0$ the stationary solution is given by equation,

$$u(\mathbf{x}) = \alpha w_l(|\mathbf{x}-\mathbf{y}|) * f(u(\mathbf{x})) + \alpha i(\mathbf{x}), \tag{1.27}$$

where $*$ is the spatial convolution. In order to proceed to the linear stability analysis, let $\bar{u}$ be a steady state solution of equation (1.20) and $\phi(\mathbf{x},t)$ be a small perturbation around $\bar{u}$ at time t. Thus, $\phi(\mathbf{x},t) = u(\mathbf{x},t) - \bar{u}(\mathbf{x})$ and hence

$$\dot{\phi}(\mathbf{x},t) = -(\bar{u}(\mathbf{x}) + \phi(\mathbf{x},t)) + \alpha w_l(\mathbf{x},\mathbf{y}) * f(\bar{u}(\mathbf{x}) + \phi(\mathbf{x},t)) + \alpha i(\mathbf{x},t) \tag{1.28}$$

Since the non-linearity is because of firing-rate function, it is replaced by its first order Taylor expansion around $\bar{u}$. Thus,

$$\begin{aligned} f(u) &\approx f(\bar{u}) + f'(\bar{u})(u-\bar{u}) \\ f(u) &\approx f(\bar{u}) + f'(\bar{u})(\epsilon + \bar{u} - \bar{u}) \\ f(u) &\approx f(\bar{u}) + \epsilon f'(\bar{u}) \end{aligned} \tag{1.29}$$

Then injecting equation (1.29) into equation (1.28) one has

$$\begin{aligned} \dot{\phi}(\mathbf{x},t) = &-\bar{u} - \phi(\mathbf{x},t) + w_l(|\mathbf{x}-\mathbf{y}|) * f(\bar{u}) \\ &+ \alpha f'(\bar{u})(w_l(|\mathbf{x}-\mathbf{y}|) * \phi(\mathbf{x},t)) + \alpha i(\mathbf{x},t) \end{aligned} \tag{1.30}$$

Subtracting equation (1.27) from (1.30),

$$\dot{\phi}(\mathbf{x},t) = -\phi(\mathbf{x},t) + \alpha f'(\bar{u})(w_l(|\mathbf{x}-\mathbf{y}|) * \phi(\mathbf{x},t)) \tag{1.31}$$

After the linearization of the original equation around a fixed point a Fourier transform $\mathcal{F}\{g(x,t)\} = \int_{-\infty}^{\infty}\int_{-\infty}^{\infty} g(x,t)e^{-i(\omega x+kt)}dtdy$ is applied on equation (1.31) and the following expression comes

out,

$$\begin{aligned}\mathcal{F}\{\dot{\phi}(\mathbf{x},t)\} &= \mathcal{F}\{-\phi(\mathbf{x},t) + \alpha f'(\bar{u})(w_l(|\mathbf{x}-\mathbf{y}) * \phi(\mathbf{x},t))\}\\ \dot{\Phi}(\omega,k) &= -\Phi(\omega,k) + \alpha F'(\bar{u})\mathcal{W}(\omega,k)\Phi(\omega,k)\\ \dot{\Phi}(\omega,k) &= \Phi(\omega,k)\big(-1 + \alpha F'(\bar{u})\mathcal{W}(\omega,k)\big)\\ \dot{\Phi}(\omega,k) &= \mathcal{L}(\omega,k)\Phi(\omega,k)\end{aligned} \tag{1.32}$$

In equation (1.32) $\mathcal{L}(\omega,k)$ must be negative, by virtue of stability of equilibrium points. Therefore,

$$\begin{aligned}\mathcal{L}(\omega,k) &< 0\\ -1 + \alpha F'(\bar{u})\mathcal{W}(\omega,k) &< 0\\ F'(\bar{u})\mathcal{W}(\omega,k) &< \frac{1}{\alpha}\end{aligned} \tag{1.33}$$

Hence if $F'(\bar{u})\mathcal{W}(\omega,k) < 1$ for each pair of frequencies ω and k then the equilibrium point is stable, otherwise it is unstable. Moreover, because the firing-rate function $f(x)$ is a piecewise linear function according to equation (1.23), its derivative $\frac{df(x)}{du}$ is equal to 1 if $x > 0$ and 0 otherwise therefore for this specific firing rate function and within the excited region of equation (1.20) the relation (1.33) can be written as $\mathcal{W}(\omega,k) < \frac{1}{\alpha}$. This means that if this relation is true then the stationary solution of equation (1.20) is stable around a fixed point.

1.6 Lyapunov Function Analysis

In order to study the stability of a solution of a neural field, one can take advantage of the Lyapunov function analysis. The first use of a Lyapunov function on recurrent neural networks has been done by John Hopfield, in [175]. The main idea is to find a Lyapunov candidate function. A Lyapunov candidate function $\mathcal{E}(x) : \mathbb{R}^n \to \mathbb{R}$ is a positive definite function,

$$\begin{aligned}&\mathcal{E}(0) = 0\\ &\mathcal{E}(x) > 0 \quad \forall x \in \mathcal{B} \setminus \{0\}\end{aligned} \tag{1.34}$$

If its first time derivative is localy negative semidefinite then the equilibrium point of the dynamical system is stable and the system remains close to the origin over time.

However, the aforementioned definition of Lyapunov function has been done for the Hopfield neural network and therefore one has to modify it properly in order to describe the stability of a neural field. Dong, [182], introduced the Lyapunov function as,

$$\mathcal{E} = -\frac{1}{2}\sum_{ij} T_{ij}V_iV_j + \sum_i \int u_i dV_i - \sum_i \int I_i dV_i, \tag{1.35}$$

where V_i is the output of neuron i, T_{ij} is the connection matrix, u_i is the input to neuron i and I_i is the input to neuron i from other cortical layers. Then, derivating equation (1.35) one obtains

$$\begin{aligned}\frac{d\mathcal{E}}{dt} &= -\sum_i a_i \frac{du_i}{dt}\frac{dV_i}{dt}\\ &= -\sum_i a_i g_i^{-1'}\Big(\frac{dV_i}{dt}\Big)^2,\end{aligned} \tag{1.36}$$

where a_i is the positive time constant and $g_i^{-1}(V_i)$ is the monotonic increasing gain function. Therefore,

$$\frac{d\mathcal{E}}{dt} \leq 0 \tag{1.37}$$

$$\frac{d\mathcal{E}}{dt} = 0 \rightarrow \frac{dV_i}{dt} \quad \text{for all} \quad i \tag{1.38}$$

This energy (Lyapunov) function ensures that the system described in [182] converges to a stable state.

The equation proposed by Dong is still in discrete time domain and thus is not suitable for a continuous neural field. Kubota et al. in [183] developed a Lyapunov function for continuous neural fields. Moreover, Owen et al. in [184] and French in [185] use a Lyapunov function for particular equations of neural fields. Hence in order to construct a proper energy function for the equation (1.20) one has to modify all the necessary terms. Thus,

$$\begin{aligned}\mathcal{E} &= -\frac{1}{2}\int_\Omega r(\mathbf{x})\int_\Omega w_l(|\mathbf{x}-\mathbf{y}|)r(\mathbf{y})d\mathbf{y}d\mathbf{x} \\ &\quad -\int_\Omega i(\mathbf{x})r(\mathbf{x})d\mathbf{x} + \int_\Omega hr(\mathbf{x})d\mathbf{x} \\ &\quad +\int_\Omega\int_0^{r(\mathbf{x})} f^{-1}(v)dv \qquad (1.39)\\ &= -\frac{1}{2}\int_\Omega r(\mathbf{x})\int_\Omega w_l(|\mathbf{x}-\mathbf{y}|)r(\mathbf{y})d\mathbf{y}d\mathbf{x} \\ &\quad -\int_\Omega i(\mathbf{x})r(\mathbf{x})d\mathbf{x} + \frac{1}{2}\int_\Omega r^2(\mathbf{x})d\mathbf{x}, \qquad (1.40)\end{aligned}$$

where $r(\mathbf{x},t) = f(u(\mathbf{x},t))$, $f(x)$ is the firing rate function and Ω is the domain of the neural field equation defined in paragraph 1.4. Equation (1.40) described the Lyapunov candidate function for the dynamic neural field described by equations (1.20), (1.22) and (1.23). In the case of equation (1.20) the resting potential equals to zero and therefore the equation (1.39) can be rewritten as

$$\begin{aligned}\mathcal{E} &= -\frac{1}{2}\int_\Omega r(\mathbf{x})\int_\Omega w_l(|\mathbf{x}-\mathbf{y}|)r(\mathbf{y})d\mathbf{y}d\mathbf{x} \\ &\quad -\int_\Omega i(\mathbf{x})r(\mathbf{x})d\mathbf{x} + \int_\Omega\int_0^{r(\mathbf{x})} f^{-1}(v)dv \qquad (1.41)\end{aligned}$$

Taking the time derivative one ends up to,

$$\begin{aligned}\frac{d\mathcal{E}}{dt} &= -\int_\Omega \frac{\partial r(\mathbf{x},t)}{\partial t}\int_\Omega w(|\mathbf{x}-\mathbf{y}|)f(u(\mathbf{y}))d\mathbf{y}d\mathbf{x} \\ &\quad +\int_\Omega \frac{\partial r(\mathbf{x},t)}{\partial t}u(\mathbf{x})d\mathbf{x} - \int_\Omega \frac{\partial r(\mathbf{x},t)}{\partial t}i(\mathbf{x})d\mathbf{x} \\ &= -\tau\int_\Omega \frac{\partial r(\mathbf{x},t)}{\partial t}\frac{\partial u(\mathbf{x},t)}{\partial t}d\mathbf{x} \\ &= -\tau\int_\Omega f^{'}(u(\mathbf{x}))\Big(\frac{\partial u(\mathbf{x},t)}{\partial t}\Big)^2 d\mathbf{x} \qquad (1.42)\end{aligned}$$

And because $f(x) \geq 0$ the candidate energy function is a Lyapunov function since,

$$\begin{aligned} \frac{d\mathcal{E}}{dt} &\leq 0 \\ \frac{d\mathcal{E}}{dt} = 0 \Leftrightarrow \frac{\partial u(\mathbf{x},t)}{\partial t} &= 0 \quad \text{for all} \quad \mathbf{x} \end{aligned} \tag{1.43}$$

This criterion is very usefull in order to control the stability of a dynamic neural field during numerical simulations. In figure 1.6 is displayed the evolution of a solution of a two-dimensional neural field and the corresponding evaluation of energy function according to equation (1.41). At the beginning of the simulation the energy is positive, which means that the system is not near to a stable state. Instead at the end of the simulation and since the neural field has converged the energy function has received a negative value indicating that the system is close to a stable state.

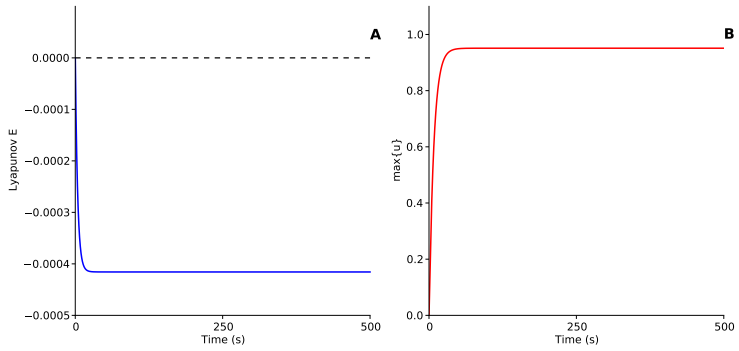

Figure 1.5: **Lyapunov function A** The Lyapunov function values during the numerical solution of equation (1.20). The dashed line indicates the x-axis. **B** The maximum value of the solution of equation (1.20) evolving during the numerical solution.

1.7 Some new DNF properties

In this section three properties of the dynamic neural fields are illustrated. These three properties have been found during the present work and are very important in the self-organization process. The first property has to do with the fitting of the maximum value of the input signal. The second one is related to the dynamic gain modulation. This means that one can adjust the width and the amplitude of a bump solution at the same time and during a simulation by changing one parameter. The last property, is related to the perturbation of a dynamic neural field in order to satisfy two different kinds of solutions. In more details, the DNF solution is either one-bump or two-bumps. All three properties have been tested numerically (experimentally), and the analytical investigation is ongoing.

1.7.1 Neural population dynamics

Dynamic neural fields are able to exhibit different behaviors depending on the connection weight of lateral connections and on parameters. In the present work, the main point is the self-organization and the emergence of topographic maps. Therefore the two-dimensional case of dynamic neural field is the most suitable for modeling the cortical sheet. In this context the activity of the dynamic neural field is used as a driving force for the self-organizing process as it

is explained in later chapters. The level of the activity has to reflect to some extent a measure of the input, e.g. a measure of the distance between the feed-forward thalamocortical connections of the most activated units (i.e. units from the bump) and the current stimulation. Using a specific set of parameters $\mathcal{P} = \{K_e, \sigma_e, K_i, \sigma_i\}$ (which has to be found) the field can achieve the following property: *for any finite input,* $i(\mathbf{x}, t)$ *the maximum activity of the field is almost equal to* $i(\mathbf{x}, t)$. In figure 1.6 is illustrated this property of dynamic neural fields in one- and two-dimensions. In the first panel the input is illustrated, where in the second panel is depicted the solution of equation (1.20). From the third panel it is obvious that the maximum level of excitation relaxes on the maximum level of the input. This third panel is a section profile of the second panel. The one-dimension case is actually similar to the section profile of the two-dimensional case and is displayed in the third panel of figure 1.6.

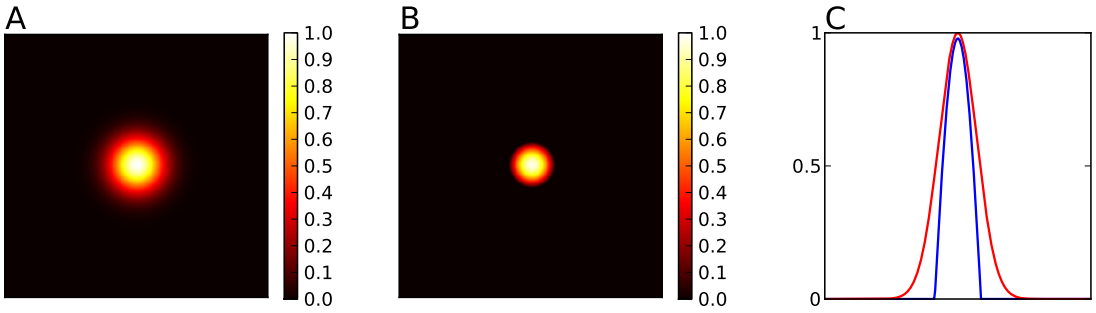

Figure 1.6: **Illustration of population dynamics A** Input to equation (1.20), **B** solution of equation (1.20) which expresses the property of maximum values, and **C** a profile of the solution of panel **B** indicating the match of activity and input highest levels. This is also the one-dimensional case of the property.

1.7.2 Dynamic gain modulation

In the field of signal processing, electronics and in neuroscience as well by the term gain is described the ability of a system to increase the amplitude of its output to a response of an input. In this work the gain is used in order to describe the alterations of excitatory and inhibitory kernels amplitude. And as gain modulation is defined to be any change in the response amplitude of a neuron that is independent of its selectivity or receptive field properties as it has been proposed by Salinas and Thier in [186].

The parameters of a dynamic neural field are of important significance, because they are the driving force of different behaviors of the latter. The gains of the lateral connections of a dynamic neural field are able to alter dramatically the behavior of equation (1.20).

A dynamic modification of the gains K_e and/or K_i of equation (1.20) can result in an increase/decrease of the amplitude of the solution of DNF simultaneously with an increase /decrease of the variance of the solution. This means that by altering the gains on the fly (real-time) during the simulation one can achieve a behavior such the one is illustrated in figure 1.7

1.7.3 The two-face DNF

Another interesting and important property of dynamic neural fields is that by using a specific set of parameters, and therefore a specific type of lateral connections, one can obtain two different kind of solutions from the same equation by modifying only a single parameter. More precisely,

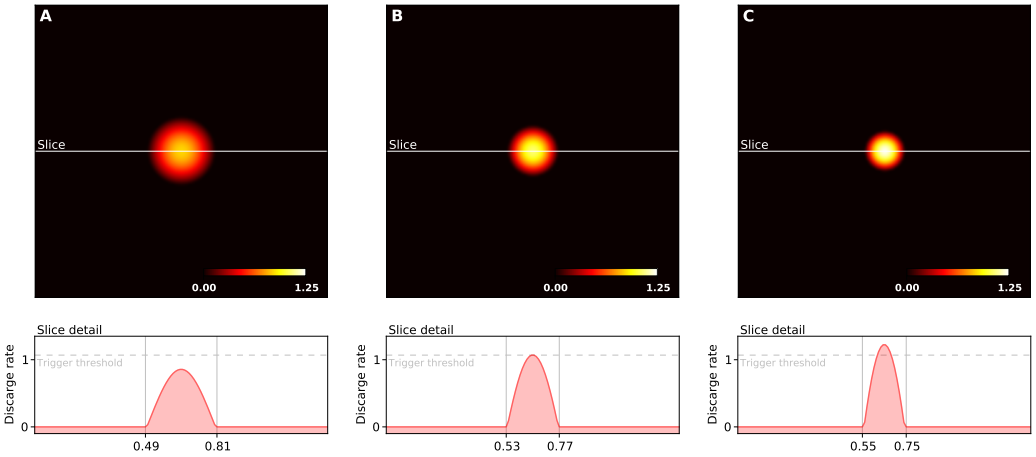

Figure 1.7: **Dynamic DNF gain modulation.** Different bump solution widths and amplitudes depending on the gain of population coupling strengths (excitatory and inhibitory). **A** Low gains are used in order to obtain a wide spreading bump solution of low amplitude, $K_e = 1.5$, $K_i = 0.75$. **B** A higher gain value, $K_e = 3.65$, $K_i = 2.4$ and **C** a more higher value of gains lead to a thiner bump solution and to an increase of amplitude. Here, $K_e = 8.0$, $K_i = 6.08$.

the lateral connections, w_l, must be of the form described by equations (1.21) and (1.22). The parameters $\mathcal{P} = \{K_e, \sigma_e, K_i, \sigma_i\}$ of the DNF must ensure that the lateral connections fade out close to the boundary of the domain Ω. Hence, the solution of the dynamic neural field is either a one-bump solution or a two-bumps solution depending *only* on the parameter K_e. In panel A of figure 1.8 is illustrated the input to the dynamic neural field equation (1.20). In the panels B and C of the same figure the bump-solutions are depicted. In panel B the parameters are $K_e = 6.17, \sigma_e = 0.1, K_i = 4.6, \sigma_i = 0.25$, and in panel C all parameters are the same as in B but $K_e = 5.6$. Hence by changing only one parameter one can end up to two different bump-solutions.

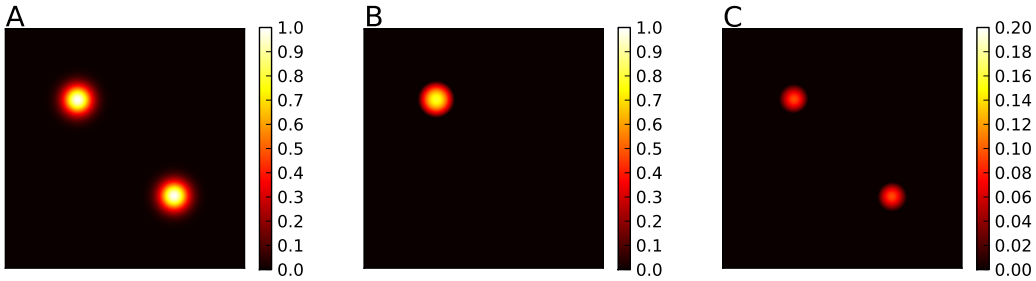

Figure 1.8: **A realization of a two-face DNF. A** Input, $i(\mathbf{x}, t)$ of the equation (1.20). The input is two Gaussian functions. **B** The solution of equation (1.20) for parameters $K_e = 6.17, \sigma_e = 0.1, K_i = 4.6, \sigma_i = 0.25$ and **C** is the solution of equation (1.20) for parameters $K_e = 5.6, \sigma_e = 0.1, K_i = 4.6, \sigma_i = 0.25$

1.7.4 Dynamic neural field parameters

The dynamic neural field that is described by equation (1.20) is characterized by five parameters K_e, σ_e, K_i, σ_i and α. Throughout this work, the variances of the lateral connections (σ_e and

σ_i) remain constants as well as the parameter α. The parameters that are allowed to change are the gains of lateral connections K_e and K_i. In order to find the proper parameters for K_e and K_i a Brute-Force attack method has been used. The width and the amplitude of the DNF

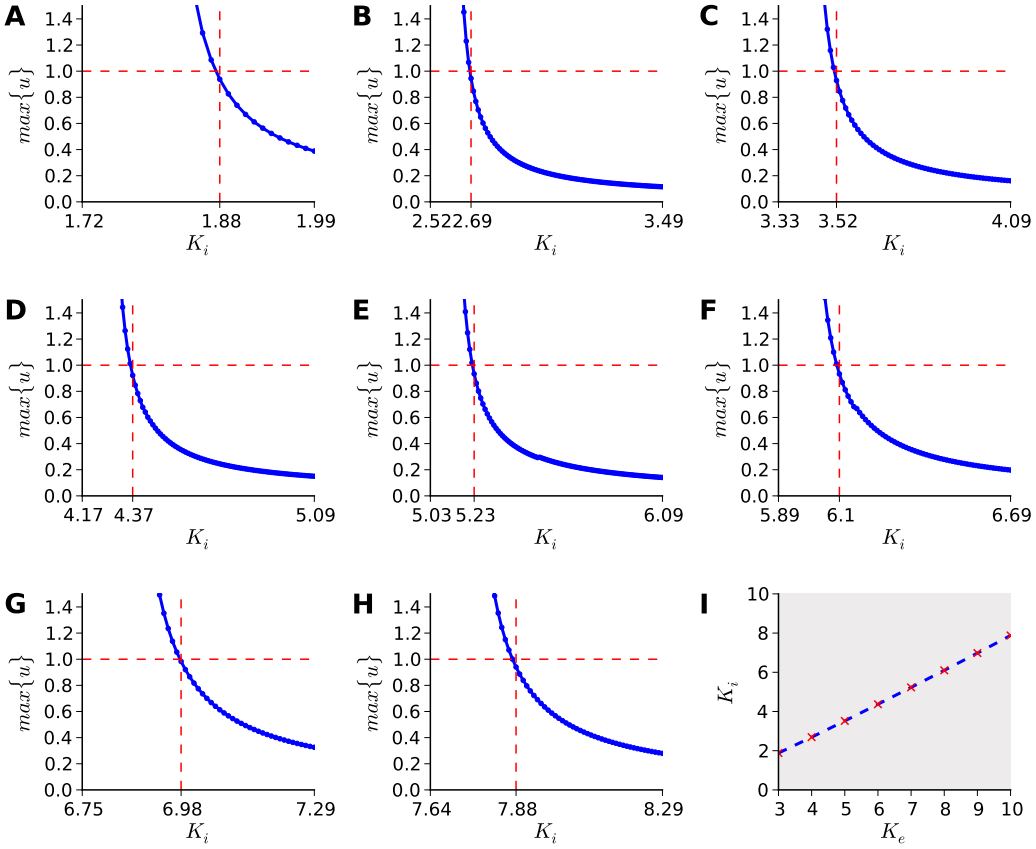

Figure 1.9: **DNF parameters.** In each subfigure K_i is plotted versus $max\{u\}$. The red dashed lines indicate the proper value of K_i for which the maximum activity of the DNF is equal to the maximum value of the input (a two-dimensional Gaussian function with zero mean, variance equals 0.08 and amplitude equals one). **A** $K_e = 3$, $K_i = 1.88$ **B** $K_e = 4$, $K_i = 2.69$ **C** $K_e = 5$, $K_i = 3.52$ **D** $K_e = 6$, $K_i = 4.37$ **E** $K_e = 7$, $K_i = 5.23$ **F** $K_e = 8$, $K_i = 6.1$ **G** $K_e = 9$, $K_i = 6.98$ **H** $K_e = 10$, $K_i = 7.88$ **I** In this subfigure, the values of K_e are depicted versus the values of K_i. A linear relation has been revealed between the two parameters. The crosses indicate the pairs of values (K_e, K_i) for which the maximum value of input is equal to the maximum value of the DNF solution. The thick blue line is the interpolation of those points (cubic splines).

bump solution depend on the values of K_e and K_i as it has been described earlier. Therefore, one has to find the range of values of K_e and K_i for which the aforementioned properties of DNF hold. In this context, the values of K_e have been taken to be in the range $1, 2, \ldots 10$. Hence, one has to find the corresponding values of K_i for which the dynamic neural field converges to a solution (bump) and in addition the property of relaxing its solution to the maximum value of input remains. In addition and according to the theory of dynamic neural field as it has been stated in previous sections, K_e must be greater than K_i. Therefore in order to search for the proper values of K_i one has to start with a fixed value of K_e and a set of values for K_i keeping in mind the inequality $K_e < K_I$. Then for each value of K_i, equation (1.20) has to be solved. If the maximum value of the DNF solution is smaller than a threshold, then that value is stored in

an array (and the corresponding values of K_e and K_i, as well). Hence, at the end of the method, one has three arrays, containing the values of K_e, K_i and $max\{u\}$. In figure 1.9 are illustrated eight realizations of the aforementioned method. The values of K_e are $\{3, 4, 5, 6, 7, 8, 9, 10\}$ and the corresponding values of K_i are depicted in the subfigures. In addition, an interpolation of the pairs (K_e, K_i) has been done by using the method of cubic splines in order to investigate further the relation between K_e and K_i. It is apparent from figure 1.9**I** that the relation between K_e and K_i is linear.

1.8 Summary

This work is mainly based on Amari's neural fields and dynamic neural fields. These integro-differential equations describe the spatial and temporal dynamics of a neural population (or more in the case of coupling equations). Neural fields have different kinds of solutions depending on the kernel and the firing rate functions that they used. For instance, neural fields are capable of producing fronts, travelling waves, oscillators and bumps. Bump solutions are of particular meaning because they can be used in several different cases. One such interesting case is the self-organization process. In addition, a dynamic neural field with a bump solution has some interesting properties. First, it is able to relax its solution at the same level of its input (if the neural field is inhomogeneous) and second, it can accept as a solution one or two bumps by changing only one parameter of the equation without changing anything else in the equation.

The best material model of a cat is another, or preferably the same, cat.

(Norbert Wiener, 1894-1964)

2 Self-organizing Maps

Contents

According to Camazine [187] "self-organization is a process in which pattern at a global level of a system emerges solely from numerous interactions among the lower-level components of the system". These lower-level components are the artificial neurons in the case of self-organizing

maps. A self-organizing map is a kind of neural network which has the ability to organize itself according to the input data. At the end of the self-organization the features of the input space have been learned and each neuron of the network represents a part of the input space.

This topographic organization of the receptive fields of the neurons is a result of both cooperation and competition of each neuron with each other. As the input reaches the neurons they compete with each other in order to approach the input (minimize the distance from the input), and then they cooperate locally in order to share the input properties and features. This lead to the following principle: *"Similar neighboring inputs represented by neighbor neurons"*. Some examples coming from biology are the orientation selectivity of visual cortex (V1), tonotopic organization of auditory cortex and skin topography of somatosensory cortex.

A self-organization process was originally described mathematically in biological systems and morphogenesis by Alan Turing in [188]. The notion of a computational self-organizing map (SOM) was firstly introduced by Teuvo Kohonen in 1982 when he published his seminal article [171]. But the idea of self-organization at that time was not new. At that period Grossberg and Von der Malsburg were working independently on self-organization [189] and [190], respectively. However, it is now more frequent to refer to self-organizing maps as Kohonen self-organizing maps (SOMs). Besides the SOM there are a lot of different versions of this algorithm. In the next sections such a variation of SOM, the DSOM, is discussed.

2.1 The problem of Vector Quantization

In the field of signal processing, the term quantization is the mapping process of a high dimensional data set to a lower dimensional one. Or in simple words, quantization is the process of representing a continuous large set of values by using a finite discrete set of values. For instance, if one would like to quantize the interval of real numbers $[0, 6.5]$ they have to use a finite discrete set, which in this case is $\{0, \ldots, 6\}$. It is obvious that a lot of information has been lost and the noise of the original signal can be inherent to the quantized signal. Furthermore a quantization process is irreversible and non-linear.

A special case of quantization is the Vector Quantization (VQ). The VQ process is used to model a probability density function by the distribution of prototype vectors (or codebooks). This means that any point of the modeled distribution can be represented by a prototype vector, like in the $k-$means method, [191]. In the rest of this chapter the definitions and the notation introduced by [192] are used.

In a more mathematical context, let $f(x)$ be a probability density function defined on a compact manifold $\Omega \in \mathbb{R}^d$, and a VQ be a function $\Phi : \Omega \to X$, where X is a finite subset of n code words, $X = \{\mathbf{w}_i \in \mathbb{R}^d\}_{1 \leq i \leq n}$. A cluster is defined to be $C_i = \{x \in \Omega | \Phi(x) = \mathbf{w}_i\}$ and it forms a partition of Ω. The distortion of the VQ process is defined by the following mathematical formula,

$$\xi = \sum_{i=1}^{n} \int_{C_i} ||x - \mathbf{w}_i||^2 f(x) dx \tag{2.1}$$

If a finite set of observations is known, but the probability density function is unknown, then the distortion given by equation (2.1) can be computed approximately by,

$$\xi = \frac{1}{p} \sum_{i=1}^{n} \sum_{x_j \in C_i} ||x_j - \mathbf{w}_i||^2 \tag{2.2}$$

where x_j is a set with cardinal number p.

2.2 Kohonen Self-organizing Map

Before going further into self-organized maps, it is necessary to provide some definitions and terms.

Definition. *A neural map is a projection $\Phi : \Omega \to N$, where N is a set of n neurons, where each neuron i has a code word $\mathbf{w}_i \in \mathbb{R}^d$ and the set of all the code words is called codebook, $\{\mathbf{w}_i\}_{i \in N}$.*

Definition. *The mapping from Ω to N is a closest-neighbor winner-take-all (WTA) rule such that any vector $\mathbf{v} \in \Omega$ is mapped to a neuron i with the code $\mathbf{w}_\mathbf{v}$ being closest to the actual presented stimulus vector $\mathbf{v}$,*

$$\Phi : \mathbf{v} \to \arg\min_{i \in N}(||\mathbf{v} - \mathbf{w}_i||) \tag{2.3}$$

Definition. *The neuron $\mathbf{w}_\mathbf{v}$ is called the winning element (neuron) and the set $C_i = \{x \in \Omega | \Phi(x) = \mathbf{w}_i\}$ is called the receptive field of the neuron i.*

A self-organized map defines a projection function from one set of any dimension to another regular set usually one- or two-dimensional. The resulting map (the projection) must be ordered and more precisely, it must be topologically ordered. This means that the code words must preserve an analogy to the input ordering keeping the information of the input signal as invariant as possible. In simple words, the topology of the input defines a neighbor relation of the code words. Hence, neighbor code words must represent similar inputs.

2.2.1 The Kohonen self-organizing map

In 1982 Teuvo Kohonen in [171] introduced the so-called SOM. SOM was the first self-organized map neural network and was firstly introduced in order to visualize distributions of metric vectors. The SOM was based on the previously works of Stephan Grossberg, Shun-ichi Amari and Christoph Von der Malsburg.

Definition. *A SOM is a neural map equipped with a structure (usually a hypercube or hexagonal lattice) and each element i is assigned a fixed position $\mathbf{p}_i \in \mathbb{R}^q$, where q is the dimension of the lattice (usually 1 or 2).*

SOM as already mentioned is an artificial neural network, which is able to compute projections from a large input data set to a smaller regular finite set (code words). This process of mapping can be done using an unsupervised learning rule that can train the neural network and succeed to self-organize the code books according to the input vectors. The learning process is an iterative one and it starts from an initial time $t = 0$ and ends when iterations reach the final time $t = t_f \in \mathbb{N}$. During the iterative learning process the input vectors $\mathbf{v} \in \mathbf{\Omega}$ are sequentially presented to the map with respect to the probability density function $f(x)$ at each time step t. Then equation (2.3) is applied. This means that the distance between the code words and the input is measured according to a distance function. The distance function can be defined by the Minkowski formula. Hence, let $\mathbf{x}, \mathbf{y} \in \mathbb{R}^d$.

$$d(\mathbf{x}, \mathbf{y}) = \Big(\sum_{i=1}^{n} |x_i - y_i|^r \Big)^{\frac{1}{r}} \tag{2.4}$$

One can notice that from the Minkowski distance one can derive other distance functions for specific values of r. Therefore, for $r = 2$ the Euclidean distance is derived and for $r = 1$ the Manhattan distance.

Once a distance has been defined and it has been used within equation (2.3) a winner neuron, $s \in N$, can be found. This means that there is a neuron for which its distance from the input vector $\mathbf{v}$ presented at time t is the minimum. The winner neuron s is the one that defines the update of all the codes $\mathbf{w}_i$, in a neighborhood $V_{d(\mathbf{x},\mathbf{w}_s)}(\mathbf{w}_s; t)$, by shifting all of them towards input vector $\mathbf{v}$ according to the following relation,

$$\Delta \mathbf{w}_i = \epsilon(t) h_{\sigma(t)}(t, i, s)(\mathbf{v} - \mathbf{w}_i) \tag{2.5}$$

where $\epsilon(t) : \mathbb{R} \to \mathbb{R}$ is a time function describes the learning rate of the learning process, $h(t, i, s)$ is the neighbor function that depends on the time and the winner neuron as well as its index. Finally, $\sigma(t) : \mathbb{R} \to \mathbb{R}$ is the width of the neighborhood function. These three functions are defined respectively as,

$$\epsilon(t) = \epsilon_i \Big(\frac{\epsilon_f}{\epsilon_i}\Big)^{\frac{t}{t_f}} \tag{2.6}$$

$$h(t, i, s) = \exp\Big(- \frac{||\mathbf{p}_i - \mathbf{p}_j||^2}{2\sigma(t)^2}\Big) \tag{2.7}$$

$$\sigma(t) = \sigma_i \Big(\frac{\sigma_f}{\sigma_i}\Big)^{\frac{t}{t_f}} \tag{2.8}$$

In the aforementioned equations ϵ_i and ϵ_f are the initial and final learning rate respectively. σ_i and σ_f are the initial and final neighborhood width, respectively. In addition, the following must be held, $\epsilon_f << \epsilon_i$ and $\sigma_f << \epsilon_i$. The learning rate function as well as the neighborhood width function can be linear or exponential monotonically decreasing. But the learning rate can also be kept constant during the training process. In both cases a convergence can be achieved at least for the one-dimensional case of Kohonen SOM, as it has been proved mathematically. All the necessary theorems can be found at the article of Fort, [193]. In panel 2.1 there is an algorithmic description of Kohonen SOM.

Algorithm 2.1 Kohonen Self Organizing Map Algorithm

Require: $t_f, n, \sigma_i, \sigma_f, \epsilon_i, \epsilon_f, \Omega$.
Ensure: Codebook $\mathbf{w}$.

```
w ← rand()
for t = 0 to t_f do
    Select randomly an input vector v ∈ Ω.
    s ← arg min_n d(v, w_i)
    for i = 0 to n do
        σ(t) ← σ_i (σ_f/σ_i)^(t/t_f)
        ε(t) ← ε_i (ε_f/ε_i)^(t/t_f)
        G ← h_σ(t)(t, i, s)
        Δw_i ← ε(t) G (v − w_i)
    end for
end for
```

2.2.2 Error of the Kohonen SOM

In computer science and in the field of VQ, the performance of a VQ algorithm is measured in terms of distortion (see equation (2.1)). One known VQ algorithm is the k-means. This

algorithm is pretty much the same as the SOM algorithm, but the topology. The k-means algorithm receives as input a collection of observations of n dimensions each and clusters them into k, $k \leq n$ sets S. The classification process obeys the minimization of,

$$\arg\min_{s} \sum_{i=1}^{k} \sum_{\mathbf{x}_j \in S_i} ||\mathbf{x}_j - \mu_i||^2 \tag{2.9}$$

where μ is the mean of points in S_i. One can observe that $k - means$ and Kohonen SOM have in common the minimization of a distortion measure and every time there is a distance between the input vectors that it has to be computed. The main difference is the lack of topology in the case of $k - means$ instead of SOM, where the codebooks are aligned on a predefined grid and the topology remains even after the convergence of the algorithm. Furthermore, other VQ algorithms have to minimize a distortion measure in order to ensure acceptable performances. In this context the SOM algorithm has to minimize a distortion error, which is approximated by equation (2.1) and empirically by equation (2.2).

2.2.3 Kohonen SOM organization measures

According to [194] a SOM is considered organized when the codebooks have the same probability of response (this means that the more frequent inputs are represented with more codebooks than the non-frequent) and all the codebooks are ordered. From the aforementioned statements it is apparent that the topology of the code books must be preserved and the topographic map must preserve the relationships between the input data. Several measures of the neighborhood preservation have been developed. In [195] one can find a description of all the existing measures. Indicatively, the topographic product and the $C-$measure are two out of the five most used measures.

Another codebooks organization measure is the $dx - dy$ representation, introduced by [194]. The $dx - dy$ representation is a graphical representation of all input weights distances (grid index) versus the corresponding distances in the output space (codebooks). This representation is a kind of correlation diagram and provide a lot of valuable information. On the one hand if the map is not organized at all the result of the $dy - dy$ representation is a cloud of points without any kind of correlation between the dx and dy quantities. On the other hand, if a rectangular map is organized then the $dx - dy$ representation has a linear form with some slope. The slope of the line is the weight distance between two consecutive neurons. In figure 2.1 is illustrated a realization of the $dx - dy$ representation for randomly initialized codebooks. It is apparent that there is not correlation at all between the codebooks. This means that there is no topographic organization. On the contrary, in panel B of figure 2.2, the $dx - dy$ representation of a SOM after convergence is illustrated. It is obvious that there is a strong correlation between physical and weights (codebooks) distances.

2.2.4 Convergence of Kohonen SOM

The convergence of the Kohonen SOM has been studied by many researchers. A collection of some mathematical and technical details can be found in the book provided by Kohonen [196]. On the one hand the convergence of one-dimensional map stability is fully described in [196]. In this case the transition form one state to another during learning and updating the code books is considered as a Markov chain and using some of its properties and probability theory one can prove the convergence of the algorithm. On the other hand the two-dimensional convergence

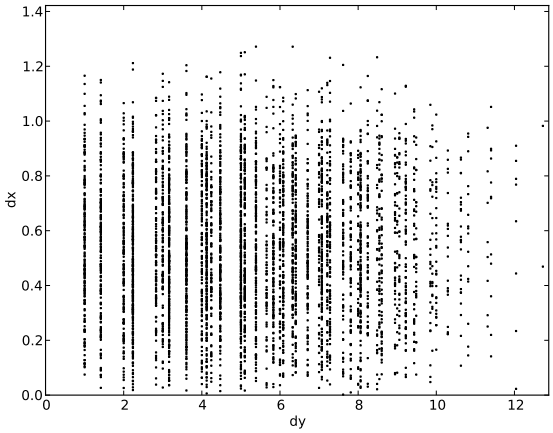

Figure 2.1: **A realization of $dx - dy$ representation.** The representation $dx - dy$ has been computed over a randomly chosen set of codebooks, just before the learning process.

problem remains open since it cannot be found a global energy functional. This means that there is no mathematical quantity to be minimized in order to ensure the convergence of the algorithm.

2.2.5 SOM examples

In this section two basic examples of a SOM are illustrated. The first example is a rectangular uniform distribution and the second one is a ring uniform distribution. The case of the ring distribution is harder for the SOM instead of the rectangular distribution. This is due to the "hole" of the ring, which creates a gap between the input vectors. In both examples the algorithm

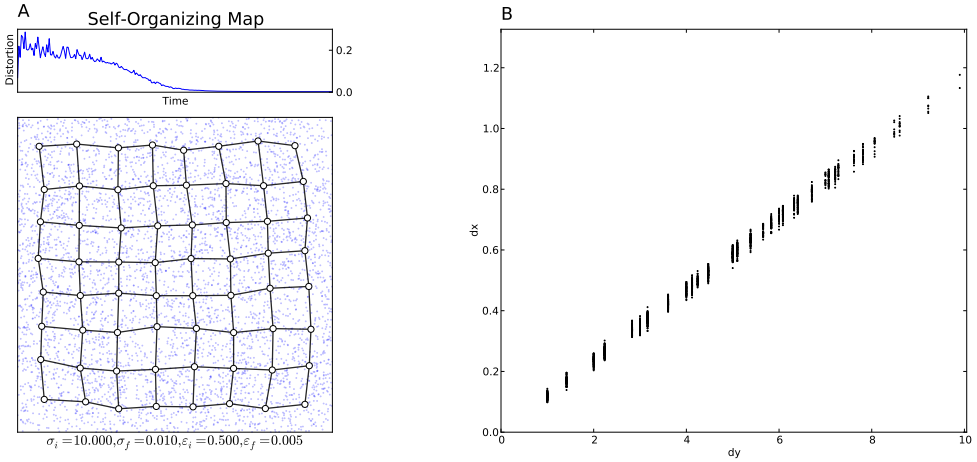

Figure 2.2: **SOM on a uniform rectangular distribution. A** Uniformly drew input data on a rectangle. The white discs and the black grid represent the SOM neurons and the connections of them, respectively. The Distortion is computed during the simulation and it is depicted over time on the top of this panel. **B** The $dx - dy$ representation of the present SOM.

2.1 has been used. The final time has been set to $t_f = 25000$ and the rest of the parameters have also been set to $\epsilon_i = 0.5$, $\epsilon_f 0.005 =$, $\sigma_i = 10.0$ and $\sigma_f = 0.01$ in both simulations.

In figure 2.2 is illustrated the rectangular uniform distribution. The input vector $\mathbf{v} \in \mathbb{R}^2$ is two-dimensional and in the figure is represented as the blue dots. The code words $\mathbf{w}$ are self-organized on a grid (white empty discs) and the connections are represented as black edges. The distortion ξ of the SOM for the regular uniform distribution indicates that the error is minimized and therefore the self-organization has emerged. In addition in the $dx - dy$ representation the cloud of the distances are organized around a line indicating that there is a strong correlation between the input and output space points and hence the topology is preserved. This can also be verified by a visual inspection to the self-organized code words. They tend to cover the input space implying a quantization of the input data.

The second simulation concerning the ring uniform distribution is illustrated in figure 2.3. In this case, as already mentioned, there is a "hole" in the distribution making the self-organization process more difficult. After the simulation one can claim that the SOM minimized the error in terms of distortion as it is depicted at the distortion panel in figure 2.3. In the same figure is illustrated also the input to the SOM as blue dots and the code books of the network at time t_f. A self-organized maps has formed and this can be confirmed also by the $dx - dy$ representation. The $dx - dy$ representation is depicted in the same figure in panel B revealing a correlation between the input and the output space points.

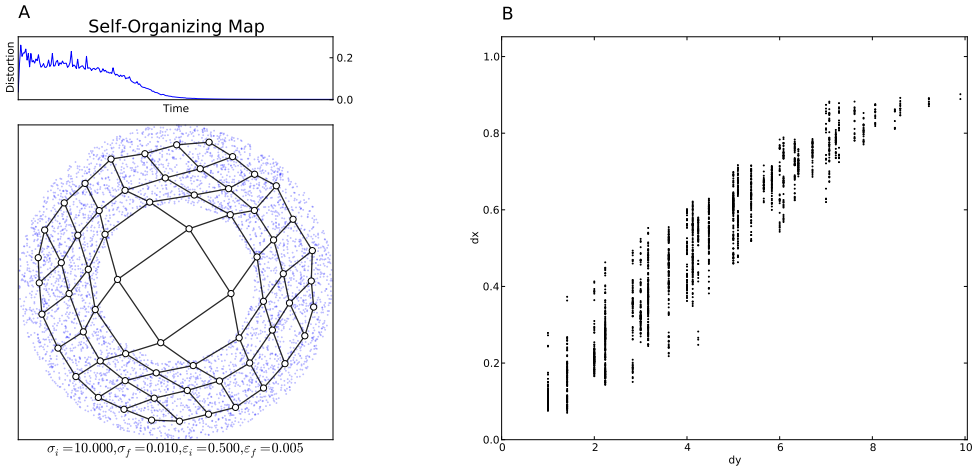

Figure 2.3: **SOM on a uniform ring distribution. A** Uniformly drew input data on a ring. The white discs and the black grid represent the SOM neurons and the connections of them, respectively. The Distortion is computed during the simulation and it is depicted over time on the top of this panel. **B** The $dx - dy$ representation of the present SOM.

2.2.6 Is SOM a good model of cortical phenomena?

Since now it has been mentioned that SOM is the firstly introduced self-organized map and its impact to computer science and machine learning is undeniable. The SOM is a fast and easy way to compute self-organized maps from large input data sets. The one-dimensional of SOM is already known that converges and creates topographic maps. But there are also some problems about SOM. Some of them have been described by Teuvo Kohonen, himself and other by the many researchers that have been developing several variations over time. One problem is the boundary effect. The SOM is not able to cover the whole input space because there is a border effect, which limits the self-organization near the boundary of the input space. This problem is caused by the borders of the input space and a possible way to avoid this problem is to implement

the model on a torus. Another well-known problem is that of magnification factor. This term describes the density of the code books depending on the frequency of the input vectors presented at a unit time. In simple words, if the distribution of the input is not uniform but some of the inputs data are more dense at somewhere the self-organized map will reflect this phenomenon to its codebook. Other types of problems have also been referred by Kohonen, such as the pitch problem and the collapse problem (for more details look at [171]).

Another problem of the SOM is the time-dependent learning. According to the learning process of the SOM and the algorithm described in 2.1 it is apparent that a SOM learns over a predefined time interval and after that time period the model is considered fixed. This means that the codebooks cannot be updated further after the convergence of the learning process algorithm. This phenomenon is in accordance with some neurophysiological data of visual cortex and area V1. It is known that the cortical areas are organized according to a topography (e.g. the orientation selectivity of area V1 of primary visual cortex emerges through a self-organization process according to the retinal input, therefore it follows a retinotopic organization). In 1972 Hubel and Wiesel, [17], found that the area V1 of the primary visual cortex of cats after a time window of learning (the so-called critical period) is not able to reorganize itself. This means that the retinotopic organization of V1 is fixed and cannot alter over time, as exactly a SOM does. Hence, the SOM is a suitable tool for studying cortical phenomena and the cortical self-organization. That was true but not for long enough, because in 1983 John Kaas and Michael Merzenich found evidence in the primary somatosensory cortex of monkeys that the fixed cortex is not the case. They studied cases of sensory deprivations and they found that the area 3b of the primary somatosensory cortex is able to reorganize itself in the presence of a lesion. This means that a SOM cannot model area 3b. Therefore, there is a need for a better model, which is able to model more reliable cortical phenomena and cortical self-organization.

2.3 Dynamic Self-organizing Map (DSOM)

2.3.1 Need for continuous learning

In the field of computer science, an algorithm that is able to process its input data continuously and in a serial fashion without having knowledge of other inputs than the present one is called an online algorithm. Instead, an algorithm that process all the input data at once and has a prior knowledge of the future states is called offline algorithm. The SOM learning process is a off-line process and that's a problem from a biological point of view as it has already mentioned.

2.3.2 The DSOM

Rougier and Boniface introduced in 2011 a version of a SOM, which learns in a time-independent way, and hence its learning process is an online method. The new version is named DSOM after the Dynamic Self-organized Map and is fully described in [192]. DSOM takes advantage of a new concept, the elasticity. Elasticity permits to neglect the time dependency of neighborhood and learning rate equations, leading to a new learning rule completely dynamic and adaptable to the continuous alterations of a dynamic input space.

Definition. *DSOM is a neural map equipped with a structure (a hypercube or hexagonal lattice) and each neuron i is assigned a fixed position $\mathbf{p}_i \in \mathbb{R}^q$, where q is the dimension of the lattice.*

The learning process is similar to the one of SOM and it has been described in the previous section. The main differences with the learning process of SOM are the neighbor function, which

is now given by

$$h_\eta(i, s, \mathbf{v}) = \exp\Big(- \frac{1}{\eta^2} \frac{||\mathbf{p}_i - \mathbf{p}_w||^2}{||\mathbf{v} - \mathbf{w}_s||^2_\Omega} \Big) \tag{2.10}$$

where η is the elasticity or plasticity parameter, $\mathbf{p}_i$ is the position of neuron i and $\mathbf{p}_w$ is the position of winner neuron. One can notice that the neighborhood function is now independent of time t. Instead, it is dependent on the input vector $\mathbf{v}$. It is obvious that the update rule of the code words has also to change in order to be consistent with the new online learning process of DSOM. Hence,

$$\Delta \mathbf{w}_i = \epsilon ||\mathbf{v} - \mathbf{w}_i||_\Omega h_\eta(i, s, \mathbf{v})(\mathbf{v} - \mathbf{w}_i) \tag{2.11}$$

where, now, the learning rate ϵ is a constant and time-independent.

The DSOM has a simple way to generate self-organized maps. The input is presented sequentially to the network and equations (2.10) and (2.11) are computed. This computation leads the winner neuron s to adapt its code words and all the neighbor neurons to do the same. The neighbor of the updated neurons is now defined according to elasticity parameter. This treatment drives the winner s and its neighbor neurons to update their code words and not the rests. On contrary, if there is no neuron close enough to the data, then every neuron update their code words. The DSOM learning process is described algorithmically in 2.2.

Algorithm 2.2 Dynamic Self-organizing Map

Require: $t_f, n, \epsilon, \eta, \Omega$.
Ensure: Codebooks $\mathbf{w}$.

```
w ← rand()
for t = 0 to t_f do
    Select randomly an input vector v ∈ Ω.
    w_s ← arg min_n d(v, w_i).
    for i = 0 to n do
        G ← exp( − (1/η²) ||p_i − p_s||² / ||v − w_s||²_Ω )
        Δw_i ← ε||v − w_i||_Ω G(v − w_i)
    end for
end for
```

2.3.3 Elasticity

The most important parameter of the DSOM is the elasticity, η. Elasticity controls the size of the neighborhood of codebooks and therefore the neurons that will learn the new representations. High values of elasticity lead to a strong coupling of neurons forming a dense pack of neurons. On the opposite, if elasticity is too low then neurons preserve a very light coupling and they are not able to self-organize their codebooks according to the input vectors. In principle, there is no standard method to find the optimal value for elasticity.

2.3.4 Neighborhood preservation and convergence

The DSOM is able to preserve neighbor relations of the input space to the output space. In the previous section, the $dx - dy$ representation was introduced in order to qualify the neighborhood

preservation of a self-organized map. For the DSOM qualification, the $dx - dy$ representation is also used.

The proof of DSOM convergence is an easier process of that of SOM. This is because in DSOM one can find a case where the number of neurons is less than the number of nodes and the DSOM does not converge (for more details the reader can refer to [192]).

2.3.5 DSOM examples

As in the case of SOM the two uniform distributions examples are used. A rectangular and a ring uniform distributions are presented to the DSOM, while at the same time the distortion of the DSOM is computed. After convergence the self-organized map is tested by using the $dx - dy$ method in order to validate the topology preservation. In both simulation cases the elasticity parameter and the learning rate are the same, $\eta = 2.0$ and $\epsilon = 0.1$. The final time has been set to $t_f = 25000$ and 5000 different input vectors $\mathbf{v}$ have been used. The results of

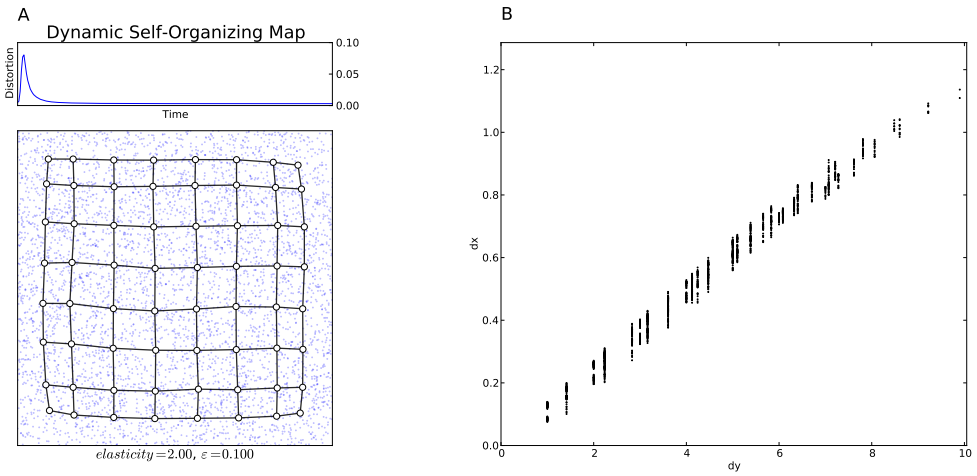

Figure 2.4: **DSOM on a uniform ring distribution. A** Uniformly drew input data on a rectangle. The white discs and the black grid represent the DSOM neurons and the connections of them, respectively. The Distortion is computed during the simulation and it is depicted over time on the top of this panel. **B** The $dx - dy$ representation of the present DSOM.

the uniform rectangular distribution and the uniform ring distribution are illustrated in figures 2.4 and 2.5, respectively. In both figures, in the panel A, the distortion of the DSOM over time is depicted, indicating the minimization of the error during learning process. In the same panel, at the bottom, is also illustrated the input vectors as blue dots and the codebooks after convergence as white empty discs. In both cases the topology is preserved according to the $dx - dy$ representation that reveals a linear correlation in the case of the rectangular distribution and a quasi-linear correlation in the case of the ring.

2.3.6 Is DSOM a proper model of cortical phenomena?

As already mentioned, DSOM is a variation of SOM algorithm. It does not use any kind of time dependency. Instead, a parameter, called elasticity, controls the size of the neighborhood function and therefore drives the self-organization process. Hence, DSOM provide a mechanism for on-line and continuous learning process, which leads to the formation of self-organized maps, rendering the DSOM able to be used in the modeling of cortical phenomena. This is because

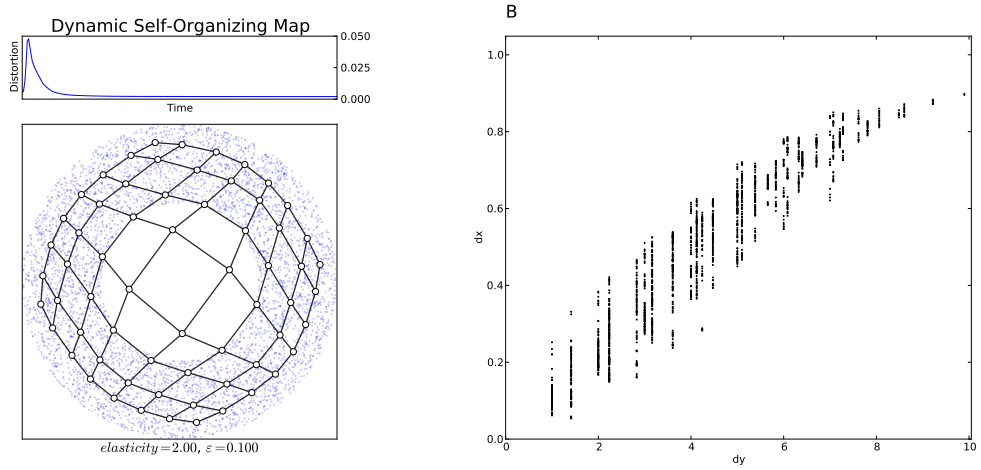

Figure 2.5: **DSOM on a uniform ring distribution. A** Uniformly drew input data on a ring. The white discs and the black grid represent the neurons and the connections of them, respectively. The Distortion is computed during the simulation and it is depicted over time on the top of this panel. **B** The $dx - dy$ representation of the present DSOM.

the learning is not frozen after a time period and can continue for ever. But if DSOM is capable of modeling cortical phenomena then what's wrong about it? From a biological point of view DSOM captures the structure of the input data and not the density. In somatosensory cortex, for instance, this is not true since the density and the structure of the input are both mapped. From a computational point of view, DSOM is sensitive to the elasticity parameter. Elasticity can affect the whole learning process and if it's not finely tuned, the self-organized map could be not-organized at all.

2.4 Laterally Interconnected Synergetically Self-organizing Map (LISSOM)

2.4.1 The LISSOM

Until now, two main self-organized maps have been presented. The original version of SOM and the DSOM. The main points of both have been discussed in the previous sections, but a significant similarity of both models remains. Both models use a mathematical way to find out which is the winner neuron s at each time step t. This is not biological plausible since there is no any such device into the central nervous system. This means that there is a need for a more biological plausible model and another mechanism of measuring the distance between the input vector $\mathbf{v}$ and the codebooks $\mathbf{w}_i$. At this point another computational model comes to fill this gap. The model is called LISSOM after the Laterally Interconnected Synergetically Self-Organizing Map. This model was firstly described by Sirosh and Miikkulainen in [197, 198, 199]. The idea behind LISSOM is the exploitation of the lateral connections within a neural population. Mammals brain cortex is characterized by lateral connections, which play an important role in the formation and maintenance of topographic cortical maps (see chapter 1). LISSOM has the ability to learn not only the feed-forward codebooks but also the lateral codebooks.

According to LISSOM each neuron exhibits an initial response η_{ij} to the input (in this chapter the terminology and the notations of Miikkulainen and Sirosh are used in order to make

comparisons easier to the reader) according to the following equation,

$$\eta_{ij} = \sigma\left(\sum_h \mu_{ij,h}\xi_h\right), \tag{2.12}$$

where the function $\sigma(x)$ is a piecewise linear approximation of a sigmoid function given by

$$\sigma(x) = \begin{cases} 0 & x \leq \delta \\ \frac{(x-\delta)}{(\beta-\delta)} & \delta < x < \beta \\ 1 & x \geq \beta \end{cases} \tag{2.13}$$

δ and β are parameters that introduce a soft threshold and a nonlinearity, respectively, into the response. Moreover the sigmoid function limits the range of values of the response within the interval $[0, 1]$.

The learning process of the model starts with the drawing of a random input pattern with respect to a distribution. Then the input is applied on the model and the response of the neurons according to equation (2.12) are left to settle. After the settling of the response, the feed-forward and the lateral codebooks are updated according to a normalized Hebb rule, given by

$$\mu_{ij,h}(t + \Delta t) = \frac{\mu_{ij,h}(t) + \alpha\eta_{ij}\xi_h}{\sum_h[\mu_{ij,h}(t) + \alpha\eta_{ij}\xi_h]} \tag{2.14}$$

where μ_{ijh} is either the feed-forward codebooks or the lateral codebooks. α is a gain factor, ξ is the presynaptic (input) activity and η_{ij} is the postsynaptic activity of the neurons and is provided by

$$\eta_{ij}(t) = \sigma\left(\sum_h \mu_{ij,h}\xi_h + \sum_{k,l} \gamma_{kl,ij}\eta_{kl}(t - \Delta t)\right), \tag{2.15}$$

$\gamma_{kl,ij}$ is the lateral connection weight on the connection from unit (k, l) to unit (i, j), and $\eta_{kl}(t - \Delta t)$ is the activity of unit (k, l) during previous time step. In addition the lateral connections at the beginning of the simulation have a specific “Mexican hat" form as it is described by

$$\gamma_{kl,ij} = \begin{cases} \gamma_E & |k-i|, |l-j| \leq d \\ -\frac{\gamma_E}{\rho} & (|k-i| > d \text{ or } |l-j| > d) \text{ and } |k-i|, |l-j| \leq 3d+1 \\ 0 & \text{otherwise} \end{cases} \tag{2.16}$$

where the parameter d controls the width of the interaction between neurons, γ_E it's the strength and ρ the ratio of excitation/inhibition. This form of lateral connections corresponds to the short-range excitation and long-range inhibition connectivity pattern found in the brain cortex (e.g primary visual cortex).

LISSOM algorithm provides a new insight to the self-organizing maps, since the activity drives the whole process of self-organization. The activity after some time steps forms a bump which represents the activity of the neurons close enough to the input data and hence these neurons modify their codebooks (both feed-forward and lateral) according to equation (2.14). After some time convergence has reached and the feed-forward codebooks have converged to a topographic map representation of the input data.

2.4.2 LISSOM applications

LISSOM was used, principally, by Sirosh and Miikkulainen in order to model the ocular dominance in primary visual cortex, V1. LISSOM was able to reproduce pinwheel maps of ocular dominance by learning the feed-forward thalamocortical connections and the lateral intracortical connections.

LISSOM has also been used in many different applications. For instance, Wilson et al. in [200] built a model, based on LISSOM. Wilson's model is a self-organizing map that simulates the topographic organization of layers 2/3 of primary somatosensory cortex of rats. The model is able to produce topographic maps of somatotopic organization of rats whiskers and pinwheels of whiskers directions.

2.4.3 Some comments on LISSOM

LISSOM is a significant improvement of self-organized maps, since it has the ability to learn on-line and continuously the representations of the input vectors. LISSOM algorithm updates both the feed-forward and the lateral codebooks, following a Hebb rule. The use of Hebb rule renders the LISSOM more biologically plausible than Kohonen SOM and DSOM. In addition, comparing to Kohonen SOM and DSOM, LISSOM takes the advantage of updating the lateral codebooks leading to a more flexible learning process. In both Kohonen SOM and DSOM the neighborhood function is not learned but it is considered more or less fixed in terms of learning.

LISSOM is a self-organized map that lacks any kind of distance function useful to decide the winner neuron s and to locate its index. The activity of the LISSOM drives the self-organization process, rendering the model more biological plausible than Kohonen SOM and DSOM. Another advantage of LISSOM is the local driven evolution of lateral connections. The lateral connections of the neurons evolve according to a normalized Hebb rule and therefore the proper associations are permitted to develop. By learning the lateral connections LISSOM is able to mimic the developmental process of the cerebral cortex and to establish more stable activity over time. In addition, LISSOM can respond better to a lesion rather than a SOM or a DSOM because it will relearn the lateral connections according to a new connectivity pattern of cortex. In addition, by learning lateral connections, LISSOM is devoid of time-dependent learning rates and neighborhood functions.

In oppose, LISSOM has also some disadvantages. The most important is the boundary effect. LISSOM cannot, as it has been proposed by Sirosh and Miikkulainen, surpass some boundary problems as Kohonen SOM and DSOM do. In addition LISSOM suffers from a dimensionality reduction problem. Another problem of LISSOM is the scalar product that it uses. If one observe the equations describing LISSOM, they will notice that all the equations are based on the scalar product. This condition requires a normalization of codebooks. This normalization also prevents LISSOM codebooks from running away during learning (since the Hebb rule used in LISSOM is the very basic). Another serious problem of the LISSOM is the direction of the input vectors. If the input vectors point to the same direction, then LISSOM is not able to distinguish them and therefore is impossible to map a $n-1$-dimensional map of a n-dimensional input space. At this point Sirosh and Miikkulainen introduced a technical way to avoid such problems, let alone the normalization of the codebooks (for more details reader can refer to [197]). Furthermore, all the technical treatment and the relevant large number of the parameters used in LISSOM, make it a highly parametrized model. This means that one has to finely tune a lot of parameters in order to make the model operational. Moreover, from a mathematical point of view LISSOM does not exhibit any interesting property, which could be used in combination with biological

data in order to build a more biological plausible model.

At this point it is worth making a speculation about LISSOM, which might be of some interest from a mathematical point of view. In [201] Harker et al. introduced an analysis about the Map Seeking Algorithm (MSA), [202]. MSA algorithm is able to find the optimal combination of discrete given transformations in order to find the best fit in between a template image and a transformed one. LISSOM, in contrary, is able to self-organize the codebooks, after some geometrical computations of scalar products (in reality those scalar products, are rotations in the context of LISSOM). Therefore, one could claim that LISSOM acts more or less like a MSA but on a more restrict and specific way in order to perform self-organization learning.

2.5 Why Kohonen SOM, DSOM and LISSOM are not enough?

Kohonen SOM is the very self-organized map in the history of self-organized maps, and it is the most studied. There is an enormous number of studies, variations and applications of Kohonen. The pros and cons of Kohonen SOM have been already discussed as well as of DSOM and LISSOM. From the three aforementioned models, LISSOM is the most biologically plausible, because it takes advantage of the Hebb rule and it is able to learn both, feed-forward and lateral codebooks. LISSOM also offers an on-line and continuous learning process. So, why none of the aforementioned models is not enough to model and used in favor of studying cortical phenomena?

To begin with, cortex is a multilayer structure containing multiple different types of neurons and cells performing complex computations using complex communication mechanisms, as it has been described in chapter one. These neurons, especially in primary sensory areas, are able to perform competitive and cooperative operations in order to form self-organized maps of the input space, which is highly complex and of high dimensionality also. In the present work it is proposed that a computational model of self-organized maps, used in the study of cortical phenomena, must fulfill some characteristic properties.

Proposition 1. *Cortical self-organization and reorganization can be achieved in a biological plausible way if the computational model fulfills the following properties:*

- **Neural dynamics** *The mathematical equations of the model must describe the interactions of neurons, the dynamics, and the activation patterns.*
- **Driving forces** *The same mathematical equations must drive somehow the cooperation and the competition of neurons within the cortex in order to form cortical self-organized maps.*
- **Biological factors** *The equations must not contain any kind of non-biological plausible terms, such as distance functions. The dynamics of the equations must be capable of measuring everything.*
- **Lesions** *Different cortical phenomena, such as cortical lesions, must be possibly modeled and reproduced by the model.*
- **Simplicity** *The model itself must be as simple as possible and keeping only a minimal finite set of parameters. The parameters of the model, have to be in accordance with the physiology and the biology of the problem, otherwise the model is an engineering approach of the problem, which is not the case.*
- **Autodidacticism** *The model has to be completely unsupervised, in any sense.*

- **Distributed-ness** *From a computational point of view the model must be distributed.*
- **Continuity** *Finally, the model must be able to learn in a on-line and continuous fashion.*

According to the aforementioned manifest of what the model must do and must not do, it is apparent that Kohonen SOM and DSOM are excluded immediately as possible candidates of such a model. This is because DSOM and Kohonen SOM lack the ability of modeling the cortex, the interactions of neurons and the activity patterns. In addition both SOMs are not distributed and completely unsupervised in the sense of choosing a winner neuron. This means that the index of the winner neuron has to be assigned according to a distance function. Furthermore, cortical lesions for instance is impossible to be studied by using Kohonen SOM. By using DSOM it could be possible but it is not parameter free making the problem very hard to be solved. On contrary, LISSOM can be distributed and uses also a biological plausible way to learn both, the feed-forward and the lateral codebooks. In addition LISSOM is able to recover from lesion cases, but it is not parameter-free model. One has to take care of a lot of parameters in order to make the model operational. In addition a lot of LISSOM parameters do not reflect any biological property. Their existence is only up to solving some technical problems of LISSOM, as they have been explained in the previous subsection.

Concluding one can claim that none of the Kohonen SOM, DSOM and LISSOM are able to model and being used in a study of cortical phenomena. Therefore, one has to devise a model, which will be able to capture the aforementioned characteristic properties. And since the model must be able to study cortical phenomena, it could be a spiking neural network described by a bunch of ordinary differential equations or a rate model. A rate model is more suitable candidate, because it offers a complete mathematical and computational way to study neural populations. Furthermore, in the context of self-organization a rate model could be used to drive self-organization process and to correlate different parameters with biological factors. Such models are the Wilson and Cowan and Amari's neural fields. In previous chapter, there is a complete analysis of the neural fields and a bibliographic remark of some of the rate models.

In previous chapter, the neural field theory has been described and some of their properties such as the ability of a neural field to relax its activity on the maximum value of its input. Neural fields can be used in modeling of cortical sheets and as it has been shown one can interconnect different neural fields in order to construct cortical hypercolumns and model all the cortical layers. Depending on the properties of neurons and the lateral connections, one can embed these properties into neural fields equations. Furthermore, neural fields have been used also in the past in self-organization. This has been done by Amari, himself and more recently by Lucian Alecu, during his dissertation [203]. The last model is a two-populations neural field that is inspired by the Pinto-Ermentrout model, [204], and can produce self-organized maps. That model fulfills the characteristic properties described in proposition 1 but the rule of the simplicity and the parameters. The model is not parameter-free and one has to put a lot of effort in order to make that model fully operational. Hence, in the next chapter a self-organized map based on neural fields theory is proposed that fulfills all the properties of proposition 1 and in addition can exploit several different cortical phenomena, let alone the self-organization.

2.6 Summary

Kohonen's self-organizing maps or SOM is a kind of a vector quantizer and it is able to project a large set of input data to a smaller finite set of code words. Kohonen learning process is not continuous, since the model is capable of learning only within a time-window. That's because the

learning rate and the neighborhood functions of the model are time-dependent. After that period the codebooks are frozen and the SOM cannot learn any new representation. A better variation of Kohonen SOM is the DSOM. DSOM is able to learn using an on-line and continuous learning process. DSOM can succeed that by taking advantage of one parameter, the elasticity. Elasticity controls the coupling of neurons promoting the self-organization. Another better model of SOM is the LISSOM. LISSOM is a bunch of scalar products equations and it uses a normalized Hebb learning rule by virtue of learning. LISSOM has the ability to learn continuously and on-line. All three models have been used in studies of cortical phenomena and cortical organization, but none of the three offers a realistic cortical model.

In the context of cortex modeling and self-organization in primary sensory areas, seven rules have to be fulfilled in order a model to be able to succeed in cortical modeling. Such a model must be related somehow to the biological aspects of the problem. This biases the choice of the model to be a rate or a spiking neural network. In the present work a rate based model is proposed to serve as cortical model. The rate model is a dynamic neural field equation, which drives the learning process of the self-organization.

To know the brain...is equivalent to ascertaining the material course of thought and will, to discovering the intimate history of life in its perpetual duel with external forces.

(Santiago Ramon y Cajal, 1852-1934)

3

Dynamic Neural Fields Self-organizing Maps (DNF-SOM)

Contents

The purpose of the present work is the study of cortical phenomena such as the formation of topographic maps. All the primary sensory areas of the mammal brain contain topographic maps. The primary visual cortex is characterized by a retinotopic organization. The primary somatosensory cortex contains somatotopic maps of the body parts. Finally, the primary auditory cortex forms a tonotopic map, which is organized according to audio frequencies of the cochlea. Through self-organization, cerebral cortex is able to form external representations in order to exploit their properties and to make further processing optimal in terms of dimension reduction, distributed-ness and redundancy.

Three different computational self-organized maps have been described in the previous chapter, as well as the advantages and the disadvantages of each of the maps. Those models, Kohonen SOM, DSOM and LISSOM cannot satisfy all the properties described in proposition 1, as it was already explained in the previous chapter. The proposed model is called DNF-SOM (Dynamic Neural Fields - Self-organizing Map) and is based on the theory of neural fields and an Oja-like learning rule. This chapter is organized as follows. First the model(architecture, input and computations) is is introduced. Then some very simple examples of self-organization are illustrated. Then the problem of modeling area 3b of the primary somatosensory cortex is introduced and the results of the model are illustrated and discussed as well. The results concern the formation and maintenance of topographic maps of area 3b, reorganization in the face of cortical lesion or a sensory deprivation and finally the effects of attention on neurons of area 3b. Moreover, the model fulfills the requirements stated at proposition 1 and the three following remarks as well.

- First, the model has to be in accordance with real experimental data.
- Second, the context of the model has to be defined. This means, what is the problem that the model solves and on what kind of data can be applied.
- The third and last requirement has to do with the new insights that the model reveals. In simple words, the model has to extend the already existing, from experimental data, knowledge by making predictions.

DNF-SOM is a continuous model based on dynamic neural fields equations and provides spatial and temporal information at the same time. It is completely unsupervised and fully described by a system of two coupled equations, a finite set of five parameters (regarding the dynamic neural field), and a difference of Gaussian functions serving as lateral connections kernel. These characteristics of the model render it computationally simple. The model is suitable to parameters alterations, and only four different parameters control the behavior of the model (see chapter 1). Additionally, DNF-SOM can simulate cortical phenomena and the results are in accordance with neurophysiological experimental data and is also capable of making predictions about several cortical phenomena, such as attention. The rest of the chapter is organized as follows. First, the basic mathematical/computational model is introduced as well as some very important properties of the model. Then, preliminary results are presented, followed by the model of the area 3b of the primary somatosensory cortex. Finally, some older models of primary somatosensory cortex are compared with the DNF-SOM.

3.1 The model

The DNF-SOM is composed of two levels. An input level preparing and providing the input stimuli to the cortical model, which is the second and higher level. At this latter level a dynamic

neural field models a cortical sheet and all the necessary calculations for self-organization take place at this level. These two levels are interconnected via afferent fibers supported by a set of synaptic strengths, the feed-forward thalamocortical connections. At the cortical level, neurons are inter-connected with each other with lateral synaptic strengths, named lateral connections.

The cortical level is modeled by a dynamic neural field equation such the one introduced by equation (1.20). The lateral connections, w_l, can be a difference of Gaussian (DoG) or a difference of exponential functions (DoE). Both, DoG and DoE, correspond to the short-range excitation and long-range inhibition cortical connectivity pattern. In addition, the firing rate of the model is a rectification, which is positive for positive values or zero otherwise. This type of firing rate function reflects the static properties of neurons, when they act as linear operators, [205, 206]. In order to be completed, the model needs also a learning rule. The learning rule is given by an Oja-like continuous differential equation. Because the dynamic neural field equation receives as input the thalamic signal $s(\mathbf{z}, t)$ that is conveyed through the feed-forward thalamocortical connections $w_f(\mathbf{x}, t)$ one can assume that the neural field equation and the learning rule are coupled. Hence a non-linear coupling system of differential equations describes the DNF-SOM model.

$$\left.\begin{aligned} \tau\frac{\partial u(\mathbf{x},t)}{\partial t} &= -u(\mathbf{x},t) + \int_{\Omega} w_l(\mathbf{x},\mathbf{y})(\alpha f(u(\mathbf{y},t)))d\mathbf{y} + \alpha\Big(1 - \frac{1}{k}\sum_{i=0}^{k}|s_i(\mathbf{z},t) - w_f^i(\mathbf{x},t)|\Big) \\ \frac{\partial w_f(\mathbf{x},t)}{\partial t} &= \gamma\left(s(\mathbf{z},t) - w_f(\mathbf{x},t)\right)\int_{\Omega} w_e(\mathbf{x},\mathbf{y})(\alpha f(u(\mathbf{y},t)))d\mathbf{y} \end{aligned}\right\} \tag{3.1}$$

The function u describes the neural population activity at a position $\mathbf{x}$ of the cortical sheet. α is a constant parameter of the neural field, k is the cardinal of the finite set of input receptors, and the resting potential h has been set to zero. The input receptors is a finite set of points on the plane that are used during the sampling process of the actual stimulus. This sampling process mimics the actual biological process. Of course the model is able to form self-organizing maps without the use of any kind of input receptors. This implies that in some simple cases the model can achieve a self-organization by just applying the stimuli directly to the model without any kind of preprocessing.

Equation (3.1) is used in the context of DNF-SOM in order to drive the self-organization process by exploiting the properties of population dynamics. As it has been discussed in chapter one of the second part the main property of population dynamics states that if one tunes properly the gain parameters of a dynamic neural field, then the maximum of the neural field activity is equal to the maximum value of the input. This property has been introduced in [207] and can ensure the convergence of self-organization using dynamic neural fields. In a more mathematical context a dynamic neural field, given by equation (3.1), has the ability to relax its population activity to the maximum value of its input, if the input is finite, continuous or constant. A counterexample is the case of a hills-valleys function, where the dynamic neural field converges close to the global maximum value. This means that the dynamic neural field could serve as both a measure of the input and a global maximizer. In the rest of the chapter the model is explained in full detail.

3.1.1 Input to the DNF-SOM

The first level of the model is the input layer. At this level the input stimulus to the model are applied and transmitted through afferent connections to the cortical level. Normally, one would expect to find some more relay stations in between the two levels, representing the sub-

and thalamic nucleus according to the neuroanatomy of the central nervous system. However such a condition is not the case for the DNF-SOM. This means that the DNF-SOM does not contain any intermediate level in between the input and the cortical levels. If one would like to add some more intermediate layers (relays), is able to do so. This is because of the abstraction and the generality of the core of the model, which is the system (3.1). One can have as many preprocessing or relay modules, as they will. Back in the modeling of area 3b, the conveyed information from the input level to the cortical one is given by the following equation,

$$i(\mathbf{x},t) = 1 - \frac{1}{k}\sum_{i=0}^{k} |w_f^i(\mathbf{x},t) - s_i(\mathbf{z},t)| \tag{3.2}$$

where $\mathbf{x} \in \Omega, \Omega \subseteq \mathbb{R}^2$ is the position of a neuron on the grid of neurons (see chapter 1 for more details), $w_f^i(\mathbf{x},t)$ is the $i-$th feed-forward thalamocortical connection (weight) and $\mathbf{z} \in \Theta, \Theta \subseteq \mathbb{R}^2$ the stimulus applied on the skin (Θ is the input space). k is the size of each receptive field of neurons.

The size of the receptive fields of the neurons is assumed to be the same for all the neurons and it has to do with the size of the input area that a neuron has access to. For instance, if the input space is the one-dimensional line of real numbers, then $k = 1$ and the feed-forward connections are a one-dimensional array. Thus $s(\mathbf{z},t)$ is a scalar representing the single value of the input. In more general cases, $s(\mathbf{z},t)$ is a vector or a matrix representing the input to the model.

3.1.2 Response of the DNF-SOM

At the next level of the model is the cortical one. The core of that layer is a dynamic neural field given by equation 1.20. A solution of this equation represents the activity (response) of the cortex in terms of modeling. This means that in the presence of a stimulus, the neurons that respond to the input contribute to the solution. The rest of the neurons remain silent.

More precisely, if the stimulus intensity is high enough there is a high probability for the neurons to overpass the firing threshold and to respond to the stimulus. In contrast, if the stimulus is not so effective neurons remain subthresholded and thus silent without any response to that stimulus. In more mathematical terms if $\Omega \in \mathbb{R}^n$ (where n usually is 1 or 2) is the domain of the dynamic neural field (cortical sheet) then a subset of neurons will be excited responding to a stimulus if there is a region R for which the following holds,

$$R = \{\mathbf{x} \in \Omega | u(\mathbf{x},t) > 0\} \tag{3.3}$$

R defines the excited region of the dynamic neural field, which reflects the activity of the responding neurons. R was previously introduced by equation (1.15) in chapter one. This activity of the dynamic neural field is used in later processing steps of self-organization as it is explained later.

3.1.3 Plasticity rule of the model

The response of the dynamic neural field drives the self-organization process. This process promotes the formation and the maintenance of topographic maps at the level of thalamocortical afferents (the feed-forward connections). Therefore, the most important part of the model is the plasticity rule (learning rule), which updates (adapts) the feed-forward connections. Unlike

the updating of feed-forward connections, the lateral connections remain stable during specific developmental periods.

The plasticity rule is inspired by the dynamic self-organizing map algorithm that has been proposed by [192] and it has been described briefly in section 2.3 of chapter 2. The main idea of the learning rule of DSOM is that the original time-dependent learning rate and neighborhood learning function has been replaced by a time-invariant learning rule. Instead, a dynamic neighborhood function has been introduced that depends explicitly on the distance of the winner neuron to the presented stimulus. On the one hand, if the distance of a winner neuron is very close to the stimulus, the ϵ-neighborhood undergo a shrinkage and the neighbor neurons learn the new representations by updating their weights. Neurons that are not in that ϵ-neighborhood of the winner neuron does not learn (they do not adapt their weights). On the other hand, when the winner neuron is very far from the stimulus, the ϵ-neighborhood undergoes an expansion and every neuron of the network adapts its weights according to the new representation.

Taking advantage of the DSOM learning rule and making use of the properties of dynamic neural fields about the level of cortical activity as it has been explained in section 1.7.1 of chapter 1 the learning rule of the model, firstly introduced by [208], is given by the following equation,

$$\frac{\partial w_f(\mathbf{x},t)}{\partial t} = \gamma L_e(\mathbf{x})\left(s(\mathbf{z},t) - w_f(\mathbf{x},t)\right) \tag{3.4}$$

where γ is the learning rate and $L_e(\mathbf{x})$ is the total excitation received at the point $\mathbf{x}$ which is given by the two-dimensional spatial convolution between the excitatory part of the lateral connections function and the field activity. More precisely,

$$L_e(\mathbf{x},t) = \int_{\Omega} f(u(\mathbf{y},t))w_e(|\mathbf{x}-\mathbf{y}|)d\mathbf{y} \tag{3.5}$$

Where w_e is the excitatory part of the lateral connections function as it is given by equation (1.22). The main advantage of this learning rule is the explicit modulation of learning according to the sum of excitation received at a point $\mathbf{x}$ while the inhibition only serves during the competition stage. At the early stage of the training, because of the randomness of the feed-forward weights, any stimulus can cause a weak response of the model at a random place within the field. As the learning process is ongoing and the feed-forward weights converge according to equation (3.4), the response of the model becomes stronger and occupies a specific spatial location.

The learning rule given by equation (3.4) is an Oja-like learning rule. As it has been proposed by Abbott and Nelson in [209] this learning rule may reflect some of the properties of the synaptic scaling in combination with LTP and LTD and therefore is a suitable biological plausible learning rule promoting the modeling of cortical plasticity. Therefore the aforementioned learning rule is used to drive the self-organization process leading to the emergence of topographic maps. Moreover, equation (3.4) offers a mechanism for continuous learning. This means that the model is able to learn new representations at any time and/or reorganize itself in the presence of cortical lesions or sensory deprivations.

3.2 DNF-SOM in action

The architectures of the one- and two-dimensional models are depicted in figures 3.1 and 3.2, respectively. In the former figure, the DNF-SOM is composed by a one-dimensional neural sheet (DNF), which represents the cortex and an input layer which represents the thalamus. The input is conveyed via thalamus to the neurons of the neural field according to the feed-forward

connections. The neurons within the neural field are interconnected with a short-range excitation long-range inhibition pattern given by equation (1.21). In the same figure, blue lines indicate the inhibitory connections and red ones the excitatory connections. In the latter figure, 3.2, the input

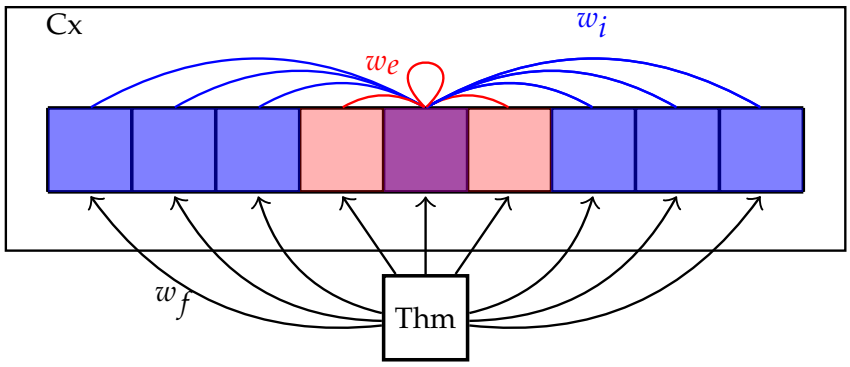

Figure 3.1: **One-dimensional DNF-SOM model.** Blue boxes and lines represent inhibitory neurons and connections, respectively. Red boxes and lines represent excitatory neurons and connections, respectively. w_f is the feed-forward connections, w_e the excitatory and w_i the inhibitory connections given by equation (1.22).

to the model is formed by using several receptors which sample the stimulus and convey it to the cortical layer through the feed-forward connections. Feed-forward connections are represented in that figure as an independent layer, w_f. Within cortical layer all neurons are interconnected with a short-range excitation long-range inhibition pattern of connectivity (i.e. w_l is given by a DoG or a DoE). An important remark is that any neuron of the cortical level has access to all the available information at any time. This kind of information availability is important during the self-organization process, because it provides a global information to each neuron. At the end of the learning process each neuron will have learnt some specific features of the input by shaping its receptive field. Using the one-dimensional DNF-SOM, illustrated in figure 3.1, and a slightly modified version of the two-dimensional DNF-SOM, one can obtain self-organized maps. More precisely, and for the sake of simplicity, the two-dimensional DNF-SOM has been modified at the input level by neglecting the skin receptors. This means that the input $s(\mathbf{z}, t)$ is provided directly to the DNF-SOM via the feed-forward connections. In simple words, the input is not sampled by any kind of receptors, instead, it is given to the DNF-SOM *talis qualis*.

Before proceeding to the simulation details and the results of the model, it is important to define some qualification quantities in order to measure empirically the quality and the convergence of the model. The first measure is the average evolution of feed-forward weights, w_f, and it has been used in [208] in order to measure convergence. The average evolution error is defined by

$$\bar{\mathcal{E}}_i = |\mathbb{E}[w^i_{f_{new}}] - \mathbb{E}[w^i_{f_{old}}]| \tag{3.6}$$

Where $\mathbb{E}[]$ and $|\cdot|$ represent the expected value and the absolute value, respectively. The average evolution $\bar{\mathcal{E}}$ can be computed on-line during the learning process and it requires only to store the previous values of the feed-forward weights. The second measure, the mean-squared error (MSE) of the feed-forward weights is defined as

$$\text{MSE}[w_f] = \frac{1}{M}\sum_{i=0}^{M}(\hat{\mathbf{w}}^i_f - \mathbf{w}^i_f)^2 \tag{3.7}$$

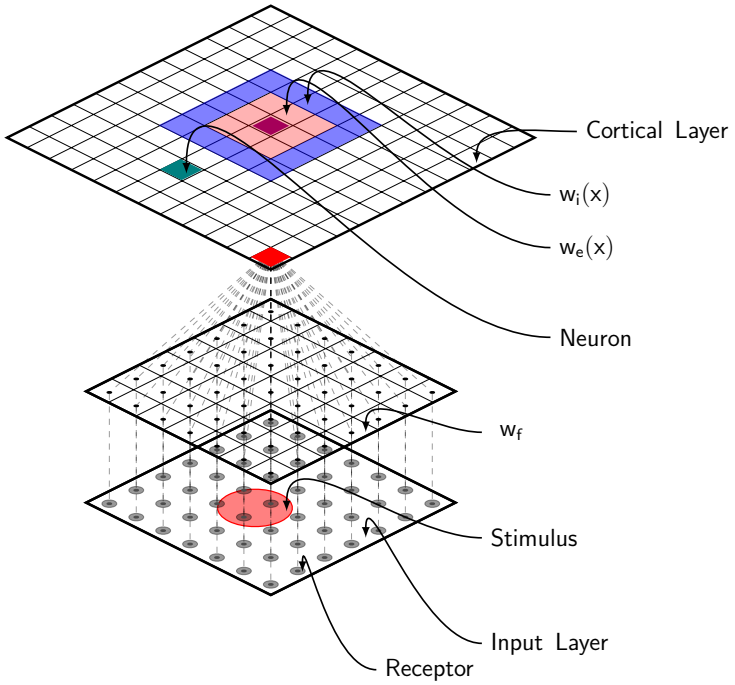

Figure 3.2: **Two-dimensional model.** Blue rectangles represent inhibitory neurons, light red rectangles represent excitatory neurons. The red square indicates a neuron, which receives an input via feed-forward connections, w_f. The gray discs represent skin receptors and the red circle represents a stimulus applied on the skin. Finally, the navy colored rectangle represents a simple neuron.

This error dependents on a set of ideal values of the feed-forward connections, w_f. Therefore $\hat{\mathbf{w}}_{\mathbf{f}}{}_f^i$ is the $i-$th ideal feed-forward connection of the map and $\mathbf{w}_f^i$ is the $i-$th current feed-forward connection. If the DNF-SOM has converged the MSE is a decayed exponential function converging to zero with some small amplitude oscillations. These oscillations are present because of the dynamic nature of the model, indicating that the model is not frozen after the convergence and rendering it able to continue the learning process. On the other hand, if the DNF-SOM has not converged, the MSE function is completely noisy and oscillatory. Finally, if the DNF-SOM model converges with a delay, that can be reflected to MSE as a very slow decaying curve. Both measures, the average evolution error and the MSE cannot predict the convergence nor ensure it, but they offer a way to measure at some point the behavior of the DNF-SOM during the learning process. The first test case is a one-dimensional DNF-SOM trained over a discrete input set,

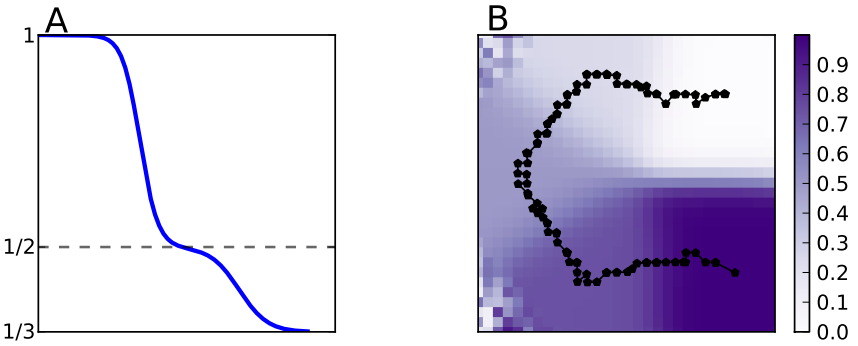

Figure 3.3: **1D and 2D DNF-SOM over 1D input. A** One-dimensional DNF-SOM trained for 3000 epochs over the set $\mathcal{I} = \{\frac{1}{3}, \frac{1}{2}, 1\}$. In this panel is illustrated the feed-forward weights w_f after the convergence of the learning process. It is apparent that the feed-forward weights have been converged to the input values 1, $\frac{1}{2}$, and $\frac{1}{3}$. **B** Two-dimensional DNF-SOM trained for 5000 epochs over the set $\mathcal{I} = \{0, \frac{1}{4}, \frac{1}{2}, \frac{3}{4}, 1\}$. The thick black dotted line indicates the continuity of the feed-forward weights w_f after the convergence of the learning process. One can observe that there is a continuous topographic organization starting from 0 and moving towards 1.

$\mathcal{I} = \{\frac{1}{3}, \frac{1}{2}, 1\}$. The DNF equation is discretized by using 128 nodes and the learning process lasts 3000 epochs. At each time step of the learning process a value from the input set $\mathcal{I}$ is presented to the DNF equation (3.1) and the feed-forward weights are updated. In order to solve numerically equation (3.1) the forward Euler's method is used. In this test case the input to equation (3.1) is given by

$$i(x,t) = 1 - |s(x,t) - w_f(x,t)| \tag{3.8}$$

Because this test case is a non-toric implementation of the model, there are some boundary effects. In order to avoid these effects, the input is multiplied at each time by a Gaussian function, $G(x;\mu,\sigma)$ with zero mean and a high variance ($\mu = 0$, $\sigma = 2.1$). The initial feed-forward weights are randomly chosen and after 3000 epochs, the model has converged to a self-organized map. The map is illustrated in panel A of figure 3.3. The three values of the input set $\mathcal{I}$ has been learnt and the weights (codebooks) represent the values $\frac{1}{3}$, $\frac{1}{2}$ and 1. It is apparent that there is also a *continuity* regarding the representations. The DNF-SOM has learnt the input values in a consistent way (e.g. in this particular case in a descending order from maximum to minimum value). The next test case concerns a two-dimensional DNF-SOM over a discrete input set, $\mathcal{I} = \{0, \frac{1}{4}, \frac{1}{2}, \frac{3}{4}, 1\}$. In this case the DNF equation is discretized in a 32×32 grid of nodes and the forward Euler's method is used in order to solve numerically the equation (3.1). The DNF-SOM

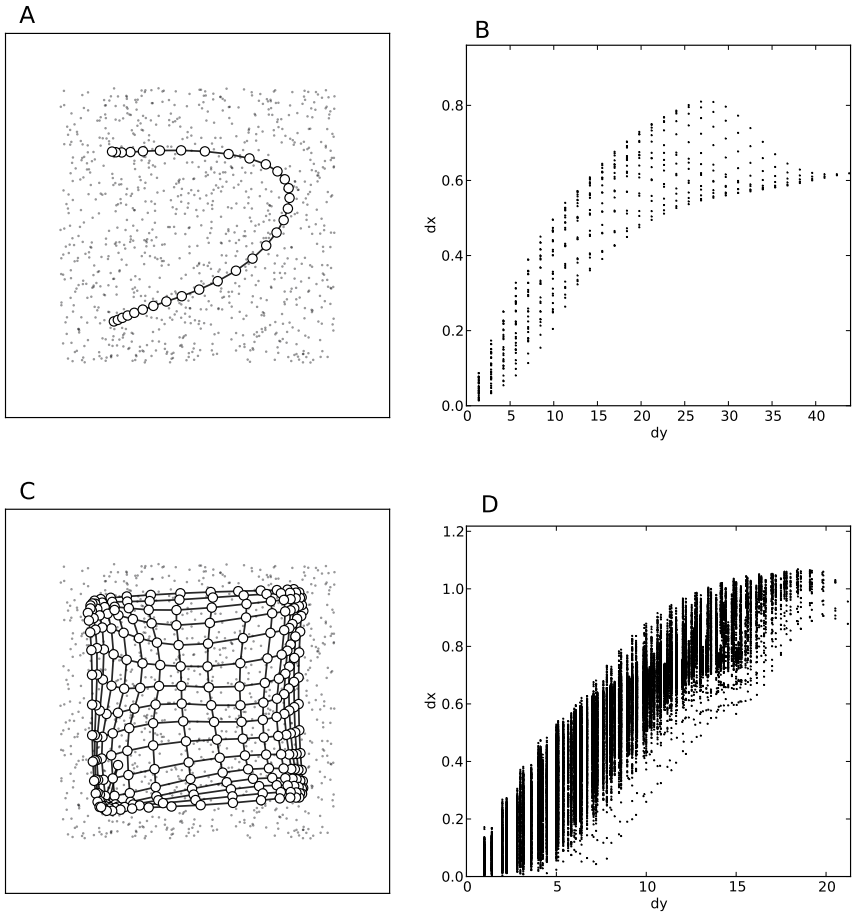

Figure 3.4: **1D and 2D DNF-SOMs over a 2D rectangle.** **A** One-dimensional DNF-SOM trained for 10000 epochs over uniformly distributed plane points of a rectangle, **B** the corresponding $dx - dy$ representation. **C** Two-dimensional DNF-SOM trained for 10000 epochs over uniformly distributed plane points of a rectangle. White vertices are the neurons and black edges the connections among neurons, **D** and the $dx - dy$ representation.

is trained for 5000 epochs. The input is computed at each time step by equation (3.8) and it is multiplied by $G(x;\mu,\sigma)$, because the DNF-SOM is the non-toric version.

In panel B of figure 3.3 it is illustrated the self-organized map after the convergence of the DNF-SOM algorithm. The color variation indicates different level of values according to the input set $\mathcal{I}$. The black pentagon markers point out the *continuity* of the self-organized map, starting from the lowest value and going to the highest one.

In order to test more thoroughly the DNF-SOM, a higher dimension distribution has to be used. Thus a set of uniformly distributed points on the plane is presented to the DNF-SOM. The two aforementioned DNF-SOM models are kept the same with the same parameters, but the input which is different this time. First, the one-dimensional DNF-SOM (the same as previously) is trained over an input set $\mathcal{I} = \{(x,y) \in \mathbb{R}^2 | 0 < x < 1, 0 < y < 1\}$ for 10000 epochs. At each time step a stimulus, randomly drawn from the input set $\mathcal{I}$, is presented to the model and the actual input is computed by equation (3.2), where $k = 2$. In panel A of figure 3.4 is depicted the self-organized map after the training process. The gray dots represent the (x,y) inputs spread on the plane $[0,1] \times [0,1]$. The white discs represent the feed-forward weights, w_f, of the model. It is obvious that the model in this case fails to represent the input space since a two-dimensional input space has to be mapped on a one-dimensional map. This leads one to test a two-dimensional DNF-SOM. Therefore, the previously two-dimensional DNF-SOM is used again here. Only the discretization is different, since a grid of 16×16 nodes is used in this case. In panel B of figure 3.4 the white discs represent the feed-forward weights of the DNF-SOM that have mapped almost the entire input space. A border effect is apparent since the present model is a non-toric and the input vectors have borders promoting this effect (the border effect has been discussed in the previous chapter).

It is obvious from the panel B and D of figure 3.4 that the DNF-SOM can produce a self-organized map. The $dx - dy$ representation indicates a strong correlation between the neurons space and the weights space. The abnormalities are due to the border effect which tends to act as a repellor to the system.

The uniform distribution on a rectangle is a classical test-case used in self-organized maps. It is a simple example, which cannot exploit all the weak points of a self-organized map. Therefore, another test must be used, more difficult. Hence, a uniform distribution on a ring is used in order to test the performance of the model. This kind of distributions have some topological constraints such as holes, rendering the self-organization process more difficult. The same configuration of DNF-SOM as in the case of the rectangular distribution is used. After 10000 iterations the algorithm has converged and the results are illustrated in figure 3.5. In panel A the one-dimensional version of the DNF-SOM has converged to a self-organized map, without such good results. This is obvious if one takes a look at the $dx - dy$ representation in panel B. The correlation is not so strong. The two-dimensional case, illustrated in panel C, is better but still there are some issues. The self-organized map is compressed because of the boundaries of the model. A solution to that problem would be a toric version of the model. This means that the input vectors have not any kind of border or restriction. Later in this chapter, the toric version of the model will be explained further. The DNF-SOM has been tested in two more test cases. The first test case has to do with a distribution of one-dimensional Gaussian functions. The mean μ of each Gaussian function is taken to lie on a partition node of interval $[0,1]$. The partition of this interval has been done using $n = 32$ nodes. This means, for instance, that the center of the first Gaussian is at point 0 the second one is at point 0.1 and so on. Therefore, at each time step a vector of dimension 32×1 containing a one-dimensional Gaussian is presented to the model that has been discretized as a 64×1 grid. The input is computed according to equation (3.2) and the learning process is driven by equation (3.1). After 25000 epochs the DNF-SOM

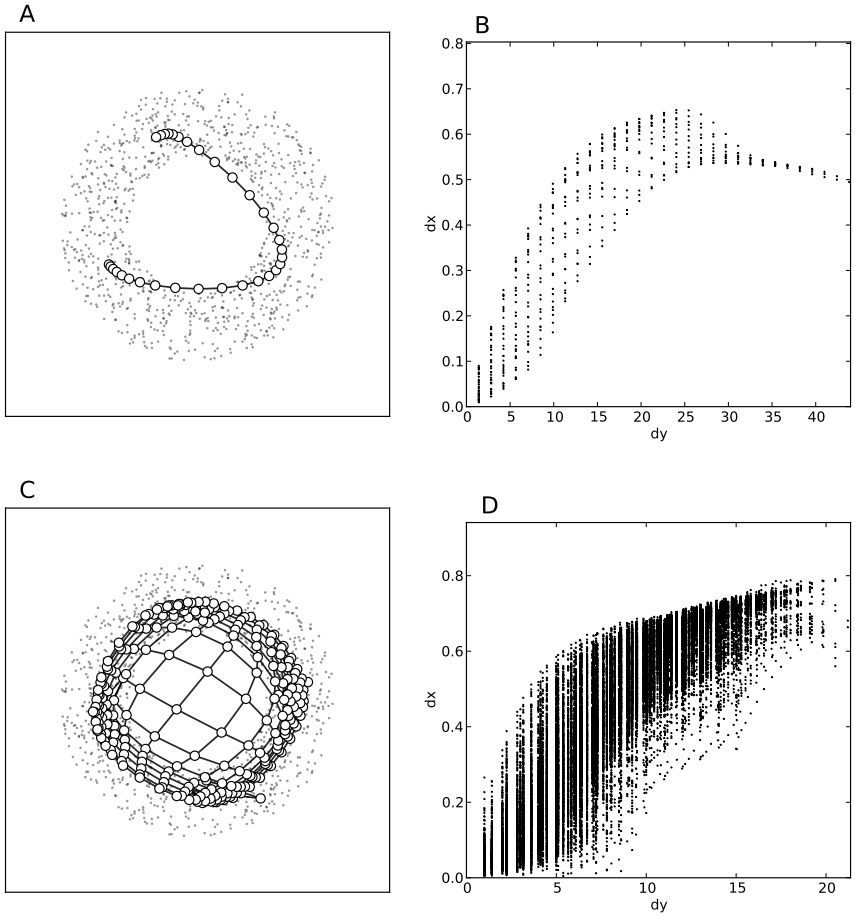

Figure 3.5: **1D and 2D DNF-SOMs over a 2D ring. A** One-dimensional DNF-SOM trained for 10000 epochs over uniformly distributed plane points of a ring, **B** the corresponding $dx - dy$ representation. **C** Two-dimensional DNF-SOM trained for 10000 epochs over uniformly distributed plane points of a ring. White vertices are the neurons and black edges the connections among neurons, **D** and the $dx - dy$ representation.

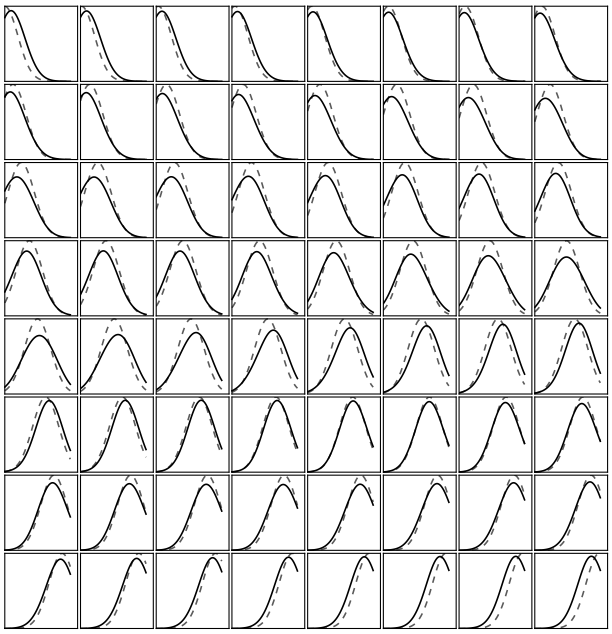

Figure 3.6: **1D DNF-SOM over n-dimensional Gaussians.** A one-dimensional DNF-SOM model of 64 units has been trained over one-dimensional Gaussian functions. Each Gaussian has a resolution of 32 nodes, implying that the interval $[0, 1]$ has been partitioned in 32 equal parts. Therefore the feed-forward weights matrix dimension is 64×32. Each unit has access to the whole input space. Each block of the figure illustrates the final feed-forward weights after the learning process. The dashed lines indicate the input Gaussian functions centered on the 32 nodes. Because of lack of space the weights have been depicted as a matrix, instead of a 64×1 vector.

has converged to a self-organized map as it is illustrated in figure 3.6. The self-organized map shows a continuous organization from left to right. The self-organized map has learnt, actually, the centers of the Gaussians. In the same figure, the black curves represent the feed-forward weights while the dashed curves represent the original corresponding inputs.

The DNF-SOM has been also examined in the same two-dimensional problem. The plane $[0,1] \times [0,1]$ is discretized in a grid of 64×64 nodes and two-dimensional elongated Gaussian functions with a specific direction are centered on those nodes. In addition, the orientation of the elongated Gaussian functions vary between 0 and π. The model is discretized using a 32×32 grid and the input is computed by equation (3.2). After 25000 iterations the model has converged to a self-organized map as it is depicted in figure 3.7. By visual inspection of the self-organized map, it is clear that there is a continuity to the representations of the Gaussians. The direction follows a specific pattern of organization and same directions have been clustered together. In addition, the transition from one to another representation is almost smooth due to the gradually altered direction.

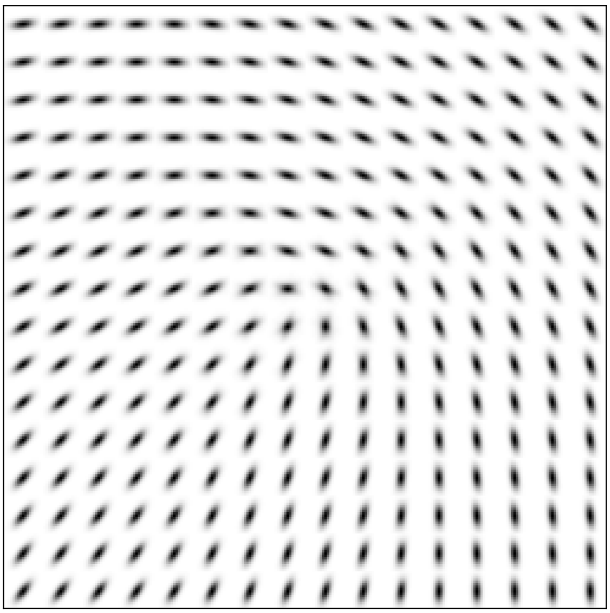

Figure 3.7: **2D DNF-SOM over n-dimensional Gaussians.** A 16×16 DNF-SOM model has been trained over elongated and rotated two-dimensional Gaussian functions. Each Gaussian has been centered on a node after a partitioning of the interval $[0,1] \times [0,1]$ in 64×64 equipartitioned intervals. Moreover, the orientation of each Gaussian varies between 0 and π. After the convergence of the learning process the model has converged to a topographic organization and the orientation of the Gaussian functions indicates a continuous topographic organization.

3.3 Transition to neuroscience modeling

So far the DNF-SOM and all the previous models (Kohonen, DSOM and LISSOM) have been discussed from a pure computational and mathematical point of view. Some of the applications of each model have been discussed as well as their advantages and disadvantages. A more interesting perspective is that of computational neuroscience. In the context of computational neuroscience, one has to be able to build models able to simulate, explain and predict neurosci-

entific phenomena.

As it has been also discussed, one of the goals of the present work is the study of area 3b of SI (i.e. primary somatosensory cortex). This means that one has to pick or to build a computational model in order to study cortical phenomena taking place in area 3b. None of the three self-organized maps, Kohonen, DSOM and LISSOM, satisfies the requirements of proposition 1. This means that these models are not biologically plausible and cannot explain all the aspects of cortical phenomena. This is the reason why in the present work a new model has been proposed. The DNF-SOM satisfies all the requirements of proposition 1 and therefore it is suitable to study self-organization, reorganization and other phenomena in area 3b of primary somatosensory cortex. In the next section the area 3b is modeled by using the DNF-SOM and three major aspects are discussed. The first, has to do with the development of the area 3b. How this area forms the body skin representations and how the touch sense is encoded by the receptive fields of area 3b neurons. The second, is the reorganization of area 3b in the presence of cortical lesions and/or sensory deprivation. And the third one is the effect of attention on neurons of area 3b and on their receptive fields.

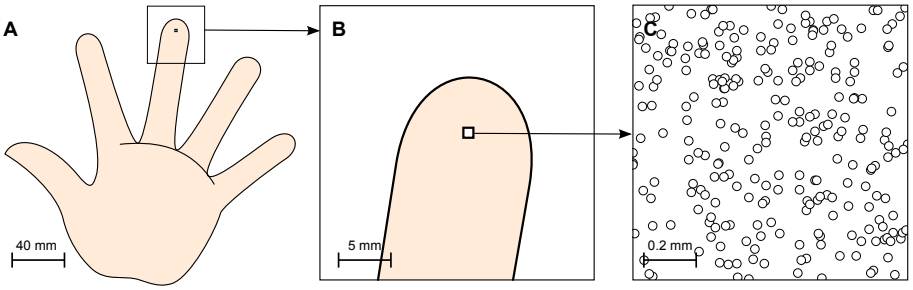

Figure 3.8: **Skin modeling. A** A palmar schematic of the hand. **B** Location and relative size of the modeled skin patch. **C** Magnification of skin patch indicating the topology of receptors.

3.4 Modeling the area 3b of the SI

The primary somatosensory cortex (SI) as it has already been described in the first part of the present work, consists of four areas, 1, 2, 3a and 3b. Each area is devoted to a specific type of sensory information (modality) transmitting by several and different types of receptors spreading on all over the body. Area 3b processes information about the skin surface and touch. Information from four different types of skin mechanoreceptors reach the area 3b. In this section only one part of that information is used in order to model area 3b. The chosen sensory modality is the sensation of touch. The responsible mechanoreceptors for conveying the relevant information are the Merkel's discs. Therefore, one has to model both the skin and the cortex in order to succeed a more biologically plausible model and to study better the underlying cortical phenomena. In the rest of the present section the modeling of area 3b is introduced as well as the development (formation and maintenance) of skin topographic maps. After the development of a topographic map, cortical lesions and sensory deprivations are examined in order to study the behavior of the model under such circumstances. In the end, the effects of attention on area 3b are examined.

3.4.1 Skin model

The skin model provides the proper input to the cortical model through a bunch of receptors that sample the actual stimulus. Equation (3.2) describes the input to the model from a mathematical point of view. The real stimulus is given by the $s(\mathbf{z}, t)$, where $s(\mathbf{z}, t)$ represents the input conveying by the skin receptors (see figure 3.2).

The skin receptors used by the present model are the so-called Merkel ending complexes (MECs) (see chapter 2 for more details). The MECs have been assumed to be on a two-dimensional skin sheet and they are specialized on conveying information related to the modalities of touch sensation and pressure. In figure 3.8 is illustrated a schematic of the MEC receptors on a skin patch of the index finger. This skin patch acts as input layer in the present model, providing the input to the next level of the model.

The skin patch is approximately of size of 1mm^2, using a receptor density of $250/\text{mm}^2$ [55]. It has been modeled as a planar surface $[0, 1] \times [0, 1]$ (arbitrary units) and it is considered that 256 MEC's are arranged in a regular grid over the whole surface with a location jitter of 5%. This results in a quasi-uniform distribution consistent with actual distribution of MEC as reported in [54] and illustrated in figure 3.8C. Each receptor is fully described by its Cartesian coordinates, namely (R_{x_i}, R_{y_i}), where $i \in \{1, \ldots, 256\}$. We assume that when a stimulus is applied at a given location (x, y) of the skin patch, the mechanic property of the skin extends the pressure level to nearby locations [210] such that the response s of any receptor $(R_x,\ R_y)$ is given by:

$$s(R_x, R_y) = \exp\left(-\frac{1}{2}\sqrt{\frac{1}{\sigma}((R_x - x)^2 + (R_y - y)^2)}\right) \tag{3.9}$$

This equation describes the input transduction by skin receptors on a planar rectangular grid, concerning a plain implementation of the model. The toric implementation of the model requires another equation, that best describes the toric nature of the input manifold. Hence,

$$\begin{aligned} d_x &= \min\{|R_x - x|, 1 - |R_x - x|\} \\ d_y &= \min\{|R_y - y|, 1 - |R_y - y|\} \\ s(R_x, R_y) &= \exp\left(-\frac{1}{2}\sqrt{\frac{1}{\sigma}(d_x^2 + d_y^2)}/\sqrt{2}\right) \end{aligned} \tag{3.10}$$

Where the square root of two is a scaling factor due to the distance between two diagonal points. Two diagonal points have a distance either zero or square root of two (i.e. if one applies the Pythagorean theorem on the orthogonal triangle formed by the edges of the skin surface $[0, 1] \times [0, 1]$ ends up to the square root of two, the length of the diagonal). Both equations (3.9) and (3.10) are used with the equations (1.21), (3.4). In addition equation (1.20) is used in order to describe the strength of horizontal cortical connections. By combining all the aforementioned equations and by using a simple sequential training paradigm one can achieve topographic organized maps, as it is discussed in the next sections.

3.4.2 Cortical model

The cortical model is a DNF equipped with a learning rule governed by a differential equation, as it is described by equation (3.1). In order to implement this model a discretization of the DNF equation into a 32×32 grid is used. An FFT algorithm computes the spatial convolution integral of equation (3.1). The lateral connections of the model have been chosen to be a DoG or

a DoE function. The DNF equation each time receives an input and responds with a persistent activity solution (bump). This solution is computed numerically by Euler's forward method (temporally).

In order to be consistent the model with the neurophysiological data, it must follow some general rules and assumptions. The most of the rules are the requirements of the proposition 1. In addition, the model has to follow a specific architecture, which is in accordance with the neurophysiology of area 3b and the somatosensory pathway (as it has been described in chapter two, part one).

The model must receive an input from the environment and then it has to process it in spite of self-organization. This means that a model of the skin is necessary as it has been described in previous chapters and sections. The input from the skin model then is transmitted to the somatosensory cortex for further processing. A schematic view of the architecture of the model

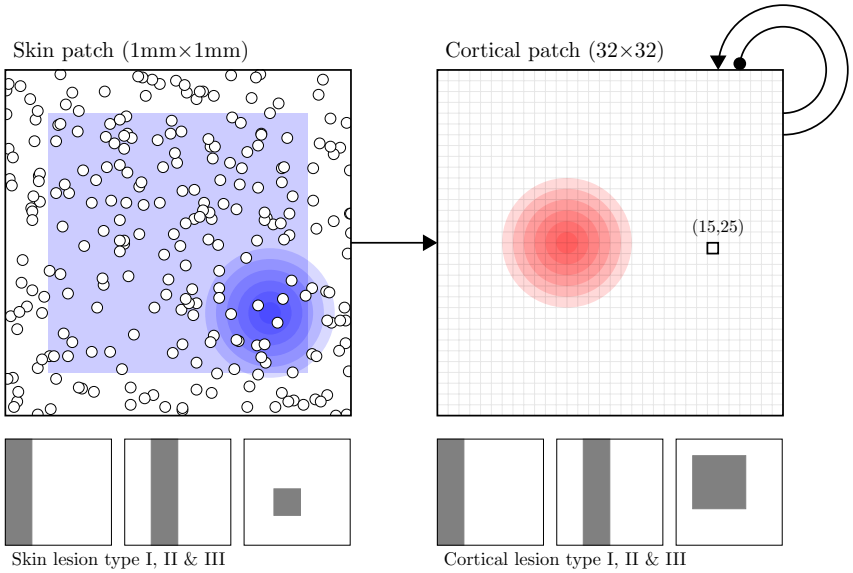

Figure 3.9: **Non-toric model of the somatosensory cortex.** The skin patch is modeled as a set of 256 mechanic receptors (white discs in the figure) with a quasi-uniform distribution that feeds the cortical patch. Blue circles represent an example of a stimulus applied on the skin patch and the blue square represents the stimulation area. The cortical patch is modeled using a neural field with a spatial discretization of size 32×32 elements using global lateral excitation and inhibition. Red circles represent a (schematic) typical cortical response after learning.

is illustrated in figures, 3.9 and 3.10. In figure 3.9 a simple realization of the model on a plane is illustrated. This model will be neglected for the rest of the chapter due to some limitations (see previous section). Instead the non-toric version of the DNF-SOM is used. The input and the cortical sheet has been presumed toric and therefore the boundary problem is vanished. In figure 3.9 the non-toric model is depicted. One can notice that there is a *pac-man* effect (as in the homonym game), where a point can traverse the input space from left to right without gaps and from top to bottom and vice-versa.

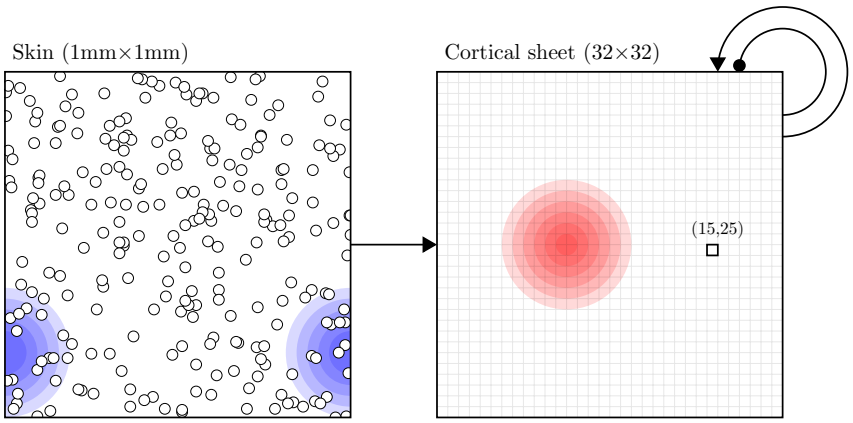

Figure 3.10: **Toric model of the somatosensory cortex.** The skin patch is modeled as a set of 256 mechanic receptors (white discs in the figure) with a quasi-uniform distribution that feeds the cortical patch. Blue circles represent an example of a stimulus applied on the skin patch and the blue square represents the stimulation area. The cortical patch is modeled using a toric neural field with a spatial discretization of size 32×32 elements using global lateral excitation and inhibition. Red circles represent a (schematic) typical cortical response after learning.

3.4.3 Data analysis methods*

Receptive Fields

In order to obtain the receptive fields (RFs) of the neurons, a previously introduced method has been used here, [208]. The RFs plots have been constructed according to the center of mass and the area (size) of each RF. The receptive field of each neuron is computed by using a set of $p \times p$ regularly distributed stimulus $\mathbf{r_i}$ over the set $[0,1]^2$. Each neuron receives input and simultaneously its activity is recorded and aggregated into a $p \times p$ matrix of activities. The center of mass $\mathcal{C}$ is given by the following equation,

$$\mathcal{C} = \frac{\sum_{i=0}^{p^2} \mathcal{V}_i \mathbf{r_i}}{\sum_{i=0}^{p^2} \mathcal{V}_i} \tag{3.11}$$

where $\mathbf{r}_i$ denotes the respective position of stimuli used to compute RF and $\mathcal{V}_i$ is the activity at position $\mathbf{r}_i$. The area of RFs is calculated by using a normalized sum of the elements of RF, p^2, that are greater than a threshold value,

$$\mathrm{RF}_{\mathrm{area}} = \frac{1}{M} \sum_{i=0}^{p^2} (\mathrm{RF}_i > \mathrm{threshold}) \tag{3.12}$$

Where M is the maximum value of $\mathrm{RF}_{\mathrm{area}}$. Using the information given by the area and the center of mass of RFs one can construct plots of RFs on the skin patch with high precision. Each RF lies on the preferred location of the skin and therefore, the topographic organization can be qualified. To some extent the migration and the size adaptation of RFs can be defined, as well. The density of RF over the skin patch has been approximated using a Gaussian filter with

standard deviation of 0.5 in each dimension. This means that for each RF of the model, the density is computed by applying a Gaussian filter according to

$$\mathbf{D}_{\mathrm{RF}} = \mathbf{RF} * G \tag{3.13}$$

Where $\mathbf{D}_{RF}$ is the density of the RF, $\mathbf{RF}$ is a $p \times p$ matrix that represents the receptive field of a neuron and G is a two-dimensional spatial Gaussian filter given by equation,

$$G(x, y) = \frac{1}{2\pi\sigma^2}\exp\Big(- \frac{x^2 + y^2}{2\sigma^2}\Big) \tag{3.14}$$

Where σ is the standard deviation of the Gaussian filter and the mean in this case has been considered zero. Throughout this work the density $\mathbf{D}_{RF}$ is used to compute the density diagrams as for instance the one illustrated in figure 3.19

Histogram of RFs sizes

Histogram of receptive field sizes have been made relatively to the reference period in order to better underline the various changes. Considering the mean size m (mean over the $p \times p$ RF) of an intact topographic map and a second set $\{X_i\}_n$ of observations (the RFs of the reorganized topographic map), histogram is build using set $\{Y_i\}_n$ such that $Y_i = 100 * (X_i - m)/m$ with fixed size bins of width 8%. Any bin with negative width abscissa indicates a shrinking in RF size while positive abscissa indicates an expansion.

Cortical representation

When attention is studied a region of interest is defined on the skin surface. This area acts as the attended skin surface and each time a stimulus is applied on that region an explicit modulation signal is sent to the cortical model (see next sections about attention for more details). In order to compute the cortical representation of RoI, $\mathbf{Cx}^{\mathrm{RoI}}_{\mathrm{area}}$, one can use the aggregation of the activity of the model. In each case the skin patch representing cortically by RoI is stimulated using 4096 well ordered stimuli. Each time the model responds to a stimulus, the response is summed up with all the previous ones. Finally the sum is normalized in order to obtain values in range $[0, 1]$. Hence the cortical representation is a $n \times n$ matrix, where $n \times n$ is the size of the dynamic neural field. Thus the cortical representation is given by,

$$\mathbf{Cx}^{\mathrm{RoI}}_{\mathrm{area}} = \frac{1}{M}\sum_{i=0}^{4096}\mathbf{V}^{\mathrm{RoI}}_{i} \tag{3.15}$$

Where $\mathbf{V}_i$ is the $i-$th $n \times n$ response of the dynamic neural field to the $i-$th stimulus and M is the maximum value of the $\mathbf{Cx}^{\mathrm{RoI}}_{\mathrm{area}}$. The stimulation concerns only the RoI and therefore the responses of the model are focused on the cortical area that represents the RoI. In figure 3.32 is illustrated the cortical representation of each case. In addition the number of non-zero elements of each cortical representation is used in order to compute the size of the cortical representation and to make a juxtapose of real cortical representations the artificial ones (in mm^2).

3.4.4 Development of SI

As it has been mentioned in section 2.2 of chapter 2 the development of the somatosensory cortex is a very complex and long-lasting process starting prenatally in the uterus and continuous

postnatal. The development can be roughly divided into four distinct periods. The most important period is the so-called critical. During this period all the necessary wiring and synapses are established and refined according to experience. After this critical period the brain is still able to learn but with a slower learning rate.

In this context, the model described in the previous sections has been used in order to study the formation and the maintenance of ordered somatotopic maps in area 3b of somatosensory cortex. In spite of achieving this self-organizing map the model (both non-toric and toric) has been trained using 50000 stimuli. The stimuli are two-dimensional Gaussian functions, applied on the skin model. The input space ($[0,1] \times [0,1]$) is discretized and Gaussian functions centers are spread on the input space in a uniform fashion. Each stimulus is a toric (or non-toric depending on the implementation) two-dimensional Gaussian (with variance equals to 0.08 and mean to be variable) reflecting the mechano-elastic properties of the skin and representing the touch modality. Furthermore, a typical stimulus covers an area of $0.24mm^2$ of the skin patch.

The stimuli then are applied and the receptors collect and transmit the corresponding information according to the equation (3.9) and (3.10) for the non-toric and toric model, respectively. The conveyed information to the cortical model is used in order to compute the actual input to the cortical model according to the feed-forward weights, w_f. This is done by equation (3.2). Then $i(\mathbf{x}, t)$ is given to equation (1.21). This last equation is solved by using the forward Euler's method. Then the learning rule, given by the equation (3.4) is applied and hence the feed-forward connections are updated. Then a reset of the activity of the dynamic neural field takes place reflecting the removal of the stimulus from the skin patch. Then the learning process continues by choosing a new input a so on. After the convergence of the learning process, which corresponds to the development stages from a prenatal period to the end of the critical period, a somatotopic map has emerged. As it is depicted in figure 3.11 the receptive fields of the neurons have covered properly the skin surface and thus a topographic map has been formed. In addition, the MSE given by equation (3.7) is illustrated in figure 3.14 suggests that the convergence of the model has been achieved after about 3000 iterations. The simulation has been continued further to 35000 epochs in order to ensure that the whole input space has been properly mapped and that the model is stable enough over time.

During the early stage of the learning process, the response of the field to a stimulus is not null even though feed-forward weights have been set to random values. It displays instead a localized but weak activity as illustrated in figure 3.12A. This is due to neural field properties that guarantee such behavior depending on the amount of lateral excitation and inhibition. This allows most active units to learn the presented stimulus proportionally to their lateral excitation (see equation (3.4)). Once the field has been trained, the response to any stimulus is stronger (see figure 3.12B) as well as the amount of lateral excitation. This results in an increased learning rate for a stimulus that is already known to the model and thus, it does not change drastically the feed-forward weights anymore. This is a key point of the model since we'll see in next subsection how this active learning rule may help to recover from lesions. The evolution of the RF of a neuron (number $[15, 32]$) is illustrated in figure 3.13 demonstrating its evolution over time. Initially, the neuron is mostly silent, but after 500, 1500, 5000 and 25000 presented stimuli, one can see the development of the RF that is finally precisely tuned for a specific set of stimulus location. This evolution has been done in two phases. In the first phase, RF is extended and covers a large part of the skin and as the training process goes on, the RF becomes refined and covers only a small part of the skin (during the second phase). Subsequently, the emergence of such an ordered topographic map tends to confirm that thalamocortical connections are an adequate site of plasticity for both the formation and the maintenance of topographic representations. In this context, lateral connections mainly serve as support for competition at the cortical level for the

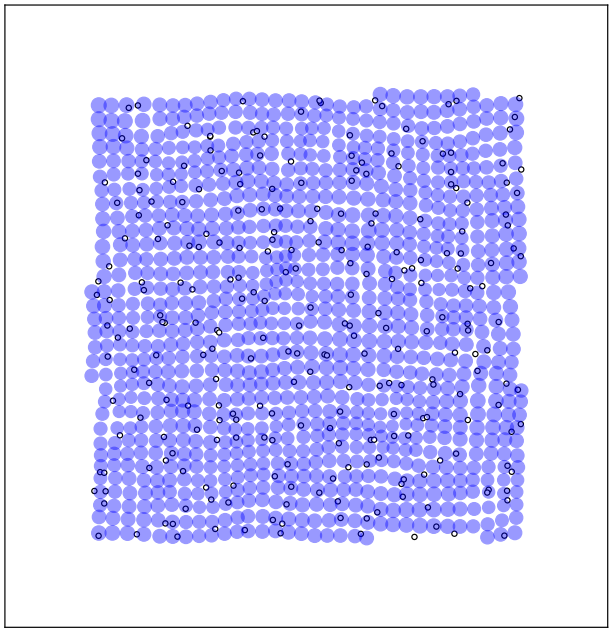

Figure 3.11: **Receptive fields of neurons on the covered skin surface.** The blue discs represent the receptive fields of neurons and the black discs represent the Merkel skin receptors. The center of mass of each RF has been computed according to equation (3.11) and the area (is reflected by the area of each disc) according to equation (3.12).

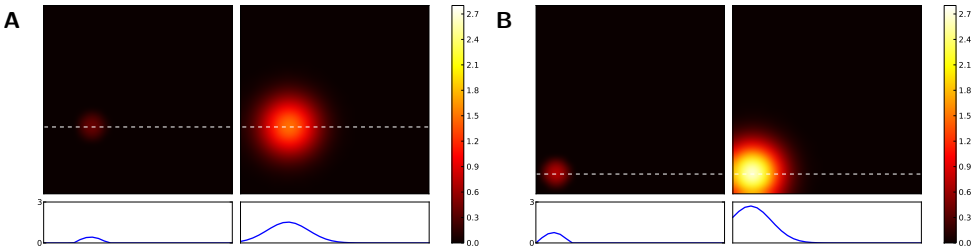

Figure 3.12: **Response of the model and lateral excitation.** The response of the model and the amount of lateral excitation at a specific site (center of activity). Plots represent the response profile corresponding to the dashed lines. **A** Before learning. **B** After learning.

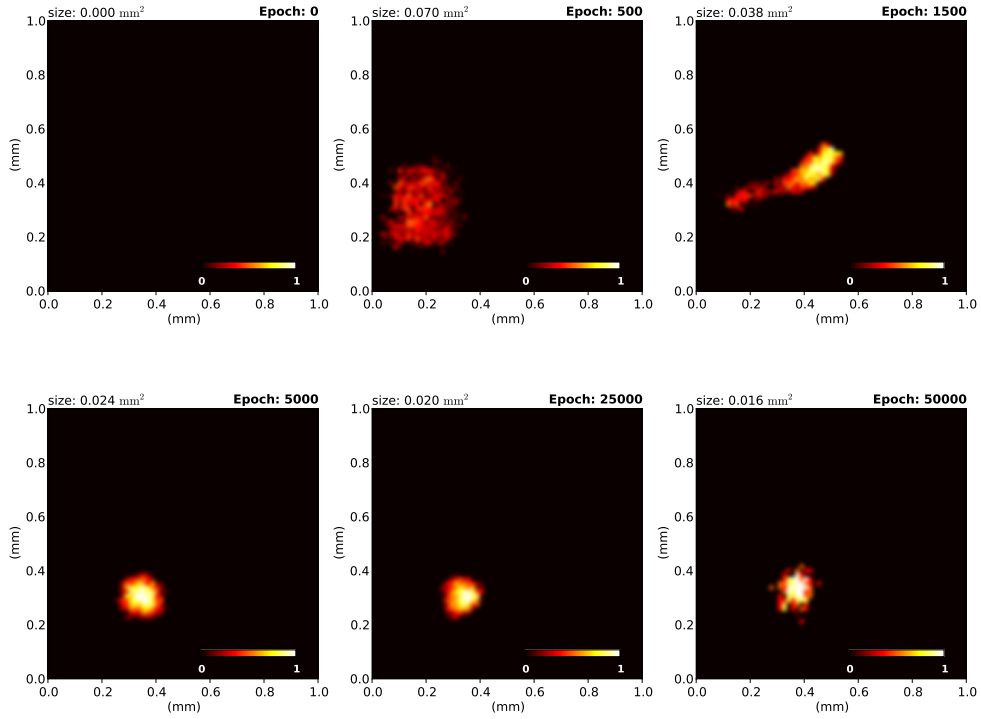

Figure 3.13: **A receptive field evolution over time.** The receptive field of neuron numbered $[15, 32]$ is illustrated as it is established during learning process. At the beginning (epoch 0) there is no at all a response to the stimuli but at the end of the learning process (epoch 50000) a well-shaped receptive field has emerged.

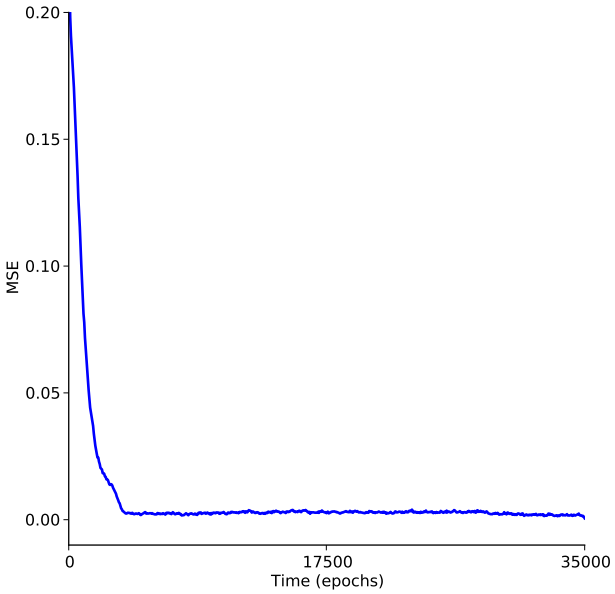

Figure 3.14: **Mean-squared-error** Equation (3.7) has been computed after the training of the model. At each epoch the feed-forward thalamocortical weights w_f are stored. After training the off-line omputation of MSE takes place.

emergence of a unique bump of activity that drives learning process.

3.4.5 Replication of DiCarlo protocol

In order to validate the model and to verify that it is capable of explaining real neurophysiological data, the DiCarlo drum protocol method has been implicated. The drum protocol is described in [211] and it has been used to investigate the two-dimensional structure of area 3b neuronal receptive fields (RFs) in alert monkeys.

Drum protocol

The drum protocol is a direct adaptation of the protocol that has been used in [211]. The main idea is that a cylindrical drum carrying random dot patters is moving while the index finger of a monkey touches it. At the same time the activity of the neurons of area 3b is recorded. In the context of the present computational model the drum has been simulated as a plain surface of size 250mm×30mm. The skin is moved over the full length (40mm/second) before jumping back to the start and shifting up the patch by 200μm. The drum surface is made of 750 uniformly distributed dots, achieving a mean density of 10 dots/cm^2. Using a sample timestep of 5ms, the model is fed with 120000 samples for a complete sweep of the drum surface. Activity of all neurons are recorded at once without centering the drum onto each individual receptive field.

Extended Receptive Fields

The extended receptive fields (eRFs) of the neurons are computed by applying the drum protocol according to [211]. In this article the analysis of the receptive fields has been done by using a method similar to reverse correlation. The proposed in [211] method is a generalization of reverse correlation and thus is more exact. Therefore, the predicted impulse rate of a neuron in response to the nth stimulus is called $r_{\text{predicted}}$. $r_{\text{predicted}}$ is defined to be the sum of the effects of each skin subregion to the neuron (see drum protocol for more details). Hence,

$$r_{\text{predicted}} = b_0 + \sum_{i=1}^{p} b_i x_i(n) \tag{3.16}$$

Where n is the number of the stimuli, p is the number of the different skin subregions, x_i is the stimulus relief, b_0 is the background firing rate and b_i is the strength of the effect of a dot (since the stimulus each time is a random dot pattern). Rewriting equation (3.16) in vector form one ends up to,

$$\mathbf{r}_{\text{predicted}} = \mathbf{Xb} \tag{3.17}$$

Where $\mathbf{r}$ is a $n \times 1$ vector of the firing rates, $\mathbf{X}$ is a $n \times p$ matrix with values of ones in the first column and the stimuli in the remaining columns. Finally $\mathbf{b}$ is a $p \times 1$ vector, which contains the weights of the effect of a stimulus to the neuron. This term is actually the extended receptive field of a neuron, since its values indicate the way that a stimulus affect the firing rate properties of a neuron. In addition, $\mathbf{b}$ can be used in order to investigate further the optimality of each stimulus, in terms of neural responses. Besides the predicted firing rates, a vector of observed discharge rates for every neuron is used, $\mathbf{r}_{observed}$.

In order to compute the vector $\mathbf{b}$, which minimizes the mean-squared error between $\mathbf{r}_{\text{predicted}}$ and $\mathbf{r}_{\text{observed}}$, one has to solve the linear normal equations $\mathbf{X}^T\mathbf{Xb} = \mathbf{X}^T\mathbf{r}_{\text{observed}}$. Therefore, in

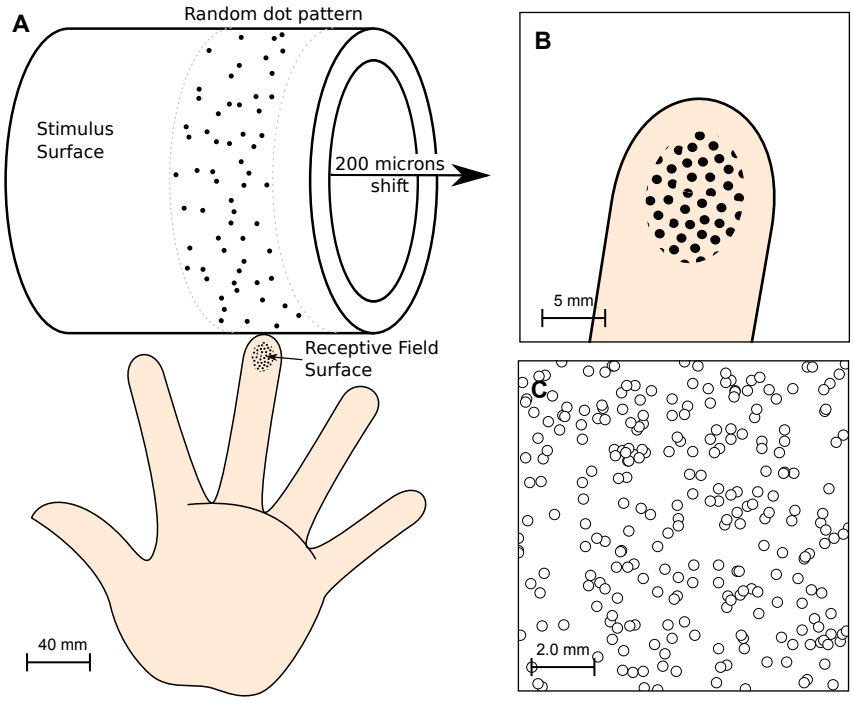

Figure 3.15: **Stimulus.** The stimulus pattern is a field (28×250 mm) of randomly distributed, raised dots mounted on the surface of a drum [211]. The drum rotates at a constant angular velocity to produce proximal-to-distal motion at 40 mm/sec. After each rotation, the drum is translated by 200 μm along its axis of rotation. The recording period yielding the data for a single RF estimate typically involved 100 revolutions and lasted 14 min for a total of 120000 samples. **Fingerpad.** The fingerpad patch is approximately of size 10mm^2, using a (sparse) receptor density of 2.5/mm^2. It has been modeled as a plain surface and it has been considered that 256 MEC's are arranged in a regular grid over the whole surface with a location jitter of 5%. This results in a quasi-uniform distribution consistent with actual distribution of MEC as reported in [54].

order to solve the equations, the inverted stimulus autocorrelation matrix is used and thus,

$$\mathbf{b} = (\mathbf{X}^T\mathbf{X})^{-1}\mathbf{X}^T\mathbf{r}_{\text{observed}} \tag{3.18}$$

By applying this method one can compute the extended receptive fields, **b** for all the neurons. This method indicates the spots on the skin that contribute positively to the firing rate (excitatory part) or negatively (inhibitory part). For more details about this method refer to [211].

Signal-to-noise ratio (SNR) and Noise Index (NI)

When the threshold method is applied (see below section "Structure of extended receptive fields"), the SNR and the Noise Index are computed as well. From signal processing definition, noise is defined to be the residual of the subtraction between an original signal s and the filtered one $\bar{s}$ In this work, the original signal is the receptive field and the filtered signal is the receptive field after the application of a Gaussian filter with zero mean and variance 1.7. SNR is given by $SNR = 10\log_{10}\left(\frac{S}{N}\right)$, where S is the power of the original signal s and N is the noise power. The SNR for each RF was measured and the mean values of SNR was 8 (S.D.=1.5).

In addition, and in accordance with DiCarlo et al. [211], the Noise Index (NI) has been also computed according to equation $NI = 100\frac{\text{Var}[noise]}{\max\{|s|\}}$. NI is given in terms of the absolute peak of the original signal s. The Noise Index for each of the RF was measured and the mean value was 1.5% (S.D.=0.01). Conclusively, both measures SNR and Noise Index pinpoint that the noise was eliminated.

Spatial Event Plot

The alignment of the stimulus and the responses of a specific neuron, during the execution of the drum protocol, has been done by applying the spatial event plot method, described in [212] and also used by DiCarlo et all in [211]. The latter uses a variation of SEP method in order to achieve better resolution. In this work the very first version of the method is used, since the main results are outcomes of a computational model and therefore there is no need for a high resolution method.

The receptive field (eRFs) of a specific neuron is isolated. Then the drum protocol is applied as it has been described in previous paragraphs. During the execution of the protocol a recording of all responses of the neuron are recorded. After the simulation of the protocol, the array of the responses is processed by assigning ones to that elements that contain an evoked response and zeros otherwise. Because the events array is one-dimensional, a transformation is necessary in order to fit the responses on the proper locus of the drum (input space). Therefore, starting from the lower right corner of the drum (where the first stimulus was applied) and continuously skimming the array one can assign correctly the response events to the corresponding stimuli. The SEP of the drum protocol is illustrated in figure 3.16**B**.

In addition to SEP, the predicted responses plot has been also used. In this case the stimuli (dot patterns) are convolved with the extended receptive field (RF) of a specific neuron in order to obtain a prediction of the responses to each stimulus. This method leads to the results depicted in figure 3.16**A**.

Structure of extended receptive fields

Following the learning stage where RFs have been shaped (see [208]), the structure of the receptive fields by applying the DiCarlo's protocol has been studied. The results are illustrated in figure

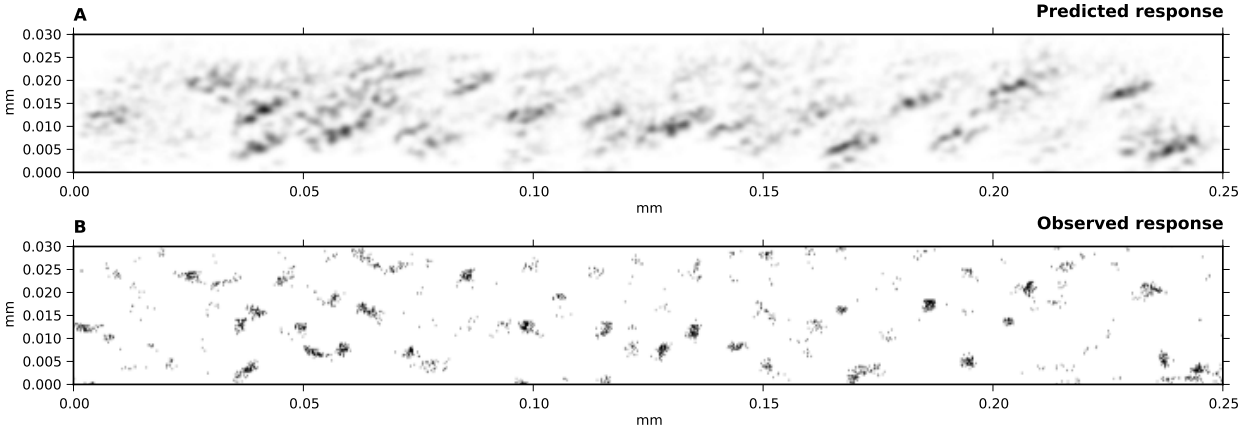

Figure 3.16: **Observed and predicted responses. A** Neural impulse rates of the neuron $(20, 16)$. In order to obtain this plot, a convolution of eRF of the neuron with the random dot stimulus is necessary. **B** Spatial event plot of neuron $(20, 16)$. Each dot represents the side where a stimulus triggers a response of the neuron. The axis x and y represent the length and the width of the drum (drum protocol, see the main text) in mm, respectively.

3.15. In order to reduce the noise one can follow the proposed method in [211] and, for each matrix representing a receptive field, first can convolve it with a Gaussian filter ($\mu = 0$ and $\sigma = 1.7$) and apply a thresholding (10% of the absolute peak value) on every value. If a value was below the threshold, it is set to zero. Each pixel of the receptive field is let to have at least two of the four neighbors non-zero and of the same sign such that isolated islands of positive or negative values are not allowed if they have a total area less than $0.7mm^2$. Each time a RF is computed, the signal-to-noise ratio (SNR) as well as the noise index are computed, in order to constraint them to low values. After this preprocessing stage, the respective size of excitatory (positive) and inhibitory (negative) areas is measured. The minimum, mean and maximum values of excitatory RFs are 7.7, 13, $20mm^2$, respectively. In same order, the values of the inhibitory RFs are 4.24, 15, $26mm^2$, respectively. Furthermore, in logarithmic scale the mean, the standard deviation and the geometric mean for both the excitatory and the inhibitory RFs have been computed. Hence, for the excitatory RFs are 1.12, 0.06, 13.22 ($\log_{10}$ units) and for the inhibitory ones 1.16, 0.11, 15, respectively. Moreover, the Pearson correlation points out no any significant correlation between the excitatory and inhibitory distributions ($\rho = 0.17$). Figure 3.17 shows the bivariate plot of excitatory versus inhibitory area. A k-means classification of the RFs was applied on the RFs in order to compare the number of RFs classes of our model with [211]. The k-means classification separated 16 different classes depending on the topology of the excitatory and inhibitory areas (homogeneity = 0.39, completeness = $1, 0$, V-measure = 0.56). As in [211], receptive fields whose excitatory area is surrounded by the inhibitory one as well as receptive fields whose excitatory area is opposite the inhibitory area, have been found. It is to be noted that figure 3.17 shows a remarkable similarity with physiological results of DiCarlo (on three alert monkeys), where most of the RFs are centered around a central point of 15mm^2 (excitatory) / 15mm^2 (inhibitory). The spread is larger in the case of DiCarlo but this is expected since a toric stimulation model has been used and the RFs have not been centered.

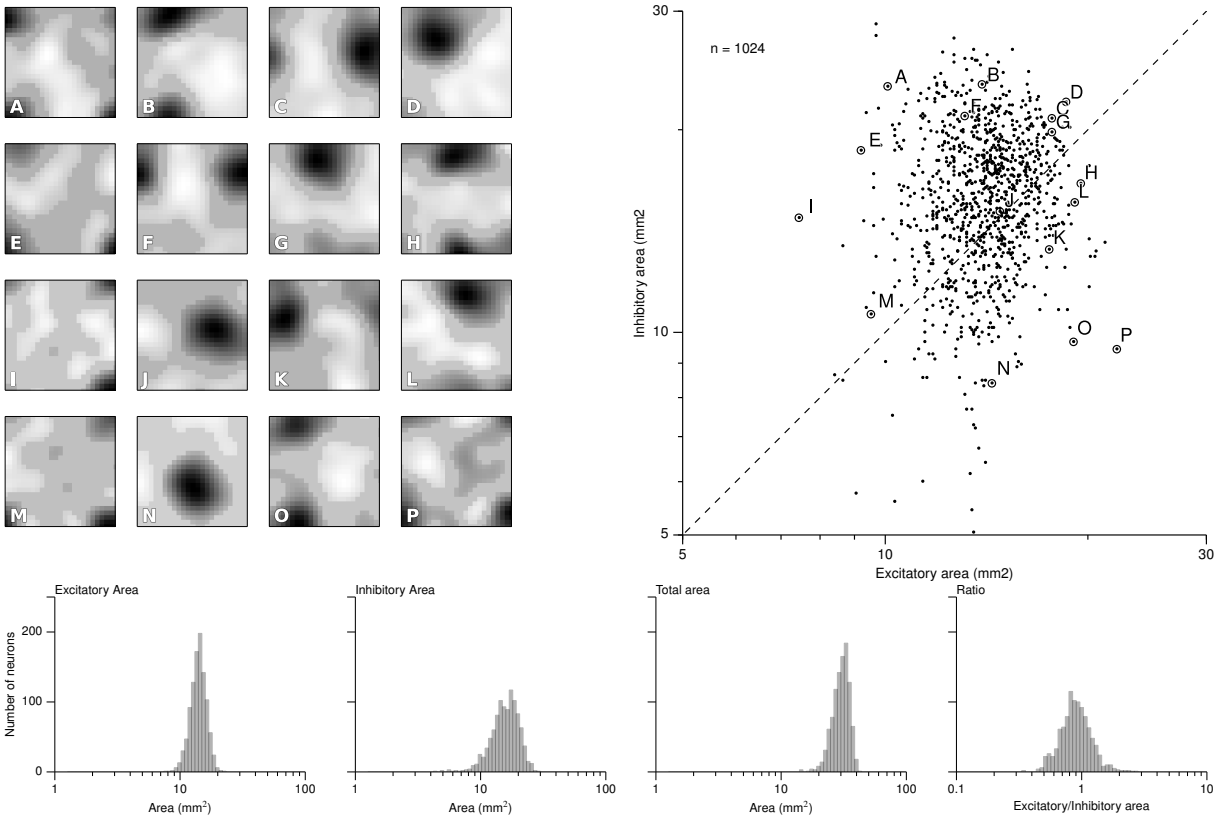

Figure 3.17: **Extended RFs.** From the experimental drum protocol of [211], 120000 responses for each of the 1024 neurons of the model are recorded and the same analysis has been applied in order to obtain the respective RF (non centered). The scatter plot on the *right* displays the balance between excitatory and inhibitory components of each RF. Excitatory area was measured as the total positive area in the thresholded RF (positive RF regions with values greater or equal than 10% of the peak absolute RF value). Inhibitory area was measured as the total negative-thresholded RF area (negative RF regions with absolute values less or equal of 10% of the peak absolute RF value). The *left* part of the figure illustrates the diversity of RFs and the letter above each RF is keyed to a point in the scatter plot. The bottom row shows the distributions of the sizes of RFs. The y-axis indicate the number of neurons (n=1024) and the x-axis, from left to right displays the excitatory area of RFs, the inhibitory area, the total area (is the sum of the excitatory and inhibitory areas) and the ratio of excitatory area to inhibitory one.

3.4.6 SI cortical lesions

As it has been mentioned in chapter 2 of first part, somatosensory topographic maps are able to reorganize themselves in the presence of a cortical lesion or a sensory deprivation. In this section, cortical lesions have been taken into consideration and the reorganization of somatosensory topographic maps is under investigation.

In simple words a cortical lesion is nothing more than a damage of neurons. This means that previously operational neurons, after a cortical lesion are dead and cannot respond to any kind of information. This, in turn, causes a dramatic alteration of topographic organization, since many of the body representations does not exist after a cortical lesion, rendering many of the body functions problematic. In the context of the present model a cortical lesion corresponds to a mask applied on the cortical sheet and on the feed-forward connections, making them completely silent. A lesion mask is nothing more than a matrix with the same dimensions of the dynamic neural field (for the feed-forward weights is used the same mask but in a higher dimension depending each time on the experimental set up) containing ones and zeros. When a cortical lesion is caused the non-zero elements of the mask have to be defined. The zeros are put where one would like to apply the lesion (kill the neurons). At each time time step of the model simulation (learning process) the activity, the lateral connections and the feed-forward thalamocortical connections of the model are multiplied in an element-wise fashion with the mask. In a similar way one can cause a skin lesion by applying the same types of masks but of different size. In a more mathematical context a lesion can be considered as a Hadamard product. Thus if $\mathbf{L}$ is the lesion mask matrix and $\mathbf{V}$ is, for instance, the activity of the dynamic neural field then $\mathbf{V}_{\text{lesioned}}$ is the lesioned activity given by,

$$\mathbf{V}_{\text{lesioned}} = \mathbf{V} \circ \mathbf{L} = V_{ij} \cdot L_{ij} \tag{3.19}$$

In figure 3.9 are illustrated the three main types of lesions that have been applied throughout the present work. Type I is a stripe-like cortical lesion applied at the border of cortical sheet. Type II is a stripe-like cortical lesion applied within the cortical sheet. This particular kind of lesion divide the cortical sheet into two separate parts. Finally, Type III cortical lesion is a rectangular-like lesion, applied at the center of cortical sheet.

All the aforementioned lesion masks have been used in order to study the reaction of the model in a lesion condition, and how it reorganizes the cortical representations by virtue of recovery. Therefore, all the three types of lesion are almost 25% of the cortical sheet in extent. After the convergence of the learning process and the emergence of a topographic map as it has been described in the previous section, a mask of Types I, II and III are applied and after 50000 presented stimuli a reorganization of the topographic map has taken place. In figure 3.18 are illustrated the histograms of receptive fields sizes of a topographic map before and after cortical lesions. Comparing the RFs size before and after cortical lesion, they have been clearly altered. After lesion, RFs tend to become larger and consequently to respond to larger skin areas. More precisely, RFs size after lesion is almost twice bigger compared to pre-lesion ones. This is quite consistent with [113] who reported similar results with the noticeable difference, that weeks after a lesion, cortex is able to completely recover, having its neurons RFs sharpened. This is because of re-establishment of inhibitory connections and/or sprouting of neural axons as it has been proposed by [70]. Consequently, the refinement of RFs arises in two phases. During the first phase, there is an expansion of RFs towards lost territories followed by a shrinkage. In this model such a shrinkage has not been noticed because the lateral connections are fixed and a modification is not permissible. This leads to the assumption that lateral connections are crucial for development of stable representational maps. Neurons are not able to precisely refine

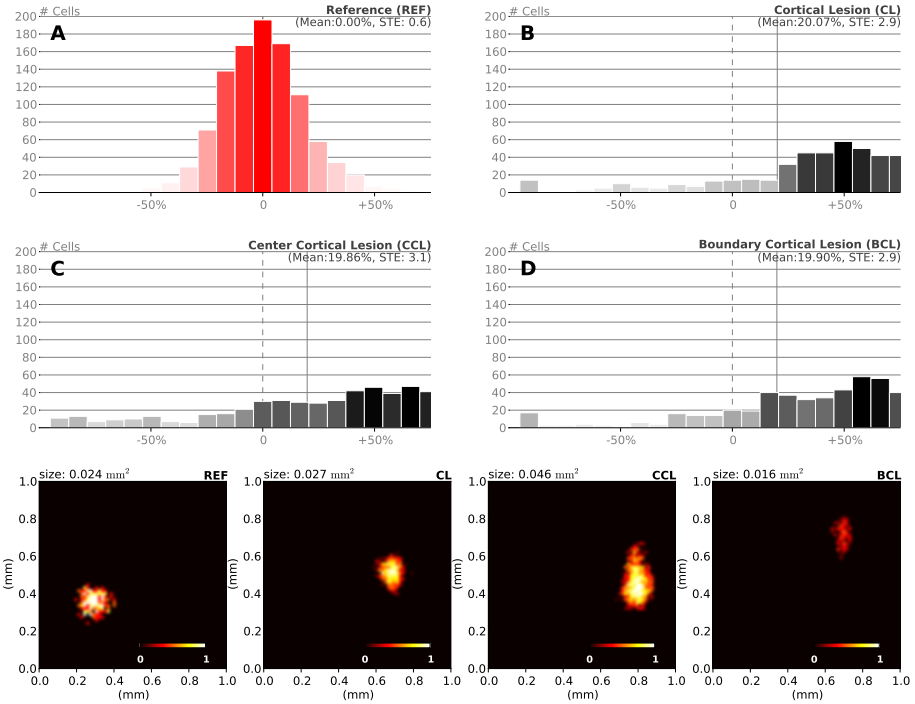

Figure 3.18: **Size histogram of cortical lesions.** **A** Histogram of receptive fields sizes of reference case. Reference case is the intact topographic map as it has emerged through the learning process described in previous section. **B** Size histogram of receptive fields of cortical lesion of Type II. **C** Size histogram of receptive fields of cortical lesion of Type III and **D** Type I. At the bottom row is illustrated a receptive field of a specific neuron after reorganization due to cortical lesions.

their RFs since there is no balance mechanism between excitation and inhibition within cortical circuits. In [82] it is indicated that intralaminar excitatory connections are the major factor for expansion of RFs.

Another interesting and important part of reorganization is the migration of RFs of neurons. This migration of neurons takes place in order to cover the whole skin surface again and non-functional representations (just after lesion) have been *recaptured* by neighboring units. The model is able to respond again to stimuli applied on areas innervating neurons within the lesioned cortical area. This indicates that other neurons took over and recovered from lesion by migrating their representations towards the lost ones, making the cortical patch fully functional again. In figure 3.19 are illustrated the density plots that indicate the order of neurons receptive fields migration. As it is depicted in the figure 3.19, migration takes place and the remaining intact

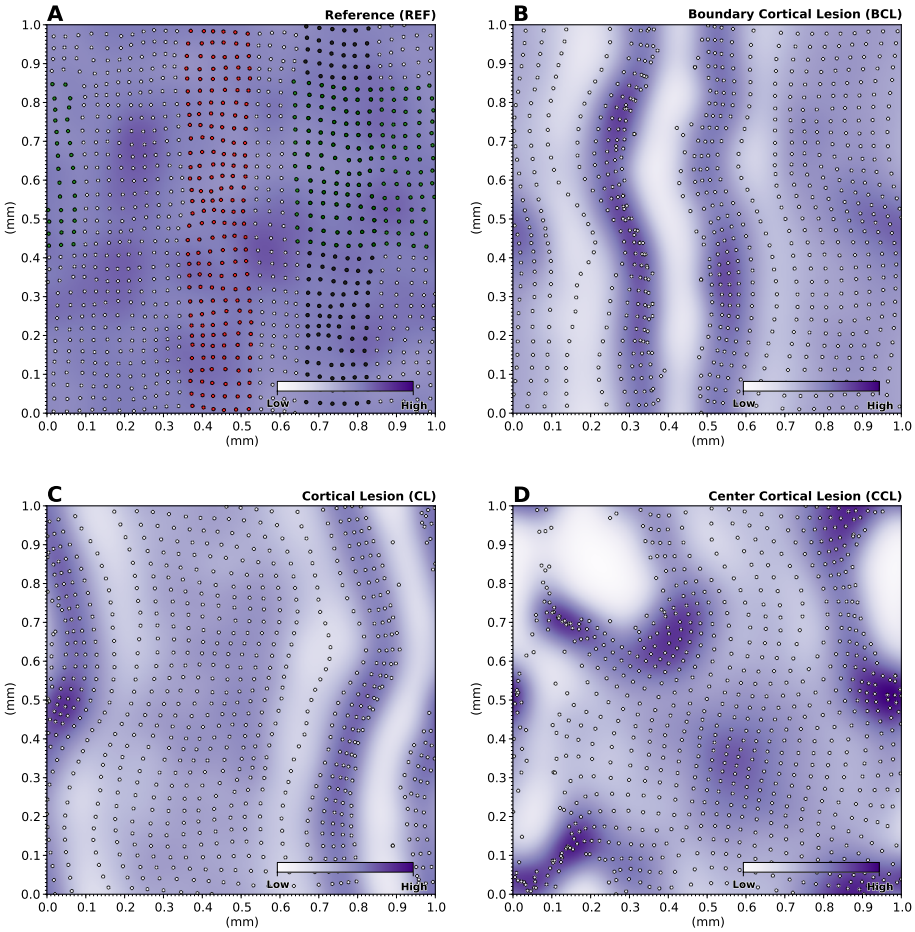

Figure 3.19: **Density and migration graphs.** Density is represented as a mauve color and the white dots represent the center of masses of receptive fields of **A** intact topographic map, **B** cortical lesion of Type II, **C** Type III and **D** Type I. The colored dots in panel A represent the affected neurons receptive fields. Red dots indicate the boundary lesion (type I), black dots represent the cortical lesion (type II) and greed dots designate the center cortical lesion (type III).

neurons try to cover the non-representative part of the skin. An interesting remark is the abnormal gathering of neurons receptive fields on the borders of the lesion. The density graph of the intact topographic map expresses an almost uniform distribution of receptive fields on the

skin patch. In the lesion cases represented in panels B, C and D of figure 3.19 the density of the receptive fields has changed dramatically. Furthermore, a high density of receptive fields is observed around the skin representation of damaged neurons, indicating the trying of the intact neurons to take over. In this case, if the lateral connections are allowed to reorganize it is likely to obtain a fully reorganized topographic map.

3.4.7 Sensory deprivations and SI

Beyond cortical lesions, there exist also other kinds of lesions, which can cause reorganization of the somatosensory topographic maps. Such lesions have to do directly with the sensory information provided by the skin receptors to the somatosensory cortex. This kind of lesion is named sensory deprivation and it has to do with the lack of sensory input to the CNS. For instance, damaged sensory nerves or physical damages to the receptors can lead to the lack of sensory information.

In the present thesis such a lesion is modeled by silencing a specific amount of skin receptors ($\sim 45\%$ in all simulations) such that only a subpart of previously sensory information is available to the cortex. A lesion is made onto two specific areas which are referred to as lesion type I and type II (see figure 3.9).

Starting from an intact topographic map, the model is let to learn 50000 stimuli, but using the lesioned skin patch. After the learning period a new topographic map has emerged. In figure 3.20 is depicted the histograms of sizes of receptive fields of sensory deprivations of Types I and II, respectively. As it is concluded from the results illustrated in figure 3.20 the size of the receptive

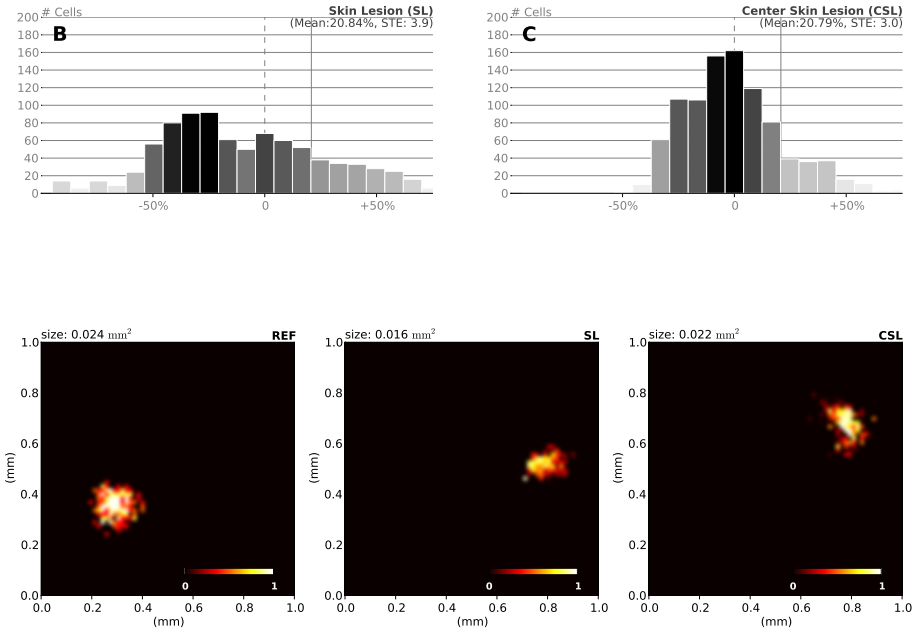

Figure 3.20: **Size histogram of sensory deprivation.** **A** Histogram of receptive fields sizes of reference case. Reference case is the intact topographic map as it has emerged through the learning process described in development section. **B** Size histogram of receptive fields of sensory deprivation of Type I. **C** and of Type II. At the bottom row is illustrated a receptive field of a specific neuron after reorganization due to cortical lesions.

fields is affected directly by the sensory deprivation. Affected neurons by sensory deprivation,

tend to expand their receptive fields in order to capture new inputs. The most dramatic changes take place in the case of sensory deprivation of Type I. In this case the relative size of receptive fields has moved to the right indicating an expansion of receptive fields. Although, the size of the receptive fields remain large and there is no shrinkage during learning. This is due to the fixed lateral connections. This means that neurons are able to receive proper excitation and inhibition conserving the competitive nature of the reorganization process. Nevertheless, a better refinement could be possible by using a learning rule also for the lateral connections (it has been left as future work).

Furthermore, reorganization has been achieved in two major phases. At the beginning, each neuron innervated by deprived skin area, undergoes an expansion of its RF simultaneously with a spatial shifting in order to capture a new skin area (first phase). This lasts almost during the whole retraining process. Near the end of training process the affected neuron has shrinked its RF (second phase). Similar to this finding, Foeller in [126] proposes a three-phases model of the RFs reorganization. In the first phase and due to reduction of inhibitory connections the RFs expand their size. During the second phase, a further increase of RFs size is taking place because of homeostatic plasticity of GABA circuits. Finally, in the third phase, a shrinkage of RFs around their new centers occurring as it is driven by re-established inhibitory connections. After a sensory deprivation there exist also a migration of receptive fields of neurons towards new territories just like in the case of a cortical lesion. In this case the neurons tend to move their receptive fields far away from the damaged area in contrary to the cortical lesion, where neurons tend to move their receptive fields toward the body representations that they have lost their representative neurons. This migration towards the unaffected skin regions take place in order to provide new information to the neurons. In figure 3.21 the receptive fields density graph is illustrated for three different cases. In the first panel there is the intact topographic map receptive fields density, which is more or less uniform. In the panel B of the same figure a stripe-like skin deprivation in the middle of the skin patch forces the neurons to move their receptive fields away from the damaged area. In the third panel (C) a skin deprivation centered at the middle of the skin patch causes the migration of the neurons also away from the damaged area. Neurons, in both sensory deprivation cases, establish new input connections and therefore a migration of their receptive fields to the new skin regions takes place.

3.4.8 Some results of the non-toric version

In this section are illustrated the results of the non-toric version of the model and a more detailed neurophysiological interpretation of the results as well. As it has been mentioned, the model has been implemented on a torus in order to avoid some well-known boundary effects. However, a non-toric version of the model has been implemented, which reflects some interesting properties as well. This means that the equation (3.1) has been used and solved on a two-dimensional plane surface and not on a torus. The receptors sample the applied stimulus each time according to equation (3.9) and the interval of stimulation is the rectangle $[-0.75, 0.75]^2$ instead of $[0, 1]^2$ of the toric version.

In order to train the model in this case a set of 10000 two-dimensional Gaussians has been used. The center of each Gaussian is randomly chosen during the training and lies within the interval $[-0.75, 0.75]^2$. During the early stage of the learning process, the response of the field to a stimulus is not null even though feed-forward weights have been set to random values. It displays instead a localized but weak activity due to neural field properties that guarantee such behavior depending on the amount of lateral excitation and inhibition.

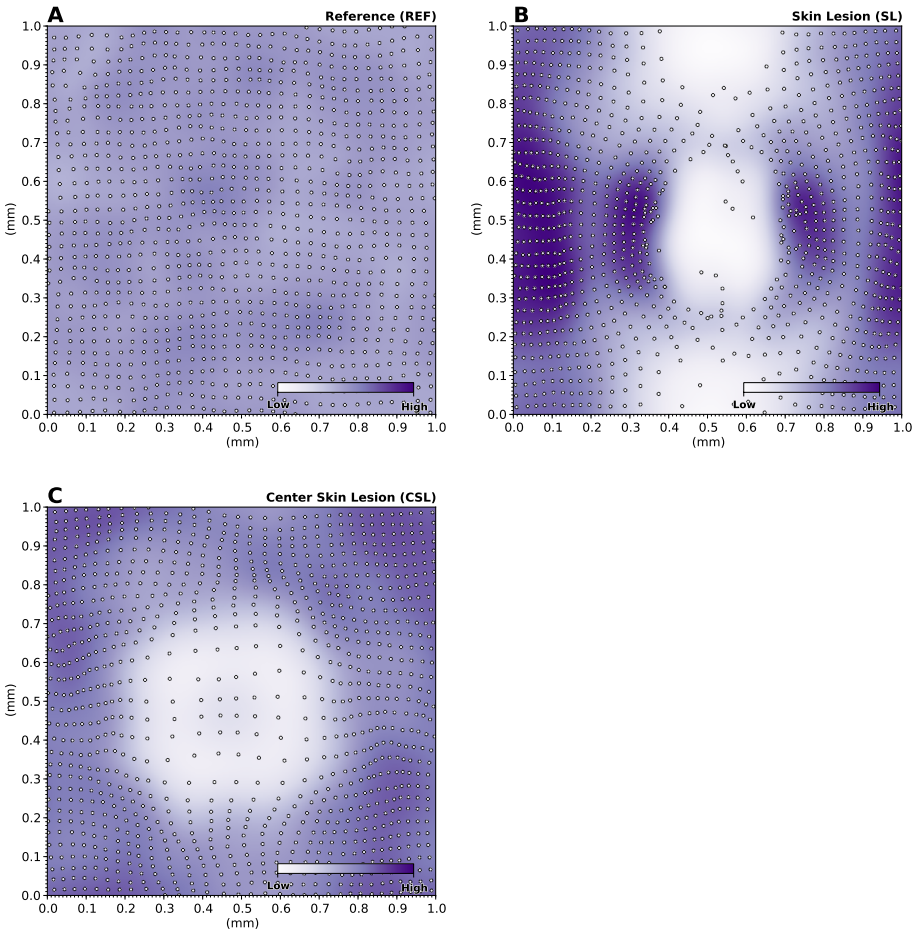

Figure 3.21: **Density and migration graphs.** Density is represented as a mauve color and the white dots represent the center of masses of receptive fields of **A** intact topographic map, **B** sensory deprivation of Type I, **C** and Type II.

Emergence of ordered topographic maps

After the training period the model has converged to a topographic map as it is illustrated in figure 3.22. The evolution over time of the RF of the neuron (number $(25, 15)$) is depicted in figure 3.22A. Initially, the neuron is mostly silent, but after 1500, 3500 and 10000 presented stimuli, one can see the development of the RF that is finally precisely tuned to a specific set of stimulus location. This evolution occurs in two phases. In the first phase, the RF is extended and covers a large part of the skin, then in a second phase, as the training process goes on, the RF shrinks and covers only a small part of the skin.

Each neuron now responds preferentially to a specific skin region. Moreover, figure 3.22C shows the response of the model (after training) to 10×10 different stimuli. It is quite clear that a topographic map has emerged. Each block in this figure represents a response of the model to a specific stimulus (e.g. the block at the upper left corner represents the response of the model to a stimulus at the upper left corner of the skin grid) providing a way to verify self-organization and also provides a frame of reference of the receptive field location on the skin patch. Similar results are illustrated in figure 3.22B where equation (3.11) has been used in order to compute the location of each receptive field on the skin patch. The radius of each circle has been calculated by using the size of each RF.

In addition, the distribution of RF sizes can undergo alterations during training. Panel 3.22E shows the distribution of RF sizes before any learning occurs in the model. As one expects, there is no RFs at all since the neurons have not yet learned anything. However, once learning is finished, one can see in figure 3.22F the normal-like distribution of the RF sizes. There is a high-value component near zero which indicates a large number of very small RF sizes that is due to side (border) effects of the neural field. Other RF sizes follow a normal-like distribution with mean 0.02246 (SD= 0.01190). This indicates that there is a better acquisition of RFs at the center of the field than at the periphery. Combining all the aforementioned results one can conclude that the model has achieved proper self-organization. Subsequently, the emergence of such an ordered map tends to confirm the initial hypothesis that thalamocortical connections are an adequate site of plasticity for both the formation and the maintenance of topographic representations. In this context, lateral connections mainly serve as support for competition at the cortical level for the emergence of a unique bump of activity that drives learning.

Reorganization after a skin lesion

As in the case of the toric version of the model, the sensory deprivation test case has been applied on the non-toric version as well. The sensory loss can be caused by damaged sensory nerves or physical damages to the receptors. This has been modeled by silencing a specific amount of skin receptors (25% in type I and type II skin lesions and 9% for type III skin lesion) such that only a subpart of previously sensory information is made available to the cortex.

Following a skin lesion of type I, the model has been retrained over 10000 epochs using the same set of stimuli as before but with missing values from disabled receptors. Panel 3.23A shows the temporal evolution of the receptive field of unit $(25, 15)$ and figure 3.23C shows the overall reorganization of representations that has occurred according to the response of the model to 10×10 different stimuli. This is most clearly illustrated in figure 3.23B that displays the preferred location of units that do not intersect with the skin lesioned area. Comparing the RFs illustrated in this figure with the ones in figure 3.22B, one can conclude that the sizes of RFs which were previously innervated by the lesioned skin area are now larger. This is because neurons lost their preferred input and therefore the balance of excitation and inhibition is disrupted. Therefore

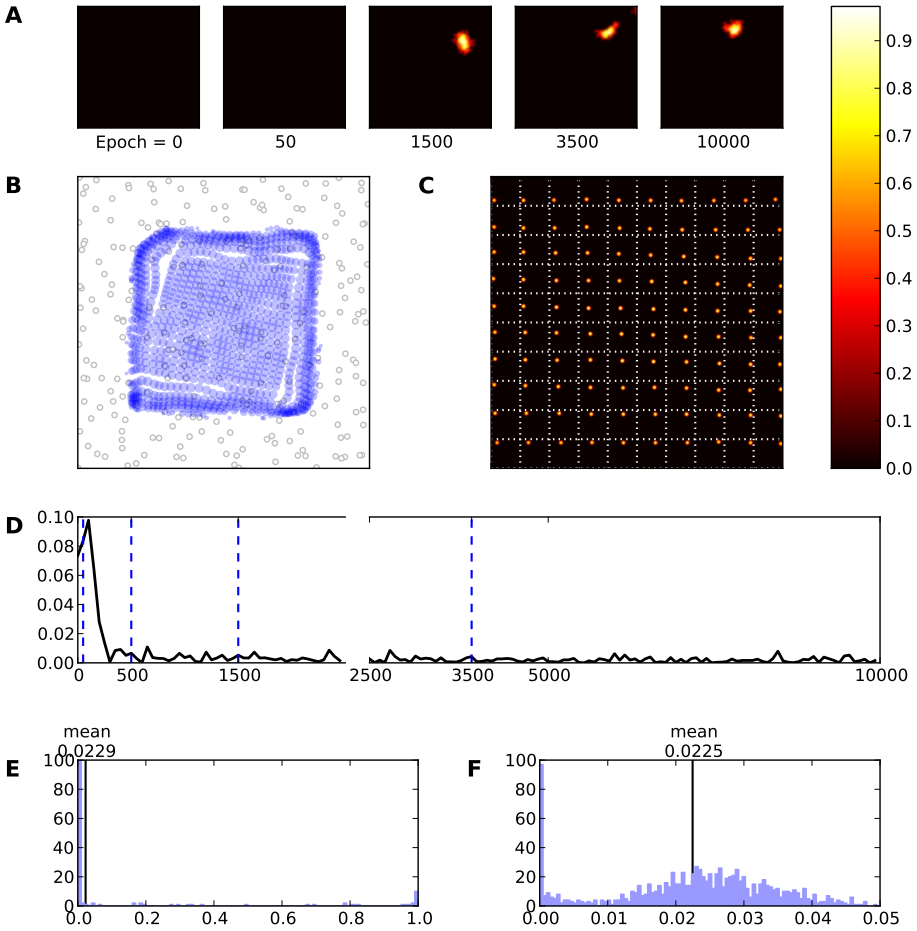

Figure 3.22: **Intact model A** Evolution of the receptive field of neuron $(25, 15)$ during learning. The neuron is initially silent (epoch 0) but learns quickly to answer to a large range of stimuli (epoch 1500) until finally settling on a narrower range of stimuli. **B** Receptive fields of the whole model. Each blue circle represents a neuron. The center of the circle indicates the (converted) receptive field center and the radius expresses the (relative) size of the receptive field. **C** Response of the model (after learning) to a set of 10×10 regularly spaced stimuli. Each square represent a response to a specific stimulus. **D** This represents the mean evolution of thalamo-cortical weights of neuron $(25, 15)$ during learning (i.e. $\mathcal{E}_{(25,15)}$). **E** & **F** Histogram of receptive field sizes (100 bins) before (E) and after (F) learning. The final distribution is Gaussian-shaped centered around a mean value of 0.02246. Is is to be noted the high number of very small receptive field size that correspond to neurons on the border of the field that are mostly silent during the whole simulation.

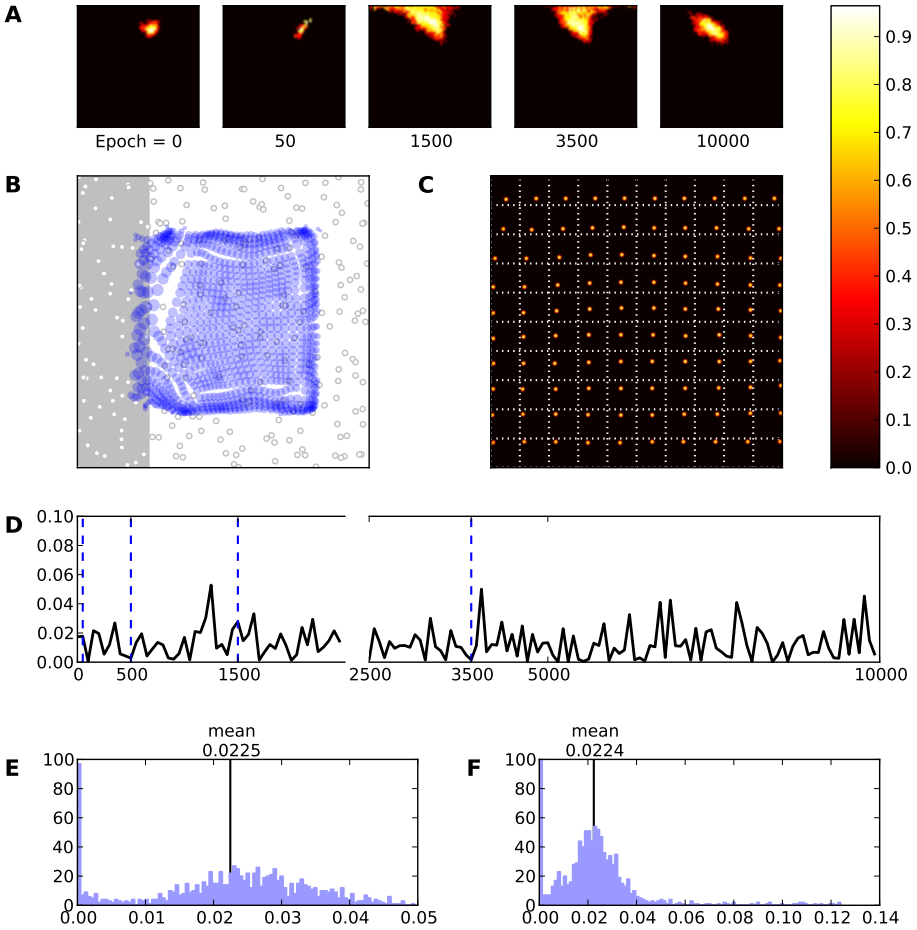

Figure 3.23: **Skin lesion type I (gray area).** **A** Evolution of the receptive field of neuron $(25, 15)$ during retraining after a skin lesion of type I. **B** Receptive fields of the whole model. **C** Response of the model (after retraining) to a set of 10×10 regularly spaced stimuli. **D** This represents the mean evolution of thalamo-cortical weights of neuron $(25, 15)$ during retraining (i.e. $\mathcal{E}_{(25,15)}$. **E** & **F** Histogram of receptive field sizes (100 bins) before (E) and after (F) skin lesion. The initial distribution is Gaussian-shaped centered around a mean value of 0.02246. However, the final distribution is a Poison-like centered around a mean value of 0.2241 with a long tail indicating that there are a lot of neurons whose RFs have underwent an expansion. At the same time an almost equivalent amount of neurons has moved toward smaller RF sizes underlying that a shrinkage of RFs has taken place.

neurons expand the size of their RFs in order to acquire new inputs. This resilient behavior can be easily explained because thalamus provides divergent inputs to the cortex. Neurons that were previously tuned to dead receptors will expand their RFs in order to reach neighboring receptors. This expansion takes place immediately after the sensory deprivation as shown in figure 3.23B and 3.23A where the RF of neuron $(25, 15)$ underwent an expansion immediately after sensory deprivation (epoch 50). Panels 3.23E and 3.23F shows the histograms before and after sensory deprivation, respectively. The former corresponds to the intact model which was discussed in previous subsection and the later corresponds to the sensory deprivation case after retraining of the model. There is a small shift of the main peak of the distribution from the value of 0.02246 towards 0.02227, but with a noticeable spreading of the RFs (SD = 0.02256) size indicating a new distribution of RF towards both smaller and larger receptive fields (while the large component at zero because of border effects remains). This alteration in the distribution tends to show that even if most RFs have shrunk, a significant portion have expanded in size.

Furthermore, in figure 3.23A (describes the temporal evolution of unit $(25, 15)$) one can observe that reorganization occurs in two major phases. At the beginning, each neuron innervated by deprived skin area undergoes an expansion of its RF simultaneously with a spatial shifting in order to capture a new skin area (first phase). This lasts almost during the whole retraining process. Near the end of training process the affected neuron has shrunk its RF (second phase). Similar to this finding, Foeller in [126] proposes a three-phases model of the RFs reorganization. In the first phase and due to reduction of inhibitory connections the RFs expand their size. During the second phase, a further increase of RFs size is taking place because of homeostatic plasticity of GABA circuits. Finally, in the third phase, a shrinkage of RFs around their new centers occurring as it is driven by re-established inhibitory connections.

However, the refinement of the RFs is not so exquisite because, according to the main hypothesis of the present work, lateral connections remain fixed and non-plastic throughout all simulations. This means that neurons are able to receive proper excitation and inhibition conserving the competitive nature of the reorganization process. Nevertheless, a better refinement could be possible by allowing lateral connections to adapt to the new conditions. Furthermore and as it has been explained, the precise type of lesion does not impact result in a significant way. Neurons that were preferentially tuned to a disabled skin area tends to have their receptive fields shifting away from the site of the lesion to neighboring locations. However, for type II and type III lesions, there is an additional topological constraint onto those neurons because they can still be part of an active bump in the field (and tune their receptive field accordingly). They can be thus attracted either to the left or to the right part of the lesion site for type II and to any border of the lesion site for type III. This explains that some neurons do not express any kind of resilience and have their preferred location still on the lesioned area even after extensive retraining (figures 3.24B and 3.25B). This also explains the increased oscillations in average evolution of feed-forward weights, $\mathcal{E}_i$ (figures 3.23D, 3.24D, 3.25D).

Reorganization after a cortical lesion

Cortical lesion cases have been addressed as well. A cortical lesion can be caused for instance by silencing some neurons in the neural field. In living tissue, such damages can be caused by a stroke, a hematoma or by a surgery either for therapeutic or experimental purposes. Subsequently, three different types of cortical lesions (i.e. type I, II and III) were caused by applying a mask to the self-organized representational map as it has been previously described for the toric version. These lesions were of an extent of 25% of the total amount of neurons. After retraining of the network using 10000 stimuli patterns for each of these lesion cases, a new representational

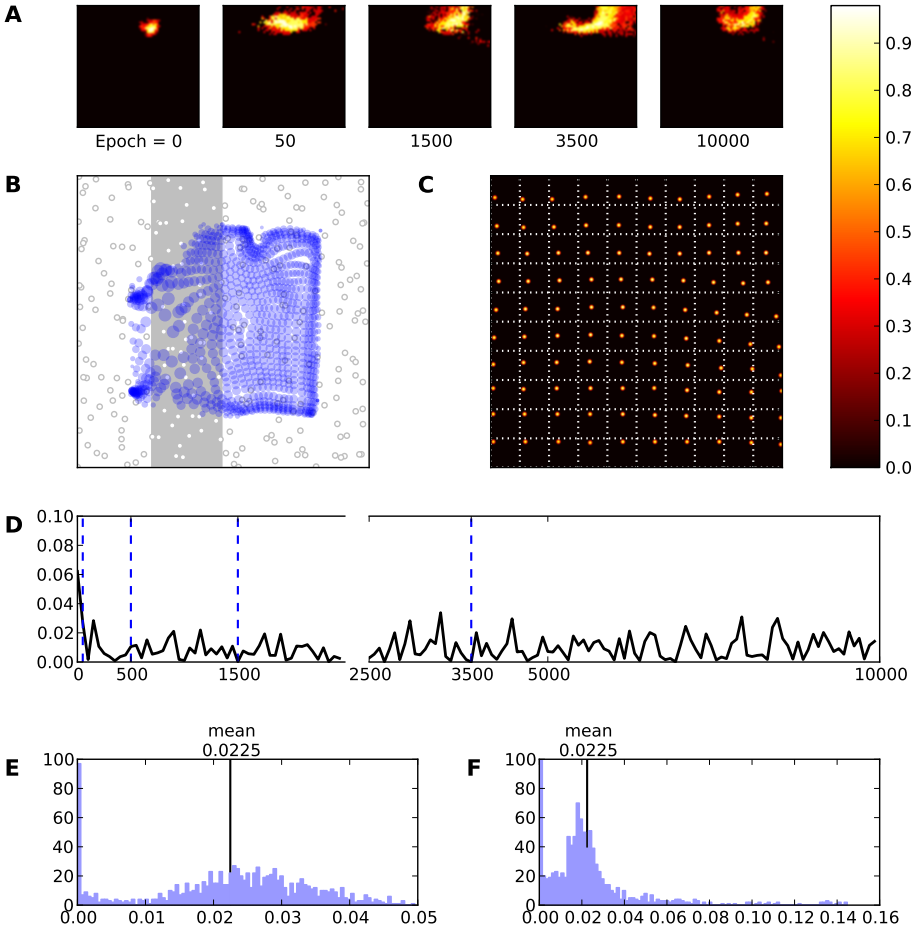

Figure 3.24: **Skin lesion type II (gray area).** **A** Evolution of the receptive field of neuron $(25, 15)$ during retraining after a skin lesion of type II. Immediately following skin lesion (epoch 50), RF tends to expand. This phenomenon persists until the final epoch is reached where a shrinkage takes place. **B** Receptive fields of the whole model. **C** Response of the model (after retraining) to a set of 10×10 regularly spaced stimuli. **D** This represents the mean evolution of thalamo-cortical weights of neuron $(25, 15)$ during retraining (i.e. $\mathcal{E}_{(25,15)}$). **E** & **F** Histogram of receptive field sizes (100 bins) before (E) and after (F) skin lesion. The initial distribution is Gaussian-shaped centered around a mean value of 0.02246. However, the final distribution is a Poisson-like centered around a mean value of 0.2241 with a long tail indicating that there are a lot of neurons whose RFs have underwent an expansion. At the same time an almost equivalent amount of neurons has moved toward smaller RF sizes underlying that a shrinkage of RFs has also taken place.

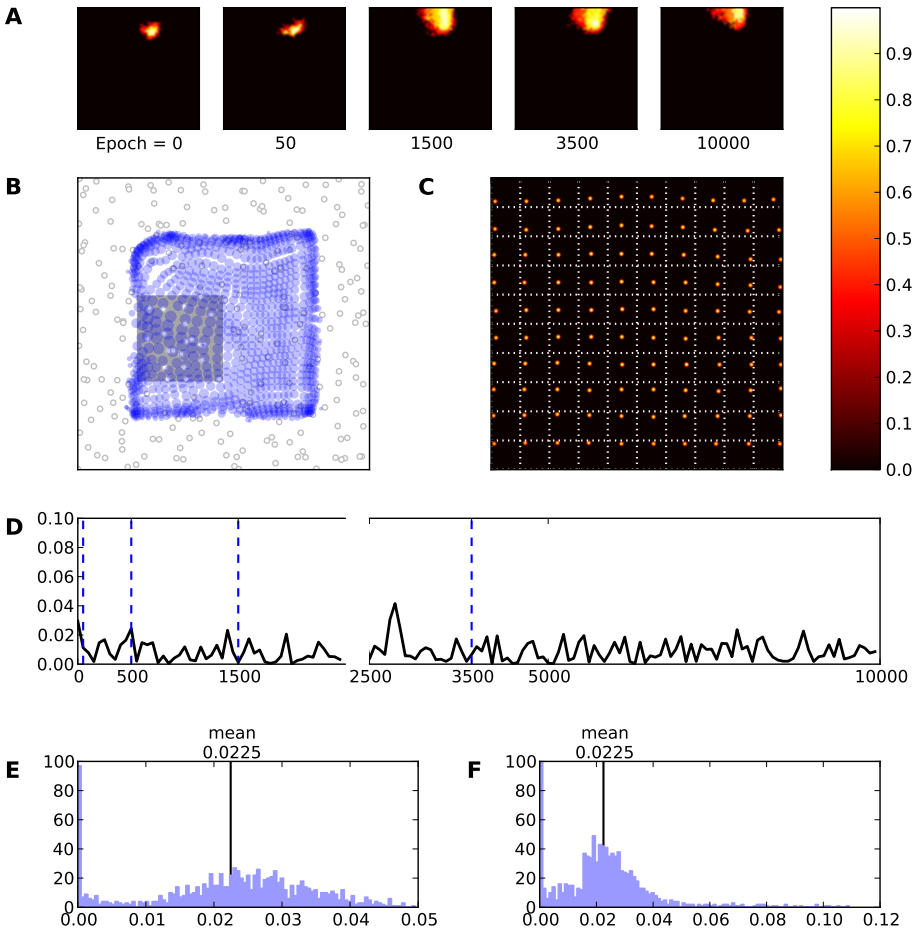

Figure 3.25: **Skin lesion type III (gray area).** **A** Evolution of the receptive field of neuron $(25, 15)$ during retraining after a skin lesion of type III. **B** Receptive fields of the whole model. **C** Response of the model (after retraining) to a set of 10×10 regularly spaced stimuli. **D** This represents the mean evolution of thalamo-cortical weights of neuron $(25, 15)$ during retraining (i.e. $\mathcal{E}_{(25,15)}$. **E** & **F** Histogram of receptive field sizes (100 bins) before (E) and after (F) skin lesion. The initial distribution is Gaussian-shaped centered around a mean value of 0.02246. Although, the final distribution is a Poison-like centered around a mean value of 0.2248 with a long tail indicating that there are a lot of neurons whose RFs have underwent an expansion. At the same time an almost equivalent amount of neurons has moved toward smaller RF sizes underlying that a shrinkage of RFs has taken place.

map has emerged as it is depicted in figure 3.26 for type I lesion.

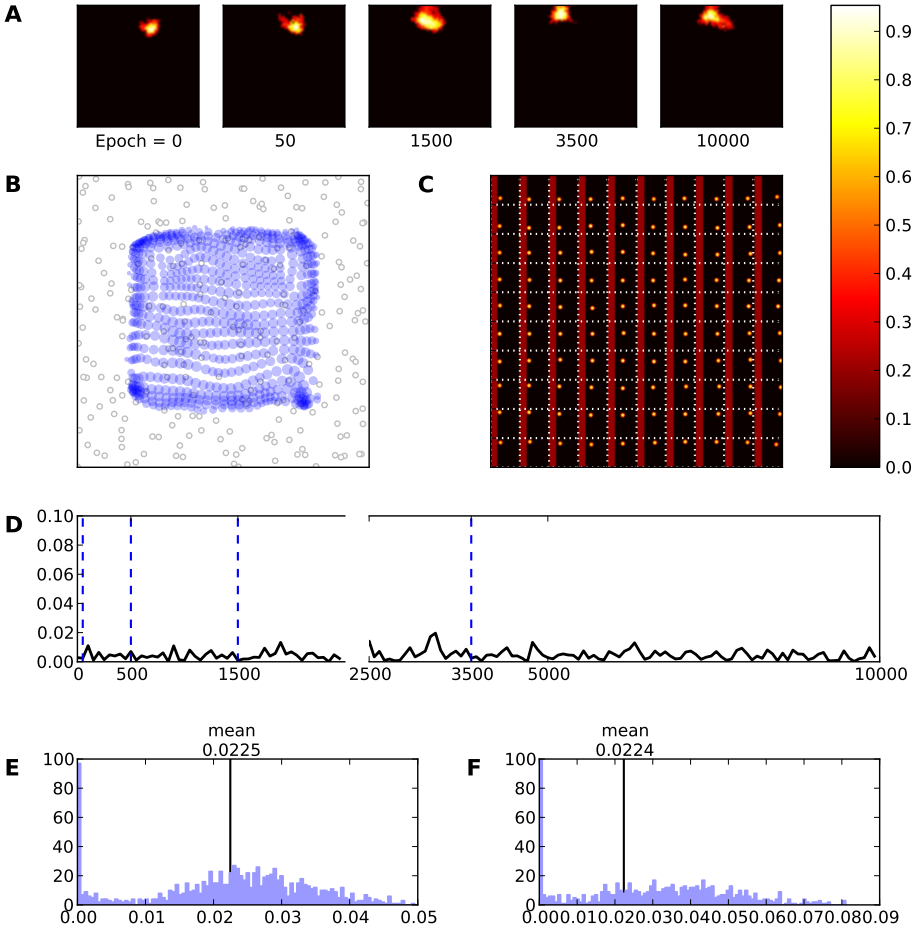

Figure 3.26: **Cortical lesion type I (red area) A** Evolution of the receptive field of neuron $(25, 15)$ during retraining after a cortical lesion of type I. Immediately following the lesion (epoch 50), RF tends to expand. This phenomenon persists until the final epoch is reached. **B** Receptive fields of the whole model. **C** Response of the model (after retraining) to a set of 10×10 regularly spaced stimuli. The activity of the model is now bound to the unlesioned area. **D** This represents the mean evolution of thalamo-cortical weights of neuron $(25, 15)$ during retraining (i.e. $\mathcal{E}_{(25,15)}$). **E** & **F** Histogram of receptive field sizes (100 bins) before (E) and after (F) skin lesion. The initial distribution is Gaussian-shaped centered around a mean value of 0.02246. However, the final distribution is a uniform-like centered around a mean value of 0.02245 (0.02235). This uniform-like distribution indicates the existence of neurons whose RFs have underwent an expansion, but not a shrinkage.

Comparing the RFs size before and after cortical lesion, they have been clearly altered. After lesion, RFs tend to become larger and consequently to respond to larger skin areas. More precisely, RFs size after lesion is almost twice bigger compared to the intact ones. As it is shown in figure 3.26A the evolution of neuron $(25, 15)$ after a cortical lesion of type I has been altered. Immediately following the lesion (epoch 50), RF has expanded itself and cover the skin patch which was previously represented by lesioned neurons. The temporal evolution of the RF indicates that this neuron has changed its preferred input in order to promote the recovery. In addition and as it is illustrated in figure 3.26B, RFs of almost all neurons have been changed.

The radii of the blue discs have been increased in size, especially around the lesion site. Taking also into account the results coming from the histograms of figures 3.26E and 3.26F concerning the intact and the lesioned cases, respectively, one can see the overall distribution of RFs size has changed in favor of a larger number of large RFs. The mean value of RFs after cortical lesion is equal to 0.02235 and the SD is equal to 0.02179 indicating a significant spread of RF sizes.

This is quite consistent with Sober [113], who reported similar results with the noticeable difference, that weeks after a lesion, cortex is able to completely recover, having its neurons RFs sharpened. This is because of re-establishment of inhibitory connections and/or sprouting of neural axons as it has been proposed by Florence [70]. Consequently, the refinement of RFs arises in two phases. During the first phase, there is an expansion of RFs towards lost territories followed by a shrinkage of the second phase. In the present computational experiments there is no such shrinkage during the second phase because of the fixed set of lateral connections as it is depicted in figures 3.26A, 3.27A and 3.28A. This leads one to ascertain that the lateral connections are crucial to the development of stable representational maps. Neurons are not able to precisely refine their RFs since there is no balance mechanism between excitation and inhibition within cortical circuits. Sur [82] has shown that intralaminar excitatory connections are the major factor for expansion of RFs. In consequence, RFs in figures 3.26A and 3.26B have successfully expanded themselves leading to larger skin area representation but have failed at shrinking themselves because of the non-plastic lateral connections. Furthermore, it is remarkable to see that neurons have migrated their RFs to cover the whole skin surface again (figures 3.26A, 3.26B) and non-functional representations (just after lesion) have been recaptured by neighboring units. The model is able to respond again to stimuli applied on areas innervating neurons within the lesioned cortical area (figure 3.26C). This indicates that other neurons took over and recovered from lesion by migrating their representations towards the lost ones, making the cortical patch functional but degraded.

Recovery from cortical lesions of type II and III is displayed in figures 3.27 and 3.28 and show the degraded response of the model with only a partial recovery of lost territories. Furthermore, figures 3.27A, 3.27B and 3.28A, 3.28B clearly show that most RFs have been shifted and expanded spatially without any kind of refinement except for a small number which have underwent a shrinkage as it is pointed out by figures 3.27F and 3.28F. This behavior can be explained quite simply in terms of topology. The first type of cortical lesion is topologically equivalent to the intact one while type II lesion introduces a separation of the cortical patch into two distinct patches and type III introduces a hole in the topology. In both cases, neurons from either sides of the lesion cannot cooperate because their influence is mostly inhibitory (due to their respective distance from each other). This means that the active population resulting from the competition cannot exist on any borders of the lesion. This brings severe constraints to the self-organization process that can only be partially overcome without relearning a new topology through the modifications of lateral connections.

3.4.9 Higher cognitive effects on SI

Higher order cognitive functions have the ability to affect different brain areas in many different ways as it has been discussed in the second chapter of the first part. Such a well-known higher order cognitive function is the attention. Attention has been studied in visual system, exhaustively. More details about attention in visual system can be found in a review by Knudsen, [135], where all the fundamental components of attention are described and presented. Although, attention does not affect only visual cortices and it is not valuable only to visual system. Other systems such as somatosensory takes advantage of attention in order to execute demanding tasks. In

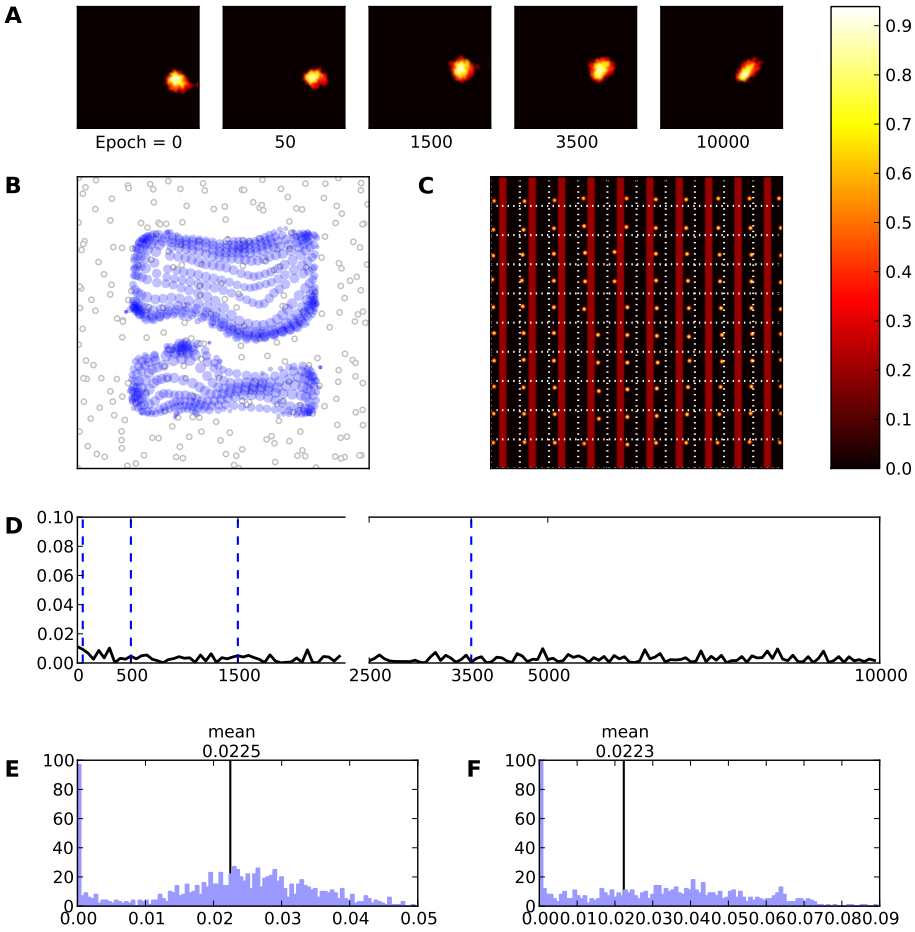

Figure 3.27: **Cortical lesion type II (red area) A** Evolution of the receptive field of neuron $(15, 25)$ during retraining after a cortical lesion of type II. This particular neuron has not expanded its RF but it has replaced its preferred location as it is depicted at the final profile (epoch 10000). **B** Receptive fields of the whole model. The cortical lesion is appeared at the preferred locations since the previously corresponding neurons are now affected by the lesion. The RFs around the lesion have been increased in size comparing with the corresponding pre-lesion figure 3.22**B**. **C** Response of the model (after retraining) to a set of 10×10 regularly spaced stimuli.The activity of the model is now bound to the unlesioned area. **D** This represents the mean evolution of thalamo-cortical weights of neuron $(15, 25)$ during retraining (i.e. $\mathcal{E}_{(15,25)}$). **E** & **F** Histogram of receptive field sizes (100 bins) before (E) and after (F) skin lesion. The initial distribution is Gaussian-shaped centered around a mean value of 0.02246. However, the final distribution is a Uniform-like centered around a mean value of 0.02233. This uniform-like distribution indicates the existence of neurons whose RFs have underwent an expansion, but not a shrinkage as in cortical lesion type I case. In this case we illustrate results regarding neuron $(15, 25)$ because neuron $(25, 15)$ lies in the lesion.

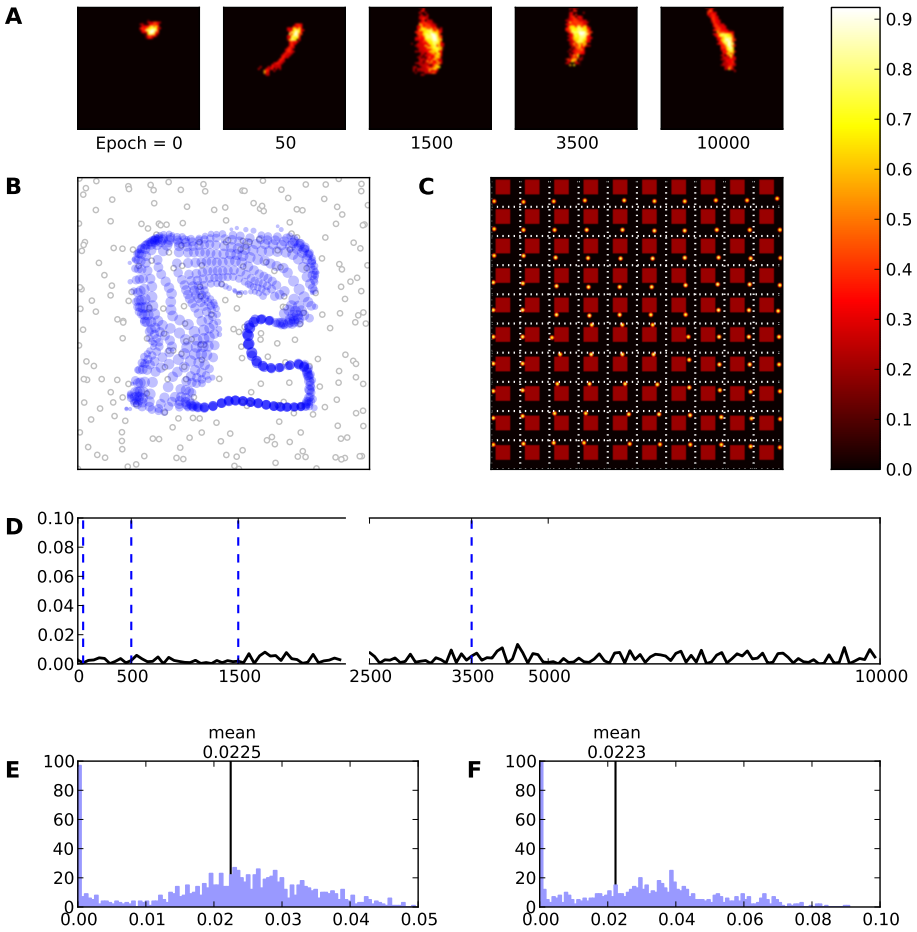

Figure 3.28: **Cortical lesion type III (red area) A** Evolution of the receptive field of neuron $(25, 15)$ during retraining after a cortical lesion of type III. This particular neuron has expanded its RF immediately after lesion and moreover it has has replaced his preferred location as it is depicted at the final profile (epoch 10000). **B** Receptive fields of the whole model. The cortical lesion is appeared at the preferred locations since the previously corresponding neurons are now affected by the lesion. The RFs around the lesion have been increased in size comparing with the corresponding pre-lesion figure 3.22**B**. **C** Response of the model (after retraining) to a set of 10×10 regularly spaced stimuli. **D** This represents the mean evolution of thalamo-cortical weights of neuron $(25, 15)$ during retraining (i.e. $\mathcal{E}_{(25,15)}$). **E** & **F** Histogram of receptive field sizes (100 bins) before (E) and after (F) skin lesion. The initial distribution is Gaussian-shaped centered around a mean value of 0.02246. However, the final distribution is a Uniform-like centered around a mean value of 0.02227. This uniform-like distribution indicates the existence of neurons whose RFs have underwent an expansion, but not a shrinkage as in cortical lesion type I case.

chapter two the neurophysiological data and the recent hypotheses around attention were discussed. In this section, an attempt to model the effects of attention on area 3b of the primary somatosensory cortex is made.

As it has been mentioned, attention affects the receptive fields of the neurons and reorganize in a way the topographic maps. The reorganization is not such brute as the one of lesions, but it is more "gentle". In addition, because some researchers have claimed that more or less the same results as attention can be acquired by using an intensive training and without taking advantage of any attentional mechanism, the idea of intensive stimulation is also in question. In this context, the topographic map of the Development section has been used also here. Four different case studies concerning attention have been examined. In addition, one case of intensive stimulation has also examined. During all these experiments the parameters described in table 3.1 have been used.

Parameter	REF	IS	LTGM+	LTGM+IS	STGM+	STGM-
K_e	3.65	3.65	3.65/8.00	3.65/8.00	3.65/8.00	3.65/1.50
σ_e	0.1	0.1	0.1	0.1	0.1	0.1
K_i	2.40	2.40	2.40/6.10	2.40/6.10	2.40/6.10	2.40/0.75
σ_i	1.0	1.0	1.0	1.0	1.0	1.0
α	0.1	0.1	0.1	0.1	0.1	0.1
γ	0.05	0.05	0.05	0.05	0.0	0.0
τ	1.0	1.0	1.0	1.0	1.0	1.0

Table 3.1: **Model parameters.** K_e and K_i are the amplitudes, σ_e and σ_i are the variances of excitatory and inhibitory lateral connections, respectively. γ is the learning rate, α is a scaling factor and τ is the synaptic temporal decay.

Intensive Stimulation (IS)

Several studies have unraveled a range of cortical phenomena following intensive and continuous training of a localized skin patch. For instance, Recanzone et al. in [213] have shown that under intensive stimulation of the fingers skin surface using vibrating stimulation, the cortical surface of the monkeys underwent an expansion simultaneously with receptive fields expansion. In the meantime, Xerri et al., [214] have shown that cortical representations in rats tend to expand after exposition to an intensive stimulation while the receptive fields decrease in size.

The purpose of this experiment aims at precisely measuring to what extent an intensive stimulation may affect the reorganization of the primary somatosensory cortex and what kind of alterations take place at the level of receptive fields. In this context, intensive stimulation relates to the increased stimulation of the region of interest (RoI) using a given frequency f. Frequency is set to 0.5, meaning that the RoI is stimulated as often as the remaining (complementary) region. However, due to the relative difference in size between the two regions, this results in an actual ratio of three to one, i.e. the RoI receives half of all stimulations while each three other equivalent subregions received each 1/6 of stimulations. The frequency f has thus to be chosen relatively low because a too high frequency could lead to severe perturbations of the self-organization. At the upper limit $f = 1$, only the RoI receives stimulations and this can be considered as sensory deprivation, leading to a complete migration of all the receptive fields into the RoI.

Using the topographic map of the Development section, the model is let to learn an extra set of 25000 random stimuli, with a distribution enforcing the aforementioned protocol. Figure 3.31B shows the new distribution of the receptive fields at the end of the retraining. Three main effects are present:

- Moderate shrinkage of the size of receptive fields, the mean of receptive fields size is 0.016 ($SD = 0.048$),
- Strong migration of the receptive fields towards the RoI as it is pointed out by figure 3.31B where the density is higher inside RoI and a solid number of center of masses of receptive fields has moved towards RoI,
- Moderate cortical expansion (0.72mm^2) instead of (0.59mm^2) as it is depicted in figure 3.32B.

Histogram of receptive fields relative size changes are illustrated in figure 3.29B. Alterations in size of receptive fields relatively to the reference period implies that intensive stimulation affects directly the size of receptive fields by diminishing that. In addition, intensive stimulation of the RoI leads to an expansion of the cortical territory representing the region as well as a moderate decrease of the size of the receptive fields, comparing reference experiment with the present one and interpreting the relative histogram of figure 3.29B.

Long-term Gain Modulation (LTGM+)

As explained earlier, the model relies functionally on the balance between lateral excitation and inhibition, allowing to widen or sharpen the peak of activity when a stimulus is present (see figure 3.30). This balance can be dynamically adjusted via gain modulation, which is assumed to influence both the response of the model and the formation of somatosensory representations. To assess this hypothesis, the dynamic modulation of the model response has been examined in order to measure the long-term effects of such modulation on the distribution of the receptive fields as well as their mean size. Using a set of 25000 random stimuli of equal size with respective positions covering uniformly the whole skin area, the gain of the model is modulated only when the position of the stimuli is lying within RoI. This modulation is made such as sharpening the model response. It is important to underline that the gain modulation is done at the whole field level but is only effective where the field is active. In this case, it is only effective in the RoI. The standard learning rule (3.4) is enforced continuously and everywhere and the overall long time effect of this modulation is a noticeable decrease in the size of the RFs as it is displayed in figure 3.29C. The mean of the receptive fields size is in this experiment 0.0014 ($SD = 0.0037$), which means that the size of receptive fields inside RoI is smaller than the ones in reference period. An interesting point in LTGM+ case is the shrinkage of cortical area representing RoI as it is illustrated in figure 3.32C. Moreover the density of the receptive fields, depicted in figure 3.31C, is more or less the same as REF case, panel 3.31A indicates that there is no migration of receptive fields towards RoI during long-term modulation of gains. The cortical size, that obtained for long-term gain modulation supports the aforementioned arguments. The cortical representation of REF case is 0.59mm^2 instead of 0.56mm^2 of LTGM+ cortical representation.

Similar results can be obtained by instantaneous modulation of the gain without retraining the model. This means that the gains can be altered at any time and at any place leading to an alteration of cortical activity having as a consequence a modification on the shape and the size of the receptive fields. This phenomenon is temporary and cannot affect the feed-forward connections (w_f). Therefore, a short-term gain modulation (STGM+) can, for instance, leads

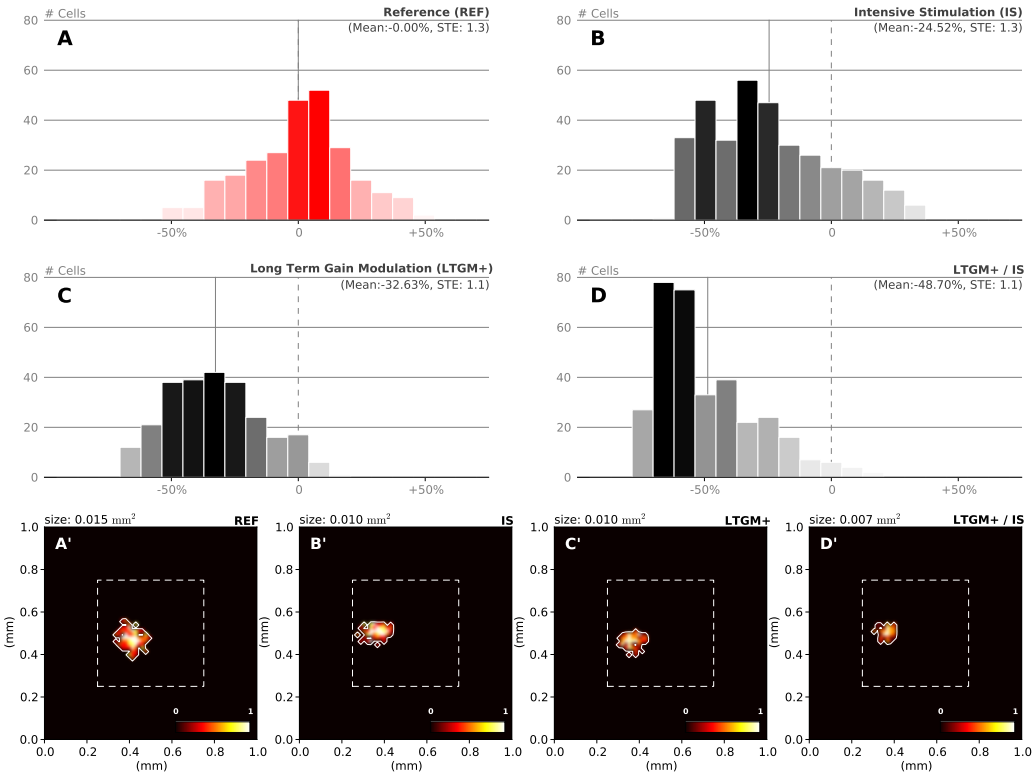

Figure 3.29: **Relative change of receptive field sizes in the RoI compared to the reference.** Histogram of receptive field relative sizes in the RoI after **A.** initial training (25000 samples). **B.** intensive stimulation in the RoI (1/1 ratio) using 25000 extra samples, **C.** long term gain modulation in the RoI using 25000 extra samples, **D.** long term gain modulation and intensive stimulation (1/1 ratio) in the RoI using 25000 extra samples. **Bottom row.** Receptive field of a single cell recorded at the end of each of the aforementioned experiments. The receptive field size in the LTGM+/IS experiment (0.007 mm^2) has shrunk to one half of the reference size (0.015 mm^2).

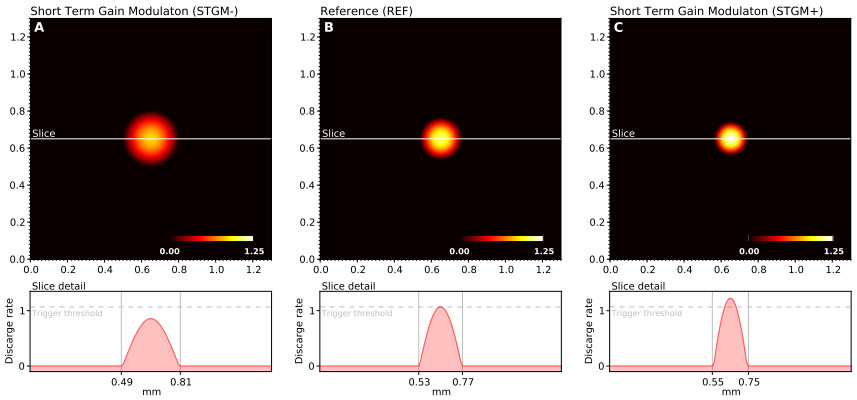

Figure 3.30: **Dynamic modulation of the cortical answer.** The response of the model depends functionally on the balance between lateral excitation (K_e) and inhibition (K_i), allowing to widen (panel **A**) or sharpen (panel **C**) the peak of activity when a stimulus is presented. If we consider the trigger threshold to be peak of nominal response (panel **B**), the same stimulus can either trigger a sharp response or not trigger any response at all, depending on the modulation. This modulation is believed to be to a form of somatosensory attention.

to a decrease of the size of receptive fields (mean is 0.014 ($SD = 0.0025$)) but it cannot affect the cortical size of RoI cortical representation as it is illustrated in figure 3.32C. In addition the size of cortical representation in this case is 0.59mm^2, same as the cortical representation of RoI in reference period. The aforementioned results suggest that the long- or short-term gain modulation is not sufficient by itself to promote the dramatic changes that have been observed in other studies, [147, 149, 146] about attention effects on receptive fields and cortical representations.

Long Term Gain Modulation and Intensive Stimulation

On the one hand intensive stimulation can lead to a new reorganized topographic map with smaller and more numerous receptive fields within RoI. On the other hand long-term and short-term gain modulation can lead to smaller receptive fields within RoI making one to assume that a possible mechanism for explaining the effects of attention on primary somatosensory cortex could be the combination of both intensive stimulation and long-term gain modulation. The joint effect of long-term modulation and intensive stimulation has been measured by combining the two aforementioned protocols. Using a frequency $f = 0.5$ and a set of random stimuli of equal size with respective positions covering uniformly the whole skin area, the model gain was modulated only when the position of the stimuli was lying in the RoI. This results in a dramatic shrinkage of the size of the receptive fields in the RoI as it is displayed in the relative histogram in figure 3.29D, that encompasses previous results. Almost all of the receptive fields that are contained within RoI are now smaller than the reference period since the mean value of size of receptive fields is 0.0011 ($SD = 0.0040$). Furthermore, there is also a strong migration of the receptive fields towards the RoI as it is suggested by the interpretation of density figure 3.31D. RoI is more dense, indicating there are more receptive fields in the RoI compared to the other cases. In addition the size of cortical representation is also much larger (0.74mm^2) than other cases, pointing out that the migration is highly efficient (one can see the expansion of RoI cortical representation in figure 3.32D).

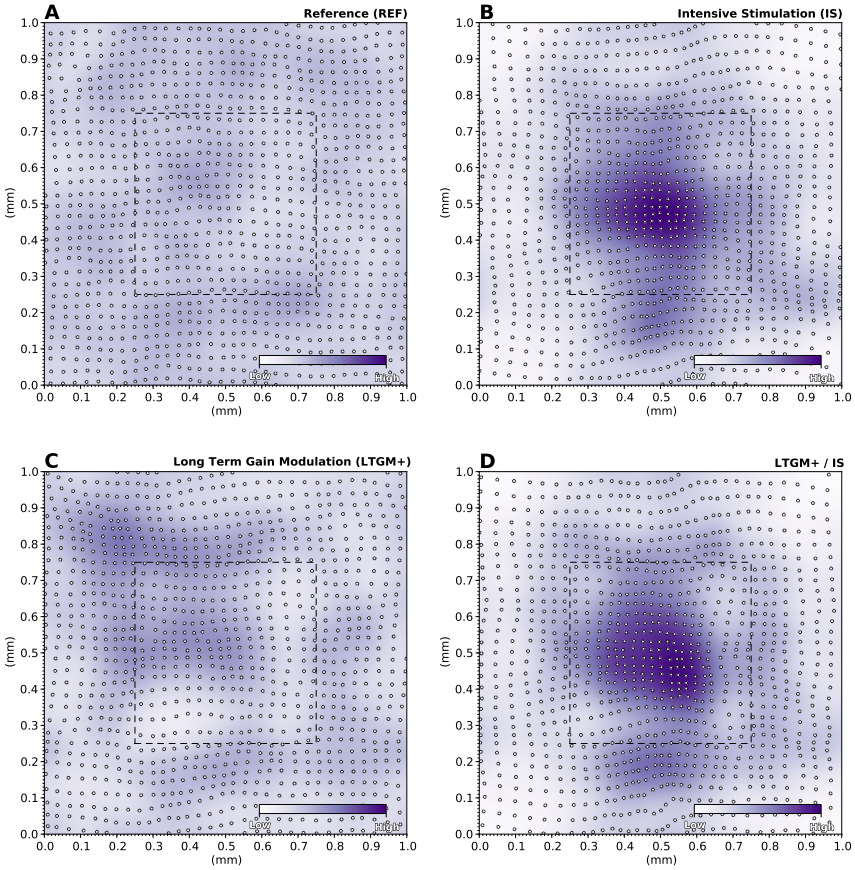

Figure 3.31: **Distribution and relative density of receptive field over the skin patch area A.** Initial training (25,000 samples). **B.** Intensive stimulation in the RoI (1/1 ratio) using 25,000 extra samples. **C.** Long-term gain modulation in the RoI using 25,000 extra samples. **D.** Long-term gain modulation and intensive stimulation (1/1 ratio) in the RoI using 25,000 extra samples.

A more precise picture about the effect of attention on receptive fields of somatosensory cortex is provided by figure 3.29 in panels from A' to D'. A receptive field of a single specific neuron is illustrated during reorganization in the four different experiments. The size of that receptive field decreases starting from the reference period (A') and going to the case of long-term gain modulation and intensive stimulation combination (B'). This is another argument that supports the hypothesis that attentional mechanisms affect the receptive fields of somatosensory cortex through gain modulation of horizontal synaptic connections. However, this mechanism is not sufficient to achieve both the shrinkage of the receptive fields and their migration towards RoI. This suggests that neurons of the primary somatosensory cortex require both training and attention in order to improve performance.

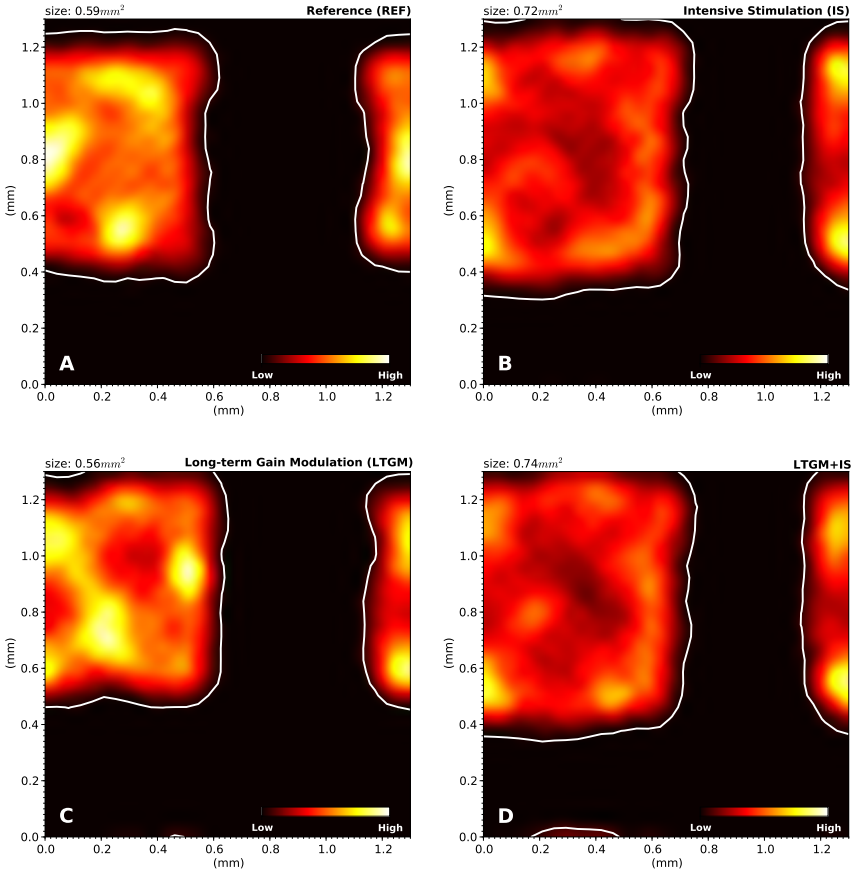

Figure 3.32: **Relative change in the size of the cortical area representing the RoI A** RoI cortical representation of reference period. The size in mm^2 is equal to 0.56. **B** Cortical representation of RoI after retraining using 25000 stimuli as intensive stimulations. The size in mm^2 is equal to 0.72. **C** RoI cortical representation after reorganization of cortical topographic map using 25000 stimuli and long-term gain modulation. The size of the representation in this case is $0.54mm^2$. **D** Finally, the cortical representation of RoI after long-term gain modulation and intensive stimulation. 25000 stimuli has been used and the acquired cortical size is $0.74mm^2$.

3.4.10 Parameters of the model

In order to study the robustness of the model in the presence of parameters perturbation one has to measure the impact of those perturbations. Therefore the two main parameters of the self-organization have been put under investigation. The skin receptors distribution has perturbed in principle by adding a location jitter of 5% to each receptors coordinates. This means that the skin receptors distribution is not a regular grid, but a quasi-uniform rectangular distribution. In order to investigate further how this jitter affects the self-organization, six different values of jitter have been applied on the model. In a similar way the effect of the learning rate has also been investigated by applying different learning rates in several simulations and measuring the MSE and inspecting the final self-organizing maps.

Skin receptors distribution

The distribution of the skin patch receptors can affect at some extent the learning process and as a consequence the self-organization of the map. In order to examine at which degree the skin receptors distribution affects the self-organization, six simulations was used. In each simulation different jitter values have been used. The jitter is used in order to add some noise to the original regular and rectangular receptors distribution. Thus, starting from a jitter of 0% and going on to 5%, 10%, 25%, 50%, 75% and finally to 100% the results of the simulations are depicted in figure 3.33. In each panel of that figure, is illustrated on the left side the distribution of receptive fields on the skin surface and on the right side the MSE of the system during learning. The MSE has been computed according to equation (3.7). In every case the as original $\hat{w}_f$ feed-forward connections matrix has been considered the converged topographic map of zero noise case. This means that the regular receptors distribution has been taken as the ideal case of topographic organization and all the comparison has been done based upon it.

The results of each simulation reveal that the skin receptors distribution does not affect the self-organization process, except the case where the jitter is 25%. This happens because the skin patch is divided into two separated pieces and this causes a topological reformation of the skin patch. This results a self-organizing map that is not well-organized. As it is depicted in figure 3.33 the MSE indicates that the feed-forward weights converge in any case but the case of 25% location jitter. In this case the MSE seems normal, although the organization is not good. There is a cut in the topographic organization of that map due to the distribution of the receptors. Therefore, the normal MSE comes from that organization and the very fast oscillations of the trailing part of MSE are due to the gaps in the topographic map. The neurons during the self-organization process try to converge to some locus of the skin, but the skin receptors and therefore the sampling of the stimuli is not sufficient to drive properly those units. The rest of the topographic maps are fine and their MSE as well, pointing out that the noise of the skin receptors distribution does not affect the self-organization process.

Learning rate

The second factor that affects the learning and therefore the self-organization is the learning rate, γ, (see equation (3.4)). The learning rate determines how fast or slow the self-organization takes place. A high learning rate leads to an aggressive oscillation of feed-forward weights, w_f, rendering the model unstable. This is because all the neurons tend to migrate towards the winner neuron. On the other hand, if the learning rate is low, then the self-organization process can be considered as frozen, and one needs many times more iterations during learning in order to stabilize the model at a self-organizing map.

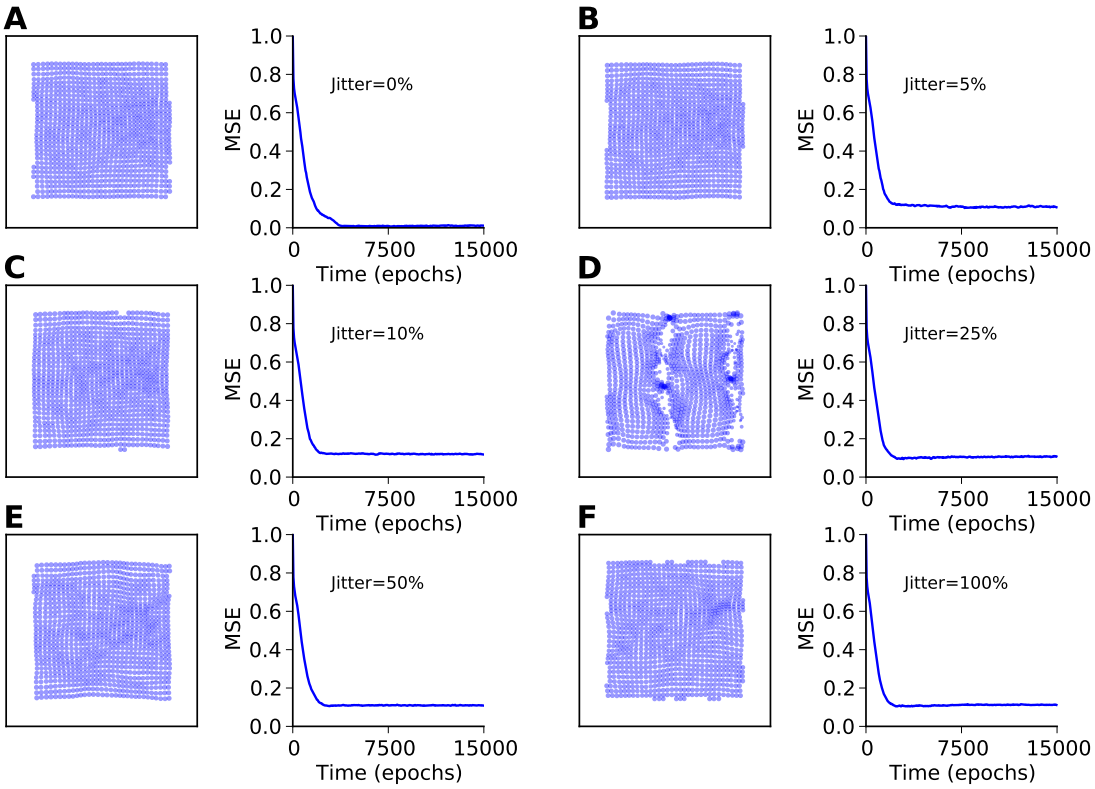

Figure 3.33: **Perturbation of DNF-SOM (different skin receptors distributions)** In each panel is illustrated the distribution of the receptive fields on the skin surface (left subfigure) and the MSE of them model during learning (right subfigure). MSE has been computed according to (3.7). The jitter of skin receptors distribution is indicated as inset text in each subfigure. For the sake of simplicity only 15000 iterations of learning have been used for illustrating MSE figures.

In order to test the effect of different learning rate values, six simulations have been done. In each simulation a different value of learning rate has been used. In figure 3.34 are illustrated the receptive fields of the neurons on the skin surface (distribution of receptive fields on the skin surface) and the corresponding MSE of the system. It is apparent that learning rates $0.02, 0.07$ and 0.2 can result a self-organizing map with a uniform distribution of receptive fields. Although, in the case when the learning rate is equal to $0.001, 0.005$ and 0.4 the distribution of the feed-forward weights cannot updated properly. The MSE in each case confirms that results. For instance, in figures 3.34**A** and 3.34**F** are illustrated the results of the cases where the learning rate is equal to 0.001 and 0.4, respectively. One can observe that in the former case the MSE reveals that there is no convergence of the learning process at all and in the latter case the very fast and violent oscillations of MSE reflects the aggressively fast learning process. In both cases the learning the final topographic map is not organized.

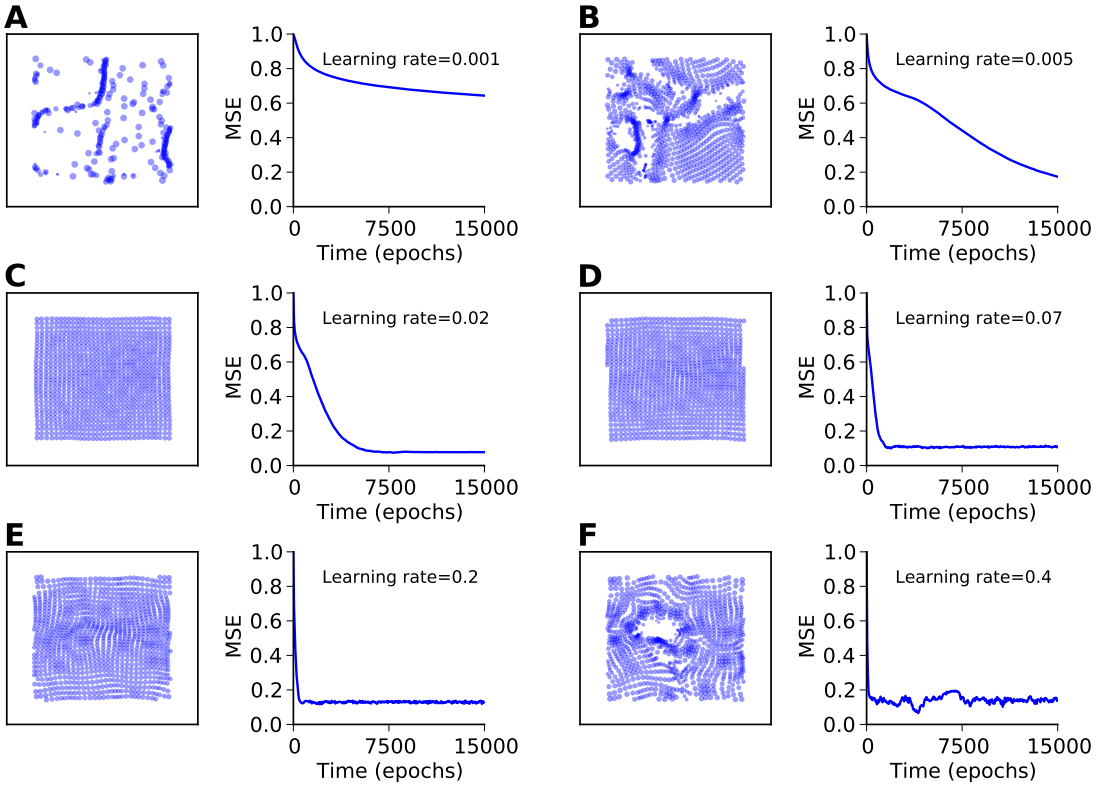

Figure 3.34: **Perturbation of DNF-SOM (different learning rates)** The MSE of six different simulations has been computed according to equation (3.7). The learning rate is indicated as inset text in each subfigure. In each panel are illustrated the distribution of the receptive fields on the skin at the end of the learning process (left side) and the MSE of the model during the learning process (right side). For the sake of simplicity only 15000 iterations of learning have been used for illustrating MSE figures.

3.4.11 Simulation details

The initial training stimuli set of the model is generated using two-dimensional Gaussians with variance 0.08 and mean to be variable and actually depending on the side of the skin patch where a stimulus is applied on. The stimulus is considered toric (or non-toric) as well as the skin

patch. When the stimuli and the skin are considered toric then if a stimulus is located on any of the border side of the skin, the missing part appears on the other side of the skin (pacman effect). Before each simulation, a set of 50000 uniformly distributed stimuli is created over the plane $[0, 1] \times [0, 1]$. The elevated number of stimuli guarantees a good discretization of the skin patch and ensures the smooth transition from one area to another on the topographic map. In addition, all the thalamocortical feed-forward connections, w_f, are initialized to random values between 0 and 1.

Each stimulus is used for training the model only once. During one iteration, the model receives an input according to equations (3.10) or (3.9). Then the forward Euler's method is implicated in order to solve numerically the dynamic neural field system, (3.1) (temporally) and an FFT is used in order to compute the spatial integrals. Therefore, the persistent activity of the dynamic neural field (a.k.a. bump solution) drives the self-organization as it is described by equation (3.1). Then a reset of the field activity takes place and a new stimulus is received. After 50000 stimuli (or 25000 for the attention and the intensive training) the model converges to a topographic organization.

Simulations were performed on a HP Z800 Workstation. The source code of all simulations is written in Python (Numpy, Scipy and Matplotlib) and some core computations have been also done in C (using the libraries FFTW3 and LAPACK). During a simulation of 50000 stimulations, the program consumed $\sim$ 45MB of physical memory and required $\sim$ 30 minutes of real time (measured with *time* Unix command) until convergence.

3.4.12 Time complexity of the model

The algorithm describes the model is quite simple and mainly consists of three basic steps. All the three steps take place in a main loop that reflects the training period. During one iteration there is a preparation of the current thalamocortical input, the numerical solution of a dynamic neural field and the update of the learning rule and finally the reset of the activity of the model. One can summarize the algorithm as it manifested in 3.1.

Algorithm 3.1 Dynamic Neural Field - Self-organizing Map

Require: time, n, dt, T, W_e, W_i.
Ensure: W_f.
$W_f \leftarrow$ rand()
$S \leftarrow$ Gaussian()
$W_{e_f} = FFT\{W_e\}$, $W_{i_f} = FFT\{W_i\}$
for $t = 0$ to time **do**
  Compute I according to equation (3.10)
  for $i = 0$ to T with step dt **do**
    $Z = FFT\{V\}$
    $Le = FFT^{-1}\{Z * W_{e_f}\}$
    $Li = FFT^{-1}\{Z * W_{i_f}\}$
    $U+ = (-U + (Le - Li) + I) * dt * tau$
    $W_f+ = (\gamma * Le * (W_f - S)) * dt$
    $V = max\{U, 0\}$
  end for
  $U = 0, V = 0$
end for

In algorithm 3.1, $*$ represents an element-wise multiplication. U and V are $1 \times n$ array represents the activity of the dynamic neural field, where n is the number of dynamic neural field units. W_e and W_i are $1 \times n$ arrays represent the lateral connections, excitatory and inhibitory respectively. W_f is a $n \times m$ matrix containing the feed-forward thalamocortical connections, where m indicates the number of receptors of the skin patch. dt is the time discretization of the dynamic neural field and T is the learning time window.

In order to compute the time complexity of algorithm 3.1 one has to take into consideration the time complexity of each function and calculation. Therefore, FFT and FFT^{-1} algorithms have time complexity of order $O(n \log n)$. Addition, subtraction and element-wise multiplication have a time complexity of $O(n)$. $max\{\cdot,\cdot\}$ function has a time complexity of $O(n)$ and assigning the values of U and V to zero costs $O(n)$, as well. Therefore, the asymptoticly total time complexity of the algorithm is computed to be $O(k \cdot m \cdot n + \frac{k \cdot n \cdot \log n}{dt})$ where k is the number of iterations of the learning process (lines 4 to 14). In the same context, when the discretization of the dynamic neural field and the feed-forward weights are implemented as two-dimensional (matrices) then the time complexity of algorithm (3.1) is $O(k \cdot m^2 \cdot n^2 + 2\frac{k \cdot n^2 \cdot \log n}{dt})$.

3.4.13 Some neuroscientific predictions of the model

As it is clear so far the proposed model is able to form topographic maps according to the somatotopic organization of the skin and its receptors. The formation of the topographic maps is achieved by using a modified Oja learning rule. The classical Oja learning rule can provide a way to build up associations between neurons and in addition is able to model the synaptic scaling. The proposed version of Oja learning rule is first a continuous one and second it has been modified in order to be more biological plausible. It exploits the dynamics of the neural population and it is devoted of the polynomial term of the original learning rule. Furthermore, the model is able to replicate real neurophysiological data (DiCarlo's experiment) and it is one of the very few (probably the only one) computational models of area 3b that does that in a fairly abstract and generic way (i.e. the model has not been designed to model specific parts of area 3b nor to interpret specific experimental data).

The model is able to recover from cortical lesions and responds to sensory loss as well. The reorganization in real cerebral cortex takes place in three different phases and involves also two main mechanisms. In real brain tissue at the beginning of a cortical lesion a subpopulation of neurons is dead and the connections of those neurons to other brain areas and to the neighbor neurons have been lost. Therefore at the beginning of the lesion there is no response to any stimulus applied on the lesioned representations. After some time, some of the thalamocortical inputs promote the generation of new connections. This causes the establishment of connections between neuron neighborhoods that before the lesion they did not communicate with each other. This provides the ability to the cortical tissue to reorganize itself and to recover some of the lost functions. In the proposed model this is the case as it was demonstrated in the previous paragraphs. The model is able to reorganize the topographic organization in the face of a cortical lesion pinpointing that the feed-forward thalamocortical connections are capable of promoting a reorganization. However, the lateral connections have been considered fixed and therefore the last phase of the reorganization (the refinement of RFs) is not present in the proposed model.In this last phase the cerebral cortex refines the receptive fields of the reorganized neurons. The exact biological mechanism in not yet fully known, but it is attributed to the lateral connections (horizontal) of the neurons. When a lesion takes place some of the well-known developmental mechanisms of the brain are activated. This means that the brain-derived neurotrophic factor (BDNF) and the Nogo receptors play a key role. It has been shown that the Nogo is down-

regulated after a lesion in oppose to BDNF which is up-regulated after a lesion. This indicates that the mechanisms of axon growing are active during reorganization. At the end of reorganization an inverse condition takes place, [215]. Something similar happens when the cerebral cortex confronts a sensory loss, but in this case the sprouting and the axons growing is more vivid because the neurons are in good condition and they search for new inputs. In the context of the proposed model this could be done by modulating the variance of the lateral connections σ_e and σ_i reflecting the dynamic sprouting and growing of lateral connections as it has been shown by [102].

The other side of the same coin is the synaptic learning. Therefore, so far the two known underlying mechanisms that are activated in the face of a lesion are the sprouting of lateral connections and/or the unmasking of preexisting suppressed connections. Once the new connections have been established they have to be enhanced or weaken according to some synaptic plasticity rule. This is the hard part of reorganization since a lot of different biological (molecular) mechanisms are involved. For instance, it is now known that GABA and NMDA receptors play a key role to synaptic plasticity especially during the reorganization of the cortex. It has been shown that GABA is extremely important during the third and last phase of reorganization. It promotes the refinement of the receptive fields by suppressing the excitatory activity of the pyramidal neurons and providing a balance between excitation and inhibition. This last part is the one that the proposed model lacks. The lateral connections have been considered steady and not plastic. This means that one has to devise a way in order to describe mathematically and computationally the synaptic and the homeostatic mechanisms which regulate the balance between excitation and inhibition. Nevertheless, the model is able to reorganize its topographic organization pinpointing that the cortex is probably able to reorganize its somatotopic organization of area 3b after a lesion only using the feed-forward thalamocortical connections and a fundamental system of horizontal connections.

Other aspects that the proposed model covers are the attention and its effects on area 3b. As it has been mentioned previously the results of the proposed model points out that attention affects the receptive fields of neurons of area 3b but it is not capable of causing migration of receptive fields towards the attended side of the skin. Instead of attention, intensive training of the skin region of interest causes a massive migration of the receptive fields and a shrinkage of them as well. A combination of both, attention and intensive training, can cause an extremely massive migration of receptive fields towards the attended area and a huge reduction of the size of RFs. The proposed model confirms the existing theories of attention and disprove the theory of continuous training. According to the latter, an exhausting training can increase dramatically the performance of a subject during the execution of a demanding task without any implication of attention. This theory might be not true, since attention is always present during learning and experimentalists must be very careful in how they treat and destruct attention during a task. This suggests that experiments should be conducted with high fidelity. In addition, experimentalists should devise and conduct experiments where attention and training mechanisms should be separated. Finally, according to the results of the proposed model, attention is crucial for learning and performance of a subject and in a combination with intensive training can increase tremendously the performance.

3.5 Other computational models of SI

Modeling cortical phenomena is not something new. In bibliography there are several computational models that simulate different cortical phenomena. In this section, four different models of

primary somatosensory cortex are presented and shortly described. In addition a model of neural fields that is able to develop self-organization maps is also presented, because of the relation to this work.

Joublin et al. in [216] introduced a computational model of the primary somatosensory cortex. The model is based on experimental data that have been acquired from the authors. The equation that governs the model is given by Wilson-Cowan model and the learning rule is a mixed of Hebb and a non-Hebbian rule. The architecture of the model is a four layer neural network. The first layer represents the hindpaw sensors, the second one is the pre-cortical cells and is based on a Kohonen map. The third level is the excitatory neurons population and the fourth one is the inhibitory neurons population. The model is able to explain in high precision the neurophysiological phenomena, that have been found during the experimental work of the authors. However, authors have not studied lesions and moreover the use of a Kohonen self-organizing map renders the model not biologically plausible. Instead, the model can be characterized as a powerful tool in order to study the corresponding neurophysiological data.

One of the most dated models about somatosensory cortex is that provided by Pearson et al. in [217]. This model is based on Edelman's theory of neural groups. The model consists of four digits, a palm and a cortical sheet. The training of the models has been done in a continuous fashion and takes advantage of a synaptic plasticity rule that simulates the open/close gates of synapses. In addition, two populations of neurons are used, one excitatory and one inhibitory. Inhibitory population acts through a shunting inhibition mechanism and a sigmoid function is used as firing rate function. The model is able to develop topographic maps, but suffers from some boundary problems, which lead to somehow not so nice topographic maps. Furthermore, authors study the reorganization in the presence of a persistent stimulation of one digit and reorganization after sensory deprivation of digit one and two.

A slightly different model based on spiking neural networks is provided by Xing and Gerstein in [218, 219, 220]. The model can simulate a plethora of cortical phenomena such as organization of topographic maps, reorganization in the presence of a cortical lesion and reorganization of cortical representations after sensory deprivation. The architecture of the model is a three layer network consisting of an input layer, a thalamic layer and a cortical layer. The cortical layer, in turn, consists of excitatory and inhibitory interconnected neurons. In addition the model is highly dependent on a variety of parameters.

All the aforementioned models can exploit cortical phenomena of the primary somatosensory cortex such as the formation and the maintenance of topographic maps. In addition they are able to treat some cortical lesion and sensory deprivation cases. They satisfy the most of the requirements of proposition 1, but there is a vulnerability in common for all the these three models. They either model something specific according to some experiments conducted by the authors themselves or they use as self-organized maps model the Kohonen SOM. Only the model of Pearson et al. is independent of specific experimental results. This renders the model more abstract and generic. However the model does not include a detailed skin model and exhibits some other issues that have been discussed previously.

3.6 Summary

The area 3b of primary somatosensory cortex is a nice candidate of modeling and studying self-organization and the emergence of topographic maps. The area 3b of somatosensory cortex of mammals, as it has already been mentioned, contains topographic organizations of skin body parts. Furthermore, these representations are dynamic and can undergo a reorganization under

several circumstances. For instance, in the presence of a cortical lesion area 3b is capable of reorganization of itself in order to circumvent the functional problems that have been developed due to the lesion.

Therefore, a computational model of self-organization and reorganization of area 3b of the primary somatosensory cortex has been proposed in this chapter. The model is based on neural fields and an Oja-like learning rule. The model consists of a skin patch, which contains receptors and transmits the input to the cortex, and a cortical model, which is a dynamic neural field and process further the incoming information. The model is named DNF-SOM from the dynamic neural field - self-organizing maps. The DNF-SOM model is able to manage simple self-organization tasks such as capturing features of a one- or a two-dimensional input space in different configurations (rectangles, circles). In addition it has the ability to generate self-organizing maps of higher dimensional objects. Furthermore, it is robust, distributed, and completely unsupervised. The strongest point of the model is the four parameters that it needs in order to work properly. This renders the model really simple and useful in contrary to other highly parametrized and tunable models.

The DNF-SOM model has been used throughout this thesis in order to study the formation and the maintenance of somatosensory topographic maps. A $1mm^2$ part of the index finger has been modelled and it has been used as input space. A 32×32 cortical model (dynamic neural field) drives the self-organization process providing the proper post-synaptic activity to the Oja-like learning rule. The DNF-SOM model after learning is able to produce self-organizing maps and in the presence of a cortical lesion (i.e. a damage to the neurons of the cortical model) or a sensory deprivation (i.e. a damage to the receptors of the skin model) it is able to reorganize itself. Moreover, higher order cognitive functions, such as attention, are capable of causing gain modulations in the model and therefore they can cause alterations to the receptive fields of the model. This, in turn, can promote a soft-reorganization of the topographic map of the model.

General Conclusions

A computational model of the primary somatosensory cortex has been proposed and described in this thesis. The model is able to develop topographic maps, maintain and reorganize them in face of cortical lesions, sensory deprivation and under the influence of attention. A dynamic neural field has been used as mathematical and computational framework. The dynamic neural field has a persistent activity solution (aka bump), which acts as post-synaptic activity and drives the learning process. The learning process is governed by an Oja-like learning rule, which is able to simulate synaptic scaling and other synaptic properties of learning. Among several different applications and test cases of the model the most important is the investigation of the topographic organization of the area 3b of the primary somatosensory cortex. This area receives information about touch by the mechanoreceptors of the skin of the hand. The complete model, the skin and the neural field with the feed-forward connections between them is able to produce topographic maps of the skin surface and is also able to respond to any input after the self-organization. In addition, the model recovers from a cortical lesion or a sensory deprivation. This means that the model is able to reorganize itself in the presence of such a damage.

The major finding of the present model is that a topographic map can emerge as a consequence of the interaction between thalamus and cortical excitatory afferent connections. These feed-forward connections are capable of causing the reorganization of a topographic map even in the presence of a cortical lesion or a sensory deprivation. Bruno in [78] has shown that excitatory thalamocortical connections can synchronize themselves in order to drive cortical neurons without making of use of any kind of cortical amplification mechanism. This enhanced the hypothesis that states that the main effort of the emergence and reorganization of a topographic map can be promoted by thalamocortical connections.

As it has been proposed by [126, 29], RFs are capable of refinement and shrinkage during a long-term reorganization process of a topographic map in the presence of a deprivation. DNF-SOM model, due to non-labile lateral connections, is not able to refine the RFs during the reorganization of a topographic map. This leads one to claim that lateral connections is a major moderator of RFs, especially in reorganization process of cortical sheet. An expansion of RFs takes place during reorganization indicating that RFs are able to represent a larger skin area rather than they did before lesion. However, this is only one part of the whole picture as it is only one out of two (or maybe three) reorganization phases. This second phase is what DNF-SOM model lacks. During the second phase of reorganization, a shrinkage of RFs takes place due to adaptation of lateral connections, the sprouting of new intracortical connections and the left over unaffected thalamocortical connections. In addition, lateral connections must be an important and valuable mechanism of the balance between excitatory and inhibitory neural populations, which, in turn, steers to the reorganization of robust topographic maps.

Subsequently, the present model indicates that without re-learning lateral connections, cortical sheet is able to recover from a lesion of type I or II. A lesion of type I or II does not affect explicitly the topology of the whole field. In a lesion of type I, the field is degraded topologically into a new one holding almost the same circuitry. During a lesion of type II, the field is divided

into two different topological pieces, holding the connections stable. Instead, a lesion of type III topologically transforms the field into a new one with a hole within it. Thus the recovery from this condition is not so easily obtainable, rendering this lesion case the most noxious.

Furthermore, two major characteristics of a cortical lesion (or ablation) could be responsible for a proper reorganization and recovery of a cortical sheet. First, is the location of the lesion, *Where the lesion is located?* and second the extent of the lesion, *What is the amount of the dead neurons?*. Both, location and extent are intertwined, in a fashion that the former pervades the later and vice versa. Therefore, two different cases of lesion can be discriminated. First, if the lesion is located at the borders of two or more cortical representations and it is extended not in a large area, then recovery is easily achievable. This is because of the large amount of left over neurons and afferent connections. Instead, if the extent of the lesion is large then the representations cannot recover completely and sometimes they cannot recover at all. Second, if the lesion is located within a single representation, recovery is only a matter of the extent of the lesion, itself. That is because, if a significant amount of neurons is affected by the lesion, there is no sufficient number of neurons to deploy their RFs and revive previously lost functions of the dead neurons by virtue of remaining afferent connections. Yet, in a localized lesion case, in the vicinity of the lesioned area, there are some neurons which do not respond so intensively as the others and those neurons drive other neurons leading them to reorganize themselves.

In this study it has not been taken into account any kind of homeostatic mechanism and/or metaplasticity, which have been proposed by [42] as moderator factors of lateral connections. The former conserves and regulates the average activity of brain circuits by scaling neural synapses and the later prevents them from saturation effects, [45]. Homeostatic mechanisms and/or metaplasticity can prevent networks from saturation effects in the same way metaplasticity may affect neural circuits of the brain.

Another interesting aspect that investigated throughout this thesis is the effect of attention on the area 3b of the primary somatosensory cortex and the alterations of receptive fields of neurons that are provoked by attentional phenomena. The evidence for the effects of attention on SI in the literature are somehow contradictory. Hsiao [138] has shown that attention is engaged in the modification of RFs of both primary and secondary somatosensory cortices. Similarly, Braun and colleagues [139] have reported such engagement of attention in the primary somatosensory cortex using neuroimaging techniques. On the other hand, [221] have claimed that attention is not important in enhancing performance during a discrimination task even though consecutive training or pairing stimulations leading to co-activation can affect the RFs and the cortical representations increasing the performance of the subjects.

In the case of intensive stimulation (without any kind of modulation), the model tends to show a large expansion of the cortical territory with a simultaneous shrinkage of the receptive fields as well as strong migration of their center towards the region of interest. These findings are contradictory with psychophysical studies such as [222, 221, 213], where authors noticed that the cortical representation undergoes an expansion but at the same time the RFs undergo a similar expansion. However, other neurophysiological and neuroimaging studies have shown that when cortical representation expand, RFs sizes are shown to decrease [223, 214]. These latter results are also consistent with early findings of Sur and colleagues [224]. They found, from neurophysiological recordings and mappings that the magnification factor of cortical representations is related to the size of the RFs. More precisely, the magnification factor is proportional to the size of the RFs (the smaller the RFs the larger the cortical representation). The model findings indicate and confirm that cortical representations, in the case of intensive stimulation, increase in cortical size while RFs shrink. However, in the case of long-term modulation, the model is capable of showing very clearly that it is possible to have a shrinkage of the receptive fields with-

out any migration on the skin patch nor any cortical magnification. This finding indicates that there are two distinct processes at work, namely modulation and stimulation, that are believed to be present simultaneously in most cases, while there may exist a few cases where only one process is active. This may reconcile the aforementioned contradictory results. To confirm these findings, it would thus be necessary to set up new experiments where modulation and stimulation would be carefully dissociated. This can be done by precisely controlling the amount of training received by a subject and by distracting the subject such as drifting attentional process away from the primary task.

Another concept that has to be mentioned, is that of co-activation of cortical representations in order to achieve better performance in a tactile discrimination task. In this case, two (or more) stimuli are applied simultaneously on the skin and, following a training period of variable length, the subject is able to discriminate the most salient stimulus. Such an example is the two-point discrimination test [225] that is used mostly by neurologists in order to examine neurological pathologies. Neurologists apply at the beginning two stimuli far apart and after getting the response of the patient, they reduce the distance between the two stimuli. At some point the patient perceives only one stimulus instead of two which are applied on their skin. The same protocol has been applied on subjects for the purpose of investigating perception and discrimination at the somatosensory cortical level. The key idea is the co-application of two stimuli on the skin which leads to the development and the establishment of multi-receptive fields (mRFs) on the somatosensory cortex. This condition implies the engagement of a Hebbian learning rule which builds up associations between the two stimuli. A side-effect of this condition is the increase in size of the cortical representation as it has been reported by [226, 221]. Such condition can lead to inconsistent results. The mRFs are larger than the normal RFs by definition and therefore a neuron of mRF may be capable of responding to two simultaneously applied stimuli, increasing the performance of the subject in the two-points discrimination test. In addition the mRFs could lead to an increase of the cortical representations. Present findings of the model related to intensive stimulation reveal a migration of RFs of neighboring neurons of cortical representation of RoI towards this latter representation. Additionally, the RFs sizes within cortical representation of RoI undergo a decrease in size. These findings are consistent with the neurophysiological findings provided by Xerri and Elbert.

The present experimental results are also consistent with several neurophysiological and computational studies, [146, 147, 148] and [149], respectively. In these studies authors have found that when a stimulus lies on the center of a RF of a neuron, the neuron tends to shrink its RF around the stimulus. Nevertheless, when a stimulus is located close to the center of the RF (but outside of the center) the neuron shifts the RF towards the stimulus position by expanding the RF. In the one-dimensional neural network model of Compte and Wang, an explicit attentional signal is provided to the model. In our case, the model is continuous and two-dimensional and we only modulate lateral connections gain without using any kind of explicit attentional signal. Furthermore, when this modulation is combined with intensive stimulation, results are dramatically enhanced. This leads one to believe that the combination of attentional mechanisms and intensive stimulation can lead to a better refinement of RFs as well as cortical representations. This is evident and substantiated by the findings of the DNF-SOM model experiments. The RFs outside the cortical representation of RoI have undergone an expansion, despite the fact that the RFs within cortical representation of RoI have undergone a shrinkage. These results plus the fact that only the synaptic gain of lateral connections (K_e and K_i) is modified, indicate that a modulation of the gain is sufficient to change the cortical organization. This means that an explicit attentional signal as an additional input to the model (such the one that is used by Compte and Wang) is not necessary in order to trigger cortical reorganization and RFs alter-

ations. Such result is significant because of its parsimonious nature: the system does not require extra parameters for the expression of attention (compared to the nominal regime).

A possible mechanisms and neural circuitry that could convey the attentional signal has not been yet mentioned. From several studies on attention, one can conclude that the origin of the attentional mechanism most probably involves many different networks from both cortical and sub-cortical areas and involves as well different higher order cognitive functions such as working memory, planning and prediction. The present model is not able to shed light on the underlying mechanisms of attention. However, since the factor that triggers cortical alterations is the synaptic gain of lateral connections, this implies that a higher order signal is necessary. Such a signal could be of a cholinergic nature as it has been described in a review by Sarter et al. [140] and by the work of Juliano et al. [142]. The former proposes a complete circuit that engages the basal forebrain corticopetal cholinergic system. The latter indicates that the cholinergic depletion prevents expansion of somatosensory topographic maps. These works provide evidence for the involvement of some cholinergic substances such as acetylcholine (ACh) in attention mechanisms. Moreover this cholinergic system is affected by the prefrontal cortex and therefore it can be considered as an output of the prefrontal cortex to the somatosensory cortices. Another interesting finding is provided by Tremblay et al. [143, 144] and Rasmusson and Dykes in [145], where authors have shown that the co-activation of somatosensory cortex by cutaneous stimulation and the basal forebrain leads to an enhancement of the activity response of the neurons of somatosensory cortex (in cats). This cholinergic system may reflect to some extent the modulation of gains of lateral connections in DNF-SOM model. A rational speculation is that the cholinergic release in somatosensory cortex affects the gains of lateral connections that in turn leads to the cortical representations expansion and the re-tuning of RFs, which is consistent with the previously discussed experimental data.

Even if a cholinergic substance is believed to be the underlying molecular mechanism, which plays the key role in attention (and/or in other high cognitive processes), cortical and subcortical circuitry involved in such attentional function remains largely unknown. According to [140] there are two distinct networks one bottom-up and a top-down. DNF-SOM model does not take into account the whole picture since there is no modeling of cortical areas outside SI. Therefore, the attentional signal may reach the SI through the basal forebrain system after the implication of a more complex network. This last network has been proposed to be a switching system involving insular cortex, dorsolateral prefrontal cortex, posterior parietal cortex, ventromedial prefrontal cortex, posterior cingulate cortex and anterior cingulate cortex. This complex network has been proposed by Manon and Uddin, [141] and the main point is that the insular cortex acts as a switch between two different prefrontal networks leading to an attentional effect through saliency occurring in anterior insular cortex. From anatomical data is is known that some insular areas talk to SI and SII, something which leads one to suspect that this complex network might be a candidate for attention. In the context of DNF-SOM model the top-down mechanism is the attentional signal that triggers the modification of lateral synaptic strength gains and the bottom-up mechanism is the reorganization of feed-forward corticothalamic connections. Both affect the whole system at the same time by different ways leading to a new topographic map and new properties of RFs of neurons. This implies that both top-down and bottom-up mechanisms are necessary and work synergetically in order to achieve better performances guiding by higher order brain cortical centers. Of course it remains to determine the exact underlying top-down and bottom-up mechanisms in terms of neurophysiology.

One major perspective of this work is the understanding of the perception of the body and the touch. It has been shown that the perception of touch can be divided into two distinct processes. The detection and the localization. The former is related to the detection of a stimulus on the

skin surface and the second has to do with the localization of that stimulus on the skin. Several psychophysics schemas have been proposed based on psychological or psychophysics experiments on humans (for an extended review one can read [150] and [227]). Therefore the main idea of those propositions the combination of different modalities, such as touch and proprioception with higher mental functions. These mental functions are able to execute the final transformations in order to promote perception and spatial localization of touch. These theories can explain some phenomena of touch localization or tactile object recognition. However, they cannot explain how the brain can acquire the knowledge of where a stimulus is over development or they do not explain in details which is the exact mental mechanism in the brain. What is the exact brain circuitry which implements that kind of behaviors.

Therefore, in order to study in a more detailed way the spatial localization of touch, one has to take into account the brain weave together sensory modalities and motor actions. It has been shown that the primary somatosensory and the primary motor cortices are the first in raw of development, [21] while early motor activity drives the development of somatosensory cortex, [99, 31] and [228]. This implies that the spatial localization of touch is not a simple process and it can be acquired through a closed-loop circuitry implemented by sensorimotor brain areas. During prenatal development the primary motor cortex due to spontaneous activity produces several movements which lead to a feed-back of the primary somatosensory cortex, induces the formation of somatotopic maps. This later, can lead to the detection of a stimulus on the skin. Nevertheless, for the spatial localization of touch the information provided by the area 3b of primary somatosensory cortex (touch modality) is not enough. Therefore, the proprioceptive modality must be taken into account. The proprioceptive modality consists the so-called postural schema with the motor commands. Thus, the touch modality, the *a priori* knowledge of body metrics (size and shape), the proprioceptive modality and the motor commands can weave together and lead to the solution of the spatial localization of touch problem. One possible biological plausible implementation is the integration of different modalities in multimodal topographic maps such the second somatosensory cortex (SII) and/or the area 5 of parietal cortex (both are involved in touch information process). In this context, so far, the model explains the detection of a touch (in normal conditions, after lesions, sensory deprivations and how attention affects the detection). The same mechanism can be used in order to model proprioception areas (such as area 3a), secondary somatosensory cortex (SII) and associative areas (area 5). In combination with a motor map the phenomenon of touch spatial localization can be studied and investigated further.

Summarizing, the proposed model is a one-equation neural field model that integrated information from a skin model of Merkel's mechanoreceptors. The dynamic neural field represents two neural populations, one excitatory and one inhibitory in one single cortical layer. The input to the dynamic neural field is provided by the thalamus and any in between relay stations have been omitted in favor of simplicity. The model requires four (in reallity two) parameters in order to perform a self-organization process. This renders the model robust enough and very simple without need for hard parameters tuning and searching in high dimensional search spaces. The nature of the dynamic neural fields equations permits the distributed implementation and maybe a synchronous/asynchronous implementation, according to [229]. The model is offered to model cerebral areas due to its simplistic nature. As future work, it would be nice to add some extra terms into the equation according to neurophysiological data in order to render the model more realistic and more useful to people who conduct experiments and not only.

Bibliography

[1] Purves Dale, Augustine George J, Fitzpatrick David, Katz Lawrence C, LaMantia Anthony-Samuel, McNamara James O, and Williams S Mark. *Neuroscience*. Sinauer Associates, 2004.

[2] Larry Squire, Darwin Berg, Floyd E Bloom, Sascha du Lac, Anirvan Ghosh, and Nicholas C Spitzer. *Fundamental neuroscience*. Academic Press, 2012.

[3] Roger W Sperry. Hemisphere deconnection and unity in conscious awareness. *American Psychologist*, 23(10):723, 1968.

[4] Sally P Springer and Georg Deutsch. *Left brain, right brain (rev.* WH Freeman/Times Books/Henry Holt & Co, 1985.

[5] Francisco Aboitiz, Arnold B Scheibel, Robin S Fisher, and Eran Zaidel. Fiber composition of the human corpus callosum. *Brain research*, 598(1):143–153, 1992.

[6] Eric R Kandel, James H Schwartz, Thomas M Jessell, et al. *Principles of neural science*, volume 4. McGraw-Hill New York, 2000.

[7] Christian Giaume, Annette Koulakoff, Lisa Roux, David Holcman, and Nathalie Rouach. Astroglial networks: a step further in neuroglial and gliovascular interactions. *Nature Reviews Neuroscience*, 11(2):87–99, 2010.

[8] Larry R Squire. Memory and the hippocampus: a synthesis from findings with rats, monkeys, and humans. *Psychological review*, 99(2):195, 1992.

[9] VS Chakravarthy, Denny Joseph, and Raju S Bapi. What do the basal ganglia do? a modeling perspective. *Biological cybernetics*, 103(3):237–253, 2010.

[10] Andrea Stocco, Christian Lebiere, and John R Anderson. Conditional routing of information to the cortex: a model of the basal ganglia role in cognitive coordination. *Psychological review*, 117(2):541, 2010.

[11] Edward J Fine, Catalina C Ionita, and Linda Lohr. The history of the development of the cerebellar examination. In *Seminars in neurology*, volume 22, pages 375–384. Copyright© 2002 by Thieme Medical Publishers, Inc., 333 Seventh Avenue, New York, NY 10001, USA. Tel.:+ 1 (212) 584-4662, 2003.

[12] Kenji Doya. Complementary roles of basal ganglia and cerebellum in learning and motor control. *Current opinion in neurobiology*, 10(6):732–739, 2000.

[13] Ying-Wan Lam and S Murray Sherman. Functional organization of the somatosensory cortical layer 6 feedback to the thalamus. *Cerebral Cortex*, 20(1):13–24, 2010.

[14] Andreas Burkhalter. Many specialists for suppressing cortical excitation. *Frontiers in neuroscience*, 2(2):155, 2008.

[15] Vernon B Mountcastle. The columnar organization of the neocortex. *Brain*, 120(4):701–722, 1997.

[16] Daniel P Buxhoeveden and Manuel F Casanova. The minicolumn hypothesis in neuroscience. *Brain*, 125(5):935–951, 2002.

[17] David H Hubel and Torsten N Wiesel. Laminar and columnar distribution of geniculocortical fibers in the macaque monkey. *Journal of Comparative Neurology*, 146(4):421–450, 1972.

[18] David H Hubel and Torsten N Wiesel. Receptive fields of single neurones in the cat's striate cortex. *The Journal of physiology*, 148(3):574–591, 1959.

[19] Jon H Kaas. Plasticity of sensory and motor maps in adult mammals. *Annual review of neuroscience*, 14(1):137–167, 1991.

[20] Dean V Buonomano and Michael M Merzenich. Cortical plasticity: from synapses to maps. *Annual review of neuroscience*, 21(1):149–186, 1998.

[21] Nitin Gogtay, Jay N Giedd, Leslie Lusk, Kiralee M Hayashi, Deanna Greenstein, A Catherine Vaituzis, Tom F Nugent, David H Herman, Liv S Clasen, Arthur W Toga, et al. Dynamic mapping of human cortical development during childhood through early adulthood. *Proceedings of the National Academy of Sciences of the United States of America*, 101(21):8174–8179, 2004.

[22] Alvaro Pascual-Leone, Amir Amedi, Felipe Fregni, and Lotfi B Merabet. The plastic human brain cortex. *Annu. Rev. Neurosci.*, 28:377–401, 2005.

[23] Kevin Fox. The cortical component of experience-dependent synaptic plasticity in the rat barrel cortex. *The Journal of neuroscience*, 14(12):7665–7679, 1994.

[24] Gordon MG Shepherd, Thomas A Pologruto, and Karel Svoboda. Circuit analysis of experience-dependent plasticity in the developing rat barrel cortex. *Neuron*, 38(2):277–289, 2003.

[25] Kevin Fox, RO Wong, et al. A comparison of experience-dependent plasticity in the visual and somatosensory systems. *Neuron*, 48(3):465, 2005.

[26] Mriganka Sur and John LR Rubenstein. Patterning and plasticity of the cerebral cortex. *Science Signaling*, 310(5749):805, 2005.

[27] MB Calford. Dynamic representational plasticity in sensory cortex. *Neuroscience*, 111(4):709–738, 2002.

[28] Jerome N Sanes and John P Donoghue. Plasticity and primary motor cortex. *Annual review of neuroscience*, 23(1):393–415, 2000.

[29] Sherre L Florence, Neeraj Jain, and Jon H Kaas. Plasticity of somatosensory cortex in primates. In *Seminars in neuroscience*, volume 9, pages 3–12. Elsevier, 1997.

[30] Megan S Steven and Colin Blakemore. Cortical plasticity in the adult human brain. In Michael S Gazzaniga, editor, *The cognitive neurosciences III*, pages 1243–1254. MIT Press, 2004.

[31] Rustem Khazipov, Heiko J Luhmann, et al. Early patterns of electrical activity in the developing cerebral cortex of humans and rodents. *Trends in neurosciences*, 29(7):414–418, 2006.

[32] Charles F Stevens and John F Wesseling. Augmentation is a potentiation of the exocytotic process. *Neuron*, 22(1):139–146, 1999.

[33] LF Abbott, JA Varela, Kamal Sen, and SB Nelson. Synaptic depression and cortical gain control. *Science*, 275(5297):221–224, 1997.

[34] SF Cooke and TVP Bliss. Plasticity in the human central nervous system. *Brain*, 129(7):1659–1673, 2006.

[35] Tim VP Bliss, Graham L Collingridge, et al. A synaptic model of memory: long-term potentiation in the hippocampus. *Nature*, 361(6407):31–39, 1993.

[36] Daniel E Feldman. Synaptic mechanisms for plasticity in neocortex. *Annual review of neuroscience*, 32:33, 2009.

[37] Peter V Massey, Zafar I Bashir, et al. Long-term depression: multiple forms and implications for brain function. *Trends in neurosciences*, 30(4):176–184, 2007.

[38] Donald Hebb. The organization of behavior, 1968.

[39] Natalia Caporale and Yang Dan. Spike timing-dependent plasticity: a hebbian learning rule. *Annu. Rev. Neurosci.*, 31:25–46, 2008.

[40] Antonio Rodriguez-Moreno, Ana Gonzalez-Rueda, Abhishek Banerjee, A Louise Upton, Michael T Craig, and Ole Paulsen. Presynaptic self-depression at developing neocortical synapses. *Neuron*, 77(1):35–42, 2013.

[41] Gina G Turrigiano, Kenneth R Leslie, Niraj S Desai, Lana C Rutherford, and Sacha B Nelson. Activity-dependent scaling of quantal amplitude in neocortical neurons. *Nature*, 391(6670):892–896, 1998.

[42] Gina G Turrigiano and Sacha B Nelson. Hebb and homeostasis in neuronal plasticity. *Current opinion in neurobiology*, 10(3):358–364, 2000.

[43] Gina G Turrigiano and Sacha B Nelson. Homeostatic plasticity in the developing nervous system. *Nature Reviews Neuroscience*, 5(2):97–107, 2004.

[44] Wickliffe C Abraham and Mark F Bear. Metaplasticity: the plasticity of synaptic plasticity. *Trends in neurosciences*, 19(4):126–130, 1996.

[45] Wickliffe C Abraham. Metaplasticity: tuning synapses and networks for plasticity. *Nature Reviews Neuroscience*, 9(5):387–387, 2008.

[46] Elie L Bienenstock, Leon N Cooper, and Paul W Munro. Theory for the development of neuron selectivity: orientation specificity and binocular interaction in visual cortex. *The Journal of Neuroscience*, 2(1):32–48, 1982.

[47] Yoshiaki Iwamura. Hierarchical somatosensory processing. *Current opinion in neurobiology*, 8(4):522–528, 1998.

[48] Oleg V Favorov, Mathew E Diamond, and Barry L Whitsel. Evidence for a mosaic representation of the body surface in area 3b of the somatic cortex of cat. *Proceedings of the National Academy of Sciences*, 84(18):6606–6610, 1987.

[49] Robert M Friedman, Li Min Chen, and Anna Wang Roe. Modality maps within primate somatosensory cortex. *Proceedings of the National Academy of Sciences of the United States of America*, 101(34):12724–12729, 2004.

[50] P.R. Burgess and E.R. Perl. Cutaneous mechanoreceptors and nociceptors. In Ainsley Iggo, editor, *Somatosensory System*, volume 2 of *Handbook of Sensory Physiology*, pages 29–78. Springer Berlin Heidelberg, 1973.

[51] MJ Prud'homme and JOHN F Kalaska. Proprioceptive activity in primate primary somatosensory cortex during active arm reaching movements. *Journal of neurophysiology*, 72(5):2280–2301, 1994.

[52] Raf J Schepers and Matthias Ringkamp. Thermoreceptors and thermosensitive afferents. *Neuroscience & Biobehavioral Reviews*, 33(3):205–212, 2009.

[53] Kenneth O Johnson. The roles and functions of cutaneous mechanoreceptors. *Current opinion in neurobiology*, 11(4):455–461, 2001.

[54] M. Pare, A.M. Smith, and F.L. Rice. Distribution and terminal arborizations of cutaneous mechanoreceptors in the glabrous finger pads of the monkey. *The Journal of Comparative Neurology*, 445:347–359, 2002.

[55] R. Moll, I. Moll, and W.W. Franke. Identification of merkel cells in human skin by specific cytokeratin antibodies: changes of cell density and distribution in fetal and adult plantar epidermis. *Diferentiation*, 28(2):136–154, 1984.

[56] LR Mills, CA Nurse, and J Diamond. The neural dependency of merkel cell development in the rat: the touch domes and foot pads contrasted. *Developmental biology*, 136(1):61–74, 1989.

[57] Jonathan Bell, Stanley Bolanowski, and Mark H Holmes. The structure and function of pacinian corpuscles: A review. *Progress in neurobiology*, 42(1):79–128, 1994.

[58] GR Fisher, Brian Freeman, and Mark J Rowe. Organization of parallel projections from pacinian afferent fibers to somatosensory cortical areas i and ii in the cat. *Journal of neurophysiology*, 49(1):75–97, 1983.

[59] David T Blake, Steven S Hsiao, and Kenneth O Johnson. Neural coding mechanisms in tactile pattern recognition: the relative contributions of slowly and rapidly adapting mechanoreceptors to perceived roughness. *The Journal of neuroscience*, 17(19):7480–7489, 1997.

[60] Benoni B Edin, Gregory K Essick, Mats Trulsson, and KA Olsson. Receptor encoding of moving tactile stimuli in humans. i. temporal pattern of discharge of individual low-threshold mechanoreceptors. *The Journal of neuroscience*, 15(1):830–847, 1995.

[61] Stanley J Bolanowski Jr, George A Gescheider, Ronald T Verrillo, and Christin M Checkosky. Four channels mediate the mechanical aspects of touch. *The Journal of the Acoustical society of America*, 84:1680, 1988.

[62] RW Dykes, M Sur, MM Merzenich, JH Kaas, and RJ Nelson. Regional segregation of neurons responding to quickly adapting, slowly adapting, deep and pacinian receptors within thalamic ventroposterior lateral and ventroposterior inferior nuclei in the squirrel monkey (saimiri sciureus). *Neuroscience*, 6(8):1687–1692, 1981.

[63] Gerhard Werner and Barry L Whitsel. The topology of dermatomal projection in the medial lemniscal system. *The Journal of physiology*, 192(1):123–144, 1967.

[64] A Vania Apkarian and Charles J Hodge. Primate spinothalamic pathways: Iii. thalamic terminations of the dorsolateral and ventral spinothalamic pathways. *The Journal of comparative neurology*, 288(3):493–511, 2004.

[65] Maria Antoniou Patestas and Leslie P Gartner. *A textbook of neuroanatomy.* Blackwell Pub., 2006.

[66] Martin Grunwald. *Human Haptic Perception.* Birkhaeuser Verlag AG, Boston Basel Berlin, 2008.

[67] Edward G Jones. Cortical and subcortical contributions to activity-dependent plasticity in primate somatosensory cortex. *Annual review of neuroscience*, 23(1):1–37, 2000.

[68] George Paxinos and Jurgen K Mai. *The human nervous system.* Academic Press, 2004.

[69] H Künzle. Projections from the primary somatosensory cortex to basal ganglia and thalamus in the monkey. *Experimental Brain Research*, 30(4):481–492, 1977.

[70] Sherre L Florence, Hilary B Taub, and Jon H Kaas. Large-scale sprouting of cortical connections after peripheral injury in adult macaque monkeys. *Science*, 282(5391):1117–1121, 1998.

[71] Edward G Jones and Tim P Pons. Thalamic and brainstem contributions to large-scale plasticity of primate somatosensory cortex. *Science*, 282(5391):1121–1125, 1998.

[72] O. Foerster. The dermatomes in man. *Brain*, 56(1):1–39, 1933.

[73] Robert A Kuhn. Organization of tactile dermatomes in cat and monkey. *Journal of neurophysiology*, 16(2):169–182, 1953.

[74] Gerhard Werner and Barry L Whitsel. Topology of the body representation in somatosensory area i of primates. *Journal of Neurophysiology; Journal of Neurophysiology*, 1968.

[75] Peter T Fox, Harold Burton, and Marcus E Raichle. Mapping human somatosensory cortex with positron emission tomography. *Journal of neurosurgery*, 67(1):34–43, 1987.

[76] Leah A Krubitzer and Jon H Kaas. The organization and connections of somatosensory cortex in marmosets. *The Journal of Neuroscience*, 10(3):952–974, 1990.

[77] Stefan Geyer, Axel Schleicher, and Karl Zilles. Areas 3a, 3b, and 1 of human primary somatosensory cortex: 1. microstructural organization and interindividual variability. *Neuroimage*, 10(1):63–83, 1999.

[78] Randy M Bruno and Bert Sakmann. Cortex is driven by weak but synchronously active thalamocortical synapses. *Science*, 312(5780):1622–1627, 2006.

[79] Wilder Penfield and Edwin Boldrey. Somatic motor and sensory representation in the cerebral cortex of man as studied by electrical stimulation. *Brain: A journal of neurology*, 1937.

[80] Michael M Merzenich, Randall J Nelson, Jon H Kaas, Michael P Stryker, William M Jenkins, John M Zook, Max S Cynader, and Axel Schoppmann. Variability in hand surface representations in areas 3b and 1 in adult owl and squirrel monkeys. *The Journal of comparative neurology*, 258(2):281–296, 1987.

[81] Mriganka Sur, John T Wall, and JH Kaas. Modular distribution of neurons with slowly adapting and rapidly adapting responses in area 3b of somatosensory cortex in monkeys. *Journal of neurophysiology*, 51(4):724–744, 1984.

[82] Mriganka Sur, Preston E Garraghty, and Charles J Bruce. Somatosensory cortex in macaque monkeys laminar differences in receptive field size in areas 3b and 1. *Brain research*, 342(2):391–395, 1985.

[83] Herbert P Killackey and S Murray Sherman. Corticothalamic projections from the rat primary somatosensory cortex. *The Journal of neuroscience*, 23(19):7381–7384, 2003.

[84] Leah Krubitzer, Kelly J Huffman, Elizabeth Disbrow, and Gregg Recanzone. Organization of area 3a in macaque monkeys contributions to the cortical phenotype. *The Journal of comparative neurology*, 471(1):97–111, 2004.

[85] Kelly J Huffman and Leah Krubitzer. Area 3a topographic organization and cortical connections in marmoset monkeys. *Cerebral Cortex*, 11(9):849–867, 2001.

[86] Michael M Merzenich, Jon H Kaas, Mriganka Sur, and Chia-Sheng Lin. Double representation of the body surface within cytoarchitectonic area 3b and 1 in si in the owl monkey aotus trivirgatus. *The Journal of comparative neurology*, 181(1):41–73, 1978.

[87] Robert W Dykes, Douglas D Rasmusson, and Perry B Hoeltzell. Organization of primary somatosensory cortex in the cat. *Journal of neurophysiology*, 43(6):1527–1546, 1980.

[88] Ruth Izraeli and Linda L Porter. The effects of localized inactivation of somatosensory cortex, area 2, on the cat motor cortex. *Somatosensory & Motor Research*, 10(2):189–202, 1993.

[89] ED Adrian. Double representation of the feet in the sensory cortex of the cat. *Journal of Physiology*, 98:16, 1940.

[90] Wilder Penfield and Herbert Jasper. Epilepsy and the functional anatomy of the human brain. *Southern Medical Journal*, 47(7):704, 1954.

[91] Simon B Eickhoff, Axel Schleicher, Karl Zilles, and Katrin Amunts. The human parietal operculum. i. cytoarchitectonic mapping of subdivisions. *Cerebral Cortex*, 16(2):254–267, 2006.

[92] Simon B Eickhoff, Katrin Amunts, Hartmut Mohlberg, and Karl Zilles. The human parietal operculum. ii. stereotaxic maps and correlation with functional imaging results. *Cerebral Cortex*, 16(2):268–279, 2006.

[93] Paul J Fitzgerald, John W Lane, Pramodsingh H Thakur, and Steven S Hsiao. Receptive field properties of the macaque second somatosensory cortex: evidence for multiple functional representations. *The Journal of neuroscience*, 24(49):11193–11204, 2004.

[94] J Ruben, J Schwiemann, M Deuchert, R Meyer, T Krause, G Curio, K Villringer, R Kurth, and A Villringer. Somatotopic organization of human secondary somatosensory cortex. *Cerebral Cortex*, 11(5):463–473, 2001.

[95] Peter N Steinmetz, A Roy, PJ Fitzgerald, SS Hsiao, KO Johnson, and E Niebur. Attention modulates synchronized neuronal firing in primate somatosensory cortex. *Nature*, 404(6774):131–133, 2000.

[96] Dennis DM O'Leary, Naomi L Ruff, and Richard H Dyck. Development, critical period plasticity, and adult reorganizations of mammalian somatosensory systems. *Current opinion in neurobiology*, 4(4):535–544, 1994.

[97] David K Warland, Andrew D Huberman, and Leo M Chalupa. Dynamics of spontaneous activity in the fetal macaque retina during development of retinogeniculate pathways. *The Journal of neuroscience*, 26(19):5190–5197, 2006.

[98] Shatz CJ. Katz LC. Synaptic activity and the construction of cortical circuits. *Science*, 1996.

[99] Ileana L Hanganu, Werner Kilb, and Heiko J Luhmann. Spontaneous synaptic activity of subplate neurons in neonatal rat somatosensory cortex. *Cerebral Cortex*, 11(5):400–410, 2001.

[100] Lawrence C Katz, Justin C Crowley, et al. Development of cortical circuits: lessons from ocular dominance columns. *Nature Reviews Neuroscience*, 3(1):34–42, 2002.

[101] Antonio M Persico, Elisa Mengual, Rainald Moessner, Scott F Hall, Randal S Revay, Ichiro Sora, Jon Arellano, Javier DeFelipe, José Manuel Giménez-Amaya, Monica Conciatori, et al. Barrel pattern formation requires serotonin uptake by thalamocortical afferents, and not vesicular monoamine release. *The Journal of Neuroscience*, 21(17):6862–6873, 2001.

[102] Sally A Marik, Homare Yamahachi, Justin NJ McManus, Gabor Szabo, and Charles D Gilbert. Axonal dynamics of excitatory and inhibitory neurons in somatosensory cortex. *PLoS biology*, 8(6):e1000395, 2010.

[103] Takao K Hensch. Critical period plasticity in local cortical circuits. *Nature Reviews Neuroscience*, 6(11):877–888, 2005.

[104] Liisa Tremere, T Philip Hicks, and Douglas D Rasmusson. Role of inhibition in cortical reorganization of the adult raccoon revealed by microiontophoretic blockade of gabaareceptors. *Journal of neurophysiology*, 86(1):94–103, 2001.

[105] W Bryan Wilent and Diego Contreras. Dynamics of excitation and inhibition underlying stimulus selectivity in rat somatosensory cortex. *Nature neuroscience*, 8(10):1364–1370, 2005.

[106] Henry H Yin, Shweta Prasad Mulcare, Monica RF Hilário, Emily Clouse, Terrell Holloway, Margaret I Davis, Anita C Hansson, David M Lovinger, and Rui M Costa. Dynamic

reorganization of striatal circuits during the acquisition and consolidation of a skill. *Nature neuroscience*, 12(3):333–341, 2009.

[107] Preston E Garraghty, Jon H Kaas, et al. Functional reorganization in adult monkey thalamus after peripheral nerve injury. *Neuroreport*, 2(12):747, 1991.

[108] Neeraj Jain, Hui-Xin Qi, Christine E Collins, and Jon H Kaas. Large-scale reorganization in the somatosensory cortex and thalamus after sensory loss in macaque monkeys. *The Journal of Neuroscience*, 28(43):11042–11060, 2008.

[109] Fred A Lenz and Nancy N Byl. Reorganization in the cutaneous core of the human thalamic principal somatic sensory nucleus (ventral caudal) in patients with dystonia. *Journal of neurophysiology*, 82(6):3204–3212, 1999.

[110] J Bruggemann, Vasco Galhardo, and A Vania Apkarian. Immediate reorganization of the rat somatosensory thalamus after partial ligation of sciatic nerve. *Journal of Pain*, 2:220–228, 2000.

[111] Brenda Rapp, Sharma K Hendel, and Jared Medina. Remodeling of somotasensory hand representations following cerebral lesions in humans. *Neuroreport*, 13(2):207–211, 2002.

[112] Shaheen Hamdy, John C Rothwell, Q Aziz, David G Thompson, et al. Organization and reorganization of human swallowing motor cortex: implications for recovery after stroke. *Clinical science*, 99(2):151–157, 2000.

[113] Samuel J Sober, Jeanne M Stark, Dwayne S Yamasaki, and William W Lytton. Receptive field changes after strokelike cortical ablation: a role for activation dynamics. *Journal of neurophysiology*, 78(6):3438–3438, 1997.

[114] Mariko Nishibe, Scott Barbay, David Guggenmos, and Randolph J Nudo. Reorganization of motor cortex after controlled cortical impact in rats and implications for functional recovery. *Journal of neurotrauma*, 27(12):2221–2232, 2010.

[115] M Carlson and H Burton. Recovery of tactile function after damage to primary or secondary somatic sensory cortex in infant macaca mulatta. *The Journal of neuroscience*, 8(3):833–859, 1988.

[116] Hubert R Dinse, Patrick Ragert, Burkhard Pleger, Peter Schwenkreis, and Martin Tegenthoff. Pharmacological modulation of perceptual learning and associated cortical reorganization. *Science Signalling*, 301(5629):91, 2003.

[117] Bryan Kolb, Russell Brown, Alane Witt-Lajeunesse, and Robbin Gibb. Neural compensations after lesion of the cerebral cortex. *Neural plasticity*, 8(1-2):1–16, 2001.

[118] MM Merzenich and Jon H Kaas. Reorganization of mammalian somatosensory cortex following peripheral nerve injury. *Trends in Neurosciences*, 5:434–436, 1982.

[119] PR Manger, TM Woods, and EG Jones. Plasticity of the somatosensory cortical map in macaque monkeys after chronic partial amputation of a digit. *Proceedings of the Royal Society of London. Series B: Biological Sciences*, 263(1372):933–939, 1996.

[120] Neeraj Jain, Kenneth C Catania, and Jon H Kaas. Deactivation and reactivation of somatosensory cortex after dorsal spinal cord injury. *Nature*, 386:495–498, 1997.

[121] Thomas Elbert and Brigitte Rockstroh. Reorganization of human cerebral cortex: the range of changes following use and injury. *The Neuroscientist*, 10(2):129–141, 2004.

[122] Lotfi B Merabet and Alvaro Pascual-Leone. Neural reorganization following sensory loss: the opportunity of change. *Nature Reviews Neuroscience*, 11(1):44–52, 2009.

[123] Neeraj Jain, Sherre L Florence, and Jon H Kaas. Reorganization of somatosensory cortex after nerve and spinal cord injury. *Physiology*, 13(3):143–149, 1998.

[124] Ephron S Rosenzweig, Gregoire Courtine, Devin L Jindrich, John H Brock, Adam R Ferguson, Sarah C Strand, Yvette S Nout, Roland R Roy, Darren M Miller, Michael S Beattie, et al. Extensive spontaneous plasticity of corticospinal projections after primate spinal cord injury. *Nature neuroscience*, 13(12):1505–1510, 2010.

[125] Barbara M Faggin, Kevin Tri Nguyen, and Miguel AL Nicolelis. Immediate and simultaneous sensory reorganization at cortical and subcortical levels of the somatosensory system. *Proceedings of the National Academy of Sciences*, 94(17):9428–9433, 1997.

[126] Elisabeth Foeller and Daniel E Feldman. Synaptic basis for developmental plasticity in somatosensory cortex. *Current opinion in neurobiology*, 14(1):89–95, 2004.

[127] KD Alloway, P Rosenthal, and H Burton. Quantitative measurements of receptive field changes during antagonism of gabaergic transmission in primary somatosensory cortex of cats. *Experimental brain research*, 78(3):514–532, 1989.

[128] Cheng X Li, Joseph C Callaway, and Robert S Waters. Removal of gabaergic inhibition alters subthreshold input in neurons in forepaw barrel subfield (fbs) in rat first somatosensory cortex (si) after digit stimulation. *Experimental brain research*, 145(4):411–428, 2002.

[129] SA Chowdhury and DD Rasmusson. Effect of gaba b receptor blockade on receptive fields of raccoon somatosensory cortical neurons during reorganization. *Experimental brain research*, 145(2):150–157, 2002.

[130] JD Churchill, N Muja, WA Myers, J Besheer, and PE Garraghty. Somatotopic consolidation: a third phase of reorganization after peripheral nerve injury in adult squirrel monkeys. *Experimental brain research*, 118(2):189–196, 1998.

[131] Daniel B Polley, Eugen Kvaš&ncaron, et al. Naturalistic experience transforms sensory maps in the adult cortex of caged animals. *Nature*, 429(6987):67–71, 2004.

[132] Michael L Platt and Paul W Glimcher. Neural correlates of decision variables in parietal cortex. *Nature*, 400(6741):233–238, 1999.

[133] Francis Crick and Christof Koch. A framework for consciousness. *Nature neuroscience*, 6(2):119–126, 2003.

[134] Rebecca Elliott. Executive functions and their disorders imaging in clinical neuroscience. *British Medical Bulletin*, 65(1):49–59, 2003.

[135] Eric I Knudsen. Fundamental components of attention. *Annu. Rev. Neurosci.*, 30:57–78, 2007.

[136] Raphaë lle Lépine, Pierre Parrouillet, and Valérie Camos. What makes working memory spans so predictive of high-level cognition? *Psychonomic Bulletin & Review*, 12(1):165–170, 2005.

[137] Stephen Monsell. Task switching. *Trends in cognitive sciences*, 7(3):134–140, 2003.

[138] Steven S Hsiao and Francisco Vega-Bermudez. 8 attention in the somatosensory system. *The somatosensory system: Deciphering the brain's own body image*, page 197, 2010.

[139] Christoph Braun, Monika Haug, Katja Wiech, Niels Birbaumer, Thomas Elbert, Larry E Roberts, et al. Functional organization of primary somatosensory cortex depends on the focus of attention. *Neuroimage*, 17(3):1451–1458, 2002.

[140] M. Sarter, M.E. Hasselmo, J.P. Bruno, B. Givens, et al. Unraveling the attentional functions of cortical cholinergic inputs: interactions between signal-driven and cognitive modulation of signal detection. *Brain Research Reviews*, 48(1):98–111, 2005.

[141] V. Menon and L.Q. Uddin. Saliency, switching, attention and control: a network model of insula function. *Brain Structure and Function*, 214(5):655–667, 2010.

[142] S.L. Juliano, W. Ma, and D. Eslin. Cholinergic depletion prevents expansion of topographic maps in somatosensory cortex. *Proceedings of the National Academy of Sciences*, 88(3):780–784, 1991.

[143] N. Tremblay, R.A. Warren, and R.W. Dykes. Electrophysiological studies of acetylcholine and the role of the basal forebrain in the somatosensory cortex of the cat. i. cortical neurons excited by glutamate. *Journal of neurophysiology*, 64(4):1199–1211, 1990.

[144] N. Tremblay, R.A. Warren, and R.W. Dykes. Electrophysiological studies of acetylcholine and the role of the basal forebrain in the somatosensory cortex of the cat. ii. cortical neurons excited by somatic stimuli. *Journal of neurophysiology*, 64(4):1212–1222, 1990.

[145] DD Rasmusson and RW Dykes. Long-term enhancement of evoked potentials in cat somatosensory cortex produced by co-activation of the basal forebrain and cutaneous receptors. *Experimental Brain Research*, 70(2):276–286, 1988.

[146] T. Womelsdorf, K. Anton-Erxleben, and S. Treue. Receptive field shift and shrinkage in macaque middle temporal area through attentional gain modulation. *The Journal of Neuroscience*, 28(36):8934–8944, 2008.

[147] K. Anton-Erxleben, V.M. Stephan, and S. Treue. Attention reshapes center-surround receptive field structure in macaque cortical area mt. *Cerebral Cortex*, 19(10):2466–2478, 2009.

[148] A.S. Quevedo and R.C. Coghill. Attentional modulation of spatial integration of pain: evidence for dynamic spatial tuning. *The Journal of Neuroscience*, 27(43):11635–11640, 2007.

[149] A. Compte and X.J. Wang. Tuning curve shift by attention modulation in cortical neurons: a computational study of its mechanisms. *Cerebral Cortex*, 16(6):761–778, 2006.

[150] Andrea Serino, Patrick Haggard, et al. Touch and the body. *Neuroscience and biobehavioral reviews*, 34(2):224, 2010.

[151] R.L. Beurle. Properties of a mass of cells capable of regenerating pulses. *Philosophical Transactions of the Royal Society of London. Series B, Biological Sciences*, 240(669):55–94, 1956.

[152] H.R. Wilson and J.D. Cowan. Excitatory and inhibitory interactions in localized populations of model neurons. *Biophysical journal*, 12(1):1–24, 1972.

[153] H.R. Wilson and J.D. Cowan. A mathematical theory of the functional dynamics of cortical and thalamic nervous tissue. *Biological Cybernetics*, 13(2):55–80, 1973.

[154] S. Amari. Dynamics of pattern formation in lateral-inhibition type neural fields. *Biological cybernetics*, 27(2):77–87, 1977.

[155] T.D. Sanger. Neural population codes. *Current opinion in neurobiology*, 13(2):238–249, 2003.

[156] S. Coombes. Waves, bumps, and patterns in neural field theories. *Biological Cybernetics*, 93(2):91–108, 2005.

[157] SE Folias and PC Bressloff. Breathers in two-dimensional neural media. *Physical review letters*, 95(20):208107, 2005.

[158] V. Markounikau, C. Igel, A. Grinvald, and D. Jancke. A dynamic neural field model of mesoscopic cortical activity captured with voltage-sensitive dye imaging. *PLoS Computational Biology*, 6(9):e1000919, 2010.

[159] S. E. Folias and G. B. Ermentrout. New patterns of activity in a pair of interacting excitatory-inhibitory neural fields. *Phys. Rev. Lett.*, 107:228103, Nov 2011.

[160] J. Fix, J. Vitay, and N. Rougier. A distributed computational model of spatial memory anticipation during a visual search task. *Anticipatory Behavior in Adaptive Learning Systems*, pages 170–188, 2007.

[161] J.S. Johnson, J.P. Spencer, S.J. Luck, and G. Schöner. A dynamic neural field model of visual working memory and change detection. *Psychological Science*, 20(5):568–577, 2009.

[162] G. Faye, J. Rankin, and P. Chossat. Localized states in an unbounded neural field equation with smooth firing rate function: a multi-parameter analysis. *Journal of Mathematical Biology*, pages 1–36, 2012.

[163] Warren S McCulloch and Walter Pitts. A logical calculus of the ideas immanent in nervous activity. *The Bulletin of Mathematical Biophysics*, 5(4):115–133, 1943.

[164] Alan L Hodgkin and Andrew F Huxley. A quantitative description of membrane current and its application to conduction and excitation in nerve. *The Journal of physiology*, 117(4):500, 1952.

[165] Richard FitzHugh. Impulses and physiological states in theoretical models of nerve membrane. *Biophysical journal*, 1(6):445–466, 1961.

[166] Wulfram Gerstner and Werner M Kistler. *Spiking neuron models: Single neurons, populations, plasticity*. Cambridge university press, 2002.

[167] Frank Rosenblatt. Perceptron simulation experiments. *Proceedings of the IRE*, 48(3):301–309, 1960.

[168] John J Hopfield. Neural networks and physical systems with emergent collective computational abilities. *Proceedings of the national academy of sciences*, 79(8):2554–2558, 1982.

[169] John A Hertz, Anders S Krogh, and Richard G Palmer. *Introduction to the theory of neural computation*, volume 1. Westview press, 1991.

[170] S. Grossberg, Boston University. Center for Adaptive Systems, Boston University. Dept. of Cognitive, and Neural Systems. *Letter to the Editor: Physiological Interpretation of the Self-organizing Map Algorithm.* Technical report CAS/CNS. Boston University, Center for Adaptive Systems and Department of Cognitive and Neural Systems, 1994.

[171] T. Kohonen. Self-organized formation of topologically correct feature maps. *Biological cybernetics*, 43(1):59–69, 1982.

[172] Michael A Arbib. *The handbook of brain theory and neural networks.* Bradford Book, 2003.

[173] B. Ermentrout. Neural networks as spatio-temporal pattern-forming systems. *Reports on progress in physics*, 61:353, 1998.

[174] O. Faugeras, F. Grimbert, J.J. Slotine, et al. Abolute stability and complete synchronization in a class of neural fields models. *SIAM Journal of Applied Mathematics*, 61(1):205–250, 2008.

[175] J.J. Hopfield. Neurons with graded response have collective computational properties like those of two-state neurons. *Proceedings of the national academy of sciences*, 81(10):3088, 1984.

[176] JG Taylor. Neural bubble dynamics in two dimensions: foundations. *Biological Cybernetics*, 80(6):393–409, 1999.

[177] P.C. Bressloff. Spatiotemporal dynamics of continuum neural fields. *Journal of Physics A: Mathematical and Theoretical*, 45(3):033001, 2011.

[178] S. Kubota, K. Hamaguchi, and K. Aihara. Local excitation solutions in one-dimensional neural fields by external input stimuli. *Neural computing & applications*, 18(6):591–602, 2009.

[179] H. Werner and T. Richter. Circular stationary solutions in two-dimensional neural fields. *Biological Cybernetics*, 85(3):211–217, 2001.

[180] E. Salinas and LF Abbott. A model of multiplicative neural responses in parietal cortex. *Proceedings of the national academy of sciences*, 93(21):11956, 1996.

[181] C. Malsburg and J.D. Cowan. Outline of a theory for the ontogenesis of iso-orientation domains in visual cortex. *Biological cybernetics*, 45(1):49–56, 1982.

[182] D.W. Dong and J.J. Hopfield. Dynamic properties of neural networks with adapting synapses. *Network: Computation in Neural Systems*, 3(3):267–283, 1992.

[183] S. Kubota and K. Aihara. Existence of lyapunov functional for neural field equation as an extension of lyapunov function for hopfield model. Technical report, Mathematical Engineering Technical Reports of the University of Tokyo, METR 2004-08, 2004.

[184] MR Owen, CR Laing, and S. Coombes. Bumps and rings in a two-dimensional neural field: splitting and rotational instabilities. *New Journal of Physics*, 9:378, 2007.

[185] DA French. Identification of a free energy functional in an integro-differential equation model for neuronal network activity. *Applied mathematics letters*, 17(9):1047–1051, 2004.

[186] Emilio Salinas and Peter Thier. Gain modulation: a major computational principle of the central nervous system. *Neuron*, 27(1):15–21, 2000.

[187] S. Camazine, J.L. Deneubourg, N.R. Franks, J. Sneyd, G. Theraula, and E. Bonabeau. *Self-organization in biological systems*. Princeton University Press, 2003.

[188] Alan Mathison Turing. The chemical basis of morphogenesis. *Bulletin of mathematical biology*, 52(1):153–197, 1990.

[189] S. Grossberg. A theory of human memory: Self-organization and performance of sensory-motor codes, maps, and plans. *Progress in theoretical biology*, 5:233–374, 1978.

[190] C. Malsburg. Self-organization of orientation sensitive cells in the striate cortex. *Biological Cybernetics*, 14(2):85–100, 1973.

[191] James MacQueen et al. Some methods for classification and analysis of multivariate observations. In *Proceedings of the fifth Berkeley symposium on mathematical statistics and probability*, volume 1, pages 281–297. California, USA, 1967.

[192] N. Rougier and Y. Boniface. Dynamic self-organising map. *Neurocomputing*, 74(11):1840–1847, 2011.

[193] Jean-Claude Fort. Som's mathematics. *Neural Networks*, 19(6-7):812–816, 2006.

[194] Pierre Demartines. Organization measures and representations of kohonen maps. In *First IFIP Working Group*, volume 10. Citeseer, 1992.

[195] H-U Bauer, Michael Herrmann, and Thomas Villmann. Neural maps and topographic vector quantization. *Neural networks*, 12(4):659–676, 1999.

[196] T. Kohonen. *Self-organizing maps*, volume 30. Springer Verlag, 2001.

[197] R. Miikkulainen. Self-organizing process based on lateral inhibition and synaptic resource redistribution. In *Proceedings of the International Conference on Artificial Neural Networks*, pages 415–420. Citeseer, 1991.

[198] J. Sirosh and R. Miikkulainen. Self-organizing feature maps with lateral connections: Modeling ocular dominance. In *Proceedings of the 1993 Connectionist Models Summer School*, page 31. Lawrence Erlbaum, 1994.

[199] J. Sirosh and R. Miikkulainen. How lateral interaction develops in a self-organizing feature map. In *Neural Networks, 1993., IEEE International Conference on*, pages 1360–1365. IEEE, 2002.

[200] Stuart P Wilson, Judith S Law, Ben Mitchinson, Tony J Prescott, and James A Bednar. Modeling the emergence of whisker direction maps in rat barrel cortex. *PloS one*, 5(1):e8778, 2010.

[201] SR Harker, CR Vogel, and T Gedeon. Analysis of constrained optimization variants of the map-seeking circuit algorithm. *Journal of Mathematical Imaging and Vision*, 29(1):49–62, 2007.

[202] David W. Arathorn. *Map-seeking circuits in visual cognition: A computational mechanism for biological and machine vision*. Stanford University Press, 2002.

[203] Lucian Alecu. *Une approche neuro-dynamique de conception des processus d'auto-organisation*. These, University of Lorraine, June 2011.

[204] David J Pinto and G Bard Ermentrout. Spatially structured activity in synaptically coupled neuronal networks: Ii. lateral inhibition and standing pulses. *SIAM Journal on Applied Mathematics*, 62(1):226–243, 2001.

[205] David J Heeger et al. Half-squaring in responses of cat striate cells. *Visual neuroscience*, 9:427–427, 1992.

[206] Jeffrey S Anderson, Ilan Lampl, Deda C Gillespie, and David Ferster. The contribution of noise to contrast invariance of orientation tuning in cat visual cortex. *Science*, 290(5498):1968–1972, 2000.

[207] Nicolas P Rougier and Georgios Is Detorakis. Self-organizing dynamic neural fields. In *Advances in Cognitive Neurodynamics (III)*, pages 281–288. Springer, 2013.

[208] G.I. Detorakis and N.P. Rougier. A neural field model of the somatosensory cortex: Formation, maintenance and reorganization of ordered topographic maps. *PloS one*, 7(7):e40257, 2012.

[209] L.F. Abbott and S.B. Nelson. Synaptic plasticity: taming the beast. *Nature neuroscience*, 3:1178–1183, 2000.

[210] AW Goodwin, AS Browning, and HE Wheat. Representation of curved surfaces in responses of mechanoreceptive afferent fibers innervating the monkey's fingerpad. *The Journal of neuroscience*, 15(1):798–810, 1995.

[211] J J DiCarlo, K O Johnson, and S S Hsiao. Structure of receptive fields in area 3b of primary somatosensory cortex in the alert monkey. *The Journal of neuroscience : the official journal of the Society for Neuroscience*, 18(7):2626–2645, 1998.

[212] JR Phillips, KO Johnson, and SS Hsiao. Spatial pattern representation and transformation in monkey somatosensory cortex. *Proceedings of the National Academy of Sciences*, 85(4):1317–1321, 1988.

[213] Gregg H Recanzone, Michael M Merzenich, William M Jenkins, Kamil A Grajski, and HUBERT R Dinse. Topographic reorganization of the hand representation in cortical area 3b owl monkeys trained in a frequency-discrimination task. *Journal of Neurophysiology*, 67(5):1031–1056, 1992.

[214] Christian Xerri, Judith M Stern, and Michael M Merzenich. Alterations of the cortical representation of the rat ventrum induced by nursing behavior. *The Journal of neuroscience*, 14(3):1710–1721, 1994.

[215] Raffaele Nardone, Yvonne Holler, Francesco Brigo, Martin Seidl, Monica Christova, Jurgen Bergmann, Stefan Golaszewski, and Eugen Trinka. Functional brain reorganization after spinal cord injury: systematic review of animal and human studies. *Brain research*, 2013.

[216] F Joublin, F Spengler, S Wacquant, and HR Dinse. A columnar model of somatosensory reorganizational plasticity based on hebbian and non-hebbian learning rules. *Biological cybernetics*, 74(3):275–286, 1996.

[217] John C Pearson, Leif H Finkel, and Gerald M Edelman. Plasticity in the organization of adult cerebral cortical maps: a computer simulation based on neuronal group selection. *The Journal of neuroscience*, 7(12):4209–4223, 1987.

[218] Jing Xing and George L Gerstein. Networks with lateral connectivity. i. dynamic properties mediated by the balance of intrinsic excitation and inhibition. *Journal of neurophysiology*, 75(1):184–199, 1996.

[219] Jing Xing and George L Gerstein. Networks with lateral connectivity. ii. development of neuronal grouping and corresponding receptive field changes. *Journal of neurophysiology*, 75(1):200–216, 1996.

[220] Jing Xing and George L Gerstein. Networks with lateral connectivity. iii. plasticity and reorganization of somatosensory cortex. *Journal of neurophysiology*, 75(1):217–232, 1996.

[221] Ben Godde, Beate Stauffenberg, Friederike Spengler, and Hubert R Dinse. Tactile coactivation-induced changes in spatial discrimination performance. *The Journal of Neuroscience*, 20(4):1597–1604, 2000.

[222] Karin Pilz, Ralf Veit, Christoph Braun, and Ben Godde. Effects of co-activation on cortical organization and discrimination performance. *Neuroreport*, 15(17):2669, 2004.

[223] Thomas Elbert, Christo Pantev, Christian Wienbruch, Brigitte Rockstroh, and Edward Taub. Increased cortical representation of the fingers of the left hand in string players. *Science*, 270(5234):305–307, 1995.

[224] Mriganka Sur, Michael M Merzenich, Jon H Kaas, et al. Magnification, receptive-field area, and hypercolumn size in areas 3b and 1 of somatosensory cortex in owl monkeys. *J Neurophysiol*, 44(2):295–311, 1980.

[225] ES Dellon, K Keller, V Moratz, and AL Dellon. The relationships between skin hardness, pressure perception and two-point discrimination in the fingertip. *The Journal of Hand Surgery: British & European Volume*, 20(1):44–48, 1995.

[226] Xiaoqin Wang, Michael M Merzenich, Koichi Sameshima, William M Jenkins, et al. Remodelling of hand representation in adult cortex determined by timing of tactile stimulation. *Nature*, 378(6552):71–75, 1995.

[227] Matthew R Longo, Elena Azañón, and Patrick Haggard. More than skin deep: body representation beyond primary somatosensory cortex. *Neuropsychologia*, 48(3):655–668, 2010.